January 2015

Genetic Regulation of Maize and Sorghum under Abiotic Stress

Alexandar Lewis Renaud
Purdue University

Graduate School Form 30
(Revised 08/14)

PURDUE UNIVERSITY
GRADUATE SCHOOL
Thesis/Dissertation Acceptance

This is to certify that the thesis/dissertation prepared

By Alexandar Lewis Renaud

Entitled
GENETIC REGULATION OF MAIZE AND SORGHUM UNDER ABIOTIC STRESS

For the degree of Doctor of Philosophy

Is approved by the final examining committee:

Mitchell Tuinstra

Michael Mickelbart

Guri Johal

Hyonho Chun

To the best of my knowledge and as understood by the student in the Thesis/Dissertation Agreement, Publication Delay, and Certification/Disclaimer (Graduate School Form 32), this thesis/dissertation adheres to the provisions of Purdue University's "Policy on Integrity in Research" and the use of copyrighted material.

Mitchell Tuinstra

Approved by Major Professor(s): _____

_____

Approved by: Joe Anderson 01/20/2015

Head of the Department Graduate Program Date

GENETIC REGULATION OF MAIZE AND SORGHUM UNDER ABIOTIC STRESS

A Dissertation

Submitted to the Faculty

of

Purdue University

by

Alexandar Lewis Renaud

In Partial Fulfillment of the

Requirements for the Degree

of

Doctor of Philosophy

May 2015

Purdue University

West Lafayette, Indiana

“I grew up on the land, on a small farm in northeast Iowa. Life was not always easy. I experienced the economic depressions of the 1930s, and from the experience, I felt that families on the land needed help from scientists, and I dedicated my life to science, and especially to food production.” – Norman Borlaug

ACKNOWLEDGEMENTS

I would like to sincerely thank my advisor Mitch Tuinstra for his guidance both scientifically and academically throughout my time at Purdue. He leads by example and his passion for agriculture is inspiring. Additionally, I would like to thank my committee members Drs. Michael Mickelbart, Guri Johal, and Hyonho Chun for the advice and accessibility throughout my graduate tenure. Their insights and suggestions to my research were extremely valuable and essential to the development of my project.

Cinta Romay and Alex Lipka were excellent collaborators at Cornell University and their aid and expertise were welcomed additions to completing this project. Special thanks to Drs. Emma Mace, David Jordan, Andrew Borrell, and Barbara George-Jaeggli for collaborative interactions on the stay-green in maize and sorghum projects.

Fellow graduate students and friends, Ray Lindsey, Michael Popelka, and Molly McKneight provided excellent feedback and support to my research project during my time at Purdue. Kartik Krothapalli and Andy Linvill were excellent sources of technical help, both in the lab and field, and I'm grateful for their advice and friendship. Furthermore, I would like to thank my dear friends at CIMMYT-Asia, Purdue University, USAID and others for providing me the opportunity to attend graduate school and experience international research. Finally, I would like to thank any other graduate or

undergraduate students that have contributed to data collection and lab work during my time at Purdue University.

I would like to express my deepest thanks and gratitude to Kurt McConnell for his friendship and mentorship over the last 3 years. His humility and impact on my life are profound and encouraging as I move forward.

I am deeply thankful and appreciative to my wife, Amanda, for her support and love during graduate school. Lastly, I would like to acknowledge my family for their encouragement and instilling in me a passion for agriculture.

TABLE OF CONTENTS

Page

Page

Page

Page

LIST OF TABLES

Table Page

Appendix Table

LIST OF FIGURES

Figure Page

Figure Page

Figure Page

Figure Page

Appendix Figure

Appendix Figure Page

Appendix Figure Page

ABSTRACT

Renaud, Alexandar L Ph.D., Purdue University, May 2015. Genetic Regulation of Maize and Sorghum under Abiotic Stress. Major Professor: Mitchell Tuinstra.

Climate extremes of temperature, drought and flooding continue to challenge global agricultural production and food security. If modeling studies are accurate, climate variability and drought will be a more prevalent occurrence in the future, not only inhibiting grain yield but also stressing water resources. Thus, it is critical to breed for improved climate resilience in agronomic crops and understand the genetic mechanisms conferring adaptation to water-limited environments.

Sorghum is an important crop grown in drought prone locations around the world and serves as a model crop for studying plant adaptation to water-limited environments. Sorghum breeders have been successful in developing drought-tolerant sorghum hybrids using stay-green as a phenotype. The ability of annual crop species to delay senescence or "stay-green" throughout the grain filling period has been associated with increased yield, decreased lodging, and stalk rot resistance. Genetic analyses of stay-green in sorghum suggest the trait is controlled by four to six loci that have been integrated into commercial programs by marker-assisted breeding.

The goal of my research is to characterize the genetic architecture of stay-green in maize. Maize exhibits substantial genetic variation for stay-green. We evaluated the

Nested Association Mapping (NAM) populations of maize and testcross hybrids with PHZ51 for variation in stay-green in multi-location trials. Joint linkage mapping was used to identify multiple QTL for stay-green across several linkage groups with sources of stay-green alleles coming from diverse genetic backgrounds. Association mapping was conducted using maize stay-green data to characterize gene families potentially associated with these phenotypes. Genetic associations from these studies were validated in the Ames Diversity Panel. Advancements in comparative genomics and statistics provide powerful tools for examining the biological relationships between maize and sorghum. Comparisons between maize and sorghum indicate that several genomic regions associated with stay-green are similar including major sorghum QTL Stg1, Stg2, Stg3, and Stg4. Identification and integration of stay-green genes into commercial programs may provide the opportunity to sustainably enhance the productivity of maize and sorghum in drought environments.

Additionally, our research examined the genetic regulation of premature senescence associated with sink-inhibition and hyper-senescence. When the ear of B73 is covered or removed to eliminate the sink, the plant prematurely and rapidly senesces around 800 growing degree days (GDD) post anthesis. The NAM populations of maize were used to identify candidate genes associated with this premature senescence trait and develop a potential model for the expression and regulation of the phenotype.

CHAPTER 1. BIOCHEMICAL, MOLECULAR, AND PHYSIOLOGICAL REGULATION OF ABIOTIC STRESS RESPONSES IN PLANTS

1.1 Introduction

Climate variability and abiotic stresses are detrimental forces to global agriculture production and food security. Abiotic stresses such as flooding, temperature extremes, and drought will continue to challenge the ability of scientists to develop stress tolerant hybrids and varieties, especially as food demand is expected to double within the next 30 years (Solomon et al., 2007; Foley et al., 2011). Scientific efforts to engineer climate resilient crops are slowed by the complex, quantitative nature of breeding for both yield and abiotic stress adaptation in hybrids and varieties (Duvick, 1996; Bruce et al., 2002). However, yield and production have continued to increase over time, as plants have become adapted to increased temperatures, drought and flooding (Solomon et al., 2007). New technological advances are ushering in a promising age of engineering climate resilient crops. In the area of biotechnology, advances in genome editing, marker assisted selection, and transgenics form a powerful suite of tools to combat climate variability. Advances in statistical modeling provide breeders and researchers alike with improved climate modeling and enhanced predictive power from genomic selection. In tandem, these two forms of modelling provide a robust platform for plant breeding.

Global production and demand for crops are continuing to increase in conjunction with climate variability. In order to meet the demands of the future, a second Green Revolution is needed. Plant breeders must combine knowledge of the biochemical, molecular, physiological, and genetic responses of plants under abiotic stresses with new technology to meet the demands of a variable climate.

1.2 Drought Stress Responses

Heightened global climate variability has brought forth devastating droughts in agricultural production areas and has led to a renewed focus on breeding and release of drought tolerant varieties and hybrids. In the United States, the summers of 2012 and 2013 served as a case study demonstrating the necessity for drought tolerant crop varieties and research. The United States experienced the second worst drought on record in 2012, when much of the Corn Belt was subjected to drought stress in July. This time period coincided with the majority of maize flowering time, when the crop is most susceptible to drought damage. The drought intensified throughout the grain filling months of August and September resulting in below average grain yields. The 2013 drought was significantly different than 2012. During the flowering period in July, no drought occurred in the Eastern and Central Corn Belt. However, a "flash drought" occurred during the grain filling months, negatively impacting yields (United States Drought Monitor, USDA-ARS Quick Stats). National United States maize yields were significantly lower in 2012, 123bu/ac, and 2013, 160bu/ac, compared to 2014, 174.2bu/ac (USDA-ARS Quick Stats). In 2014, there was little drought stress present on the United States Corn Belt correlating to higher yields (United States Drought Monitor). Therefore, drought variability and intensity, as demonstrated in this United States case study, can

result in different plant responses and adaptation resulting in lower grain yields. The Drought Monitor consists of 350 expert observers throughout the United States. Various calculations of drought are used to create the Drought Monitor Index (Palmer Drought Index, CPC Soil Moisture Model, USGS Weekly Streamflow, Standardized Precipitation Index (SPI), and blending of long-term and short-term drought indicator blends). Mountain streams and snow melt are difficult to predict and variable by nature and weighting of the data is common to accurately predict drought conditions.

Drought tolerance can be primarily attributed to maintaining and/or recreating the osmotic and ionic equilibrium of the plant cell. Osmotic adjustment is the accumulation of solutes that lower the osmotic potential of the cell thereby increasing water retention and providing turgor for cell expansion. Accumulation of osmolytes impact the water potential of the plant allowing for continued water uptake during a drought stress. Osmolyte accumulation manipulates the osmotic potential in the cell to become more positive thereby encouraging water update through the pressure potential. Osmolytes additionally interact in the cell through biochemical reactions and result in preventing membrane damage, protein degradation, and inactivation of important enzymes. This enables the plant to remain in cellular homeostasis and to repair damages created during the stress period. Specifically, maintaining homeostasis involves initiating a cascade of biochemical responses in a cell. This response activates drought-associated genes, molecular chaperones, osmolytes, and antioxidants to either confer drought tolerance or susceptibility (Zhu, 1998; Ishitani et al., 2000). Alternatively, plants can avoid drought damage through preventing tissue dehydration by reducing transpiration through stomatal closure, increasing water uptake (deep and extensive root system), or shedding leaves.

Another drought survival mechanism for plants is escape. Escape allows the plant to complete reproductive growth before the drought stress occurs, usually through a shortened life cycle.

One of the initial anatomical responses to a drought stress is stomatal closure, which minimizes water loss to maintain water pressure in the plant. However, stomatal closure decreases the amount of carbon dioxide assimilated into the plant. Decreased carbon dioxide assimilation negatively impacts yield (Schulze, 1986; Cornic, 2000). Stomata can either be metabolically regulated by abscisic acid (ABA) via hydroactive closure or non-metabolically regulated by evapotranspiration of water in the guard cells (Mansfield and Atkinson et al., 1990).

Plant hormones such as ABA, cytokinin, and ethylene play crucial roles in drought stress responses in a plant, especially in root-shoot signaling initiated by drying soils. Under drought conditions, the pH of xylem sap increases, encouraging the loading and transportation of ABA to the leaves thereby initiating stomatal closure (Wilkinson and Davies, 2002). Additionally, increased pH of the xylem sap increases cytokinin concentration leading to increased stomatal opening and decreased sensitivity to ABA. As will be discussed later, ABA and cytokinin are phytohormones that interact under drought conditions to initiate a specific plant response. Additionally, ethylene concentration increases under drought conditions, and this discourages leaf growth and initiates other signaling factors involved in a stress response.

Plants experiencing drought stress are genetically programmed to preserve elements of the photosynthetic chain. Stomatal closure and a slowed photosynthetic capacity under drought stress are due to declining Rubisco activity preservation

mechanisms (Bota et al., 2004). Declining rates of photosynthesis are related to the amount of carbon dioxide (CO_2) present in the environment. When in low concentrations, photosynthesis is impaired. In the cell, CO_2 deficiencies lead to the over-reduction of elements in the electron-transport chain, resulting in the formation of reactive oxygen species. The synthesis of reactive oxygen species can lead to photo-oxidation and cell death if the plant does not dispose of them in a timely manner.

Plants can respond to drought by manipulating the membrane fluidity of their cells through ion channels, aquaporins, and protein-lipid type interactions. Ultimately, these processes aid in maintaining the homeostasis of a plant by retaining turgor pressure in the cell during a drought stress.

1.3 Heat Stress Responses

Plants exhibit genetic variation for heat tolerance and susceptibility. At a certain thermal threshold, plant growth and development will become hindered, and if prolonged or increased, will result in plant death. Heat tolerance, defined as the plant's ability to maintain homeostasis and development under a high thermal temperatures, is of growing importance in agriculture as temperatures continue to increase worldwide (IPCC, 2007; Maplecroft Global Risk Analytics).

Symptoms of heat stress can present at different levels of a plants phenome. At a morphological level, heat stress presents as leaf firing, tassel blasting, and shoot and root growth inhibition. Both drought and heat stress can result in an extended anthesis-silking interval resulting in impaired grain fill.

Anatomically, heat stress presents as a reduction in cell size as well as increases in stomatal closure, trichomal and stomatal densities, and increased number of xylem

vessels (Banon et al., 2004). Additionally, heat stress damages mesophyll cells and results in greater fluidity of the plasma membrane (Zhang 2005). Lower photosynthetic capability is associated with structural changes and modification of the thylakoid membranes (Karim et al., 1997).

Photosynthetic capability is vulnerable under heat stress, primarily the elements within the thylakoid lamellae and carbon metabolism (Wise et al., 2004). Chlorophyll fluorescence has been successfully used to characterize heat tolerance and susceptibility of photosystem II (PSII) in several species (Lillo et al., 2004; Kadir et al., 2007; Moh'd I, 2010). Photosystem II is the most sensitive element of the photosynthetic chain, and susceptibility is determined by the turnover rate of the D1 subunit within the element.

Other measures of heat tolerance in a photosynthetic context are increased proportions of chlorophyll a:b and decreased proportions of chlorophyll:carotenoids. Chlorophyll a:b degradation is also more likely in younger, underdeveloped leaves compared to developed leaves (Karim et al., 1997).

Other elements of the photosynthetic chain can be adversely affected by heat stress. The Oxygen-Evolving Complex (OEC) can disassociate, resulting in an imbalance of electrons flowing from the OEC to the PSII acceptor side (Bukhov et al., 1999; De Ronde et al., 2004). Disassociation of the manganese (Mn)-stabilizing 33-kDa protein of PSII prompts release of Mn atoms resulting in impaired photosynthesis (Yamane et al., 1998).

Carbon metabolism through RuBP regeneration rates is altered during prolonged exposure to high temperatures. RuBP disruption cascades down through the electron transport chain, affecting the oxygen evolving enzymes of PSII, thus lowering

photosynthetic capacity (Crafts-Brander and Salvucci, 2004). Heat stress/shock can also lower the amount of photosynthetic pigments, soluble proteins, RuBP, and other associated enzymes and proteins. This highlights the role of heat-shock proteins and chaperones in providing protection against heat shock/stress which are discussed later in this chapter (Kepova et al., 2005). Sugar production enzymes, sucrose phosphate synthase, glucose pyrophoshoylase, and sucrose invertase, exhibit lower activity under heat stress (Chaitanya et al., 2001; Vu et al., 2001).

Cellular membrane stability under heat stress is critical to a plant's ability to maintain photosynthesis and respiration (Blum, 1988). High temperatures increase fluidity of the cellular membrane resulting in increased movement of molecules across the lipid bilayer. Membrane fluidity is further increased by the denaturing of membrane proteins and/or increased unsaturated fatty acids (Savchenko et al., 2002). As membrane and protein structures change, the permeability of the membrane is compromised, resulting in a loss of electrolytes and increased solute leakage. Furthermore, membrane stability is influenced by plant growth stage, development, and the ability to manipulate membrane fluidity (Karim et al., 1997, 1999). In some plants, lipid content and degree of lipid saturation are indicators of membrane stability or instability (Somerville and Browse, 1991).

1.4 Cold Stress Responses

Plants can withstand extremes in temperatures and are adapted for optimal production within a specific temperature range. Beyond a given threshold, temperatures are too low and will damage the plant (Lynch et al., 1990). Plants exhibit several

phenotypic presentations of cold stress, such as reduced leaf expansion, wilting, chlorosis, lower reproductive fitness, and necrosis (Wen et al., 2002).

At a molecular level, the cellular membrane is highly prone to damage during cold stress. The cellular membrane is composed of unsaturated and saturated fatty acids. Saturated fatty acids contain more hydrogen bonds as part of their structure and are a major influencer of membrane fluidity. Cold stress affects the transition state in which the cellular membrane switches from a semi-fluid state to a semi-crystalline state (Steponkus et al., 1993). The plant is more susceptible to cold stress in the crystalline state. Plants with a higher proportion of saturated fatty acids are more susceptible to cold stress because of a higher transition state temperature, which encourages the formation of ice (Mahajan, 2005). Ice formation begins in the apoplastic space and expands as unfrozen water from the cytoplasmic space migrates down the gradient into the apoplast. This creates a mechanical stress on the cell wall and plasma membrane leading to cellular damage and/or rupture (McKersie and Bowley, 1997; Olien and Smith, 1997; Uemura et al., 1997).

Cold stress begins at the anatomical level with the loss of cellular membrane integrity which is followed by cellular dehydration. It cascades into loss of compartmentalization, photosynthesis, protein synthesis, and other metabolic processes. Therefore, plants that are able to maintain cellular membrane stability in cold temperatures are more likely to survive.

Changes in calcium levels are the first physiological element of cold stress in which plants initiate a biochemical response (Monroy et al., 1995). Initially, a calcium increase occurs due to the influx of extracellular fluid containing calcium into the

apoplastic space. This influx induces cold stress genes like CRT/DRE that are controlled by COR6, KIN1 and Cas15 in alfalfa (Monroy and Dhindsa, 1995; Knight et al., 1996).

Several genes have been associated with cold stress tolerance in plants. FAD8 (fatty acid desaturase) in arabidopsis is involved in manipulating the cellular membrane lipid composition and fluidity (Gibson et al., 1994). Cold-stress induced genes can also include molecular chaperones for protein stabilization. In spinach, hsp70 (Anderson et al., 1994) and in Brassica napus, hsp90 (Krishna et al., 1994) are examples of cold-induced stabilization proteins. MAPK (mitogen-activated protein kinases) genes control and regulate expression of major stress cascades, initiating signal transduction and gene activation (Mizoguchi et al., 1993, 1996).

1.5 Salinity Stress Responses

High saline soils negatively impact 932 million hectares globally, and often times such soils are accompanied by heavy irrigation practices. Additionally, coastland flooding events deposit high salt concentrations after the water recedes (Wong et al., 2010). It is reasonable to assume that increased climate variability, with a likely greater incidence of flooding, will increase the prevalence of saline soils. This will lead to an accumulation of salts in arable land causing salt sensitive plants to become less productive. Accumulation of salt (Na^+) in the soil alters the soil texture and reduces porosity, leading to poor aeration and water conductance. Physiologically, saline and drought stresses have similar effects on plants. Both stresses create lower water potential making it difficult to uptake water and other nutrients from the soil (Manajan, 2005).

Salt stress prompts hypertonic and hyperosmotoic responses in plant cells. Disruption of the ionic equilibrium can occur when an influx of Na^+ dissipates the

cellular membrane potential causing an uptake of Cl^- down the chemical gradient. A high concentration of Na^+ can inhibit cellular expansion due to the osmotic imbalance. Na^+ is also toxic to cellular metabolism, as it specifically damages enzymes involved in photosynthesis and encourages the creation of reactive oxygen species.

Potassium (K^+) is essential to plants under saline stress. K^+ is needed for osmotic balance and the opening and closing of stomata. It also serves as a cofactor in enzymes such as pyruvate kinase. Signaling and maintenance of K^+ under saline stress can be an indicator of a positive plant response.

Calcium (Ca^{2+}) is a major signaling ion in many abiotic stresses, including salt stress. In high saline situations, Ca^{2+} increases in the apoplastic space as well as intracellular compartments (Knight et al., 1997). Thus when Ca^{2+} is present in high amounts, it initiates the biochemical signal cascade for a stress response.

Three salt stress genes have been identified and classified as SOS (salt overly sensitive) genes. SOS3 encodes a protein involved in Ca^{2+} binding, SOS2 encodes a protein kinase required for salt tolerance, and SOS1 encodes a putative Na+/K+ antiporter downstream of SOS2/SOS3 in the SOS pathway (Halfter et al., 2000; Ishitani et al., 2000; Lui et al., 2000; Qiu et al., 2002). This collection of genes contributes to saline stress tolerance in rice and other plants.

1.6 Flooding and Excess Water Stress Responses

Climate variability increases the chance of hydrological extremes in the form of excess rainfall and rising ocean levels that result in flooding of coastlands and poorly drained production fields. Agricultural production areas around the world are susceptible to excess water events during critical months of plant growth and development.

The most well-known breeding and genetics example of combating flooding stress is found in rice. Typically, rice does not tolerate more than one week of flooding. However, extreme flooding events can leave rice under water for two weeks or more. Recognizing this challenge, breeders at the International Rice Research Institute identified an ethylene-response-factor-like gene family conferring flooding tolerance. Within this gene family, three alleles were recognized to provide flooding tolerance: Sub1A, Sub1B, and Sub1C. Sub1A is considered the most valuable, as it overproduces ethylene upon submergence in flooding situations. Accumulation of ethylene results in dormancy of the rice variety, as cytokine-mediated senescence is slowed through an ethylene-cytokinin interaction (Xu et al., 2006). These breeding efforts have been successful agronomically. There is a 1-3 ton yield advantage of tolerant to susceptible varieties after 10 to 15 days of submergence. Flooding-tolerant commercial varieties of rice are currently grown in India as Swarna Sub1, in Bangladesh as Samba Mahsuri, and as IR64-Sub1 in the Philippines.

1.7 Stay-green and Senescence

Maize is most susceptible to drought stress during flowering as the plant is reaching peak water-use. Grain yields of maize are nearly double under optimal conditions compared to drought stress at flowering or grain-fill (Zhu, 2001). Water stress during the grain fill period leads to increased leaf senescence, loss of photosynthetic activity, reduction in dry matter accumulation, and reduction in yield from lower kernel weights (Ort and Baker, 2002; Xoing et al., 2002). Delaying leaf senescence, known as stay-green, under drought stress is associated with increased yields in both maize and sorghum (Borrell et al., 2000, Duvick, 2004)

Stay-green is the ability of an annual plant to delay senescence via an extended period of greenness and/or photosynthesis compared to a normal plant (Barry 2009; Thomas and Howarth 2000). Stay-green can be considered "functional" when photosynthesis and greenness are maintained throughout the grain filling period and "non-functional" when there is the loss of photosynthetic capacity. It is important to note that stay-green types are not associated with maturity or removal of reproductive organs (Crafts-Brandner et al., 1984).

Characterization of stay-green can be broken down into five different phenotypic and physiological manifestations based on the pattern of senescence. Types A and B stay-green are the most agronomically advantageous phenotypes. Type A stay-green extends from flowering until senescence at a peak photosynthetic capacity and chlorophyll content compared to a normally senscencing plant. Type B is characterized by a prolonged period of greenness resulting from high levels of chlorophyll content and photosynthetic capacity followed by a slower rate of senescence. Generally, these two phenotypes are correlated with increased yield under drought stress. Furthermore, types A and B are considered to be functional stay-green phenotypes. Type C stay-green occurs when chlorophyll pigments are retained throughout reproductive growth while photosynthetic capacity steadily decreases during senescence. Type D stay-green refers to plants harvested during a green stage of development. Types C and D are considered non-functional or visual stay-green types and have little agronomic value. Type E stay-green is manifested as an overabundance of chlorophyll where senescence is prolonged due to extended metabolization of chlorophyll pigments. The classification of stay-green

types mentioned above were first described and characterized by Thomas and Smart (1993; 2000).

Stay-green, as a form of delayed senescence, is part of a highly regulated process of nutrient remobilization resulting in the eventual programmed cell death of the plant. Senescence is age and time dependent and begins with the degradation of the chloroplast, which contains roughly 70% of the leaf protein. Photosynthetic capacity is lost during this senescence process. At a metabolic level, carbon assimilation is replaced by catabolism of chlorophyll and macromolecules such as proteins, membrane lipids, and RNA. The primary purpose of this catabolic process is the export of nutrients from the source to the sink. The process of senescence or delaying senescence is altruistic but contains some disadvantages. It is important for the fitness of the plant to remobilize nutrients to the sink for reproduction, but environmental factors can limit the yield for agronomic purposes (Lim et al., 2007). Thus, delaying leaf senescence during an abiotic stress can confer resistance but hinder agronomic value (del Rio et al., 1998).

There are numerous examples of the stay-green phenomenon, both functional and non-functional, in agronomic and horticultural systems. One of the most notable examples comes from Gregor Mendel's pea experiments. One of the traits examined by Mendel was pea seed color, where one genotype appeared green and the other yellow (Mendel, 1866). Recent analyses on this trait identified a relationship between senescence and chlorophyll degradation of the seed. Genetic characterization identified a gene, SGR, as a positive regulator of chlorophyll degradation (Darbishire 1911; Sato et al., 2007). SGR in rice is also involved in regulating chlorophyll catabolism via pheophorbide a oxygenase (PaO) regulation. This mechanism involves regular

remobilization of all proteins except the light-harvesting complexes (Jiang et al., 2007). SGR in rice is syntenous with the locus identified from Mendel's peas (Armstead et al., 2007). This follow-up study exhibits an example of a non-functional, visual form of stay-green.

The stay-green trait is observed in several crop species and has contributed to increased drought tolerance in pearl millet, barley, maize and most notably, sorghum. Extensive genetic characterization of stay-green in sorghum has revealed four to six major QTL explaining a majority of the phenotypic variation (Tuinstra et al., 1997; Crasta et al., 1999; Subudhi et al., 2000; Tao et al., 2000; Xu et al., 2000; Haussman et al., 2002; Harris et al., 2007). Stay-green sorghum genotypes under post-anthesis flowering drought stress maintain higher leaf nitrogen status as well as transpiration efficiency, which has translated to higher yield and lodging resistance (Borrell et al., 2000a, 2000b). Additionally, stay-green cultivars of sorghum have an increased resistance to charcoal rot (Rosenow et al., 1984). Furthermore, stay-green sorghum types have shown an increased amount of chlorophyll during anthesis, increased N content in the leaves, and increased leaf thickness. Thicker leaves are theorized to have more mesophyll cells and thus a higher capacity for photosynthesis. Stay-green sorghum Stg genotypes also exhibit reduced tillering resulting in increased lower leaf size, smaller upper leafs, and in some genotypes, less leaves per culm which all alter the canopy structure of the plant. By altering the canopy structure of sorghum under drought stress, stay-green genotypes are limiting pre-anthesis watering use thereby increasing water availability under grain-fill drought conditions (Borrell et al., 2014). Genetic characterization of sorghum suggests stay-green is inherited in both dominant and

additive manners (Walulu et al., 1994; van Oosterom et al., 1996). Furthermore, studies show increased senescence rates are partially dominant to slower senescence rates in sorghum (Walulu et al., 1994; van Oosterom et al., 1996).

There has been considerable discussion concerning nitrogen content and stay-green. Is stay-green a consequence of higher nitrogen content or is higher nitrogen content resulting in stay-green? Most likely, the answer is both. Higher nitrogen content in leaves could be indicative of a more expansive root system and/or a nitrogen balance between the sink and source controlling the greenness of the plant (van Oosterom et al., 2010). Both of these effects would manifest as delayed remobilization allowing for an extended period of delayed leaf senescence.

Genetic variation for stay-green in maize has been observed in inbred lines and hybrids and is commonly observed within elite United States breeding programs (Duvick et al., 2004). Identification of sources of stay-green for breeding has been limited to temperate adapted germplasm (Beavis et al., 1994; Coque et al., 2008; Zheng et al., 2009) but is beginning to be examined in an exotic and tropical context (Messmer et al., 2009). Previous studies suggest maize exhibits both dominant and additive modes of inheritance, similar to sorghum.

Other species have been examined for stay-green in both functional and non-functional forms in relation to drought such as wheat (Kirigwi et al., 2007; Kumari 2007, 2010; Bogard et al., 2011), barley (Diab et al., 2004; Tondelli et al., 2008) and rice (Campoux et al., 1995; Tripathy et al., 2000; Zhang et al., 2001; Diab et al., 2007).

Stay-green maize genotypes have exhibited similar genetic and physiological qualities as observed in sorghum. Stay-green genotypes in inbred and hybrid maize

combinations show an increase in stalk sucrose (Crafts-Brandner et al., 1984; Ceppi et al., 1987), higher nitrogen content in the leaves (Ma and Dwyer, 1998; Mi et al., 2003), increased Rubsico and PEC content in leaves (He et al., 2002; Martin et al., 2005), and increased PEPC activity and PNsat (He et al., 2002). Additionally, hybrids show increased nitrogen uptake in high and low nitrogen soil environments, but some stay-green types show equal or lower grain nitrogen content compared to wild type hybrids (Mi et al., 2003). Maize stay-green is associated with increased nitrogen uptake and the ability to be transferred into hybrid combinations through breeding (Swank et al., 1982; Crafts-Brandner et al., 1984; Crafts-Brandner and Poneleit, 1987; Ma and Dwyer, 1998; Bekavac et al., 2008). Examining alternate sources of genetic variation for stay-green will be critical for improving drought stress tolerance in maize.

An agronomic issue with stay-green hybrids in maize is dry-down. Certain genotypes have shown increased nitrogen uptake but lower nitrogen remobilization. This appears to be limited to environments with ample nitrogen supply (Subedhi and Ma, 2005). Therefore, plant breeders actively select appropriate stay-green genotypes to maximize drought-tolerance and optimize dry-down.

1.8 Premature Senescence by Pollination Inhibition

Maize senescence is a highly regulated process. In some maize genotypes, absence of ear fertilization initiates a hyper-senescence response in the plant. However, other genotypes do not display hyper-senescence responses. Conversely, they react by increasing the amount of photosynthates accumulated in the leaves and stalks (Crafts-Brandner et al., 1984; Duvick et al., 2004).

Crafts-Brandner et al. (1984) described a form of hyper-senescence associated with maize ear removal specific to B73. They observed a rapid, premature senescence 25 days post-anthesis beginning in the upper leaves of the maize plant descending downwards. When the ear was physically removed in B73xMo17 hybrids, a reddish discoloration occurred in plants with no ear, while alternate hybrids remained green throughout grain fill with the removal of the ear. Metabolomics data of B73xMo17 hybrid showed an accumulation of carbohydrates and a loss of nitrogen from the leaves occurring simultaneously with the cessation of nitrate uptake. Nitrogen flux was examined in a follow-up study by observing the leaf above the ear over a set period of days after anthesis. They observed a loss of nitrate reductase activity, reduced nitrogen, and lower carboxylating enzyme activity that appeared to be regulated during premature senescence. They concluded that the rate of nitrogen flux was regulating senescence but could not rule out effects of growth regulators or other metabolites as possible explanations of the phenotype. Due to the expression of this phenotype in hybrid combinations, it appears to be inherited as a dominant trait.

Sekhon et al. (2012) conducted a transcriptional and metabolic analysis of the observed premature senescence phenotype in B73. They observed an increase in free glucose and starch with a loss of chlorophyll in leaves 12 days after anthesis (DAA) from the highest ear-leaf. Whole plant transcriptional changes occurred with the presentation of the phenotype at 24 DAA, and transcriptional changes occurred in internodes at 30 DAA.

1.9 Root Structure and Morphology

Root development and expansion under abiotic stresses play a critical role in plant performance in challenging environments. Plants are dependent on the bulk flow of water and nutrients from the soil through the roots for growth and development. However, plants are limited in their ability to alter their root systems under abiotic stress conditions. Despite these limitations, they are able to expand the root zone deeper or wider to mine beneficial resources or increase the efficiency of absorption in the pre-existing root zone. Significant genetic variation exists for root traits in maize, but selection on these traits comes with a risk as there are negative implications for above ground structures when strongly selecting for root traits (Hochholdinger et al., 2004; Giuliani et al., 2005).

There are two strategies for expanding the root system, each with advantages and disadvantages for plants. Plants can extend their roots laterally to improve nutrient uptake, specifically phosphorus. While this can improve the stability of the plant, it comes at a consequence to primary root growth and depth. Primary growth tends to be the typical reaction of a drought stressed plant. In search of water and nitrogen at greater depth, the plant sacrifices lateral root growth.

1.10 Biochemical Elements Involved in Abiotic - Stress Signal and Reception

Crop mitigation of abiotic stresses, such as drought, heat, salt, and oxidative stress, are complicated biological processes involving many molecular, biochemical, and cellular elements. In general, biochemical signaling starts with a cellular receptor sensing the stress due to differences in calcium levels, metabolites, and cellular messengers associated with the stress. Additionally, secondary messengers such as inositol

phosphates, phytohormones, and reactive oxygen species modulate the calcium response and initiate other cascade responses. Secondary messengers often initiate and regulate protein phosphorylation pathways and transcription factors further down the signaling cascade. Various hormone responses regulate cascade events alongside previously mentioned secondary messengers. Ultimately, a stress response is elicited by the differential expression of 'stress-responsive' genes, antioxidants, and osmolytes leading to abiotic stress tolerance, growth repression, and/or plant death (Xoing et al., 2002).

1.10.1 Ion Channels

A primary signal of abiotic stress at the cellular level is an increase of calcium ions in the cell altering the electrochemical potential. Additionally, an efflux of calcium ions out of the cell through calcium ATPases and permeable calcium ion channels continues the initial signal reception (Sanders et al., 2002, Boudsocq and Sheen, 2010). Calcium ion channels can be activated in a variety of ways including hyper-polarization, depolarization, or ligand binding such as glutamate, inositol triphosphate (IP3), cyclic ADP ribose (cADPR), and cyclic nucleotide monophosphate (cNMPs) (White and Broadly et al., 2003; Hetherington et al., 2004; Boudsocq et al., 2010). Calcium ions interact with several proteins and enzymes, some of which are described below, at various stages in the cascade response. How a plant interacts with calcium and associated secondary messengers can influence the ability of the plant to mitigate an abiotic stress.

1.10.2 Histidine Kinases

Histidine kinases (HK) are at the first level of the cellular signal relay in an abiotic stress response. They primarily sense changes in the osmotic potential of the cell

(Xoing et al., 2002). The majority of HKs are membrane-bound, homodimeric proteins. They consist of amino-terminal periplasmic sensing domains coupled to a C-terminal cytoplasmic kinase domain. Throughout the HK family, the sensing domain is not as conserved as the kinase domain. Histidine kinases have conserved motifs designated as H, N, G1, F, and G2 boxes (Stock et al., 1989; Parkinson and Kofoid, 1992; West et al., 2001). HKs exist in a 'two component system' state, where the signal transduction is sensed by the kinase, and a subsequent phosphorylation event activates the response regulator (RR) protein. Specifically, the phosphorylation event occurs at His and Asp amino acid residues (West et al., 2001). Under an abiotic stress such as osmotic or water stress, increased amounts of calcium ions can be sensed by the HK domains, initiating the signaling cascade.

1.10.3 G-Protein Coupled Receptors

G-protein coupled receptors (GPCR) are transmembrane proteins that are located within the lipid bilayer of a plant cell. These proteins consist of seven transmembrane alpha-helices located throughout the extra- and intracellular spaces. The N-terminus is located in the extracellular space and the C-terminus in the intracellular space (Strasser et al., 2013). GPCRs undergo conformational changes during the transition from inactivation to activation in the cell (Kobilka and Deupi, 2007). They interact with G-protein heterodimers in the intracellular space (Oldham et al., 2006). This interaction initiates a conformational change in the protein thus beginning the signaling cascade due to the release of GDP and the binding of GTP to the ternary complex. Depending on the given G-protein interaction with the GPCR, the signal transduction changes the conformation of the protein and the subsequent response (Vauquelin et al., 2008; Strasser

et al., 2013). The conformational change in the GPCR begins the signaling cascade by phosphorylating target proteins downstream to respond to the corresponding physiological event (Strasser et al., 2013).

1.10.4 Receptor-like Kinases (RLK)

Receptor-like kinases (RLK) are a large gene family in plants involved in abiotic stress reception and signaling. They contain serine/threonine-like cytosolic domains that are similar to their animal counterpart receptor tyrosine kinases (RTKs) (Osakabe et al., 2013). Under drought stress, RECEPTOR-LIKE PROTEIN KINASE1 (RPK1), an LRR-RLK, is activated by ABA, high salt conditions, dehydration events, and/or low temperatures events (Osakabe et al., 2005). Proline-rich extension-like receptor kinases, a positive regulator of ABA, and calcium-mediated RLCK proteins are also activated during an abiotic stress and confer a positive regulator response (Bai et al., 2009; Yang et al., 2010). Some of these individual families are discussed at further lengths in other sections of this chapter, as they are involved in cascade responses past the initial signaling event. RLKs are diverse in both number and function; however, the main function of these proteins is the initial perception of an abiotic stress and proper signaling to initiate the cascade response through phosphorylation.

1.11 Biochemical Elements Involved in Abiotic Stress Signaling and Relay

1.11.1 Inositol Phosphates

Inositol phosphates (InsP) increase under abiotic stresses and regulate the release of calcium ions from intracellular stores (Schumaker et al., 1987; Morse et al., 1989; Gilroy et al., 1990; Perera et al., 1999; De Wald et al., 2001). While it is a complex biochemical process involving multiple InsP elements, this section will focus on InsP6,

which regulates the release of calcium and gene expression of plants under water stress. Previous literature suggested a larger role of InsP3 in response to an abiotic stress. Recently, InsP6 was shown to be the essential enzyme involved in water stress response and not InsP3. An increase in the phytohormone ABA results in an increase of InsP6 in the guard cells (Lemtiri-Chlieh et al., 2000; 2003). The ABA increase inhibits stomatal opening under stress while also encouraging closure. InsP6 is readily converted into compatible solutes and other molecular components that confer abiotic stress tolerance in these circumstances. InsP3 is readily converted to InsP6 in plants, where it is more potent in response to a stress (Lemtiri-Chlieh et al., 2000; 2003).

1.11.2 Phosphorprotein Cascades

1.11.2.1 Calcium-dependent Protein Kinases (CDPK)

There are various calcium sensitive enzymes and transcription factors that are induced during plant cell stress. Major molecular families of these calcium enzymes are calcium dependent protein kinases (CDPKs), calmodulins (CaMs), CaM-like proteins, and calcineurins B-like proteins. Asano et al. (2002) describe the composition of CPDKs as consisting of a "variable N-terminal domain, a protein kinase domain, an autoinhibitory region, and a calmodulin-like domain with EF hand Ca^{2+} binding sites." CDPKs are directly activated by the binding of Ca^{2+} to the calmodulin-like domain, and activated CDPKs further regulate downstream targets (Harper et al., 1991, 2004, 2005; Harmon et al., 2000; Cheng et al., 2002; Hrabak et al., 2003). CDPK location and variation is extensive throughout a cell and the plant kingdom.

CDPK3 and CDPK6 enzymes are positive regulators of stress signaling and in tandem with an ABA, regulate stomatal closure and opening. CDPK10 is involved in

calcium regulation and conferring drought tolerance in plants. Mutants of these kinases show an increased sensitivity to abiotic stresses and loss of interaction with ABA. CDPK4 and CDPK11 in arabidopsis participate in seedling processes involving ABA-related transcription factors (ABF1 and ABF4). Other CDPKs, 21, 23, and 32, are also involved in ABA signaling and abiotic stress responses in plants (Asano et al., 2012). CDPK4, 5, and 11 are implicated in abiotic stress tolerance by decreasing and regulating reactive oxygen species accumulation (Asano et al., 2012).

1.11.2.2 Salt Overly Sensitive (SOS)

Another class of signaling relay enzymes is the salt-overly sensitive (SOS) protein kinases that are involved in calcium sensing and signaling. Starting in the cytosol, a myristoylated calcium-binding protein, SOS3, receives the salt-elicited calcium signal and initiates the downstream responses. SOS3 then activates threonine/serine protein kinase SOS2. Together, SOS3 and SOS2 regulate SOS1, a calcium/hydrogen antiport. This antiport provides tolerance to abiotic stresses by controlling the cellular homeostasis through calcium/hydrogen ion exchange (Knight et al., 1997; Liu et al., 1998, 2004; Ishitani et al., 2000; Halfter et al., 2000; Shi et al., 2000, 2002; Qiu et al., 2002).

1.11.2.3 Mitogen Activated Protein Kinases

The mitogen activated protein kinases (MAPK) cascade from MAPKKK to MAPKK to MAPK are activated in abiotic stresses. These kinases are linked to various upstream receptors and downstream targets of signal transduction. MAPKs are thought to be convergence points in stress signaling. When a signal is detected, a variety of defense responses are possible ranging from programmed cell death, production of reactive oxygen species, synthesis of pathogen-related proteins/phytoalexins, and/or

transcriptional activation of abiotic stress related genes. SIMK (salt stress inducible MAPK) are activated in alfalfa under moderate hyperosmotic stress. SIPK (salicylic acid-induced kinase) is present in tobacco (Munnik et al., 2000). The complete picture of the MAPK cascade is still being determined.

As previously stated, dehydration of the cell can cause severe damage to a plant under drought stress. Early indicators of drought stress such as inositol 1,4,5-triphosphate (IP3), diacylglycerol (DAG), and phosphatidic acid (PA) are found in the phospholipid membrane. Studies have suggested that an increase in Ca^{+} ions under stress triggers the cascade of osmotic stress genes in the cell (Wu et al., 1997). Secondary messengers of osmotic stress in the plant such as phosphatidylinositol 4,5-bisphosphate (PIP2) are activated by hydrolysis with Phospholipase C (PLC), which creates IP3 and DAG. These compounds accumulate under osmotic stress in plants (De Wald et al., 1999). IP3s also increase in plants when ABA is added to guard cells (Lee et al., 1996; Xiong et al., 2001).

Phospholipase D (PLD) cleaves phospholipids, forming PA and free head groups, when a cell is osmotically stressed (Maarouf et al., 1999; Munnik et al., 2000). When the production of PLD is inhibited, plants exhibit a heightened tolerance to drought and an improved sensitivity to cold stresses. It is thought that the presence of PA, which is a product of PLD, might signal the closure of stomata under stress. PA would function similarly to ABA in this scenario (Jacob et al, 1999).

1.11.2.4 Protein Phosphatases

Protein kinases add a phosphate group to a substrate for activation of a cascade response. CDPK and MAPK are examples of this kind of enzyme. Conversely, protein

phosphatases remove a phosphate. These two enzyme groups are antagonistic yet both have important functions in abiotic stress response regulation. There are three protein phosphatase families that are involved in plant abiotic stress responses: protein phosphatase P (PPP), protein phosphatase M (PPM) and protein tyrosine phosphatase (PTP) (Chae et al., 2010).

Protein phosphatases P are divided into two groups, PP1 and PP2, based on their dependence for divalent cations. PP2 is divided into three subclasses: PP2A (independent of divalent cations), PP2B (requires calcium) and PP2C (requires magnesium). PP2C can also fall into the PPM class and consist of serine/threonine complexes. In some species, PP2C regulates MAPK signaling (Luan, 2003).

In abiotic stress responses, PP2C-type phosphatases are involved in ABA signaling and interactions. Two different phosphatases interact with ABI1 and ABI2 as negative regulators of ABA signaling pathways (Rodriguez et al., 1998; Sheen, 1998; Gosti et al., 1999; Merlot et al., 2001). Mutants of ABI1 and ABI2 showed an inhibition of the ABA signaling pathway, which presented as lack of stomatal regulation, impaired seed dormancy/germination, and increased drought stress response. ABI1 and ABI2 are active only in the phosphorylated form, and thus the loss of phosphatase leaves these genes without regulation.

1.11.3 Transcription Factors

1.11.3.1 EREBP/AP2

Ethylene responsive element binding proteins (EREBP) and APETLA2 transcription factors are found exclusively in plants. They interact with DREB1 and DREB2 proteins in abiotic stress responses. DREB (dehydration response element

binding) proteins are transcription factors involved abiotic stress tolerance. DREBs are ABA independent signal factors (Agarwal et al., 2006). The interaction of these transcription factors are involved in activating LEA-like and rd29A proteins. DRE cis-acting elements are directly involved in the activation of these subsequent proteins (Liu et al., 2000).

1.11.3.2 bZip Transcription Factors

Basic leucine zippers (bZips) are ABA induced DNA-binding factors that interact with ABA-responsive promoter elements (ABRE). RD29A and DRE elements can both be activated via ABA-dependent and independent pathways (Uno et al., 2000). ABRE elements interact with bZips in a cis-acting manner and are ABA-dependent (Huang et al., 2012).

1.11.3.3 Zinc Fingers

Zinc fingers are molecular elements that contain cysteine and histidine motifs that form localized peptide structures for the encoded function. These elements are thought to regulate reactive oxygen species scavenger mechanisms involved in abiotic stress response (Fujita et al., 2006). The zinc finger ZAT12 is involved in the repression of ascorbate peroxidase 1 (APX1), which increases the production of the reactive oxygen species, hydrogen peroxide, during abiotic stress. There are several examples of different zinc fingers that are involved in activating specific genes for an abiotic stress response in plants. Arabidopsis: Zat12 – Oxidative (Davletova et al., 2005), Cys2/His2 – Drought, cold, and high salinity (Sakamoto et al., 2004), Zat7 - Oxidative (Chen et al., 2002), Rice: OSISAP1 – Cold, dehydration, and salt stress in transgenic tobacco (Mukhopadhyay et al., 2004), DST – Drought and salt (Huang et al., 2009).

1.11.4 Reactive Oxygen Species

Reactive oxygen species are vital secondary messengers of an abiotic stress response that are oxidatively or osmotically created. Reactive oxygen species are primarily generated in the chloroplasts, peroxisomes, and mitochondria and have relationships and interactions with several plant metabolic pathways. Antioxidants, which will be discussed later, are the antagonists of reactive oxygen species and facilitate the removal of reactive oxygen species from the plant. Detrimental effects of reactive oxygen species include plant death due to oxidative stress damage and programmed cell death.

The onset of abiotic stresses affects the ability of plants to assimilate carbon dioxide. During low rates of carbon dioxide assimilation and high light intensity, the electron transport chain becomes over-reduced, leading to the inactivation of photosystem II (PSII). Photochemical quenching occurs for PSII as the protein passes electrons over to acceptors within the chloroplasts. This process creates free oxygen radicals (O_2^-) and subsequent reactive oxygen species of H_2O_2, OH^+, and $^1O_2$ (Hideg et al., 2002; Ort et al., 2002; Gill et al., 2010).

Superoxide radicals (O_2^-) are generated during photosynthesis in the chloroplasts through the partial reduction of oxygen molecules. Primarily, this process occurs in the thylakoid membrane-bound primary electron acceptor of photosystem I. From O_2^-, additional reactive oxygen species can be generated. One such example is OH^-, which can cause the perioxidation of the membrane lipids resulting in cellular weakening and possible cell death. If the O_2^- were to undergo protonation, a strong oxidizing agent HO_2 is created and leads to stress damage on cell membrane surfaces (Elstner, 1987; Gill et

al., 2010). Finally, the free oxygen radical can interact with Fe^{3+} and donate an electron to create Fe^{2+}. This reduced molecule undergoes a Haber-Weiss reaction for the formation of an iron-hydrogen peroxide complex. The iron hydrogen peroxide molecule undergoes the Fenton Reaction resulting in the detrimental free radicals OH^{+} and $^{1}O_{2}$.

Hydroxyl radicals (OH·) are considered to be the most potent reactive oxygen species in plants and in the presence of transitional metals, have the greatest potential for detrimental effects on plants. In the presence of a transitional metal, hydrogen peroxide and oxygen radicals generate hydroxyl radicals and create oxygen toxicity under neutral pH and ambient temperatures. These molecules can damage organic molecules and cellular structures and must be eliminated by the plant to avert cell and plant death (Vranová et al., 2002; Gill et al., 2010).

While plants are programed to detoxify reactive oxygen species that are produced during abiotic stresses, prolonged exposure can break down and damage photosynthetic elements. Chloroplast membranes and the plasma membrane are specifically sensitive to reactive oxygen species damage (oxidation stress). Reactive oxygen species can cause peroxidation, de-esterification of membrane lipids, protein degradation and mutations (Bowler et al., 1992). Cellular dehydration causes increased protein-protein interactions and toxic increases of solute concentrations leading to enzyme degradation. If the stress is relieved, detoxifying elements such as glutathione reductase and ascorbate peroxidase are expressed in high concentrations and can counteract the effects of photo-oxidation.

1.11.5 Antioxidants

Antioxidants are involved in the relief of oxidative stress created by drought, salt, ozone, and extreme temperatures. These stresses in combination with high light intensity

are ideal environments for the creation of reactive oxygen species. Reactive oxygen species were discussed earlier in this chapter and are detrimental to the growth and development of plants.

In general, antioxidants are metabolites and enzymes that are involved in the relief of reactive oxygen species from the plant either by removing or breaking down the adverse element. Several different transgenes in a variety of plants have been shown to increase antioxidant production leading to the removal of reactive oxygen species thereby providing evidence of the importance of these antioxidants for stress tolerance. When SOD, APX, MnSOD, CuZnSOD and CAT are overexpressed in transgenic constructs, thereby increasing the amount of antioxidants, tolerance is conferred. Some of these proteins are valuable under the stress but have a negative effect on yield under no stress (Allen, 1995; Van Breusegem et al., 1999; Wang et al., 1999, 2005; Lee et al., 2007).

Other enzymes that generated antioxidant production are glutathione-S-transferase (GST), dehydroascorbate reductase (DHAR), and monodehydroascorbate reductase (MDAR), where the latter two are part of the ascobate-glutathione pathway. Increased expression of DHAR and MDAR correlates to an increased production of ascorbic acid (vitamin C), a highly efficient antioxidant. GST, when overproduced, increases expression of SOD and CAR genes for oxidative stress relief (Eltayeb et al., 2006, 2007; Zhao and Zhang, 2006).

The final antioxidant class discussed in this section are polyamines (PA) molecules. These molecules are involved in increased activation of nucleic acids synthesis and confer oxidative stress tolerance. S-adenosylmethionine decarboxylase (SAMDC) is an enzyme critical in the production of PA and over-expression of SAMDC

results in increased tolerance to osmotic, cold, and oxidative stresses. APX, MnSOD, and GST, which have been previously discussed, have higher levels of expression in plants that overexpress PA (Walden et al., 1997; Ye et al., 1997; Wi et al., 2006).

1.12 Stress-Responsive Genes and Compatible Solutes

1.12.1 LEA-like Proteins

The exact functions of LEA proteins are unknown. However, evidence suggests they are integral, hydrophilic proteins that are involved in hydration buffering, serving as an ion sink and water replacement molecule, and protein renaturing for a variety of abiotic stresses (Wise and Tunnacliffe, 2004). Phytohormones, ABA and ethylene, are also implicated in the activation of LEA-proteins (Gechev et al., 2006).

LEA protein homologs are the largest class of genes involved in cold tolerance and are present in late embryogenesis, prior to seed desiccation, and seedling response to dehydration (Close, 1996; Ingram and Bartels, 1996; Xu et al., 1996). Many of these proteins are hydrophilic and simple in amino acid composition. Examples of these genes and their components are COR, HOS1, ICE, and associated CBF genes, which are all involved in cold tolerance and acclimation. Esk1 genotypes express excess free proline as a cryoprotectant, which serves as a form of negative regulation (Xin, 1998).

1.12.2 Heat-shock Proteins

Heat-shock proteins (HSP) are expressed at various stages of plant development in rapid response to heat stress. There are three different classes of heat shock proteins based on their molecular weight: HSP90, HSP70, and 15-30kDa. The accumulations of HSPs are dependent on the stage of development and type of plant (Wahid, 2007). Small

HSPs are found localized in specific cellular compartments and each corresponds to a specific six nuclear gene family (Waters et al., 1996).

Generally speaking, HSPs are responsible for prevention of protein denaturation and aggregation under high temperatures and are quickly activated to protect and insulate proteins within the chloroplast and/or mitochondria (Schoffl et al., 1999; Iba, 2002). Small HSPs assemble into heat-shock granules (HSGs) in the cytoplasm to protect biosynthetic machinery (Miroshnichenko et al., 2005). The ability for HSGs to form and disperse under constant heat stress correlates to plant survival.

HSP68 (HSP70 kDa class) is located in the mitochondria and is expressed at a higher rate under heat stress in several plants including maize and soybean (Neumann, et al., 1993). HSP101 (HSP 90 kDa class) is located in the nucleus as a campylobacter invasion antigen protein. It functions as a renaturation promoter under heat stress and is expressed at a higher rate in reproductive tissue than in vegetative tissue (Young et al., 2001). In maize, 64 and 73 kDa HSPs (HSP 70kDa class) accumulate quickly under heat stress in male pollen (Dupius and Dumas, 1990), and a 45-kDa HSP (Small HSP class protein) in maize correlates to heat stress recovery (Ristic and Cass, 1992). HSP70 assists in protein translation and translocation, proteolysis, protein folding/chaperoning, suppression of aggregation, and reactivation of denatured proteins (Zhang et al., 2005). Iba et al. hypothesizes that HSP70 participates in ATP-dependent protein unfolding or assembly/disassembly reactions and prevents protein denaturation during heat stress (Iba, 2002). HSP21 (Small HSP class protein) in tomato is linked to protecting photosystem II from oxidative damage and fruit storage at low temperatures (Neta-Sharir et al., 2005).

1.12.3 Osmolytes

Production of osmolytes can have advantages and disadvantages in plants undergoing abiotic stress. They can provide protection from reactive oxygen species during a stress, but when/if the stress is relieved; they can inhibit plant growth and development. Protection is provided by stabilizing protein structures, maintaining osmotic equilibrium, or removing reactive oxygen species from the cell (Zhu, 2001). Osmotic equilibrium and solute protection is critical for tolerance to water deficits and drought conditions. Under drought conditions, the osmotic equilibrium is readjusted towards a decrease in water and an increase in solute concentration from osmolytes.

Raffinose and galactinol are examples of osmoprotectents that are produced under drought stress. They do not adjust the osmotic balance in the cell. Mannitol is a sugar produced to scavenge and remove reactive oxygen species and hydroxyl radicals from the cell. It can also provide protection and stabilization of proteins under drought stress. When drought stress occurs, osmoprotectents form hydrogen bonds with specific proteins. This prevents the formation of intramolecular hydrogen bonds that can permanently damage a protein under drought stress. Trehalose is a non-reducing glucose disaccharide that also has stabilization functions for proteins under stress. Specifically, trehalose allows for continued photosynthesis by protecting photosystem II from photooxidation (Bohnert et al., 2000; Wahid et al., 2007).

1.12.4 Glycine Betaine and Proline

The osmolyte glycine-betaine, formed in a two-step oxidation pathway of choline, is synthesized by plants in response to abiotic stresses. Salt tolerance is conferred in plants that express the N-methyl transferase enzymes that are in the glycine-betaine

pathway that act to adjust osmotic balance. This is achieved by limiting the amount of Na^+ in the cell by the plasma membrane Na^+/H^+ antiporter, sequestering Na^+ ions in the plant vacuoles, and accumulating solutes, amino acids and glycine betaine (Wahid et al., 2007).

Proline is an additional compatible osmolyte involved in osmotic adjustment of plants under stress (Rhodes et al., 1999, 2002). Plants overexpressing proline exhibit increased water use efficiency in tobacco and accumulate in the leaves and nodules of alfalfa under drought stress (Irigoyen et al., 1992; Pospisilova et al., 2011). However, proline is metabolically costly to the plant due to its high molecular weight and is hard for the plant to transport (Irigoyen et al., 1992).

Plants with high levels of glycine betaine and proline in high temperature situations confer heat tolerance in arabidopsis (Sakamoto et al., 2002; Kishor et al., 2005). Glycine betaine and proline, in higher concentrations, buffer cellular redox potential under heat stress (Wahid et al., 2007).

1.12.5 Carotenoids and Anthocyanins

Carotenoids are actively involved in abiotic stress tolerance, specifically heat stress. They serve as photoprotectants from the xanthophyll pathway, specifically zeaxanthin. Zeaxanthin is hydrophobic and localizes in the periphery of the light-harvesting complexes to prevent peroxidative damages from reactive oxygen species to the membrane lipids (Horton, 2002). Other lipid membrane protectants from the carotenoid pathway are terpnoids (tetraterpenoids) such as 40C-isoprene and α-tocopherol (Havaux, 1998). These photoprotectant elements allow for membrane

stability by lowering susceptibility to lipid peroxidation and decreasing the fluidity of the membrane under heat stress (Havaux, 1998).

Anthocyanins are secondary metabolites involved in stress responses. Low levels of anthocyanin concentration in plants result in membrane instability and increased fluidity. Alternatively, when expressed in high amounts, anthocyanins confer stability (Wahid and Ghazanfar, 2006). Anthocyanins may contribute to reduced leaf osmotic potential. Lower leaf osmotic potential increases water uptake and reduces transcriptional losses under heat. This allows the plant to adapt quickly to changing environmental conditions (Chalker-Scott, 2002).

1.13 Plant Hormones and Abiotic Stresses

1.13.1 ABA

Under water stress, ABA is rapidly produced and controls plant responses through changes in gene regulation and expression. Additionally, ABA needs to be degraded promptly upon alleviation of the stress to allow the plant to return to normal metabolism and homeostasis (Zhang et al., 2006). Transcription factors ZEP, AAO, and NCED are upregulated under drought and salt stresses, which elicits an ABA response. ABA receptors induce the expression of ABA response genes. Physiologically, ABA encourages plant stomatal closure and prevents opening to inhibit the effects of photooxidation (Zhang et al., 2006). ABA has been discussed at length in several sections of this chapter.

1.13.2 Salicylic Acid

Salicylic acid (SA) is a phytohormone involved in stabilization of heat shock transcription factors, allowing them to bind to heat shock proteins and related genes. SA

confers long term tolerance as calcium ion homeostasis and antioxidant systems are in full effect. A derivative of SA, sulfo-salicylic acid (SSA), is involved in the removal of reactive oxygen species thereby conferring heat tolerance (Shi et al., 2006). Methyl salicylate (MeSA) functions as a signaling molecule for antioxidant related elements (Llusia et al., 2005).

1.13.3 Ethylene

Ethylene is involved in several stages of plant growth and development in normal and abiotic stress situations. ACC synthase is the precursory enzyme involved in the synthesis of ethylene. Under a drought stress, ACC activity is increased and corresponds to an increase in ethylene production (Apelbaum and Yang, 1981). Additionally, solar radiation can affect the amount of ACC present in the plant (Munne-Bosch et al., 2002). To confirm the relationship between ethylene and ACC, two ACC synthase enzymes were knocked out of the maize inbred B73. Ethylene synthesis in these plants decreased. An additional ACC synthase mutant, Zmac6, grown under drought situations showed increase stomatal conductance, transpiration, and carbon dioxide assimilation (Young et al., 2004). These studies suggested that ethylene is involved in regulating leaf physiology under drought conditions. Ethylene also appears to have a role in regulating senescence in arabidopsis, where ethylene sensing knockout mutant etr1-1 showed delayed senescence compared to wild-type plants (Grbic and Bleeker, 1995).

1.13.4 Cytokinin

Cytokinin and its precursor molecules are well-studied hormones involved in abiotic stress responses and plant senescence. Furthermore, stay-green genotypes exhibited excess amounts of cytokinin (He et al., 2005). Additionally, cytokinin

signaling increases nitrogen availability from the roots to the leaves in maize (Igarashi et al., 2009). In transgenic maize, cytokinin synthesizing genes, behind an enhanced promoter, displayed a Type A form of stay-green (Robson et al., 2004).

1.13.5 Auxin

Auxin is involved in many aspects of a plant's growth and development. In association with ABA, auxin can regulate the water status of a plant (Mansfield and McAinsh, 1995). Under certain concentrations and environmental conditions, auxin can aid in regulating the closure and opening of stomata, while ABA controls the stomatal aperture (Snaith and Mansfield 1982; Lohse and Hedrich 1992; Grabov and Blatt 1998; Tanaka et al., 2006). Additionally, waterflow/water-loss can be regulated by auxin (Albacete et al., 2008).

1.13.6 Hormone Cross-Talk in Abiotic Stress Conditions

Plant hormones are complex compounds that individually impact the response of a plant under abiotic stress (Peleg et al., 2011). However, interactions between these hormones increase the complexity of plant responses. For example, lateral root differentiation appears to be initiated by ethylene, which leads to a buildup of auxin in the pericycle followed by formation of lateral root primordial. Continuing with this model, cytokinin is predicted to deregulate lateral root differentiation and control gravitropism. Under drought conditions, ABA increases primary root growth. Thus, at least four hormones are involved in root development in plants in an abiotic stress.

Auxin production in transgenic arabidopsis enhanced the expression of LEA genes. However, ethylene appears to be regulating genes related to auxin synthesis, perception, and signaling (Zhang et al., 2009). The following auxin gene families are

proposed to be involved in this relationship with ethylene: auxin-responsive factors, auxin transporters, and auxin biosynthesis (Li et al., 2004, 2006; Stepanova et al., 2005, 2008; Růžička et al., 2007). Additionally, ethylene synthesis appears to be regulated by auxin. 1-amino-cyclopropane-1-carboxylate synthase (ACS) genes are rate-limiting enzymes involved in ethylene biosynthesis and also appear to be regulated by auxin (Tsuchisaka et al., 2004). Cytokinins are regulators of auxin biosynthesis where a homeostatic feedback loop exists between the two hormones to regulate root and shoot growth (Tsuchisaka et al., 2004). Each signaling group acts to maintain an appropriate concentration of the other in developing roots and shoots.

ABA is a major player by itself in regulating plant responses to abiotic stresses, primarily through governance of stomatal opening and closing. Furthermore, ABA interacts with several other hormones during abiotic stresses. Other plant hormones such as cytokinin, ethylene, brassinosteroids, jasomonic acid, salicylic acid, and nitric oxide are all involved to some degree with stomatal function. Nitric oxide interacts with ABA to regulate stomatal opening and closure as an intermediate in an ABA-mediating pathway. ABA and cytokinin interact under drought and senescence conditions in tobacco. Cytokinin synthesis was associated with gene expression in general hormone activity. Additional interactions between different hormones are brassinosteroids and cytokinin individually, brassinosteroids and cytokinins via protein phosphatase 2c, ABA and brassinosteroids under abiotic stresses, and cytokinins and brassinosteroids both indirectly and directly with ABA (Ribeiro et al., 2009; Lopez-Raez et al., 2010; Rivero et al., 2010; Peleg et al., 2011).

1.14 Conclusion

Climate variability and ensuing abiotic stress events will continue to challenge the ability of plants to adapt to adverse environments. Plants must maximize available resources and optimize biochemical responses to overcome drought, temperature, and flooding stresses and the resulting oxidative and osmotic implications. Thus far, plant breeders have been successful in engineering climate resilient crops for multiple locations and stresses. However, implementation of new technologies and selection criteria will be critical to enabling development of even higher yielding and more tolerant varieties. Because of this, plant breeders must be multifaceted in their approach to climate variability. Breeders must utilize transgenic and conventional traits in combination with genomic selection and advanced marker-assisted selection to maximize resources for product development.

The following chapters in this dissertation will discuss stay-green and sink-inhibition phenotypes in maize and sorghum. Objectively, this research sought to dissect the stay-green and sink-inhibition traits using multiple diverse populations of maize and powerful forms of association mapping. In chapter two, phenotypic characterization of three maize populations and association mapping were combined in an effort to identify potential causative gene(s) regulating the phenotypic expression of stay-green. In chapter three, data from stay-green in maize was leveraged in sorghum to examine the genomic relationships between these crop species. In chapter four, association mapping was conducted in the Nested Association Mapping Panel of maize in an effort to identify causative genes involved in premature senescence via sink-inhibition. All together, these

data provide a substantial contribution to the scientific community working to understand and develop climate resilient crops.

CHAPTER 2. GENETIC REGULATION OF STAY-GREEN IN MAIZE

2.1 Abstract

Climate variability will continue to challenge researchers and plant breeders in efforts to increase yield. Stay-green is an advantageous trait for plant breeders to exploit for yield gains under drought stress. In this study, we characterized three diverse populations of maize for stay-green under stress conditions and identified several gene families that appear to be specifically coordinated under drought stress. Specifically, calcium signaling and relay, phytohormone, general stress and transcription factors, vesicular transportation, sugar transportation, secondary messengers, and cell wall structure gene families are associated with the expression of stay-green. We report specific candidate genes, primarily related to ethylene and pectin formation that are implicated in two or more populations. Further genetic and molecular characterization of specific candidate genes as well as agronomic evaluation are needed to confirm the yield and stress advantages of specific stay-green genotypes. Once established, specific alleles and donor lines can be deployed into private and public sector breeding programs to enhance the ability of elite germplasm to mitigate drought stress. Additionally, a substantial contribution to understanding drought-stress responses in plants can be made building from these data. Finally, leveraging genomic information from maize stay-green

into other cereal species provides an avenue to further characterize and understand drought adaptation using comparative genomics.

2.2 Introduction

Agriculture and food production are highly vulnerable to climate variability. Past experiences in the United States such as the Dust Bowl of the 1930s and the 2012 drought have encouraged plant scientists to develop new technologies and practices to meet the challenges of stable food production and sustainable farming practices. Plant breeders have successfully met this challenge, most notable in the work of Dr. Norman Borlaug, by leveraging native genetic diversity of a crop into elite germplasm to combat a specific abiotic or biotic stress. It is important to note that these scientific improvements were accompanied by improved management and cultural practices in the target production area.

Climate variability is forecasted to increase the prevalence of abiotic and biotic stresses in food production areas (IPCC, 2007). The United States is expected to experience increased climate variability and potentially has the resources to successfully mitigate ensuing negative effects. However, underdeveloped countries, where food production is already difficult, are expected to take the brunt of negative climate effects.

In light of these challenges, plant breeders are being called to continue developing climate resilient crops. This will require introducing new biotechnology and statistical methods, agricultural management practices, and native genetic variation to begin what some have called the Second Green Revolution or the Blue Revolution (Renaud et al., 2013).

Maize is a global staple crop and is consequently grown in areas exposed to increased climate variability primarily drought and heat. Worldwide, maize is grown on over 177 million hectares producing over 872 million tonnes of grain (FAOSTAT, 2012). Additionally, maize exhibits exceptional genetic variation, which plant breeders are exploiting for crop improvement (Chia et al., 2012). Plant breeders across the world have access to both temperate and tropical sources of germplasm that can be implemented in crop improvement. However, it is critical that breeders identify potential yield components for crops under abiotic stress in lieu of breeding for a complex trait like yield. Additionally, breeders require genetic variation for successful genetic gain in production. Sorghum breeders have increased yield through indirect selection for stay-green under drought conditions (Borrell et al., 2000). Stay-green is a potential trait for maize drought tolerance breeding programs.

Stay-green is the ability of an annual crop species to delay senescence or "stay-green" throughout the grain filling period under stress and maintain or increase yield. Plant breeders desire functional stay-green where both chlorophyll content and photosynthetic activity are active and maintained under abiotic stress. Plant breeders anticipate that the maintenance of chlorophyll content and photosynthesis correlates to an increase in yield potential from the synthesis of additional photosynthates (Thomas and Howarth, 2000). Sorghum breeders have shown that several positive physiological and agronomic characteristics are associated with stay-green genotypes, such as increased yield and resistance to stalk lodging (Rosenow, 1984; Borrell et al., 2000). Additionally, genetic mapping suggests the trait is controlled by four to six major genetic loci and potentially smaller effect loci contributing in an additive nature (Crasta et al., 1999;

Subudhi et al., 2000; Tao et al., 2000; Xu et al., 2000; Kebede et al., 2001; Haussmann et al., 2002; Srinvias et al., 2009).

United States' maize breeding programs have utilized stay-green in inbred and hybrid development in both normal and stressful environments (Duvick et al., 2004). However, characterization of stay-green in maize has been limited to temperate sources of germplasm, and utilizing additional sources of genetic variation will be critical to improve yield under stressful situations (Duvick et al., 2004).

The Nested Association Mapping (NAM) panel and the AMES Diversity Panel are excellent sources of genetic variation and can be used to study genetic linkage (Yu et al., 2006; Romay et al., 2013). The NAM population consists of 25 founder lines that, when individually crossed to B73, to create 25 recombinant inbred families consisting of 200 individuals each. Thus the entire population is 5000 recombinant inbred lines (RILs) that have an anchor in the reference genome, B73. This population encompasses ~57% of the genetic diversity of maize (Romay et al., 2013). The population structure of the NAM allows for joint-linkage mapping of recent recombinations across all inbred families as well as a form of association mapping maximizing the ancestral recombinations of the diverse founder lines. This population has been successfully characterized for several traits in maize such as flowering time, flower and leaf architecture, and leaf diseases (Buckler et al, 2009; Tian et al., 2011, Poland et al., 2011, Kump et al., 2011; Cook et al., 2012). Genotypic data is publically available for linkage mapping with 1106 SNPs with 10cM resolution. HapMapv2 representing millions of SNPs is available for association mapping (www.panzea.org).

The AMES diversity panel represents an even larger source of genetic diversity (Romay et al., 2013). Consisting of all germplasm available in the North Central Regional Plant Introduction Station in Ames, Iowa, this population represents a broad swathe of the temperate maize germplasm and is a strong sample of tropical and exotic germplasm. This population is represented genotypically by almost one million GBS SNPs (www.panzea.org).

The goal of this study is to identify QTL and SNP-associations for stay-green in multiple populations of maize. Additionally, we expect this study to provide a platform for examining comparative genome relationships of stay-green alleles for drought in sorghum. Our hypothesis for this study is that stay-green alleles are present in multiple populations of maize representing a large portion of the genetic variation for the trait.

2.3 Materials and Methods

2.3.1 Genetic Materials and Experimental Design

2.3.1.1 Population One – Nested Association Mapping (NAM) Panel

PHZ51 Testcrosses

A subset of the NAM population was grown for testcross hybrid production. Lines with flowering dates similar to B73 (+/- 7 days) were testcrossed with the ex-PVP inbred PHZ51, a Pioneer HiBred Oh7B-Midland type pollinator (Mikel and Dudley, 2006). RILs from twenty-two of the twenty-five NAM families were selected for testcrossing (P39, IL14H, and Hp301 were excluded). Families selected were equally represented and the experimental population consisted of 1241 NAM testcross hybrids.

Field trials of the NAM testcrosses were grown in four environments in 2010: Sandhills, NC; Slater, IA; Columbia, MO; and West Lafayette, IN. Two-row plots were

used in each experiment. For each environment, an augmented block design (Federer 1961, 1975) was used with B73 and the founder inbreds included for replication within sub-blocks. The NAM testcrosses were nested by RIL family and were randomly added in the overall augmented design. Some environments split the experiment into different fields. Best linear unbiased estimators (BLUEs) were calculated across environment using ASReml (ASReml 3.0, VSN International).

2.3.1.2 Population Two – Nested Association Mapping (NAM) Panel RILs

We evaluated 1295 NAM RILs representing twenty-four of the twenty-five NAM families excluding Hp301 in 2012 and 2013. Evaluations occurred in West Lafayette, IN with two replications each year. RILs were selected from the entries used for the testcross experiment with flowering times similar to B73. Lines were planted as single-row plots 3.81m in length with 0.76m alleys between ranges and 0.76m spacing between the rows. A randomized complete block field design was used in the experiment with RILs randomized within their respective families and families randomized across the replications. Best linear unbiased estimators (BLUEs) were calculated across years and within years for spatial correction using ASReml.

2.3.1.3 Population Three – AMES Diversity Panel

The AMES Diversity Panel consists of 2813 inbreds representing a large portion of the known genetic diversity of maize. A subset of this population (n=2424) was tested in 2012 and 2013 in West Lafayette using an augmented design (Federer 1961, 1975). Genotypes were grouped into blocks based on their relative maturity in Indiana. There were six maturity groups consisting of ~400 individuals each. Lines were planted as single-row plots 3.81m in length with 0.76m alleys between ranges and 0.76m spacing

between the rows. B73 was used as a field check in both years. In 2012, P39, Mo17, B97, NC258, Mo18W, CML247, and in 2013, PHJ40, Mo17, PHG35, PHG39, CML247, DK3IH6, were used as maturity checks for each experiment.

2.3.2 Phenotypic Evaluation of Stay-green

Stay-green was measured using a ratio vegetation index (RVI) using a Chlorophyll Content Meter (CCM-200, Opti-Sciences, Inc.) that measures the ratio of transmitted light at 660nm and 940nm. Four plants from each plot were measured on the leaf above the ear-leaf, midway between the leaf tip and collar and between the midrib and leaf edge. A whole plot score was calculated as the mean of the four measurements. Testcrosses were measured in each environment at approximately 1250 growing degree days (GDDs) after the average silking date of the entire population. RILs and AMES individuals were measured twice, once at anthesis and then at approximately 1050 GDDs after the average flowering date of a given family in the NAM and on an individual inbred basis in the AMES. Families in the NAM and individuals in the AMES were measured at anthesis when half of the observed lines in the family were flowering. GDDs were calculated using Method 2 from McMaster and Wilhelm (McMaster and Wilhelm, 1997).

Four different phenotypic measurements were calculated for analysis (Table 2-1).

Table 2-1 Stay-green phenotypes collected for the NAM RILs, NAM testcrosses, and AMES Diversity Panel

Stay-green Phenotype	Population	Measurement Time Points	Calculation
Anthesis (Referred to as Stay-green Anthesis)	NAM RILs	Flowering	RVI Flowering
	AMES	Flowering	RVI Flowering
Terminal (Referred to as Stay-green Terminal)	NAM RILs	1050GDDs	RVI 1050GDDs
	AMES	1050GDDs	RVI 1050GDDs
	NAM Testcrosses	1250GDDs	RVI 1250GDDs
Difference (Referred to as Stay-green Difference)	NAM RILs	Flowering and 1050GDDs	(RVI Flowering - RVI 1050GDDs)
	AMES	Flowering and 1050GDDs	(RVI Flowering - RVI 1050GDDs)
Ratio (Referred to as Stay-green Ratio)	NAM RILs	Flowering and 1050GDDs	(RVI Flowering - RVI 1050GDDs)/ RVI Flowering
	AMES	Flowering and 1050GDDs	(RVI Flowering - RVI 1050GDDs)/ RVI Flowering

2.3.3 General Weather Information

The NAM testcrosses were planted on different dates in 2010 at four locations: May 27th in Columbia, Missouri, April 21st in Sandhills, North Carolina, May 6th in West Lafayette, Indiana, and April 22nd in Slater, Iowa. On a temperature basis, Iowa experienced its 10th warmest year of 116 years; Missouri experienced its 3rd warmest year; North Carolina and Indiana experienced the warmest year between the months of April to September. In terms of accumulated precipitation during the same time window, Iowa had its 115th wettest period, Indiana its 60th, North Carolina its 41st, and Missouri is 107th. At the beginning of the growing season, North Carolina was experiencing drought conditions (D1) based on the United States Drought Monitor (http://droughtmonitor.unl.edu). However, by the end of May, none of the testing locations were under any form of drought. This situation persisted throughout the rest of the growing season (Drought information - United States Drought Monitor; Weather information - NOAA).

The NAM RILs were planted on May 6, 2012 and May 20, 2013. The AMES population was planted on May 14, 2012 and May 20, 2013. During the growing season from April to September, Indiana experienced its 10th warmest year in 118 years in 2012 and 64th warmest year in 119 years in 2013. Indiana had its 15th driest year on record in 2012 and its 85th driest year in 2013. According to the Drought Monitor, West Lafayette started the growing season in 2012 in a D1 drought situation. By the end of May, the drought progressed into a D2 status and this condition persisted throughout June. By the end of July, West Lafayette had deteriorated into a D3 drought. However, by the end of August, the drought status slightly improved to a D2 state. In 2013, the effects of the

2012 drought were no longer present and West Lafayette started the season in a non-drought condition. This condition persisted through the end of July; however, West Lafayette was on the verge of a D1 drought status by the end of August.

2.3.4 Genotypic Information

2.3.4.1 Populations One and Two

Joint-linkage mapping was conducted using a genetic map with 1 cM resolution, based on GBS v2.3 SNPs available at www.panzea.org. For association mapping, HapMapV2 SNPs (Chia et al., 2012) were projected onto the NAM RILs based on linkage information. HapMap V2 consists of random-sheared, paired-end Illumina GAII reads from 103 maize inbreds, teosinte, and landraces with 4-30x coverage. Overall, 55+ million SNPs and indels were generated for genetic analyses. For each SNP, its values for a RIL were assigned based on the SNP value of the RIL parents and on the genotype of the flanking NAM markers in that RIL.

2.3.4.2 Population Three

Genotypic analysis of the AMES population consisted of genotype-by-sequencing SNPs aligned to B73 and distributed throughout the genome. The entire collection of GBS 2.7 SNPs is around one million individual markers (www.panzea.org). However, based in the minor allele frequency distribution within this subset, ~370,000 SNPs were used in the evaluation of stay-green phenotypes. Differing amounts of SNPs were used in each model depending on the phenotype based on the number of genotypes evaluated and quality control filtering.

2.3.5 Statistical Analyses

2.3.5.1 Spatial Analysis for Best Linear Unbiased Estimators

Best Linear Unbiased Estimators (BLUE)s were calculated to account for year and field effects using a weighted multivariate mixed model in ASReml (ASReml 3.0, VSN International). Within the model, the effects of blocks, rows, ranges, replications, and number of observations per plot were fit to identify the best model as appropriate. Additionally, first-order autoregressive for range and row were included as needed in the populations for a phenotype. When appropriate, likelihood ratio tests or Akaike's Bayesian Information Criteria for the random effects or the F-tests for the fixed effects were used to identify which factors were significant in the model for a given phenotype and thus were retained in the model. When statistical comparison between different models were not possible, the best model was chosen based on the highest significance for the variety F-test and the lowest pairwise variety mean comparison standard error. A combined mixed model across years was fitted for the NAM and AMES populations and across locations for the NAM testcrosses.

2.3.5.2 Heritability Calculations

Heritabilities were calculated on a plot and mean basis for all populations (Hung et al., 2011). Plot-based heritabilities were calculated for NAM populations, both RILs and testcrosses, using the following general equation which was modified to correctly account for the number of families, individuals, and environments used in each population:

$$h^2_p = \frac{\sigma^2_{family} + \frac{1}{26}\sum_{p=1}^{26}\sigma^2_{RIL(family)p}}{\sigma^2_{family} + \frac{1}{26}\sum_{p=1}^{26}\sigma^2_{RIL(family)p} + \sigma^2_{env*RIL(family)} + \sigma^2_{\epsilon}}$$

Line-mean heritabilities were calculated for the AMES population using an equation described by Cullis et al. (2006) shown below which was modified to correctly account for the number of families, individuals, and environments used in each population:

$$h^2_c = 1 - \frac{V_{PPE}}{2\left(\sigma^2_{family} + \sigma^2_{RIL*family}\right)}$$

VPPE (genetic variance) is the average prediction error variance for all possible pairwise comparisons which includes the checks, obtained directly from the ASReml prediction output.

Line-mean heritabilities were calculated for the NAM RILS, testcrosses, and AMES population using the following equation which was modified to correctly account for the number of families, individuals, and environment used in each population.

$$h^2_l = \frac{\sigma^2_{family} + \frac{1}{26}\sum_{p=1}^{26}\sigma^2_{RIL(family)p}}{\sigma^2_{family} + \frac{1}{26}\sum_{p=1}^{26}\sigma^2_{RIL(family)p} + \frac{\sigma^2_{env*RIL(family)}}{n_{env(l)}} + \frac{\sigma^2_{\epsilon}}{n_{plot}}}$$

Harmonic means were used to account for unbalanced data in the experiment. n_{envl} is the harmonic mean of the number of environments in which each RIL was observed and n_{plot} is the harmonic mean of the total number of plots in which each RIL was observed. For equations h^2_l and h^2_p, heritability equations were calculated based on the model selection for an individual trait. Each heritability calculation was specific to the field and location of each experiment. Heritabilities are reported in the results section in Table 2-2.

2.3.5.3 Joint-linkage Stepwise Regression (NAM Linkage Analysis)

QTL identification utilized a joint stepwise regression model described by Buckler et al. (2009) for mapping flowering time traits in the NAM populations. This method combines all NAM families evaluated to test for QTL associated with a given trait. To account for variation associated with maturity, the residual of the model below was used to obtain covariate value for days to anthesis (DTA):

$$y = b_0 + b_1 \times DTA + \varepsilon$$

y is the BLUE of the stay-green trait. DTA is the statistical covariate. b_0 is the intercept estimate and b_1 is the slope estimate. ε is the residual.

Backward stepwise selection in Tassel 4 (Bradbury et al., 2007) was used to determine which markers would be selected or removed from the model. Permutation analysis to determine the p-value threshold was conducted by permuting RVI values for a phenotype 1000 times. The lowest p-values of a single marker scan were collected after each permutation and a threshold p-value was determined at an experimental α of 0.05.

QTL were identified using a genome-wide joint linkage scan where significant markers from the stepwise regression were used as covariates in the model when analyzing family and marker within family as fixed effects. The joint-linkage protocol removed covariates in the model when a marker was within 10cM of the original covariate markers. QTL intervals were determined using a 0.01 confidence interval.

2.3.5.4 Genome-wide SNP Association (NAM Populations)

We used the statistical power of the NAM to leverage both the ancestral recombination events from the diversity of the founders and the linkage of individual recombinant inbred populations to conduct genome-wide association for stay-green.

Using HapMapV2 SNPs, we obtained SNPs projected onto the RIL progeny using linkage marker information and pedigree knowledge which is described in detail in section 2.3.4.

The protocol used for the GWAS followed the one proposed by Tian et al. (2012). For the first step, individual chromosome residuals for each trait were calculated from a model where the population term and all significant markers from the joint-linkage analysis in the other chromosomes were fitted against the mapping trait. Later, those residuals were used as phenotypes and fit into 100 stepwise linear models using a bootstrapping resampling protocol. A test statistic, bootstrap posterior probability (BPP or RMIP), was calculated corresponding to how many times a SNP was deemed significant out of the 100 total runs. Each of these 100 model runs were analyzed using 80% of the genotypes randomly subsampled from the population.

2.3.5.5 Genome-wide SNP Association (AMES Panel)

Genome-wide associations were performed for all stay-green phenotypes using a subset of the individuals from North Central Regional Plant Introduction Station in Ames, Iowa. As in the previous population, residuals from the regression model where the trait was the response variable and days to anthesis was the covariate were used as mapping traits to account for possible spurious associations with maturity. SNPs were tested using a mixed linear model without compression implemented in the GAPIT R package (Lipka et al., 2012). Population structure (Q) was accounted by including the first three principal components as covariates. A kinship matrix calculated following VanRaden (2008) was used to account for relationships between individuals. Both PC and kinship were calculated using a random sample of 10% of the SNPs from a dataset

where SNPs with two alleles and at least 20 individuals homozygous for the minor allele were kept (369,362 SNPs). For the GWAS, only those markers with MAF >10% were tested (229,460 SNPs).

2.3.5.6 Linkage Disequilibrium Analysis

Linkage disequilibrium (LD) was examined using TASSEL 5.0 and published NAM and AMES GBS SNPs (www.panzea.org). R-squared and p-values were generated using this software. LD was examined 20kb in each direction of the SNP association for an individual population. From the NAM population, linkage disequilibrium was examined using the NAM HapMapV2 SNPs available at www.panzea.org. In the AMES panel, linkage disequilibrium was examined using a subset of the AMES GBS SNPs specific to the lines tested in the stay-green experiment and is also available online at www.panzea.org.

2.4 Results

2.4.1 Stay-green Heritabilities

Significant genetic variation was detected for all stay-green phenotypes (Appendix B – ASReml Output; Appendix C – Phenotypic Distribution of Stay-green Phenotypes). Heritabilities were calculated for all stay-green phenotypes and flowering phenotypes on a line-means basis and a plot basis depending on the population. Reasonable heritabilities were detected in the NAM populations as flowering time phenotypes exhibited high values and stay-green phenotypes were generally lower. The AMES diversity panel exhibited lower heritabilities for stay-green and flowering traits. The breadth of maturity in the AMES panel introduces substantial variation in the dataset

making heritability calculations and assessment difficult for flowering and stay-green traits. Heritabilities for all populations and phenotypes are recorded in Table 2-2.

Table 2-2 Heritabilities for flowering and stay-green phenotypes in three diverse maize populations. Plot and line-means heritabilities were calculated for the respective populations.

NAM RILs	Days to Anthesis	Days to Silking	Stay-green Anthesis	Stay-green Terminal	Stay-green Difference	Stay-green Ratio
Plot-Basis (Hung et al.)	0.848	0.816	0.263	0.224	0.104	0.116
Line-Means Basis (Cullis et al.)	0.947	0.936	0.548	0.483	0.274	0.308
NAM Testcrosses	Days to Anthesis			Stay-green Terminal		
Plot-Basis (Hung et al.)	0.933			0.360		
AMES	Days to Anthesis	Days to Silking	Stay-green Anthesis	Stay-green Terminal	Stay-green Difference	Stay-green Ratio
Plot-Basis (Hung et al.)	0.445	0.519	0.307	0.249	0.125	0.157
Line-Means Basis (Hung et al.)	0.486	0.560	0.361	0.310	0.018	0.195
Line-Means Basis (Cullis et al.)	0.493	0.561	0.620	0.357	0.159	0.216

2.4.2 Stay-green Phenotype Correlations

2.4.2.1 NAM RILs

The flowering traits Days to Silking and Anthesis were highly correlated as expected (0.93136, p = <0.0001). All stay-green phenotypes were negatively correlated with days to silking and anthesis except for stay-green ratio. Stay-green ratio was correlated with days to anthesis but not to silking. Stay-green at anthesis was positively correlated to all stay-green traits except stay-green ratio. Stay-green terminal was correlated with all other traits. Stay-green difference and ratio were positively correlated with one another (Table 2-3).

2.4.2.2 NAM Testcrosses

Only two traits were examined in the NAM testcrosses: stay-green terminal and days to anthesis. These two traits were significantly correlated with an R-squared value of 0.4515 (p= <0.0001).

2.4.2.3 AMES Panel

As in the NAM RILs, the flowering traits were highly correlated in the AMES panel. All stay-green phenotypes, except stay-green ratio, were negatively and significantly correlated with flowering traits. Stay-green ratio was not significantly correlated to the flowering traits. Stay-green at anthesis was significantly correlated to stay-green terminal and difference but not correlated to stay-green ratio. Stay-green terminal was significantly correlated to both stay-green difference and ratio, while difference and ratio themselves were highly correlated (Table 2-4).

Table 2-3 Phenotypic correlations of stay-green phenotypes and flowering traits in the NAM RILs

	Days to Anthesis	Days to Silking	Stay-green Anthesis	Stay-green Terminal	Stay-green Difference	Stay-green Ratio
Days to Anthesis						
Days to Silking	0.93136 <.0001					
Stay-green Anthesis	-0.17638 <.0001	-0.18681 <.0001				
Stay-green Terminal	-0.12695 <.0001	-0.14205 <.0001	0.56096 <.0001			
Stay-green Difference	-0.06046 0.0229	-0.05039 0.0578	0.32332 <.0001	-0.59159 <.0001		
Stay-green Ratio	0.00573 0.8295	0.01823 0.4927	0.03279 0.2172	-0.78006 <.0001	0.92566 <.0001	

Table 2-4 Phenotypic correlations of stay-green phenotypes and flowering traits in the AMES Diversity Panel

	Days to Anthesis	Days to Silking	Stay-green Anthesis	Stay-green Terminal	Stay-green Difference	Stay-green Ratio
Days to Anthesis						
Days to Silking	0.96864 <.0001					
Stay-green Anthesis	-0.22902 <.0001	-0.22188 <.0001				
Stay-green Terminal	-0.05556 0.0039	-0.10145 <.0001	0.41632 <.0001			
Stay-green Difference	-0.09725 <.0001	-0.05223 0.0071	0.39236 <.0001	-0.67296 <.0001		
Stay-green Ratio	-0.03698 0.0566	0.01338 0.491	-0.00677 0.7273	-0.87397 <.0001	0.87865 <.0001	

2.4.3 Linkage and Association Mapping Results

2.4.3.1 Population One – NAM RILs

2.4.3.1.1 Stay-green Anthesis

The stay-green anthesis phenotype exhibited significant variation and was normally distributed. Values for RVI at anthesis were as low as 15.25 and as high as 80.5. Significant genetic variation was associated with this trait ($P = <0.001$, $F = 5.25$). Joint-linkage analysis was conducted to identify QTL for stay-green anthesis. Permutation analysis indicated a QTL significance threshold value of 6.1x10-5. Using this threshold, joint-linkage analysis using days-to-anthesis as a covariate identified five QTLs for stay-green anthesis. QTLs were identified on chromosome 1, 2, 3, and 5 and explained 35.24% of the phenotypic variation associated with the trait (Figure 2-1).

NAM GWAS was conducted to identify SNP associations for stay-green anthesis. 88 SNP associations were detected with RMIP >4 (Figure 2-1). Candidate genes were identified in a genomic interval of 20,000 bp flanking each significant SNP. We report annotated genes for stay-green at anthesis in Table 2-5 in the discussion section of this chapter.

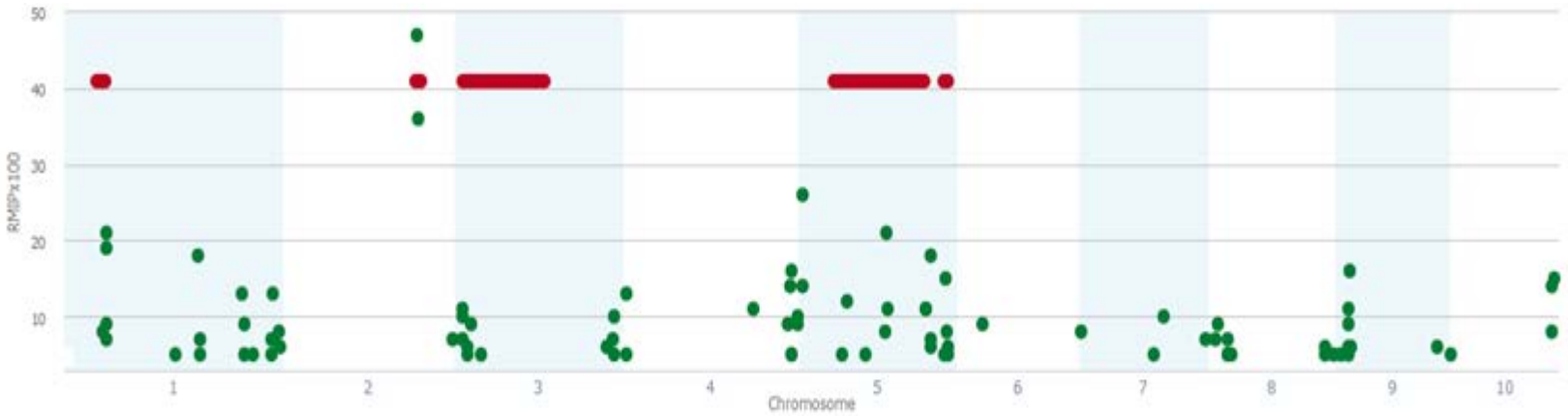

Figure 2-1 Manhattan plot for stay-green anthesis in the NAM RILs. QTL detected by joint-linkage analysis are shown as red bars. SNP associations with stay-green anthesis with a RMIP > 4 are shown as green dots.

2.4.3.1.2 Stay-green Terminal

Stay-green terminal phenotype was not normally distributed. Due to the nature of stay-green and maturity, there was a peak in low RVI values due to senescence of ~70 individuals. The frequency distribution indicated values for this trait as low as 0 and as high as 84.25. The use of the residuals of the trait against days to anthesis highly reduced this problem and normalized the distribution. Significant genetic variation was associated with this trait ($P = <0.001$, $F = 7.24$).

The QTL threshold value for the stay-green terminal phenotype was defined by permutation analysis as 8.1x10-5. Joint linkage analysis identified four QTLs for the stay-green terminal phenotype. QTLs were identified on chromosome 3, 4, 6, and 9 and explained 42.6% of the phenotypic variation associated with the trait (Figure 2-2).

NAM GWAS for the stay-green terminal phenotype identified 70 SNP associations with RMIP >4 (Figure 2-2). Candidate genes were identified in a genomic interval of 20,000 bp flanking significant SNPs. We report annotated genes for stay-green terminal in Table 2-6 in the discussion section of this chapter.

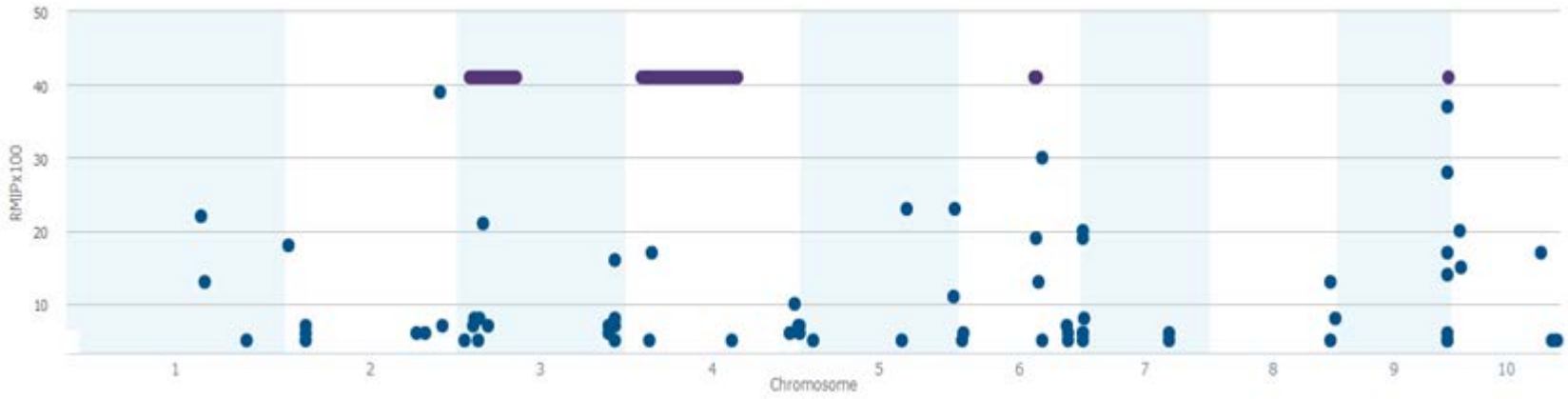

Figure 2-2 Manhattan plot for stay-green terminal in the NAM RILs. QTL detected by joint-linkage analysis are shown as purple bars. SNP associations with stay-green terminal with a RMIP > 4 are shown as blue dots.

2.4.3.1.3 Stay-green Difference

Stay-green difference phenotype was normally distributed and values ranged as low as -25.9, an indicator of increased greenness of a genotype during grain fill, and as high as 63. Significant genetic variation was associated with this trait ($P = <0.001$, $F = 6.8$).

The QTL threshold value for stay-green difference was defined by permutation analysis as 6.2x10-5. Using this threshold, joint linkage analysis identified three QTLs for stay-green difference using days-to-anthesis as a covariate in the model. QTLs were identified on chromosome 1, 3, and 5 and explained 35.3% of the phenotypic variation associated with the trait (Figure 2-3).

NAM GWAS for stay-green difference identified 57 SNP associations with RMIP >4 (Figure 2-3). Candidate genes were identified in a genomic interval of 20,000 bp flanking the each significant SNP. We report annotated genes for stay-green difference in Table 2-8 in the discussion section of this chapter.

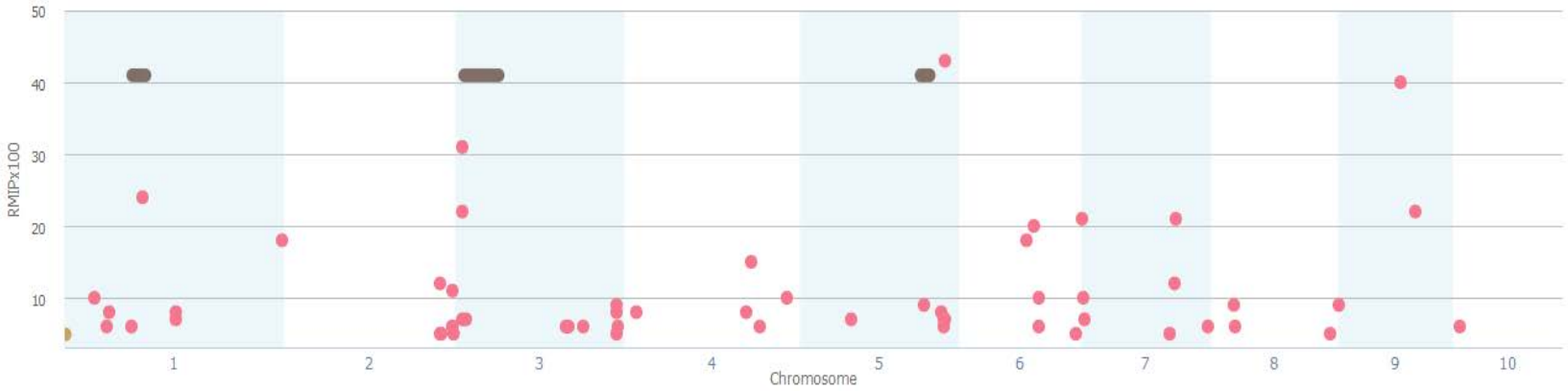

Figure 2-3 Manhattan plot for stay-green difference in the NAM RILs. QTL detected by joint-linkage analysis are shown as grey bars. SNP associations with stay-green difference with a RMIP > 4 are shown as pink dots.

2.4.3.1.4 Stay-green Ratio

Stay-green ratio exhibited normally distributed data with values as low as -1.839 and as high as 1. Significant genetic variation was associated with this trait (P = <0.001, F = 9.48). The QTL threshold value for stay-green difference was defined by permutation analysis as 5.7x10-5. Using this threshold, joint linkage analysis identified two QTLs for stay-green ratio using days-to-anthesis as a covariate in the model. QTLs were identified on chromosomes 1 and 3 and explained 35.8% of the phenotypic variation associated with the trait (Figure 2-4).

NAM GWAS for stay-green ratio identified 60 SNP associations with RMIP >4 (Figure 2-4). Candidate genes were identified in a genomic interval of 20,000 bp flanking the significant SNPs. We report annotated genes for stay-green ratio in Table 2-9 in the discussion section of this chapter.

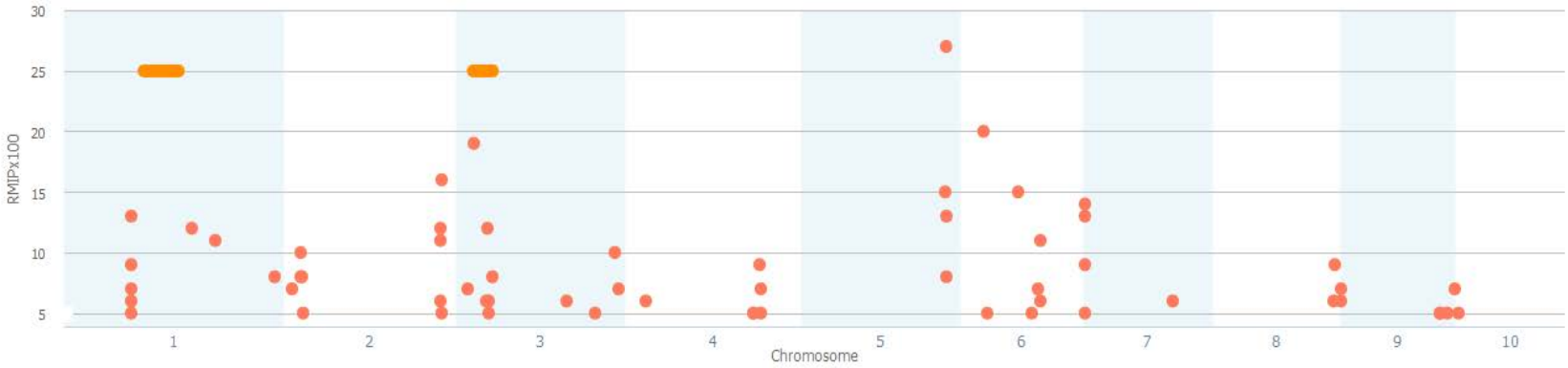

Figure 2-4 Manhattan plot for stay-green ratio in the NAM RILs. QTL detected by joint-linkage analysis are shown as orange bars. SNP associations with stay-green difference with a RMIP > 4 are shown as salmon dots.

2.4.3.2 Population Two – NAM Testcrosses

Stay-green terminal values in the NAM Testcrosses were normally distributed and were as low as -6.96 RVI (negative value due to BLUEs correction) and as high as 38.8. Significant genetic variation was associated with this trait (P = <0.001, F = 29.9). Joint-linkage analysis for stay-green terminal identified a single QTL on chromosome 2 explaining 35.3% of the phenotypic variation associated with the trait using a p-value threshold of $5.5x10^{-5}$ (Figure 2-5). NAM GWAS for stay-green ratio identified 37 SNP associations using a RMIP > 4 (Figure 2-5). Candidate genes were identified in a genomic interval of 20,000 bp flanking the significant SNP. We report annotated genes for stay-green terminal in Table 2-9 in the discussion section of this chapter.

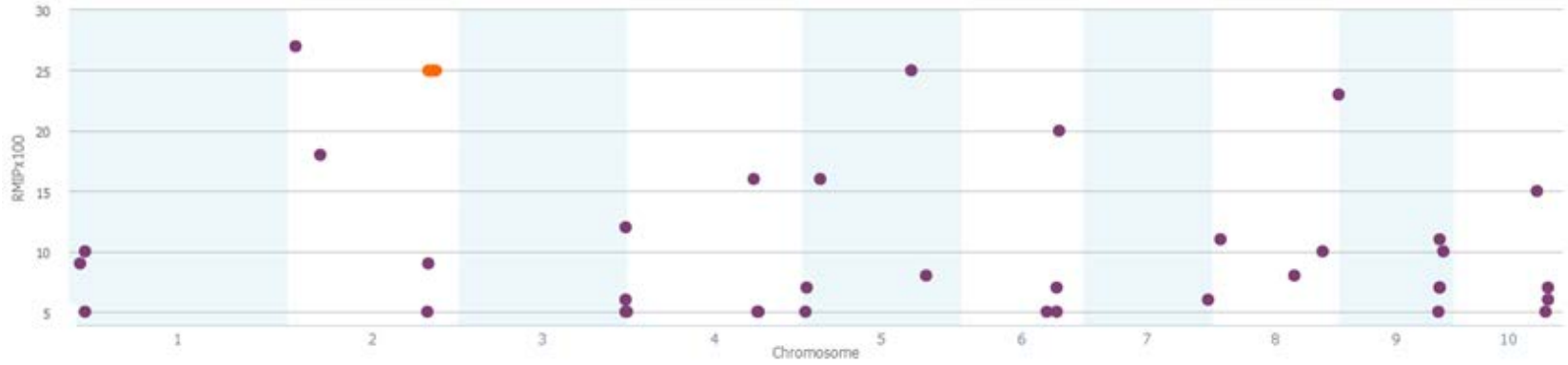

Figure 2-5 Manhattan plot for stay-green terminal in the NAM testcrosses. QTL detected by joint-linkage analysis are shown as orange bars. SNP associations with stay-green difference with a RMIP > 4 are shown as purple dots.

2.4.3.3 Population Three – AMES Panel

No significant marker associations were detected for the four stay-green phenotypes measured in the AMES in either combined or individual year analysis after false-discovery rate (FDR) correction.

We arbitrarily chose to further analyze the top fifty most significant SNPs for each trait to test for coincidence in the NAM RILs and NAM testcrosses according to the highest p-value prior to FDR correction. However, since none of these SNPs were significant after FDR correction, we were skeptical of any associations that did not collocate with the NAM RILs, testcrosses, or known sorghum stay-green positions (Chapter 3). We report the positions of AMES SNPs in Figures 2-6 to 2-9.

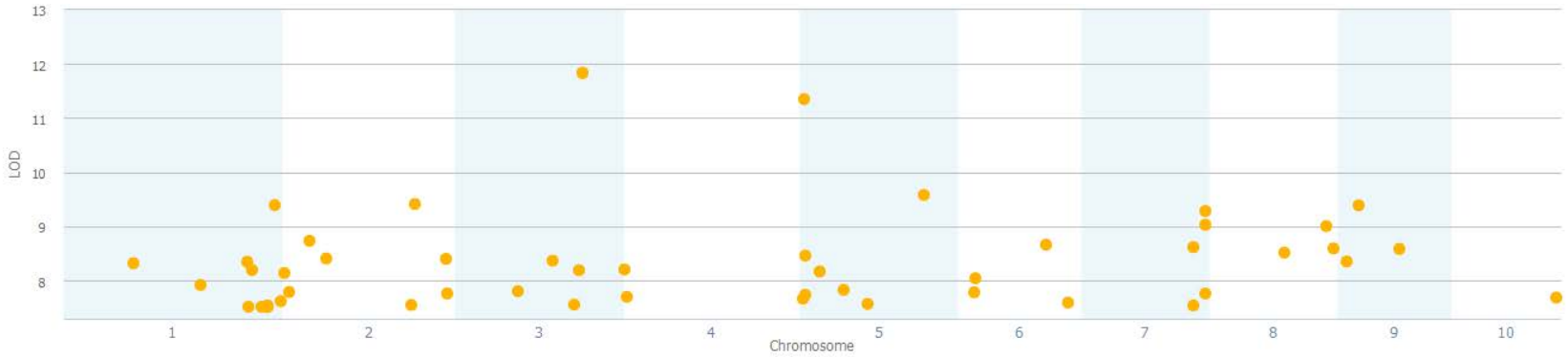

Figure 2-6 Manhattan plot from the GWAS of stay-green anthesis in the AMES Panel. SNPs (yellow dots) are reported as LODs converted from p-values before FDR correction. The top fifty most significant SNPs were selected for further characterization.

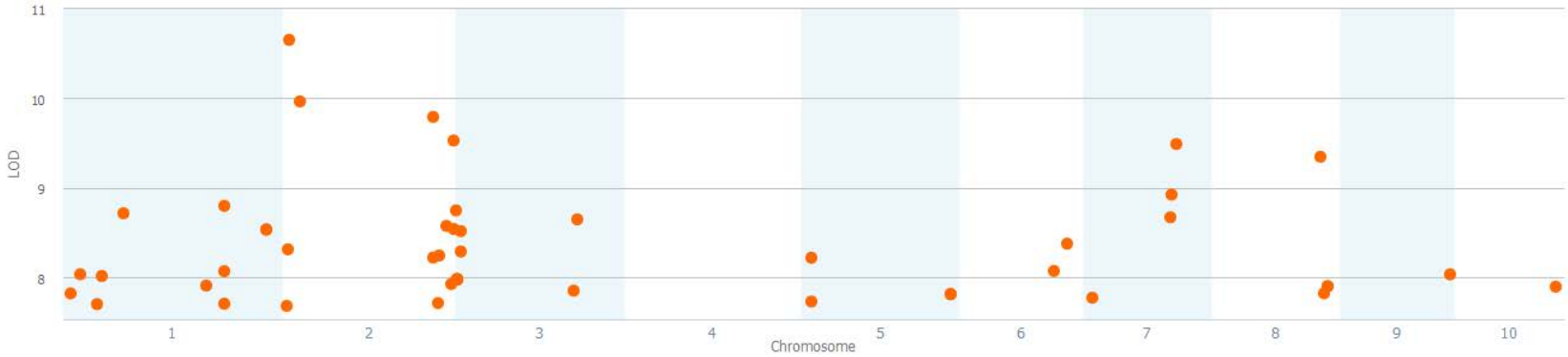

Figure 2-7 Manhattan plot from the GWAS of stay-green terminal in the AMES Panel. SNPs (orange dots) are reported as LODs converted from p-values before FDR correction. The top fifty most significant SNPs were selected for further characterization.

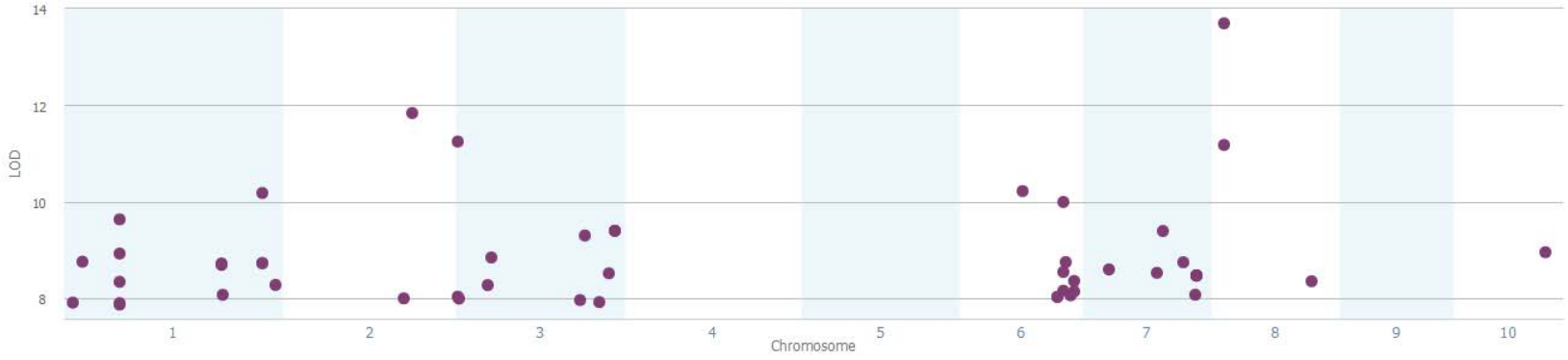

Figure 2-8 Manhattan plot from the GWAS of stay-green difference in the AMES Panel. SNPs (purple dots are reported as LODs converted from p-values before FDR correction. The top fifty most significant SNPs were selected for further characterization.

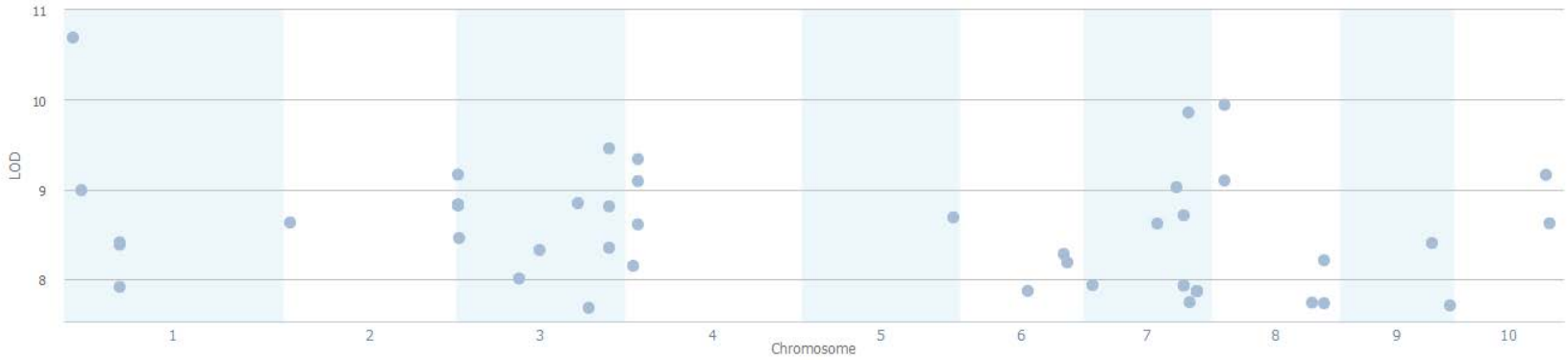

Figure 2-9 Manhattan plot from the GWAS of stay-green ratio in the AMES Panel stay-green ratio. SNPs (blue dots) are reported as LODs converted from p-values before FDR correction. The top fifty most significant SNPs were selected for further characterization.

2.4.4 Comparison of Candidate SNPs between Diverse Maize Populations

2.4.4.1 NAM RILs and AMES Panel Comparisons

2.4.4.1.1 Stay-green Anthesis

Two overlapping regions were identified for stay-green anthesis in comparisons of the NAM RILs and the AMES Diversity Panel on chromosome 1 (Figure 2-10). The first region contained RHOMBOID-like protein 15 (GRMZM2G093855) and D-arabinono-1,4-lactone oxidase family protein (GRMZM2G446350) where candidate SNPs were 53,135bp apart. The second region contained an ethylene insensitive-like 3 (AC234203.1_FG011) that was 9,315bp apart from the AMES and NAM SNPs. GRMZM2G093855 and GRMZM2G446350 were identified in the AMES population and the associated SNPs were in LD with NAM RIL SNPs. Therefore, these candidate genes would not be found in Table 2-5.

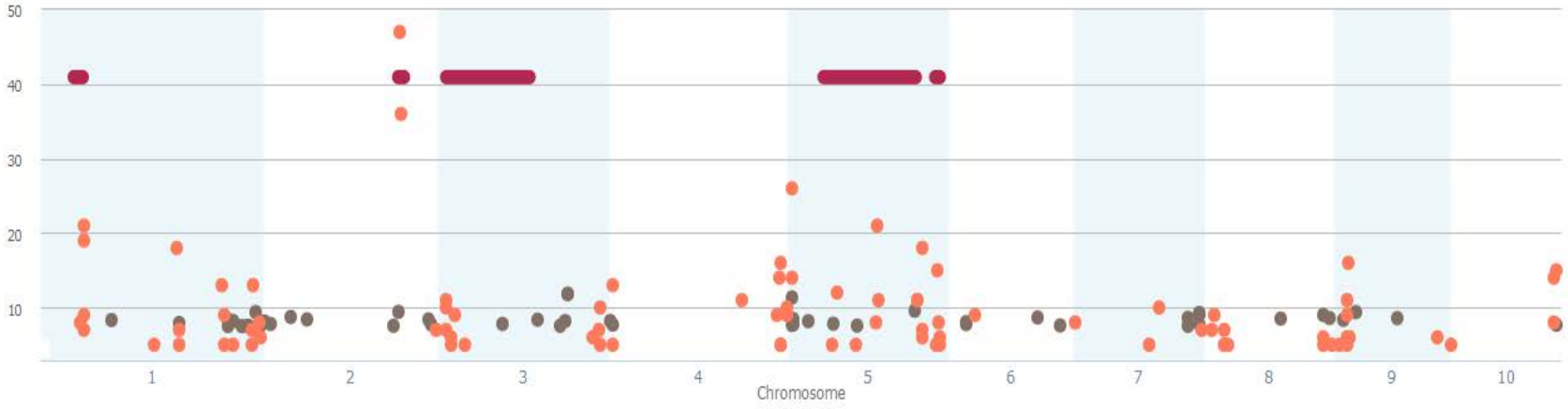

Figure 2-10 Manhattan plot showing associations for stay-green anthesis in the AMES Diversity Panel and NAM RILs. Linkage peaks are shown for the NAM RILs (red) and SNP associations (RILs – Salmon; AMES – Grey). SNP values are reported as RMIP for the RILs SNPs and LODs from p-value conversion for the AMES.

2.4.4.1.2 Stay-green Terminal

Two overlapping genomic regions were detected for stay-green terminal in comparisons of the NAM RILs and AMES Diversity Panel. An ethylene responsive binding element was detected on chromosome 10 (GRMZM2G080516) and a plant invertase/pectin methylesterase inhibitor was detected on chromosome 7 (GRMZM2G137676) (Figure 2-11). These genes can be further examined in Table 2-6.

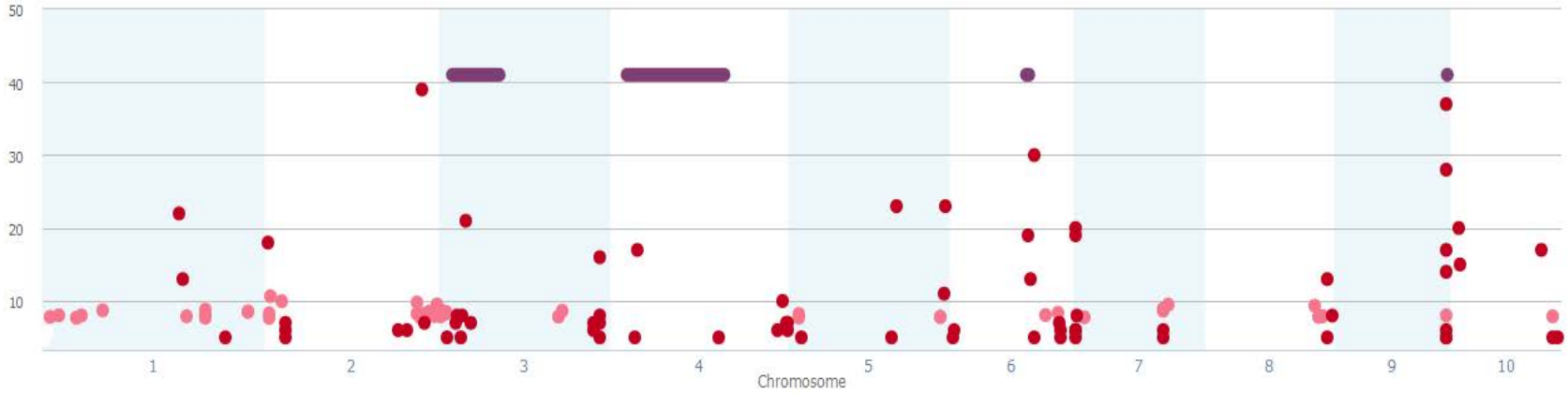

Figure 2-11 Manhattan plot showing associations for stay-green terminal in the AMES Diversity Panel and NAM RILs. Linkage peaks are shown for the NAM RILs (purple) and SNP associations (RILs – Red; AMES – Pink). SNP values are reported as RMIP for the RILs SNPs and LODs from p-value conversion for the AMES.

2.4.4.1.3 Stay-green Difference

Two overlapping genomic regions on chromosome 3 were identified for stay-green difference in comparisons of the NAM RILs and AMES panel (Figure 2-12). The first region is between the genomic positions 221,689,981 and 222,025,874 where four significant SNPs with a RMIP greater than 4 are located. Candidate genes for this region include aldehyde dehydrogenase 2C34, FTSH protease 11, and alpha/beta-hydrolases. The second region is near genomic positions 175,222,001 in the NAM RILs and 176,456,984 in the AMES Diversity Panel. A candidate gene for this region is the senescence regulator PF04520. These candidate genes can be found in Table 2-8.

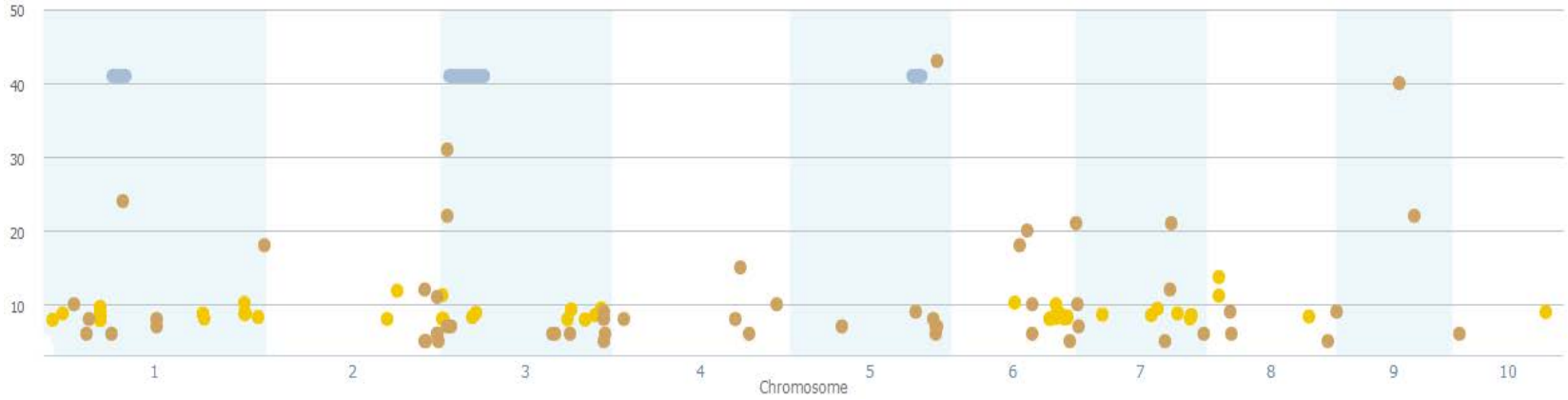

Figure 2-12 Manhattan plot showing genetic associations for stay-green difference in the AMES Diversity Panel and NAM RILs. Linkage peaks are shown for the NAM RILs (blue) and SNP associations (RILs – brown; AMES – yellow). SNP values are reported as RMIP for the RILs SNPs and LODs from p-value conversion for the AMES.

2.4.4.1.4 Stay-green Ratio

Few overlapping regions were detected for stay-green ratio in comparisons among populations. Only four regions appeared to have some genomic similarity, but the genomic distances between the SNPs mostly exceeded 1.5mb. While it is possible that these regions could be in linkage disequilibrium with one another, initial characterization did not appear promising (Figure 2-13). Candidate genes and significant SNP associations can be further examined in Table 2-9.

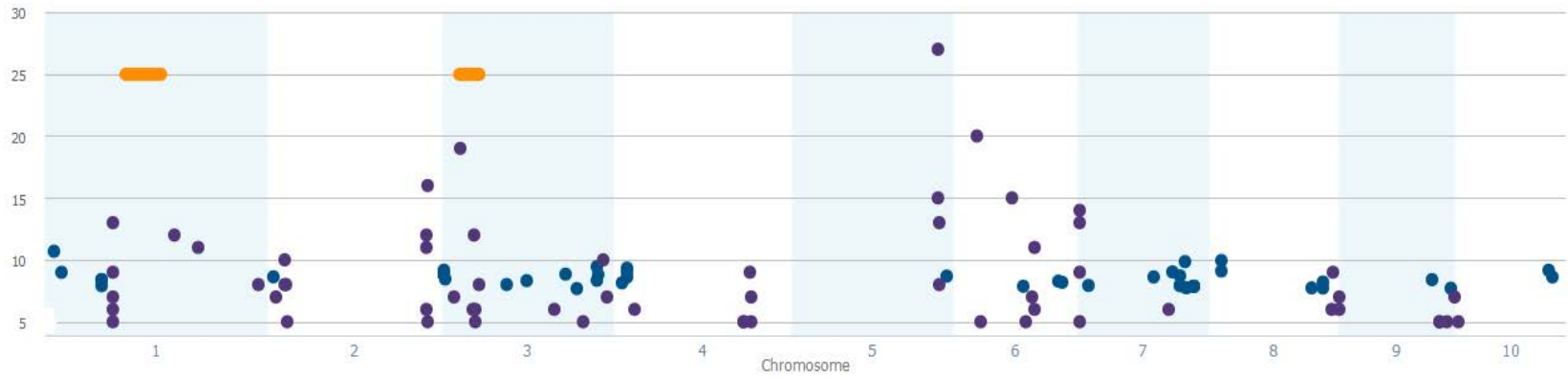

Figure 2-13 Manhattan plot showing genetic associations for stay-green difference in the AMES Diversity Panel and NAM RILs. Linkage peaks are shown for the NAM RILs (orange) and SNP associations (RILs – purple; AMES – blue). SNP values are reported as RMIP for the RILs SNPs and LODs from p-value conversion for the AMES.

2.4.4.2 Comparisons of Stay-green Terminal in the NAM RILs and NAM Testcrosses

Three overlapping genomic regions were detected for stay-green terminal in comparisons of the NAM RILs and NAM testcrosses (Figure 2-14). Chromosome 2 contained two SNPs from the NAM testcrosses (193,772,001 and 194,066,031) that were just over 1 Mb from a SNP in the NAM RILs (192,854,841). Chromosome 6 contained two SNPs from the NAM RILs (115,387,886 and 115,552,825) that were 2.5 Mb from a SNP in the NAM testcrosses 118,501,027. Chromosome 10 contained SNPs from the NAM testcrosses (NAM TC – 127,938,727) that were 2.5 Mb from a SNP from the NAM RILs (NAM RILs – 124,262,019). While it is possible that these regions could be in linkage disequilibrium with one another, initial characterization did not appear promising (Figure 2-14). These genes can be further examined in Table 2-6.

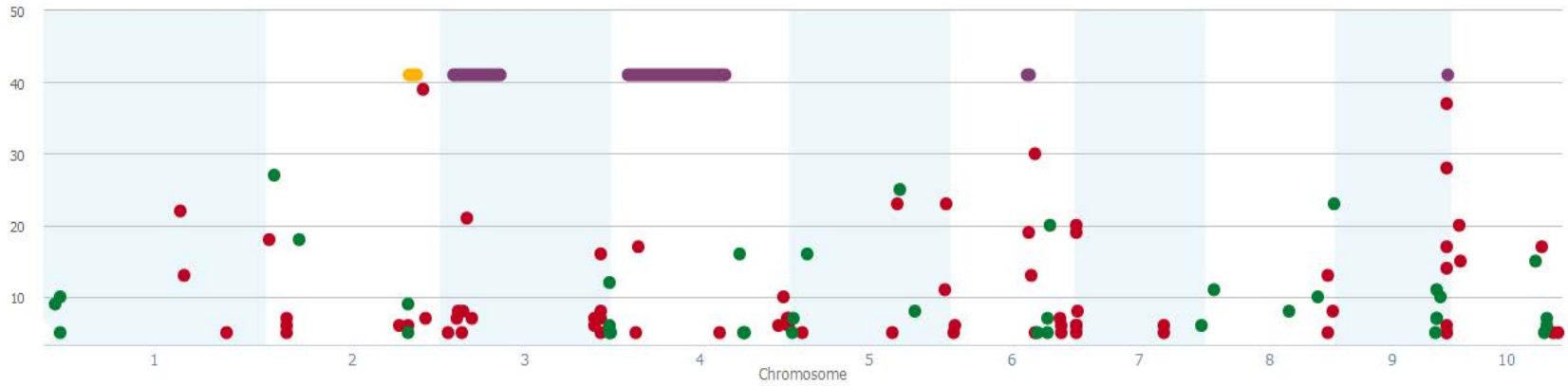

Figure 2-14 Manhattan plot showing genetic associations for stay-green terminal in the NAM RILs and NAM testcrosses. Linkage peaks are shown for the NAM testcrosses (yellow) and RILs (purple) and SNP associations (Testcrosses – Green; RILs – Red). SNP values are reported as RMIP.

2.4.4.3 Comparisons of Stay-green Terminal in the NAM Testcrosses and AMES Panel

Two overlapping genomic regions were detected for stay-green terminal in the NAM testcrosses and the AMES panel. On chromosome 1, a SNP from the NAM testcrosses (NAM TC SNP 22,205,962) was less than 1 Mb from a SNP detected in the AMES Diversity Panel (AMES SNP 23,116,667). On chromosome 8, another SNP from the NAM testcrosses (NAM TC – 151,920,141) was approximately 2 Mb away from a SNP detected in the AMES Diversity Panel (AMES – 153,858,854). While it is possible that these regions could be in linkage disequilibrium with one another, initial characterization did not appear promising (Figure 2-15). These candidate SNPs can be examined further in Table 2-6.

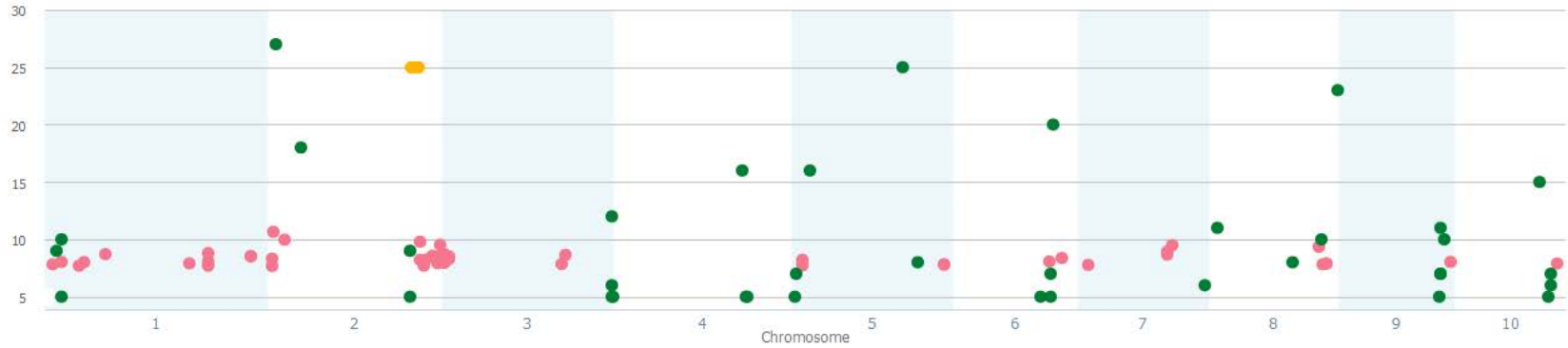

Figure 2-15 Manhattan plot showing genetic associations for stay-green terminal in the AMES Diversity Panel and NAM testcrosses. Linkage peaks are shown for the NAM testcrosses (yellow) and SNP associations (Testcrosses – Green; AMES – Pink). SNP values are reported as RMIP for the testcross SNPs and LODs from p-value conversion for the AMES.

2.4.4.4 All Maize Population Stay-green Terminal Comparisons

Stay-green terminal was the only phenotype taken in all three populations. Surprisingly, no associations occurred across all three populations within linkage disequilibrium to correlate any SNP associations (Figure 2-16).

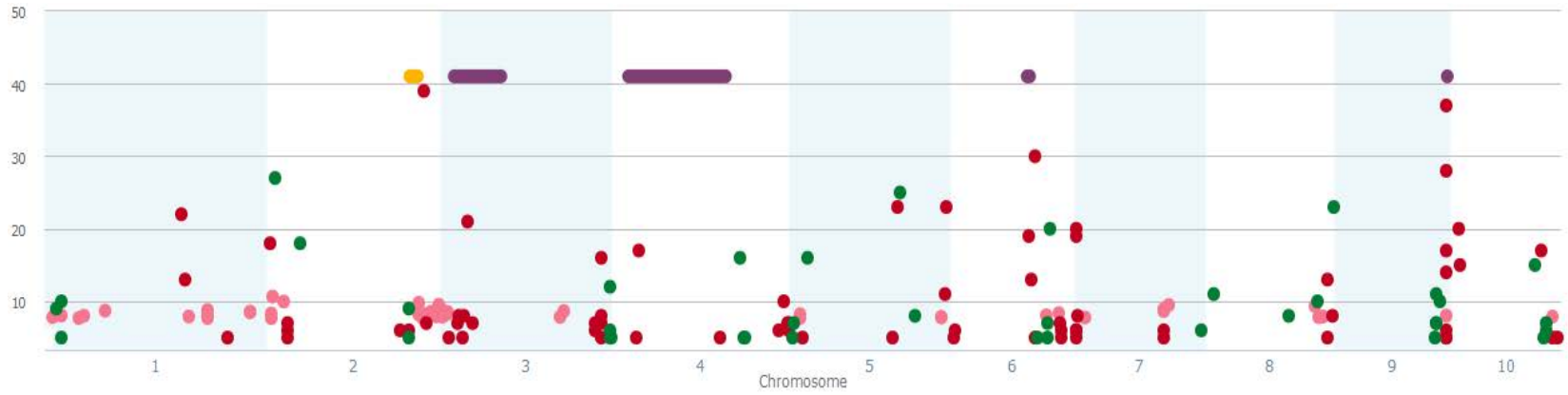

Figure 2-16 AMES Manhattan plot showing genetic associations for stay-green terminal in the AMES Diversity Panel, NAM RILs, and NAM testcrosses. Linkage peaks are shown for the NAM testcrosses (yellow) and NAM RILs (purple) and SNP associations (Testcrosses – Green; RILs – Red; AMES – Pink). SNP values are reported as RMIP for the NAM testcrosses and NAM RILs and LODs from p-value conversion for the AMES.

2.5 Discussion

In this study, the NAM population and Ames Diversity Panel were used to study the genetic variation for stay-green, a drought-related phenotype. These populations represent a large portion of the genetic diversity of maize and have been extensively characterized at a genetic and phenotypic level (Yu et al., 2006; Buckler et al, 2009; Tian et al., 2011, Poland et al., 2011, Kump et al., 2011; Cook et al., 2012). However, neither of these populations has been characterized for drought stress tolerance. Characterizing maize populations with such phenotypic diversity and sample size provides a powerful platform to dissect the genetic architecture of stay-green at a gene by gene level (Yu et al., 2006). Additionally, compelling relationships can be examined between these populations, and a model can be developed for the genetic regulation of stay-green in maize. Finally, this study provides excellent basis for examining stay-green expression and regulation in other crop species.

In our mapping process and experimental design, we accounted for variation associated with maturity because this can be a confounding factor in expression of stay-green. In the NAM populations, we constrained maturity to +/-7 days of B73. Additionally, we analyzed all of the data using days to anthesis as a covariate in our models to alleviate some of the potential statistical influence of maturity. We chose not to use days to silking as a covariate because silking is greatly influenced by drought stress (Bolanos and Edmeades, 1996). In the NAM testcrosses, flowering was further constrained by use of a common tester.

Four different phenotypic measures of stay-green were examined in this study. Each of the traits was highly heritable. We identified several SNP associations for each

stay-green phenotype throughout all populations. It can be daunting to adequately describe the annotated gene information for each association for every population. For our analyses, we focused on characterizing genes that fit the following criteria. A SNP association that only aligned in one population needed to be one of the most significant SNPs using RMIP in the NAM or p-value (prior to FDR correction) in the AMES. Additionally, genes under a SNP would be characterized if they were associated in two or more of the populations and contained collocating support from linkage mapping and LD information. It is important to note that initial characterization of linkage disequilibrium (LD) was examined within a 20 kb interval. Our analyses showed that LD blocks were less than 20 kb in all populations. Previous research suggests that LD in diverse maize lines is around 2 kb (Yu et al., 2008). For this analysis, we considered 20 kb an adequate window to examine for candidate genes unless a LD block extended past 20 kb.

In our association analyses, we organized candidate gene results into several gene families for each stay-green phenotype. These gene families suggest a potential regulation model of stay-green expression, as they are all involved in abiotic stress response or cellular signaling. These families are calcium signaling and relay, stress-related transcription factors, cell-wall related genes, phytohormones, vesicular transportation, sugar transportation, and secondary stress messengers as well as confounding gene families related to heat and disease expression.

2.5.1 Stay-green Candidate Genes

2.5.1.1 Candidate Genes for Stay-green Anthesis

Association analyses for stay-green anthesis indicated several common genomic regions in the NAM RILs and AMES Diversity Panel. NAM SNP 188,056,108 and

AMES SNP 188,065,423 are 9,315 bp away from one another on chromosome 1. There were eight genes that were in the region of interest, and seven of these genes did not have an annotated gene function. However, AC234203.1_FG011 encoded a gene annotated as ethylene-insenstive-like-3 protein (Arabidopsis best hit: AT1G73730.1) as shown in Table 2-5.

2.5.1.1.1 Ethylene Insensitive like 3 - AC234203.1_FG011

Ethylene is a well-known phytohormone involved in regulating senescence. In arabidopsis, Solano et al. (1998) showed ethylene-insensitive-3 (EIN3) and ethylene-response-factor-1 (ERF1) are sequentially activated by ethylene gas to initiate a transcriptional cascade response. Both of these are nuclear proteins, and EIN3 is necessary for ERF1 expression. This study occurred under normal conditions and was primarily concerned with dissecting the complex transcriptional hierarchy of ethylene signaling (Solano et al., 1998). Chao et al. (1997) showed that EIN3 was critical for sensing a plant response to ethylene. The inability to detect ethylene in mutants showed inhibited growth and accelerated arabidopsis senescence. This gene can be further examined in Table 2-5.

2.5.1.1.2 Candidate Genes for Stay-green Anthesis on Chromosome 1 Cluster

NAM SNP 259,884,001 and AMES SNP 259,937,136 are the second pair of SNPs in close proximity located 53,135 bp from each other on chromosome 1. There are eight genes near these SNPs, and six of them do not have any associated annotation. However, GRMZM2G093855 encodes a (AT3G58460.1) RHOMBOID-like protein 15, and GRMZM2G446350 encodes a (AT2G46760.1) D-arabinono-1,4-lactone oxidase family protein.

2.5.1.1.2.1 RHOMBOID-like protein 15 - GRMZM2G093855

Rhomboid proteins are present in almost all species and are involved in cleaving polypeptide chains as proteases. The proteolytic cleavage is irreversible and typically occurs within the lipid bilayer of the cellular membrane (EMBL-EBI, Brown et al., 2000). There has been very little characterization of these proteins in plants, and no research has associated these proteins with an abiotic stress response. This gene is not included in Table 2-5 as it was not detected in the NAM RILs dataset but was in LD with the AMES dataset.

2.5.1.1.2.2 D-arabinono-1,4-lactone oxidase family protein - GRMZM2G446350

D-arabinono-1,4-lactone oxidase family proteins are involved in catalyzing the following chemical reaction (EMBL-EBI).

$$\text{D-arabinono-1,4-lactone} + O_2 \rightleftharpoons \text{D-erythro-ascorbate} + H_2O_2$$

Little has been reported about this enzyme family in the scientific literature. However, it is specifically located in the mitochondrial membrane and is suggested to play some role in a cellular response to an oxidative stress, specifically hydrogen peroxide (Huh et al., 1994). This gene is not included in Table 2-5 as it was not detected in the NAM RILs dataset but was in LD with the AMES dataset.

2.5.1.1.3 Chromosome 4 Candidate Genes

A pair of SNPs on chromosome 4 were the next closest relationship between the NAM RILs and the AMES Diversity Panel for stay-green at anthesis. NAM SNP 4,992,844 is 83,635bp away from AMES SNP 4,909,209. There are twelve genes within this genomic region, eight of which did not have any annotated function. The four

remaining genes had the following annotations: GRMZM2G058447 – (AT4G34190.1 (SEP1)) stress enhanced protein 1, GRMZM5G877647 – (AT2G06255.1 (ELF4-L3)) ELF4-like 3, GRMZM2G058340 – (AT3G49310.1) Major facilitator superfamily protein, and GRMZM2G123996 – (AT1G51090.1) Heavy metal transport/detoxification superfamily protein. These genes are not included in Table 2-5 as they were not within an LD block initially examined.

2.5.1.1.3.1 Stress Enhanced Protein (SEP1)

In arabidopsis, stress enhanced protein 1 is localized to the thylakoid membrane and is upregulated in response to high light intensity. SEP1 is a transmembrane protein. Under high light conditions, *SEP1* and *SEP2* proteins were expressed 4 and 10 fold higher. Additionally, SEP1 is involved in chlorophyll binding and is involved in stabilizing photosystem II under high light stress (Heddad et al., 2000).

2.5.1.1.3.2 Early-Flowering (4) – like – 3

ELF4-like 3 is a transcription factor suggested to participate in the circadian clock input pathway to initiate flowering independent of phytochromeB. Research suggests that this protein has less expression when long day conditions persist. This gene is up-regulated by auxin and cytokinin and down-regulated by ABA and temperature stress. Even though flowering and maturity were controlled for in the model selection and experimental design, appearance of a flowering trait is not surprising, especially a gene implicated in abiotic stress (NCBI, Hicks et al., 2001).

2.5.1.1.3.3 Major Facilitator Superfamily Protein

The general nature of this annotation makes it difficult to ascribe any specific function. These proteins are involved in general substrate transport possibly within the

Golgi apparatus, endosome, plasma membrane, and/or trans-Golgi network (EMBL-EBI, NCBI).

2.5.1.1.3.4 Heavy Metal Transport/Detoxification Superfamily Protein

Arabidopsis provides the best insight into the potential function of this gene. Specifically, this gene is involved in response to fungal presence, in response to an ABA stimulus, and cold and drought stresses. Interestingly, this gene appears to be expressed most often during anthesis and throughout normal senescence patterns in arabidopsis (EMBL-EBI).

2.5.1.1.4 Stay-green Anthesis Candidate Gene Summary

Additionally, several genes related to calcium signaling and transduction, general-stress, growth regulators and transcription factors, sugar and secondary messengers, vesicle transport, cell-wall formation, and phytohormones were identified in individual populations (Table 2-5). Groups of genes related to disease, heat stress, expressed proteins, and unannotated proteins were also identified in the population. Only stay-green anthesis in the NAM RILs is reported in Table 2-5 as there were no significant SNPs in the AMES diversity panel and the phenotype was not collected in the NAM testcrosses. It appears that these gene groups are intimately involved in stay-green response to abiotic stress. It is important to note that significant genes in a single population can still be vital to understanding the expression of stay-green and should be thoroughly examined. These candidate genes might only be present or detectable in individual populations and characterization is needed to understand the stay-green phenotypes. Nevertheless, candidate genes present in two or more populations are

critical to the analysis of stay-green as detection in two independent dataset provides powerful insight into the expression and regulation of the phenotype.

Table 2-5 Candidate genes for stay-green anthesis in the NAM RILs.

Candidate Gene Family	Chr	SNP Position	RMIP	Gene ID	Arabidopsis/Rice/PFAM Ortholog
Calcium Signaling and Relay	10	143,670,200	15	GRMZM2G180471	AT1G34750.1: Protein phosphatase 2C family protein
	3	17,433,280	6	GRMZM2G151087	AT5G10480.3(PAS2,PEP): Protein-tyrosine phosphatase-like, PTPLA
General stress-related and transcription factors	1	58,475,918	21	GRMZM2G075502	AT3G06130.1: Heavy metal transport/detoxification superfamily protein
	5	181,386,025	18	GRMZM2G029583	AT4G24820.1: 26S proteasome, regulatory subunit Rpn7;Proteasome component (PCI) domain
	1	287,270,801	13	GRMZM2G342856	AT2G32030.1: Acyl-CoA N-acyltransferases (NAT) superfamily protein
	5	122,046,355	11	AC186500.3_FG001	AT2G42490.1: Copper amine oxidase family protein
	6	34,893,105	9	GRMZM2G305856	AT3G46130.1(ATMYB48,ATMYB48-1,ATMYB48-2,ATMYB48-3,MYB48): myb domain protein 48
	1	53,630,920	8	GRMZM2G011598	AT3G04070.1(anac047,NAC047): NAC domain containing protein 47
	1	53,630,920	8	GRMZM2G020940	AT2G39050.1: hydroxyproline-rich glycoprotein family protein
	3	17,030,869	5	AC215260.3_FG004	AT5G16450.1: Ribonuclease E inhibitor RraA/Dimethylmenaquinone methyltransferase

Table 2-5 Continued

Sugar Transport and Secondary Messengers	9	18,334,400	9	GRMZM5G838414	AT1G53290.1: Galactosyltransferase family protein
	9	19,163,887	6	GRMZM2G443985	AT4G26270.1(PFK3): phosphofructokinase 3
	9	20,459,109	6	GRMZM2G173641	AT5G11380.1(DXPS3): 1-deoxy-D-xylulose 5-phosphate synthase 3
	4	4,448,482	5	GRMZM2G039408	AT3G18830.1(ATPLT5,ATPMT5,PMT5): polyol/monosaccharide transporter 5
	9	8,020,744	5	GRMZM2G080696	AT2G03220.1(ATFT1,ATFUT1,FT1,MUR2): fucosyltransferase 1
	10	1,728,072	5	GRMZM2G130062	AT1G74040.1(IMS1,IPMS2,MAML-3): 2-isopropylmalate synthase 1
Vesicular Transport	1	183,804,764	18	GRMZM2G113840	AT4G39170.1: Sec14p-like phosphatidylinositol transfer family protein
	9	18,334,400	9	AC231745.1_FG003	AT5G45910.1: GDSL-like Lipase/Acylhydrolase superfamily protein
	1	296,649,227	8	GRMZM2G167428	PFAM ID: PF03364: Polyketide cyclase / dehydrase and lipid transport , PF10604: Polyketide cyclase / dehydrase and lipid transport
	3	17,433,280	6	GRMZM2G451327	AT2G39550.1(ATGGT-IB,GGB,PGGT-I): Prenyltransferase family protein
Phytohormone	2	185,691,621	47	GRMZM2G110107	AT1G68130.1(AtIDD14,IDD14): indeterminate(ID)-domain 14
	1	188,056,108	5	AC234203.1_FG011	AT1G73730.1: ethylene insensitive-like 3

Table 2-5 Continued

Cell Wall Structure	5	5,005,874	26	AC191251.3_FG005	AT3G20800.1: Cell differentiation, Rcd1-like protein
	4	230,895,626	16	GRMZM2G080056	AT1G14420.1(AT59): Pectate lyase family protein
	3	219,827,756	10	GRMZM2G074466	AT1G49040.1(SCD1): stomatal cytokinesis defective / SCD1 protein (SCD1)
	8	13,790,821	9	GRMZM2G477503	AT5G01220.1(SQD2): sulfoquinovosyldiacylglycerol 2
	5	204,317,772	8	GRMZM2G012044	AT1G55850.1(ATCSLE1,CSLE1): cellulose synthase like E1
	5	182,133,946	7	GRMZM2G137399	AT1G28580.1: GDSL-like Lipase/Acylhydrolase superfamily protein
	5	182,133,946	7	GRMZM2G137409	AT5G60600.1(CLB4,CSB3,GCPE,HDS,ISPG): 4-hydroxy-3-methylbut-2-enyl diphosphate synthase
	1	285,941,597	5	GRMZM2G434533	AT3G11780.1: MD-2-related lipid recognition domain-containing protein / ML domain-containing protein
	3	17,030,869	5	AC215260.3_FG003	AT5G48930.1(HCT): hydroxycinnamoyl-CoA shikimate/quinate hydroxycinnamoyl transferase
Heat	2	186,183,071	36	GRMZM2G002131	AT4G36990.1(AT-HSFB1,ATHSF4,HSF4,HSFB1):heat shock factor4
	1	285,904,918	7	GRMZM2G134917	AT5G22060.1(ATJ2,J2): DNAJ homologue 2
	2	233,674,088	7	GRMZM2G469477	AT4G14830.1(HSP1):
	9	20,459,109	6	GRMZM2G173628	AT5G23310.1(FSD3): Fe superoxide dismutase 3

Table 2-5 Continued

Disease	5	204,317,772	8	GRMZM2G011951	AT5G55850.1(NOI): RPM1-interacting protein 4 (RIN4) family protein
	7	2,360,774	8	GRMZM2G128693	AT3G50950.1(ZAR1): HOPZ-ACTIVATED RESISTANCE 1
	1	187,592,684	7	GRMZM2G132763	AT1G17750.1(AtPEPR2,PEPR2): PEP1 receptor 2
Other	5	119,472,884	8	GRMZM2G052654	AT2G02880.1: mucin-related
	5	4,944,136	14	GRMZM2G089361	AT4G18390.1(TCP2): TEOSINTE BRANCHED 1, cycloidea and PCF transcription factor 2
	3	22,568,001	9	GRMZM2G337815	AT4G34555.1: Ribosomal protein S25 family
	5	91,602,155	5	GRMZM2G174785	AT5G25060.1: RNA recognition motif (RRM)-containing protein
	7	172,488,742	7	GRMZM2G113863	AT5G27690.1: Heavy metal transport/detoxification superfamily protein
	5	204,914,413	5	GRMZM2G089454	AT5G37680.1(ARLA1A,ATARLA1A): ADP-ribosylation factor-like A1A
	9	140,431,872	6	GRMZM2G131539	AT2G29560.1(ENOC): cytosolic enolase
	5	204,317,772	8	GRMZM2G012213	AT4G16835.1: Tetratricopeptide repeat (TPR)-like superfamily protein
	8	27,648,546	5	GRMZM2G058491	AT1G64110.2: P-loop containing nucleoside triphosphate hydrolases superfamily protein
	10	1,728,072	5	GRMZM2G129954	AT3G57040.1(ARR9,ATRR4):response regulator9
	9	20,459,109	6	GRMZM2G173693	AT5G37370.1(ATSRL1): PRP38 family protein
	4	239,498,890	10	GRMZM2G169998	AT5G58130.1(ROS3): RNA-binding (RRM/RBD/RNP motifs) family protein

Table 2-5 Continued

Other	10	143,670,200	15	GRMZM2G480282	LOC_Os06g30760.1: transposon protein, putative, CACTA, En/Spm sub-class, expressed
	5	199,972,074	5	AC233960.1_FG005	AT1G06170.1: basic helix-loop-helix (bHLH) DNA-binding superfamily protein
	8	161,388,771	6	GRMZM2G423456	AT1G27320.1(AHK3,HK3): histidine kinase 3
	2	185,691,621	47	GRMZM2G110107	AT1G68130.1(AtIDD14,IDD14): indeterminate(ID)-domain 14
	4	4,992,844	13	GRMZM5G877647	AT2G06255.1(ELF4-L3): ELF4-like 3
	5	59,254,396	5	GRMZM2G084521	AT2G29960.1(ATCYP5,CYP19-4,CYP5): cyclophilin 5
	2	233,674,088	7	GRMZM2G469469	AT2G32040.1: Major facilitator superfamily protein
	8	13,790,821	9	GRMZM2G079458	AT2G38090.1: Duplicated homeodomain-like superfamily protein
	1	53,630,920	8	GRMZM2G020940	AT2G39050.1: hydroxyproline-rich glycoprotein family protein
	5	59,254,396	5	GRMZM2G385945	AT3G02790.1: zinc finger (C2H2 type) family pron
	1	297,962,777	6	AC207546.3_FG004	AT3G08947.1: ARM repeat superfamily protein
	1	183,804,764	18	GRMZM2G113726	AT3G13340.1: Transducin/WD40 repeat-like superfamily protein
	2	233,674,088	7	GRMZM2G170934	AT3G22440.1: FRIGIDA-like protein
	6	34,893,105	9	GRMZM2G305856	AT3G46130.1(ATMYB48,ATMYB48-1,ATMYB48-2,ATMYB48-3,MYB48): myb domain protein 48

Table 2-5 Continued

	4	4,992,844	13	GRMZM2G058340	AT3G49310.1: Major facilitator superfamily protein
	4	239,498,890	10	GRMZM2G169871	AT3G54170.1(ATFIP37,FIP37): FKBP12 interacting protein 37
	4	239,498,890	10	GRMZM2G169927	AT4G31120.1(ATPRMT5,PRMT5,SKB1): SHK1 binding protein 1
	5	175,865,828	11	GRMZM2G072146	AT4G39910.1(ATUBP3,UBP3): ubiquitin-specific protease 3
	1	297,962,777	6	GRMZM2G001661	AT5G16490.1(RIC4): ROP-interactive CRIB motif-containing protein 4
	3	209,021,937	6	GRMZM2G164674	AT5G19580.1: glyoxal oxidase-related protein
Other	5	199,972,074	5	GRMZM5G861093	AT5G27080.1: Transducin family protein / WD-40 repeat family protein
	10	1,728,072	5	GRMZM2G129907	AT5G43210.1: Excinuclease ABC, C subunit, N-terminal
	5	199,972,074	5	AC233960.1_FG003	AT5G45580.1: Homeodomain-like superfamily
	5	181,386,025	18	GRMZM2G031496	AT5G50960.1(ATNBP35,NBP35): nucleotide binding protein 35
	5	181,386,025	18	GRMZM2G031107	AT5G50960.1(ATNBP35,NBP35): nucleotide binding protein 35
	3	219,484,321	5	GRMZM2G306357	AT5G56930.1(emb1789): CCCH-type zinc finger family protein
	3	219,827,756	10	GRMZM5G849600	AT5G56960.1: basic helix-loop-helix (bHLH) DNA-binding family protein

Table 2-5 Continued

Other	8	13,790,821	9	GRMZM2G176568	AT5G58900.1: Homeodomain-like transcriptional regulator
	4	179,091,367	11	GRMZM2G107414	LOC_Os02g52300.1: CPuORF38 - conserved peptide uORF-containing transcript, expressed
	1	289,518,674	7	GRMZM2G101682	LOC_Os03g58850.1: uncharacterized PE-PGRS family protein PE_PGRS3 precursor, putative,
Expressed Proteins	6	34,893,105	9	GRMZM2G700901	PFAM ID: PF06813: Nodulin-like , PF00579: tRNA synthetases class I (W and Y)
	8	161,790,610	5	GRMZM2G481103	PFAM ID: PF10163: Transcription factor e(y)2
	5	204,928,300	6	GRMZM5G824439	PFAM ID: PF11573: Mediator complex subunit 23
	9	18,521,596	16	GRMZM5G800535	PFAM ID: PF05678: VQ motif
	5	182,133,946	7	GRMZM2G137375	LOC_Os02g39180.1: expressed protein
	3	209,021,937	6	GRMZM5G866432	LOC_Os01g48570.1: expressed protein
	5	204,928,300	6	GRMZM5G883043	LOC_Os02g49992.1: expressed protein
	1	188,056,108	5	AC234203.1_FG009	LOC_Os03g58340.1: expressed protein
	1	188,056,108	5	AC234203.1_FG011	AT1G73730.1: ethylene insensitive-like 3
	8	26,625,353	5	GRMZM2G413717	LOC_Os01g12190.1: expressed protein
	8	27,648,546	5	GRMZM2G058366	LOC_Os01g12670.2: expressed protein
	8	161,790,610	5	GRMZM2G180372	LOC_Os01g69100.1: expressed protein
No Annotation	2	185,691,621	47	GRMZM2G548414	
	2	186,183,071	36	GRMZM2G301582	
	2	186,183,071	36	GRMZM2G483390	
	5	5,005,874	26	GRMZM2G460635	

Table 2-5 Continued

No Annotation	5	5,005,874	26	GRMZM2G159253
	1	58,475,918	21	GRMZM2G528064
	1	58,475,918	21	GRMZM2G376395
	5	120,073,399	21	No annotated genes
	1	58,983,957	19	No annotated genes
	1	183,804,764	18	GRMZM2G113895
	1	183,804,764	18	GRMZM2G414241
	1	183,804,764	18	GRMZM5G835781
	1	183,804,764	18	GRMZM2G113718
	1	183,804,764	18	GRMZM5G831355
	1	183,804,764	18	GRMZM2G113722
	1	183,804,764	18	GRMZM2G113724
	5	181,386,025	18	GRMZM2G030606
	5	181,386,025	18	GRMZM2G331844
	5	202,484,001	15	GRMZM2G123944
	10	143,670,200	15	AC216807.3_FG009
	4	229,374,063	14	No annotated genes
	5	4,944,136	14	GRMZM2G535148
	5	4,944,136	14	GRMZM2G089425
	10	141,534,896	14	AC214233.4_FG015
	10	141,534,896	14	GRMZM2G057551
	10	141,534,896	14	GRMZM2G515381
	10	141,534,896	14	GRMZM2G515383
	1	244,459,902	13	GRMZM2G586692

Table 2-5 Continued

No Annotation	4	4,992,844	13	GRMZM2G517786
	5	66,086,001	12	No annotated genes
	3	11,032,882	11	GRMZM2G701322
	5	122,046,355	11	GRMZM2G393629
	5	122,046,355	11	GRMZM2G580248
	9	18,397,972	11	No annotated genes
	3	11,032,448	10	GRMZM2G701322
	7	115,897,484	10	GRMZM2G373937
	1	58,502,398	9	No annotated genes
	1	248,650,001	9	GRMZM2G361087
	1	248,650,001	9	GRMZM2G060718
	1	248,650,001	9	GRMZM2G519100
	3	22,568,001	9	GRMZM2G505202
	4	226,591,487	9	GRMZM2G394266
	4	239,547,934	9	No annotated genes
	6	34,893,105	9	GRMZM2G305839
	6	34,893,105	9	GRMZM2G305804
	8	13,790,821	9	GRMZM2G176562
	1	53,630,920	8	GRMZM2G587377
	5	204,317,772	8	GRMZM2G312980
	7	2,360,774	8	AC231379.2_FG010
	7	2,360,774	8	GRMZM2G704310
	7	2,360,774	8	GRMZM2G033408
	7	2,360,774	8	GRMZM2G128707

Table 2-5 Continued

No Annotation	1	58,323,293	7	No annotated genes
	1	289,518,674	7	GRMZM2G101783
	2	233,674,088	7	GRMZM2G469486
	2	233,674,088	7	GRMZM2G584410
	2	233,674,088	7	GRMZM2G584415
	2	233,674,088	7	GRMZM2G703445
	3	11,032,046	7	GRMZM2G701322
	3	217,074,714	7	No annotated genes
	5	182,133,946	7	GRMZM2G564851
	5	182,133,946	7	GRMZM2G564831
	5	182,133,946	7	GRMZM2G137371
	7	172,488,742	7	GRMZM2G414446
	7	172,488,742	7	GRMZM2G550852
	7	172,488,742	7	GRMZM2G511855
	8	10,392,672	7	GRMZM2G374085
	8	10,392,672	7	GRMZM2G526579
	8	10,392,672	7	GRMZM2G526575
	8	10,392,672	7	GRMZM2G500279
	8	26,604,001	7	GRMZM2G550451
	8	26,604,001	7	AC195899.3_FG001
	1	297,962,777	6	GRMZM2G482887
	1	297,962,777	6	GRMZM2G300698
	1	297,962,777	6	GRMZM2G300702
	1	297,962,777	6	GRMZM2G001718

Table 2-5 Continued

No Annotation	3	17,433,280	6	GRMZM2G411241
	3	17,433,280	6	GRMZM2G411238
	3	17,433,280	6	GRMZM2G573274
	3	209,021,937	6	GRMZM2G464741
	5	181,401,920	6	GRMZM2G501655
	5	181,401,920	6	GRMZM2G031496
	5	181,401,920	6	GRMZM2G331844
	5	181,401,920	6	GRMZM2G031107
	5	204,928,300	6	AC203365.3_FG007
	8	161,388,771	6	GRMZM5G872549
	8	161,388,771	6	GRMZM2G556207
	9	18,131,145	6	No annotated genes
	9	19,163,887	6	GRMZM5G861581
	9	20,459,109	6	GRMZM2G173678
	9	20,459,109	6	GRMZM2G173685
	9	20,459,109	6	GRMZM2G587636
	9	20,459,109	6	GRMZM5G807872
	9	140,431,872	6	GRMZM5G839429
	9	140,431,872	6	GRMZM2G431975
	1	154,131,933	5	GRMZM2G029936
	1	154,131,933	5	GRMZM2G500408
	1	188,056,108	5	GRMZM5G861100
	1	188,056,108	5	AC234203.1_FG008
	1	248,554,309	5	No annotated genes

Table 2-5 Continued

No Annotation	1	259,884,001	5	GRMZM5G871118
	3	17,030,869	5	GRMZM2G701355
	3	35,825,703	5	GRMZM5G820780
	3	219,484,321	5	GRMZM2G306413
	3	219,484,321	5	GRMZM2G486236
	4	4,448,482	5	GRMZM5G873972
	4	4,448,482	5	GRMZM2G333732
	4	230,907,639	5	AC186499.3_FG003
	4	230,907,639	5	GRMZM2G080050
	4	230,946,598	5	GRMZM2G078799
	4	230,946,598	5	GRMZM2G530744
	5	59,254,396	5	GRMZM5G806227
	5	199,972,074	5	GRMZM5G871673
	5	204,914,413	5	AC203365.3_FG004
	7	102,253,051	5	No annotated genes
	8	26,625,353	5	AC195899.3_FG002
	8	27,648,546	5	GRMZM2G517902
	8	27,648,546	5	GRMZM2G358977
	8	27,648,546	5	AC200099.4_FG006
	8	27,648,546	5	GRMZM2G014354
	8	31,465,928	5	No annotated genes
	8	161,790,610	5	GRMZM2G590971
	8	161,790,610	5	GRMZM5G863390
	8	161,790,610	5	GRMZM2G590973

Table 2-5 Continued

No Annotation	8	173,825,200	5	No annotated genes
	9	8,020,744	5	GRMZM2G080686
	10	1,728,072	5	GRMZM2G560695
	10	1,728,072	5	AC195137.2_FG009

2.5.1.2 Candidates Genes for Stay-green Terminal

Linkage disequilibrium for all SNPs associated with stay-green terminal were less than 20 kb in all three populations. Therefore, we considered only candidate genes within the 20 kb window as previously described in the materials and methods. Candidate genes associated with stay-green terminal in the NAM RILs are shown in Table 2-6. Candidate genes associated with stay-green terminal in the NAM RIL testcrosses are shown in Table 2-7.

We were most interested in candidate genes that had genomic relationships across two or more of the independent populations phenotyped. However, for stay-green terminal, there were no relationships across all three populations, and only the NAM RILs and AMES populations shared any genomic relationships. Therefore, the most efficient way of analyzing this phenotype is to focus on the most frequently called significant SNPs in the NAM. Further characterization of genes identified in the NAM can be supported using the AMES data.

There were two genomic regions associated with stay-green terminal that overlapped between the NAM RILs and the AMES population. On chromosome 7, NAM RIL SNPs 119,978,049 and 119,978,519 were less than 3kb away from AMES SNP 119,975,995 (Table 2-6). On chromosome 10, NAM SNP 139,882,304 was ~3kb away from AMES SNP 139,879,255. There was a single gene within the LD block on chromosome 7: GRMZM2G137676 -Plant invertase/pectin methylesterase inhibitor superfamily and a single gene in the LD block on chromosome ten: GRMZM2G080516 – ethylene response element binding factor 1 (Table 2-6).

No other extremely tight genomic relationships existed between any of the stay-green terminal populations. However, a cluster of seven SNPs were identified in the NAM RILs on chromosome 9 ranging from 150,815,418 to 152,316,001 that centered around a single AMES SNP: 151,986,054 (Table 2-6). Further characterization of stay-green terminal is needed to identify potential candidate genes from this gene-heavy region on chromosome 9.

2.5.1.2.1 Plant invertase/pectin methylesterase inhibitor superfamily – GRMZM2G137676

Golgi apparatus related genes were identified across the three populations. While there is little evidence to relate these genes to abiotic stress, they are potentially involved in regulation of pectin secretion and remodeling in conjunction with pectin methylesterases and related inhibitors. This gene can be further examined in Table 2-6.

Plant invertases/pectin methylesterases are involved in demethylesterification of cell wall polygalacturonans (Micheli, 2001). Most of these enzymes are at the beginning of the pectin biosynthetic pathway where pectin is synthesized in the Golgi apparatus and secreted into the cell wall. Additionally, in relation to abiotic stress, pectin methylesterases can regulate pectin structure in accordance to stem elongation cellular adhesion, plasticity, pH, and ionic contents of the cell wall (Pelloux et al., 2007). Thus, pectin remodeling under an abiotic stress can be critical to survival of a plant. Additionally, it highlights other association mapping results where Golgi apparatus genes (vesicular transportation family) were identified as significantly correlated with stay-green phenotypes (Tables 2-5 to 2-9).

Plant invertase/pectin methylesterase inhibitors have a direct role in regulating kiwi fruit development, carbohydrate metabolism, and cell wall extension (Giovane et al., 1995). In wheat, pectin methyl esterases and their related inhibitors were regulated under stress responses by intron retention of different alleles (Rocchi et al., 2011). French et al. (2014) identified a link between auxin, and cell wall invertases and inhibitors during grain development in rice.

2.5.1.2.2 Ethylene responsive element binding factor 1 - GRMZM2G080516

Ethylene is a major phytohormone involved in regulating gene expression and senescence under normal and abiotic stress conditions. Ethylene response elements binding factors are regulated in tandem with ethylene insensitive genes (EIN). Specifically, ethylene response factor, ERF1, activates GCC-box dependent transcription in arabidopsis leaves. It is differentially expressed in drought, salt, cold, and wounding situations by ethylene in arabidopsis via EIN2 or independent pathways (Fujimoto et al., 2000). Different alleles of ERF1 under abiotic stress could directly correspond to whether or not a plant is stay-green via modulation of ethylene response under abiotic stress conditions. This gene can be further examined in Table 2-6.

2.5.1.2.3 Stay-green Terminal Candidate Gene Summary

Candidate genes for stay-green terminal were identified and reported by their potential gene families in Table 2-5. Additional groups of genes related to disease, heat stress, expressed proteins, and unannotated proteins were identified in the NAM RILs and NAM testcrosses (Table 2-6: NAM RILs, Table 2-7: NAM testcrosses).

Table 2-6 Candidate genes associated with stay-green terminal in the NAM RILs

Candidate Gene Family	Chr	SNP Position	RMIP	Gene ID	Arabidopsis/Rice/PFAM Ortholog
Calcium Signaling and Relay	3	217,726,001	16	GRMZM5G856738	AT4G23650.1(CDPK6,CPK3): calcium-dependent protein kinase 6
	10	146,585,004	5	GRMZM2G084586	AT3G13530.1(MAP3KE1,MAPKKK7): mitogen-activated protein kinase kinase kinase 7
General stress-related and transcription factors	3	208,618,360	7	GRMZM2G022052	LOC_Os01g48810.1: transcription initiation factor TFIID subunit 11, putative, expressed
Sugar Transport and Secondary Messengers	4	240,798,443	7	GRMZM5G878607	AT1G78570.1(ATRHM1,RHM1,ROL1): rhamnose biosynthesis 1
	2	192,854,841	6	GRMZM2G181018	LOC_Os09g33800.1: arabinogalactan protein, putative, expressed
	2	27,999,843	5	GRMZM2G122618	Glucose-6-phosphate/phosphate and phosphoenolpyruvate/phosphate antiporter
Phytohormone	2	27,979,793	7	GRMZM2G122614	AT4G30080.1(ARF16): auxin response factor 16
	3	217,695,045	7	GRMZM2G041015	AT2G46225.2(ABIL1): ABI-1-like 1
	2	27,999,843	5	GRMZM2G471931	AT2G28305.1(ATLOG1,LOG1): Putative lysine decarboxylase family protein
	10	146,585,004	5	GRMZM2G084576	AT2G43060.1(IBH1): ILI1 binding bHLH 1
	10	139,882,304	5	GRMZM2G080516	AT4G17500.1(ATERF-1,ERF-1): ethylene responsive element binding factor 1

Table 2-6 Continued

	9	152,203,791	37	GRMZM5G865819	AT2G20370.1(KAM1,MUR3): Exostosin family protein
	6	115,552,825	30	GRMZM2G156255	AT3G02850.1(SKOR): STELAR K+ outward rectifier
	6	115,552,825	30	GRMZM2G156310	AT1G47480.1: alpha/beta-Hydrolases superfamily protein
Cell Wall Structure	2	5,217,793	18	GRMZM2G160523	AT1G73880.1(UGT89B1): UDP-glucosyl transferase 89B1
	9	152,252,288	14	GRMZM2G137779	LOC_Os03g05110.1: xyloglucan galactosyltransferase KATAMARI1, putative, expressed
	4	238,056,024	7	GRMZM5G846811	AT4G35020.1(ARAC3,ATROP6,RAC3,RHO1PS,ROP6): RAC-like 3
	9	151,735,364	6	GRMZM2G126682	(CVP1,FRL1,SMT2): sterol methyltransferase 2
	2	213,233,048	39	GRMZM2G021129	AT1G26690.1: emp24/gp25L/p24 family/GOLD family protein
Vesicular	9	152,316,001	28	GRMZM2G107651	AT2G20320.1: DENN (AEX-3) domain-containing
Transport	4	36,048,211	17	GRMZM2G131329	AT4G21060.2: Galactosyltransferase family protein
	6	109,837,285	13	GRMZM2G136058	AT1G09580.1: emp24/gp25L/p24 family/GOLD family protein
Disease	5	211,767,155	23	GRMZM2G463904	AT2G26330.1(ER,QRP1): Leucine-rich receptor-like protein kinase family protein
	9	152,252,288	14	GRMZM2G438840	AT4G28650.1: Leucine-rich repeat transmembrane protein kinase family protein
Other	9	152,203,791	37	GRMZM2G178072	AT3G24010.1(ATING1,ING1): RING/FYVE/PHD zinc finger superfamily protein
	5	211,767,155	23	GRMZM2G166024	AT1G23790.1: Plant protein of unknown function (DUF936)
	5	211,767,155	23	GRMZM2G166027	AT2G05940.1: Protein kinase superfamily protein

Table 2-6 Continued

Other	3	35,736,981	21	GRMZM2G122656	AT4G18590.1: Nucleic acid-binding, OB-fold-like protein
	3	35,736,981	21	GRMZM2G421742	AT5G49350.1: Glycine-rich protein family
	7	1,291,451	20	GRMZM2G120574	AT5G53890.1(AtPSKR2,PSKR2): phytosylfokine-alpha receptor 2
	7	1,291,451	20	GRMZM2G120575	LOC_Os11g16480.1: transposon protein, putative, unclassified, expressed
	10	12,542,065	20	GRMZM2G001195	AT4G33140.1: Haloacid dehalogenase-like hydrolase (HAD) superfamily protein
	4	36,048,211	17	GRMZM2G131378	AT2G38110.1(ATGPAT6,GPAT6): glycerol-3-phosphate acyltransferase 6
	9	152,138,627	17	GRMZM2G089421	AT1G57860.1: Translation protein SH3-like family protein
	9	152,138,627	17	GRMZM2G089699	AT1G65680.1(ATEXPB2,ATHEXP BETA 1.4,EXPB2): expansin B2
	9	152,138,627	17	GRMZM2G089686	AT3G24310.1(ATMYB71,MYB305): myb domain protein 305
	10	12,744,140	15	GRMZM2G063394	AT1G76390.1: ARM repeat superfamily protein
	8	166,681,172	13	GRMZM2G169412	AT5G06140.1(ATSNX1,SNX1): sorting nexin 1
	8	166,681,172	13	GRMZM2G169398	alcohol O-acetyltransferase activity
	3	23,893,603	8	GRMZM2G114552	LOC_Os01g03680.1: BBTI8 - Bowman-Birk type bran trypsin inhibitor precursor, expressed
	7	2,970,401	8	GRMZM2G350205	LOC_Os07g03140.1: ternary complex factor MIP1, putative, expressed
	8	173,028,725	8	GRMZM2G124047	AT5G65760.1: Serine carboxypeptidase S28 family protein
	2	217,010,357	7	GRMZM2G473709	LOC_Os07g48244.1: ubiquinol-cytochrome c reductase complex 6.7 kDa protein, putative,
	3	23,009,435	7	AC182482.3_FG003	AT1G16310.1: Cation efflux family protein

Table 2-6 Continued

	4	238,056,024	7	AC233922.1_FG004	AT5G64050.1(ATERS,ERS,OVA3): glutamate tRNA synthetase
	4	238,056,024	7	AC233922.1_FG005	LOC_Os02g02850.1: bifunctional protein folD
	6	148,247,279	7	AC214451.3_FG005	LOC_Os03g21660.1: transposon protein, putative, unclassified, expressed
	6	148,247,279	7	GRMZM2G175676	RNA recognition motif. (a.k.a. RRM, RBD, or RNP domain)
	4	226,356,022	6	GRMZM2G319056	AT4G10150.1: RING/U-box superfamily protein
	6	6,320,084	6	GRMZM2G412470	AT5G63190.1: MA3 domain-containing protein
	7	1,287,427	6	GRMZM2G120652	AT5G01410.1(ATPDX1,ATPDX1.3,PDX1,PDX1.3, RSR4): Aldolase-type TIM barrel family protein
	7	119,978,049	6	GRMZM2G137676	AT2G26450.1: Plant invertase/pectin methylesterase inhibitor superfamily
Other	1	248,154,405	5	GRMZM2G110298	AT5G47630.1(mtACP3): mitochondrial acyl carrier3
	3	30,054,765	5	GRMZM2G171677	Tyrosine kinase specific for activated (GTP-bound) p21cdc42Hs
	3	217,879,923	5	GRMZM2G148532	LOC_Os01g43340.1: retrotransposon protein, putative, unclassified, expressed
	5	140,089,289	5	GRMZM2G060253	AT4G23800.2: HMG (high mobility group) box
	5	140,089,289	5	GRMZM2G060167	LOC_Os02g15820.1: extra-large G-protein-related, putative, expressed
	6	5,438,107	5	GRMZM2G054946	AT3G14470.1: NB-ARC domain-containing disease resistance protein
	6	151,456,265	5	GRMZM2G059314	AT2G37790.1: NAD(P)-linked oxidoreductase superfamily protein
	6	151,456,265	5	GRMZM2G059624	AT5G59850.1: Ribosomal protein S8 family protein
	7	119,978,519	5	GRMZM2G137676	AT2G26450.1: Plant invertase/pectin methylesterase inhibitor superfamily

Table 2-6 Continued

Other	8	166,714,891	5	AC232238.2_FG008	LOC_Os01g64250.1: hemerythrin family protein, expressed
	9	150,815,418	5	GRMZM2G169384	LOC_Os09g04670.1: DAG protein, chloroplast precursor, putative, expressed
	9	150,815,418	5	GRMZM2G169365	AT5G12040.1: Nitrilase/cyanide hydratase and apolipoprotein N-acyltransferase family protein
Expressed Proteins	1	248,154,405	5	GRMZM2G408967	LOC_Os03g39820.1: expressed protein
	1	248,154,405	5	GRMZM2G110294	LOC_Os03g39830.1: expressed protein
	6	151,456,265	5	GRMZM2G059306	LOC_Os05g38219.1: expressed protein
No Annotation	2	213,233,048	39	GRMZM2G021088	No annotated gene
	2	213,233,048	39	GRMZM2G497929	No annotated gene
	2	213,233,048	39	GRMZM2G021020	No annotated gene
	2	213,233,048	39	GRMZM2G497916	No annotated gene
	2	213,233,048	39	GRMZM2G497925	No annotated gene
	2	213,233,048	39	GRMZM2G497920	No annotated gene
	2	213,233,048	39	GRMZM2G559338	No annotated gene
	2	213,233,048	39	GRMZM2G559334	No annotated gene
	2	213,233,048	39	GRMZM2G559330	No annotated gene
	2	213,233,048	39	GRMZM2G559326	No annotated gene
	2	213,233,048	39	GRMZM2G428549	No annotated gene
	2	213,233,048	39	GRMZM2G559318	No annotated gene
	9	152,203,791	37	GRMZM2G478691	No annotated gene
	5	145,727,222	23	GRMZM2G359320	No annotated gene
	5	145,727,222	23	GRMZM2G518061	No annotated gene
	5	145,727,222	23	GRMZM2G022044	No annotated gene
	5	145,727,222	23	GRMZM2G021980	No annotated gene
	5	211,767,155	23	GRMZM2G463935	No annotated gene

Table 2-6 Continued

	1	185,530,739	22	No annotated genes	No annotated gene
	7	1,291,451	20	GRMZM2G421707	No annotated gene
	7	1,291,451	20	GRMZM5G895139	No annotated gene
	10	12,542,065	20	GRMZM2G001194	No annotated gene
	6	105,842,426	19	AC219020.4_FG001	No annotated gene
	7	2,490,915	19	GRMZM2G026060	No annotated gene
	9	152,138,627	17	GRMZM2G390336	No annotated gene
	9	152,138,627	17	GRMZM5G897009	No annotated gene
	10	12,744,140	15	GRMZM2G361791	No annotated gene
	8	166,681,172	13	AC209737.3_FG009	No annotated gene
	8	166,681,172	13	GRMZM2G169391	No annotated gene
	8	166,681,172	13	GRMZM2G584348	No annotated gene
	8	166,681,172	13	GRMZM2G169405	No annotated gene
	5	211,558,679	11	GRMZM2G533819	No annotated gene
No annotation	5	211,558,679	11	AC186372.4_FG001	No annotated gene
	3	23,893,603	8	GRMZM2G114528	No annotated gene
	3	23,893,603	8	AC191265.3_FG003	No annotated gene
	3	23,893,603	8	GRMZM2G114535	No annotated gene
	3	23,893,603	8	GRMZM2G114506	No annotated gene
	7	2,970,401	8	GRMZM5G891809	No annotated gene
	7	2,970,401	8	GRMZM2G512595	No annotated gene
	8	173,028,725	8	GRMZM2G424778	No annotated gene
	2	217,010,357	7	GRMZM5G808987	No annotated gene
	2	217,010,357	7	GRMZM2G172485	No annotated gene
	3	23,009,435	7	GRMZM2G550431	No annotated gene
	3	23,009,435	7	GRMZM2G133187	No annotated gene
	3	43,150,001	7	GRMZM2G485275	No annotated gene
	3	208,618,360	7	GRMZM2G077607	No annotated gene
	3	208,618,360	7	GRMZM2G325956	No annotated gene

Table 2-6 Continued

	3	208,618,360	7	GRMZM2G078072	No annotated gene
	3	217,695,045	7	GRMZM2G500795	No annotated gene
	4	240,798,443	7	GRMZM2G549568	No annotated gene
	4	240,798,443	7	AC210218.2_FG005	No annotated gene
	6	148,247,279	7	AC214451.3_FG004	No annotated gene
	6	148,247,279	7	GRMZM2G478307	No annotated gene
	2	27,961,469	6	No annotated genes	No annotated gene
	2	192,854,841	6	GRMZM2G590927	No annotated gene
	3	209,200,001	6	GRMZM2G037789	No annotated gene
	4	226,356,022	6	GRMZM5G843584	No annotated gene
	6	6,320,084	6	GRMZM2G412459	No annotated gene
	6	151,493,339	6	AC215688.3_FG010	No annotated gene
No annotation	6	151,493,339	6	GRMZM2G036479	No annotated gene
	3	10,624,916	5	GRMZM2G113606	No annotated gene
	3	10,624,916	5	GRMZM2G113552	No annotated gene
	3	10,624,916	5	GRMZM2G113603	No annotated gene
	3	30,054,765	5	GRMZM2G585447	No annotated gene
	3	217,879,923	5	GRMZM2G571445	No annotated gene
	4	146,441,331	5	GRMZM2G536547	No annotated gene
	5	140,089,289	5	AC191751.3_FG003	No annotated gene
	6	115,387,886	5	AC212465.3_FG011	No annotated gene
	6	115,387,886	5	GRMZM2G166390	No annotated gene
	6	115,387,886	5	GRMZM2G467529	No annotated gene
	9	150,815,418	5	GRMZM2G700128	No annotated gene
	10	146,585,004	5	GRMZM2G532898	No annotated gene

Table 2-7 Candidate genes associated with stay-green terminal in the NAM Testcrosses

Candidate Gene Family	Chr	SNP Position	RMIP	Gene ID	Arabidopsis/Rice/PFAM Ortholog
Calcium Signal and Relay	4	173,557,720	16	GRMZM2G108147	AT2G25620.1(AtDBP1,DBP1): DNA-binding protein phosphatase 1
	9	137,496,465	11	GRMZM2G378852	AT2G30040.1(MAPKKK14): mitogen-activated protein kinase kinase kinase 14
General stress-related and transcription factors	2	12,267,754	27	GRMZM2G074743	AT3G22370.1(AOX1A,ATAOX1A): alternative oxidase 1A
	2	45,779,710	18	GRMZM2G021831	AT3G14180.1: sequence-specific DNA binding transcription factors
	8	11,455,569	11	GRMZM2G096358	AT1G68320.1(AtMYB62,BW62B,BW62C,MYB62): myb domain protein 62
	9	143,188,888	10	GRMZM2G147671	AT4G38630.1(ATMCB1,MBP1,MCB1,RPN10): regulatory particle non-ATPase 10
	5	170,164,966	8	GRMZM2G071484	AT3G52450.1(PUB22): plant U-box 22
	10	130,303,000	7	GRMZM2G031721	AT4G13670.1(PTAC5): plastid transcriptionally active 5
	7	171,497,509	6	GRMZM2G330690	AT4G30890.1(UBP24): ubiquitin-specific protease 24
	1	22,318,797	5	GRMZM2G107395	AT1G78300.1(14-3-3OMEGA,GF14 OMEGA,GRF2): general regulatory factor 2
	5	4,034,012	5	GRMZM2G121221	AT2G30620.2: winged-helix DNA-binding transcription factor family protein

Table 2-7 Continued

Phytohormones	2	12,267,754	27	GRMZM2G374203	PFAM ID: PF08381: Transcription factor regulating root and shoot growth via Pin3
	9	143,188,888	10	GRMZM2G156388	AT5G64813.1(LIP1): Ras-related small GTP-binding family protein
	1	16,784,972	9	GRMZM5G838098	AT1G19180.1(JAZ1,TIFY10A): jasmonate-zim-domain protein 1
	1	16,784,972	9	GRMZM2G445634	AT1G19180.1(JAZ1,TIFY10A): jasmonate-zim-domain protein 1
	1	16,784,972	9	GRMZM2G343157	AT3G43440.1(JAZ11,TIFY3A): jasmonate-zim-domain protein 11
Cell Wall Structure	6	134,840,844	20	GRMZM2G170646	AT1G28580.1: GDSL-like Lipase/Acylhydrolase superfamily protein
	5	24,216,926	16	GRMZM2G436710	LOC_Os10g35810.1: thylakoid lumenal protein, putative, expressed
	4	180,346,001	5	GRMZM2G041699	AT1G22360.1(AtUGT85A2,UGT85A2): UDP-glucosyl transferase 85A2
Disease	3	230,256,704	12	GRMZM2G439784	AT2G34930.1: disease resistance family protein / LRR family protein
	3	230,256,704	12	GRMZM2G439799	AT3G47570.1: Leucine-rich repeat protein kinase family protein
	10	131,044,766	6	GRMZM2G146809	LOC_Os02g41904.1: DEF7 - Defensin and Defensin-like DEFL family, expressed
Vesicular Transport	8	174,814,948	23	GRMZM2G055219	AT2G19950.2(GC1): golgin candidate 1
	9	136,918,065	5	GRMZM2G487359	AT4G02030.1: Vps51/Vps67 family (components of vesicular transport) protein
	6	132,416,088	5	GRMZM2G328859	AT2G18180.1: Sec14p-like phosphatidylinositol transfer family protein

Table 2-7 Continued

Other	5	24,216,926	16	GRMZM2G436707	AT1G07280.1: Tetratricopeptide repeat (TPR)-like superfamily protein
	8	151,920,141	10	GRMZM2G445338	AT1G18390.2: Protein kinase superfamily protein
	5	4,619,657	7	GRMZM2G124290	AT1G21326.1: VQ motif-containing protein
	3	229,546,961	5	GRMZM2G467086	AT1G25260.1: Ribosomal protein L10 family protein
	10	115,684,636	15	GRMZM2G042782	AT1G43690.1: ubiquitin interaction motif-containing protein
	6	134,840,844	20	GRMZM2G162702	AT1G56720.1: Protein kinase superfamily protein
	10	130,303,000	7	GRMZM2G031660	AT1G61820.1(BGLU46): beta glucosidase 46
	2	194,066,031	5	GRMZM2G530263	AT2G16030.1: S-adenosyl-L-methionine-dependent methyltransferases superfamily protein
	10	115,684,636	15	GRMZM2G042811	AT2G19130.1: S-locus lectin protein kinase family protein
	9	136,918,065	5	GRMZM2G007590	AT2G30260.1(U2B\'\'): U2 small nuclear ribonucleoprotein B
	9	136,918,065	5	GRMZM2G007514	AT2G38440.1(ATSCAR2,DIS3,ITB1,SCAR2,WAVE4): SCAR homolog 2
	9	136,918,065	5	GRMZM2G007475	AT2G38480.1: Uncharacterised protein family (UPF0497)
	8	113,868,245	8	GRMZM2G139574	AT2G41640.1: Glycosyltransferase family 61 protein
	2	45,779,710	18	GRMZM2G021464	AT3G14080.1: Small nuclear ribonucleoprotein family protein
	3	230,384,225	5	GRMZM2G054610	AT3G25100.1(CDC45): cell division cycle 45
	3	230,384,225	5	GRMZM2G353076	AT3G28917.1(MIF2): mini zinc finger 2
	10	130,303,000	7	GRMZM2G031628	AT4G21760.1(BGLU47): beta-glucosidase 47
	5	4,619,657	7	GRMZM2G124284	AT5G01230.1: S-adenosyl-L-methionine-dependent methyltransferases superfamily protein
	5	4,619,657	7	GRMZM2G124243	AT5G06560.1: Protein of unknown function, DUF593
	4	173,557,720	16	GRMZM2G344376	AT5G11090.1: serine-rich protein-related

Table 2-7 Continued

Other	4	173,557,720	16	GRMZM2G043921	AT5G11090.1: serine-rich protein-related
	5	149,752,575	25	GRMZM2G173674	AT5G17530.3: phosphoglucosamine mutase family protein
	6	118,501,027	5	GRMZM2G054468	AT5G37720.1(ALY4): ALWAYS EARLY 4
	8	151,920,141	10	GRMZM2G144021	AT5G38220.1: alpha/beta-Hydrolases superfamily protein
	3	229,546,961	5	GRMZM2G467123	AT5G45275.1: Major facilitator superfamily protein
	10	127,938,727	5	AC233888.1_FG002	AT5G57660.1(ATCOL5,COL5): CONSTANS-like 5
	9	137,496,465	11	GRMZM2G078933	AT5G58590.1(RANBP1): RAN binding protein 1
	10	127,938,727	5	AC233888.1_FG001	PFAM ID: PF05703: Auxin canalisation , PF08458: Plant pleckstrin homology-like region
	10	131,044,766	6	GRMZM2G446737	PFAM ID: PF05757: Oxygen evolving enhancer protein 3
	8	151,920,141	10	GRMZM2G144028	LOC_Os01g49529.2: OsWAK10d - OsWAK receptor-like cytoplasmic kinase OsWAK-RLCK, expressed
	4	179,080,608	5	GRMZM2G107414	LOC_Os02g52300.1: CPuORF38 - conserved peptide uORF-containing transcript, expressed
Expressed Proteins	4	173,557,720	16	AC200065.5_FG009	LOC_Os02g55580.1: hypothetical protein
	9	143,188,888	10	GRMZM2G147787	LOC_Os03g13870.1: expressed protein
	2	12,267,754	27	GRMZM5G856943	LOC_Os04g51166.1: expressed protein
	3	229,546,961	5	GRMZM2G467134	LOC_Os11g01594.1: expressed protein
No annotation	5	149,752,575	25	GRMZM2G327226	No annotated gene
	5	149,752,575	25	GRMZM2G516562	No annotated gene
	6	134,840,844	20	GRMZM2G170653	No annotated gene
	6	134,840,844	20	GRMZM2G583866	No annotated gene
	6	134,840,844	20	GRMZM2G583859	No annotated gene
	6	134,840,844	20	GRMZM5G856969	No annotated gene
	2	45,779,710	18	GRMZM2G006638	No annotated gene
	2	45,779,710	18	GRMZM2G314173	No annotated gene
	4	173,557,720	16	GRMZM5G822849	No annotated gene
	4	173,557,720	16	GRMZM2G508996	No annotated gene

Table 2-7 Continued

	4	173,557,720	16	GRMZM2G043910	No annotated gene
	4	173,557,720	16	GRMZM2G043902	No annotated gene
	4	173,557,720	16	GRMZM2G508969	No annotated gene
	4	173,557,720	16	GRMZM2G508968	No annotated gene
	5	24,216,926	16	AC196432.3_FG007	No annotated gene
	10	115,684,636	15	GRMZM2G509143	No annotated gene
	3	230,256,704	12	GRMZM2G139840	No annotated gene
	3	230,256,704	12	GRMZM2G439816	No annotated gene
	9	137,496,465	11	GRMZM2G378853	No annotated gene
	9	137,496,465	11	GRMZM5G808578	No annotated gene
	9	137,496,465	11	GRMZM2G529645	No annotated gene
	9	137,496,465	11	GRMZM2G079027	No annotated gene
	8	151,920,141	10	GRMZM2G569684	No annotated gene
	8	151,920,141	10	GRMZM2G569681	No annotated gene
No annotation	8	151,920,141	10	GRMZM2G569679	No annotated gene
	9	143,188,888	10	AC203209.3_FG004	No annotated gene
	9	143,188,888	10	GRMZM5G876445	No annotated gene
	9	143,188,888	10	GRMZM2G572049	No annotated gene
	1	16,784,972	9	AC177911.4_FG005	No annotated gene
	2	193,772,001	9	AC191363.3_FG006	No annotated gene
	2	193,772,001	9	GRMZM2G523256	No annotated gene
	5	170,164,966	8	GRMZM2G071528	No annotated gene
	5	170,164,966	8	GRMZM2G525430	No annotated gene
	5	4,619,657	7	GRMZM5G810402	No annotated gene
	5	4,619,657	7	GRMZM2G124249	No annotated gene
	5	4,619,657	7	GRMZM2G124280	No annotated gene
	6	132,329,046	7	No annotated genes	No annotated gene
	9	137,496,298	7	GRMZM5G808578	No annotated gene
	9	137,496,298	7	GRMZM2G529645	No annotated gene

Table 2-7 Continued

	9	137,496,298	7	GRMZM2G079027	No annotated gene
	9	137,496,298	7	GRMZM2G378853	No annotated gene
	10	130,303,000	7	AC195682.4_FG008	No annotated gene
	3	229,457,305	6	No annotated genes	No annotated gene
	7	171,497,509	6	GRMZM2G313742	No annotated gene
	7	171,497,509	6	GRMZM5G837729	No annotated gene
	7	171,497,509	6	GRMZM2G014754	No annotated gene
	2	194,066,031	5	GRMZM2G114022	No annotated gene
	3	229,546,961	5	GRMZM2G583006	No annotated gene
No annotation	3	229,546,961	5	GRMZM2G583003	No annotated gene
	4	179,080,608	5	AC185630.3_FG002	No annotated gene
	4	179,080,608	5	GRMZM2G107410	No annotated gene
	4	179,080,608	5	GRMZM2G546531	No annotated gene
	5	4,034,012	5	GRMZM2G555375	No annotated gene
	5	4,034,012	5	GRMZM2G555372	No annotated gene
	6	132,416,088	5	GRMZM2G516171	No annotated gene
	6	132,416,088	5	AC203331.4_FG006	No annotated gene
	6	132,416,088	5	GRMZM2G499741	No annotated gene
	9	136,918,065	5	AC203300.3_FG004	No annotated gene

2.5.1.3 Stay-green Difference Candidate Genes

The stay-green difference phenotype captures the variation of delayed plant senescence. This would be classified as either a Type A or B stay-green.

Additional groups of genes related to disease, heat stress, expressed proteins, and unannotated proteins were identified in the populations. Only candidate genes for stay-green difference in the NAM RILs are reported in Table 2-8 as there were no significant SNPs in the AMES diversity panel and the phenotype was not collected in the NAM testcrosses.

Table 2-8 Stay-green Difference Candidate Genes in the NAM RILs

Candidate Gene Family	Chr	SNP Position	RMIP	Gene ID	Arabidopsis/Rice/PFAM Ortholog
Calcium Signaling and Relay	6	110,612,431	10	GRMZM2G009703	AT4G28980.1(CAK1AT,CDKF;1): CDK-activating kinase 1AT
General stress-related and transcription factors	5	198,207,996	43	GRMZM2G044851	AT1G32450.1(NRT1.5): nitrate transporter 1.5
	5	198,207,996	43	GRMZM2G058930	AT4G14030.1(SBP1): selenium-binding protein 1
	1	108,563,398	24	GRMZM2G036567	Rice best hit: LOC_Os10g01290.1: PHLOEM 2-LIKE A10, putative, expressed
	7	129,439,412	21	GRMZM2G063517	AT2G22400.1: S-adenosyl-L-methionine-dependent methyltransferases superfamily protein
	2	215,944,843	12	GRMZM2G458437	AT5G18560.1(PUCHI): Integrase-type DNA-binding superfamily protein
	1	40,916,063	10	AC233935.1_FG005	AT3G55370.3(OBP3): OBF-binding protein 3
	5	70,689,438	7	GRMZM2G120578	AT5G53120.1(ATSPDS3,SPDS3,SPMS): spermidine synthase 3
	3	150,837,092	6	GRMZM2G082387	Rice best hit: LOC_Os01g71970.1: GRAS family transcription factor containing protein, expressed
	7	172,501,891	6	GRMZM2G113863	AT5G27690.1: Heavy metal transport/detoxification superfamily protein
Cell Wall Structure	7	302,735	21	GRMZM5G800488	AT3G09220.1(LAC7): laccase 7
	6	103,645,832	20	AC194852.3_FG007	AT1G14420.1(AT59): Pectate lyase family protein
	2	215,944,843	12	GRMZM2G158766	AT4G02620.1: vacuolar ATPase subunit F family
	4	166,980,842	8	GRMZM2G063316	AT1G24610.1: Rubisco methyltransferase family protein
	3	13,538,705	7	GRMZM5G832229	AT2G06520.1(PSBX): photosystem II subunit X
	3	13,538,705	7	GRMZM2G146627	AT2G25810.1(TIP4;1): tonoplast intrinsic protein 4;1
	8	163,904,027	5	AC233916.1_FG002	AT1G05800.1(DGL): alpha/beta-Hydrolases superfamily protein

Table 2-8 Continued

Sugar Transport and Secondary Messengers	7	302,735	21	GRMZM2G152059	AT5G01090.1: Concanavalin A-like lectin family protein
	2	233,015,071	11	GRMZM2G381766	AT2G37710.1(RLK): receptor lectin kinase
Phytohormone	1	299,119,738	18	GRMZM2G176612	AT4G17890.1(AGD8): ARF-GAP domain 8
	6	93,208,896	18	GRMZM2G048092	AT1G16540.1(ABA3,ACI2,ATABA3,LOS5,SIR3): molybdenum cofactor sulfurase (LOS5) (ABA3)
	5	70,689,438	7	GRMZM2G120539	AT1G20560.1(AAE1): acyl activating enzyme 1
	7	172,501,891	6	GRMZM2G414460	AT2G47750.1(GH3.9): putative indole-3-acetic acid-amido synthetase GH3.9
	7	120,764,288	5	GRMZM2G099049	AT1G56220.4: Dormancy/auxin associated family protein
Heat	3	9,242,298	22	GRMZM2G151444	AT4G39410.1(ATWRKY13,WRKY13): WRKY DNA-binding protein 13
Disease	1	299,119,738	18	GRMZM2G479249	AT3G02910.1: AIG2-like (avirulence induced gene) family protein
	7	127,251,952	12	GRMZM2G072240	AT3G63470.1(scpl40): serine carboxypeptidase-like 40
	7	127,251,952	12	GRMZM2G072218	AT3G63470.1(scpl40): serine carboxypeptidase-like 40
	7	2,504,001	10	GRMZM2G026083	AT3G14470.1: NB-ARC domain-containing disease resistance protein
	10	9,846,957	6	GRMZM2G388776	AT3G47580.1: Leucine-rich repeat protein kinase family protein
Other	8	163,904,027	5	GRMZM5G821267	AT1G24330.1: ARM repeat superfamily protein
	4	15,932,903	8	GRMZM2G181422	AT1G05730.1: Eukaryotic protein of unknown function (DUF842)
	5	197,603,889	6	GRMZM2G029815	AT1G65920.1: Regulator of chromosome condensation (RCC1) family with FYVE zinc finger domain

Table 2-8 Continued

Other	8	163,904,027	5	GRMZM2G700757	AT2G19490.1: recA DNA recombination family protein
	2	233,685,369	5	GRMZM2G469469	AT2G32040.1: Major facilitator superfamily protein
	7	3,008,523	7	GRMZM2G044060	AT3G18860.1: transducin family protein / WD-40 repeat family protein
	3	9,382,001	31	GRMZM5G832672	AT3G22440.1: FRIGIDA-like protein
	3	221,690,562	9	GRMZM2G071021	AT3G24503.1(ALDH1A,ALDH2C4,REF1): aldehyde dehydrogenase 2C4
	3	221,690,562	9	GRMZM2G097706	AT3G24503.1(ALDH1A,ALDH2C4,REF1): aldehyde dehydrogenase 2C4
	10	9,846,957	6	GRMZM2G388776	AT3G47580.1: Leucine-rich repeat protein kinase family protein
	7	127,251,952	12	GRMZM2G072240	AT3G63470.1(scpl40): serine carboxypeptidase-like 40
	7	127,251,952	12	GRMZM2G072218	AT3G63470.1(scpl40): serine carboxypeptidase-like 40
	2	233,685,369	5	GRMZM2G469477	AT4G14830.1(HSP1):
	3	221,690,562	9	GRMZM2G366935	AT4G32660.1(AME3): Protein kinase superfamily protein
	2	233,685,369	5	GRMZM2G170896	AT5G03800.1(EMB166,EMB175,emb1899): Pentatricopeptide repeat (PPR) superfamily protein
	1	62,555,292	8	GRMZM5G822100	AT5G07990.1(CYP75B1,D501,TT7): Cytochrome P450 superfamily protein
	5	197,603,889	6	GRMZM2G029850	AT5G17300.1(RVE1): Homeodomain-like superfamily protein
	6	160,332,779	5	GRMZM2G043943	AT5G19730.1: Pectin lyase-like superfamily protein
	3	13,538,705	7	GRMZM2G447857	AT5G66631.1: Tetratricopeptide repeat (TPR)-like superfamily protein

Table 2-8 Continued

Other	2	233,685,369	5	GRMZM2G170934	Arabidopsis best hit: AT3G22440.1: FRIGIDA-like protein
	3	9,382,001	31	GRMZM5G871126	Rice best hit: LOC_Os01g08550.1: aminoacyl-tRNA synthetase, putative, expressed
	1	299,119,738	18	GRMZM2G590033	Rice best hit: LOC_Os01g13730.1: WD domain, G-beta repeat domain containing protein, expressed
	7	3,008,523	7	GRMZM2G044174	Rice best hit: LOC_Os07g03180.1: GCRP3 - Glycine and cysteine rich family protein precursor,
Expressed Proteins	3	150,837,092	6	GRMZM2G530589	Rice best hit: LOC_Os02g48600.1: expressed protein
	4	166,980,842	8	GRMZM2G362823	Rice best hit: LOC_Os02g50110.1: expressed protein
	7	302,735	21	GRMZM2G152028	Rice best hit: LOC_Os03g01008.1: expressed protein
	6	160,332,779	5	GRMZM5G846097	Rice best hit: LOC_Os05g01330.1: expressed protein
	6	93,208,896	18	GRMZM2G047969	Rice best hit: LOC_Os06g45870.1: expressed protein
No annotation	5	198,207,996	43	GRMZM2G058943	No candidate gene
	5	198,207,996	43	AC216070.2_FG005	No candidate gene
	5	198,207,996	43	GRMZM2G517996	No candidate gene
	9	84,661,869	40	GRMZM2G396156	No candidate gene
	9	84,661,869	40	AC190675.3_FG002	No candidate gene
	3	9,242,298	22	AC204707.4_FG003	No candidate gene
	3	9,242,298	22	GRMZM2G573370	No candidate gene
	3	9,242,298	22	GRMZM2G573365	No candidate gene
	3	9,242,298	22	GRMZM2G573364	No candidate gene
	3	9,242,298	22	GRMZM2G451364	No candidate gene
	9	105,634,001	22	GRMZM5G848174	No candidate gene

Table 2-8 Continued

	7	302,735	21	GRMZM2G512515	No candidate gene
	7	129,439,412	21	AC214533.2_FG001	No candidate gene
	6	103,645,832	20	AC186818.3_FG003	No candidate gene
	2	215,944,843	12	GRMZM5G855326	No candidate gene
	7	127,251,952	12	GRMZM2G373247	No candidate gene
	7	127,251,952	12	GRMZM2G526122	No candidate gene
	7	127,251,952	12	GRMZM2G373252	No candidate gene
	7	127,251,952	12	GRMZM2G373258	No candidate gene
	2	233,015,071	11	GRMZM2G530304	No candidate gene
	1	40,916,063	10	AC233935.1_FG004	No candidate gene
	4	223,131,660	10	GRMZM2G359213	No candidate gene
	6	110,612,431	10	GRMZM2G309822	No candidate gene
	7	2,504,001	10	GRMZM5G873482	No candidate gene
	7	2,504,001	10	GRMZM2G026063	No candidate gene
No annotation	7	2,504,001	10	GRMZM2G026081	No candidate gene
	7	2,504,001	10	GRMZM2G497991	No candidate gene
	3	221,690,562	9	GRMZM2G522545	No candidate gene
	8	31,502,768	9	GRMZM2G518305	No candidate gene
	9	72,271	9	GRMZM2G354611	No candidate gene
	1	62,555,292	8	GRMZM5G864088	No candidate gene
	1	62,555,292	8	GRMZM2G358594	No candidate gene
	1	62,555,292	8	GRMZM5G830483	No candidate gene
	1	62,555,292	8	GRMZM5G802598	No candidate gene
	1	62,555,292	8	GRMZM2G703590	No candidate gene
	1	154,159,228	8	GRMZM2G029981	No candidate gene
	4	15,932,903	8	GRMZM2G591492	No candidate gene
	4	166,980,842	8	AC185474.3_FG005	No candidate gene
	4	166,980,842	8	GRMZM2G063344	No candidate gene
	1	154,094,060	7	AC196058.3_FG002	No candidate gene

Table 2-8 Continued

	3	8,568,869	7	GRMZM2G131001	No candidate gene
	3	8,568,869	7	GRMZM2G561056	No candidate gene
	3	8,568,869	7	GRMZM2G051348	No candidate gene
	3	13,538,705	7	GRMZM2G146743	No candidate gene
	3	13,538,705	7	GRMZM2G146740	No candidate gene
	3	13,538,705	7	GRMZM2G447869	No candidate gene
	3	13,538,705	7	GRMZM2G146679	No candidate gene
	3	13,538,705	7	GRMZM2G146661	No candidate gene
	5	70,689,438	7	GRMZM5G894801	No candidate gene
	5	70,689,438	7	GRMZM2G120654	No candidate gene
	7	3,008,523	7	AC204845.3_FG008	No candidate gene
	1	93,097,477	6	GRMZM2G571899	No candidate gene
	3	150,837,092	6	GRMZM2G082381	No candidate gene
	3	150,837,092	6	GRMZM2G530586	No candidate gene
No annotation	3	150,837,092	6	GRMZM2G380368	No candidate gene
	3	222,025,874	6	GRMZM2G576662	No candidate gene
	5	197,603,889	6	GRMZM2G501053	No candidate gene
	7	172,501,891	6	GRMZM2G414473	No candidate gene
	8	33,585,313	6	AC204714.3_FG001	No candidate gene
	10	9,846,957	6	GRMZM5G856076	No candidate gene
	10	9,846,957	6	GRMZM2G110374	No candidate gene
	10	9,846,957	6	GRMZM2G544885	No candidate gene
	10	9,846,957	6	GRMZM2G582312	No candidate gene
	2	233,685,369	5	GRMZM2G584410	No candidate gene
	2	233,685,369	5	GRMZM2G469486	No candidate gene
	2	233,685,369	5	GRMZM2G584415	No candidate gene
	6	160,332,779	5	GRMZM2G345798	No candidate gene
	6	160,332,779	5	GRMZM2G044048	No candidate gene
	7	120,764,288	5	GRMZM5G821047	No candidate gene

2.5.1.4 Candidate Genes for Stay-green Ratio

There was not a tight overlap in candidate genes for stay-green ratio in the NAM RILs and AMES Diversity panel. Gene families similar to those described for the other stay-green phenotypes were identified and characterized for this phenotype in the NAM RILs. Additional groups of genes related to disease, heat stress, expressed proteins, and unannotated proteins were identified in the populations. Only candidate genes for stay-green ratio in the NAM RILs are reported in Table 2-9 as there were no significant SNPs in the AMES diversity panel and the phenotype was not collected in the NAM testcrosses.

Table 2-9 Candidate genes for stay-green ratio in the NAM RILs

Candidate Gene Family	Chr	SNP Position	RMIP	Gene ID	Arabidopsis/Rice/PFAM Ortholog
Calcium Signaling and Relay	6	110,611,882	6	GRMZM2G009703	AT4G28980.1(CAK1AT,CDKF;1): CDK-activating kinase 1AT
	7	1,294,057	5	GRMZM2G120563	AT3G17980.1: Calcium-dependent lipid-binding
General stress-related and transcription factors	5	197,634,001	27	GRMZM2G029850	LOC_Os02g46030.1: MYB family transcription factor, putative, expressed
	5	197,634,001	27	GRMZM2G029815	Regulator of chromosome condensation (RCC1) repeat , PF01363: FYVE zinc finger , PF08381: Transcription factor regulating root and shoot growth via Pin3
	3	24,265,645	19	GRMZM2G011436	LOC_Os01g03570.1: transcription factor X1, putative,
	5	198,207,996	13	GRMZM2G058930	AT4G14030.1(SBP1): selenium-binding protein 1
	5	198,207,996	13	GRMZM2G044851	AT1G32450.1(NRT1.5): nitrate transporter 1.5
	1	175,638,951	12	GRMZM2G141955	AT2G45190.1(AFO,FIL,YAB1): Plant-specific transcription factor YABBY family protein
	2	215,944,843	11	GRMZM2G458437	AT5G18560.1(PUCHI): Integrase-type DNA-binding
	3	216,815,460	10	GRMZM2G064283	AT4G39370.3(UBP27): ubiquitin-specific protease 27
	4	183,922,262	9	GRMZM5G822947	AT5G27760.1: Hypoxia-responsive family protein
	8	167,982,452	9	GRMZM2G169316	AT3G55730.1(AtMYB109,MYB109): myb domain protein 109
	3	48,937,505	8	GRMZM2G420199	LOC_Os01g51140.2: helix-loop-helix DNA-binding domain containing protein, expressed
	4	185,306,610	7	GRMZM2G131516	AT3G54220.1(SCR,SGR1): GRAS family transcription factor

Table 2-9 Continued

General stress-related and transcription factors	3	41,606,364	6	GRMZM2G013378	AT1G03350.1: BSD domain-containing protein
	3	150,837,092	6	GRMZM2G082387	LOC_Os01g71970.1: GRAS family transcription factor
	4	27,763,282	6	GRMZM2G171311	AT5G65630.1(GTE7): global transcription factor group E7
	3	190,318,172	5	GRMZM2G440529	AT1G61660.1: basic helix-loop-helix (bHLH) DNA-binding superfamily protein
	3	190,318,172	5	GRMZM2G138800	AT5G54500.1(FQR1): flavodoxin-like quinone reductase 1
	10	4,676,058	5	GRMZM2G003762	AT5G19140.1(AILP1,ATAILP1): Aluminum induced protein with YGL and LRDR motifs
Vesicular Transport	8	166,834,738	6	GRMZM2G316534	AT1G08280.1: Glycosyltransferase family 29 (sialyltransferase) family protein
Cell Wall Structure	2	215,944,843	11	GRMZM2G158766	PFAM ID: PF01990: ATP synthase (F/14-kDa) subunit
	2	24,397,510	8	GRMZM2G434557	AT3G43660.1: Vacuolar iron transporter (VIT) family protein
	3	44,662,742	6	GRMZM5G840699	AT5G04930.1(ALA1): aminophospholipid ATPase 1
	4	174,920,478	5	GRMZM2G146346	AT3G49750.1(AtRLP44,RLP44): receptor like protein 44
	7	1,291,451	13	GRMZM2G120652	AT5G01410.1(ATPDX1,ATPDX1.3,PDX1,PDX1.3,RSR4): Aldolase-type TIM barrel family protein
	7	1,291,451	13	GRMZM2G120574	AT5G53890.1(AtPSKR2,PSKR2): phytosylfokine-alpha receptor 2
	10	4,676,058	5	GRMZM2G004414	AT1G08960.1(ATCAX11,CAX11): cation exchanger 11
Sugar Transport and Secondary Messengers	4	174,954,655	5	GRMZM2G312521	AT2G18700.1(ATTPS11,ATTPSB,TPS11): trehalose phosphatase/synthase 11
	9	146,210,771	5	GRMZM5G824920	AT2G01630.1: O-Glycosyl hydrolases family 17 protein
Phytohormone	2	215,636,276	12	GRMZM2G070563	AT5G65980.1: Auxin efflux carrier family protein
	3	15,048,001	7	GRMZM5G862219	AT3G51840.1(ACX4,ATG6,ATSCX): acyl-CoA oxidase 4
	4	174,920,478	5	GRMZM2G446313	AT5G57740.1(XBAT32): XB3 ortholog 2 in Arabidopsis thaliana

Table 2-9 Continued

Disease	7	2,311,738	14	GRMZM2G337881	PFAM ID: PF00931: NB-ARC domain
	2	215,644,483	6	GRMZM2G005493	AT5G57655.2: xylose isomerase family protein
	1	93,266,541	5	GRMZM2G365134	AT4G16790.1: hydroxyproline-rich glycoprotein family protein
Other	1	289,526,191	8	GRMZM2G101682	LOC_Os03g58850.1: uncharacterized PE-PGRS family protein PE_PGRS3 precursor, putative, expressed
	7	1,294,057	5	GRMZM2G120575	LOC_Os11g16480.1: transposon protein, putative, unclassified, expressed
	2	215,636,276	12	GRMZM5G873277	AT1G54610.1: Protein kinase superfamily protein
	9	155,976,827	7	GRMZM2G148090	AT2G05160.1: CCCH-type zinc fingerfamily protein with RNA-binding domain
	3	15,048,001	7	GRMZM2G165044	AT2G15530.1: RING/U-box superfamily protein
	4	174,954,655	5	GRMZM2G016362	AT2G18650.1(MEE16): RING/U-box superfamily protein
	8	167,982,452	9	GRMZM2G169329	AT2G37970.1(SOUL-1): SOUL heme-binding family protein
	2	216,690,121	16	GRMZM2G001297	AT3G06810.1(IBR3): acyl-CoA dehydrogenase-related
	10	4,676,058	5	GRMZM2G003750	AT3G26085.3: CAAX amino terminal protease family
	2	215,644,483	6	GRMZM2G306998	AT3G26330.1(CYP71B37): cytochrome P450, family 71, subfamily B, polypeptide 37
	8	166,834,738	6	GRMZM2G020728	AT4G21110.1: G10 family protein
	3	48,937,505	8	GRMZM2G420199	LOC_Os01g51140.2: helix-loop-helix DNA-binding domain containing protein, expressed
Expressed Proteins	3	150,837,092	6	GRMZM2G530589	LOC_Os02g48600.1: expressed protein
	9	155,976,827	7	GRMZM2G158293	LOC_Os03g39740.1: expressed protein
	7	1,291,451	13	GRMZM2G120572	LOC_Os07g01720.1: expressed protein
	3	222,475,972	7	GRMZM5G840887	LOC_Os01g40990.2: expressed protein
	3	222,475,972	7	GRMZM2G135120	LOC_Os01g40990.2: expressed protein
	7	1,294,057	5	GRMZM2G120572	LOC_Os07g01720.1: expressed protein
	4	183,922,262	9	GRMZM2G138936	LOC_Os11g02090.2: expressed protein

Table 2-9 Continued

	6	31,997,036	20	GRMZM2G481592	No annotated gene
	6	31,997,036	20	GRMZM2G181120	No annotated gene
	6	31,997,036	20	GRMZM2G481586	No annotated gene
	6	31,997,036	20	GRMZM2G589668	No annotated gene
	5	197,670,001	15	GRMZM2G518693	No annotated gene
	6	79,420,001	15	GRMZM2G444194	No annotated gene
	7	2,311,738	14	GRMZM2G505238	No annotated gene
	7	2,311,738	14	GRMZM2G496998	No annotated gene
	1	93,097,477	13	GRMZM2G571899	No annotated gene
	5	198,207,996	13	GRMZM2G058943	No annotated gene
	5	198,207,996	13	AC216070.2_FG005	No annotated gene
	5	198,207,996	13	GRMZM2G509724	No annotated gene
	5	198,207,996	13	GRMZM2G517996	No annotated gene
	7	1,291,451	13	GRMZM5G895139	No annotated gene
No annotation	7	1,291,451	13	GRMZM2G421707	No annotated gene
	1	175,638,951	12	AC186234.3_FG005	No annotated gene
	1	175,638,951	12	GRMZM2G568405	No annotated gene
	1	175,638,951	12	AC186234.3_FG003	No annotated gene
	1	175,638,951	12	GRMZM2G568380	No annotated gene
	2	215,636,276	12	GRMZM2G524252	No annotated gene
	2	215,636,276	12	GRMZM5G811899	No annotated gene
	2	215,636,276	12	GRMZM2G070558	No annotated gene
	2	215,636,276	12	GRMZM2G070551	No annotated gene
	2	215,636,276	12	GRMZM2G524232	No annotated gene
	3	43,280,587	12	GRMZM2G390664	No annotated gene
	3	43,280,587	12	GRMZM2G120905	No annotated gene
	3	43,280,587	12	GRMZM2G120899	No annotated gene
	1	207,811,343	11	GRMZM2G552005	No annotated gene
	2	215,944,843	11	GRMZM5G855326	No annotated gene

Table 2-9 Continued

	6	110,648,930	11	GRMZM5G840543	No annotated gene
	6	110,648,930	11	GRMZM2G066444	No annotated gene
	2	24,487,007	10	GRMZM2G026594	No annotated gene
	2	24,487,007	10	GRMZM2G499324	No annotated gene
	1	91,751,628	9	GRMZM2G038034	No annotated gene
	7	2,310,408	9	GRMZM2G505238	No annotated gene
	8	167,982,452	9	GRMZM2G584833	No annotated gene
	1	289,526,191	8	GRMZM2G101783	No annotated gene
	2	25,776,205	8	AC218093.3_FG005	No annotated gene
	3	48,937,505	8	GRMZM2G554254	No annotated gene
	3	48,937,505	8	GRMZM2G554247	No annotated gene
	3	48,937,505	8	GRMZM2G119597	No annotated gene
	3	48,937,505	8	GRMZM2G420188	No annotated gene
	1	93,098,542	7	GRMZM2G571899	No annotated gene
No annotation	2	11,116,907	7	GRMZM2G535245	No annotated gene
	4	185,306,610	7	GRMZM5G857119	No annotated gene
	4	185,306,610	7	GRMZM5G877428	No annotated gene
	4	185,306,610	7	GRMZM2G561218	No annotated gene
	9	76,962	7	GRMZM2G354611	No annotated gene
	1	93,098,238	6	GRMZM2G571899	No annotated gene
	2	215,644,483	6	GRMZM2G524232	No annotated gene
	2	215,644,483	6	GRMZM2G070551	No annotated gene
	2	215,644,483	6	GRMZM2G070558	No annotated gene
	3	41,606,364	6	GRMZM2G161613	No annotated gene
	3	44,662,742	6	GRMZM5G886583	No annotated gene
	3	44,662,742	6	GRMZM5G899881	No annotated gene
	4	185,290,753	5	No annotated genes	No annotated gene
	6	36,379,331	5	GRMZM2G400716	No annotated gene
	6	36,379,331	5	GRMZM5G871576	No annotated gene

Table 2-9 Continued

	6	36,379,331	5	GRMZM2G400683	No annotated gene
	6	97,861,447	5	GRMZM2G047775	No annotated gene
	6	97,861,447	5	GRMZM2G486900	No annotated gene
	7	1,294,057	5	GRMZM5G895139	No annotated gene
	7	1,294,057	5	GRMZM2G421707	No annotated gene
	9	135,688,774	5	GRMZM2G351951	No annotated gene
	9	135,763,373	5	No annotated genes	No annotated gene
	9	146,210,771	5	GRMZM5G820832	No annotated gene
	9	146,210,771	5	GRMZM5G844692	No annotated gene
	10	4,676,058	5	GRMZM2G485603	No annotated gene
	10	4,676,058	5	GRMZM2G485601	No annotated gene
	3	150,837,092	6	GRMZM2G082381	No annotated gene
	3	150,837,092	6	GRMZM2G530586	No annotated gene
	3	150,837,092	6	GRMZM2G380368	No annotated gene
No annotation	6	110,611,882	6	GRMZM2G309822	No annotated gene
	7	121,657,758	6	GRMZM2G431219	No annotated gene
	8	166,834,738	6	GRMZM2G485959	No annotated gene
	8	166,834,738	6	AC206610.4_FG013	No annotated gene
	8	166,834,738	6	GRMZM2G328239	No annotated gene
	8	166,834,738	6	GRMZM2G026847	No annotated gene
	9	476,632	6	GRMZM2G567592	No annotated gene
	9	476,632	6	GRMZM2G142178	No annotated gene
	9	476,632	6	GRMZM2G142185	No annotated gene
	2	27,567,458	5	GRMZM5G806743	No annotated gene
	2	27,567,458	5	GRMZM2G306735	No annotated gene
	2	27,567,458	5	GRMZM2G486496	No annotated gene
	2	27,567,458	5	GRMZM5G812121	No annotated gene
	2	27,567,458	5	GRMZM2G486490	No annotated gene
	3	44,620,604	5	No annotated genes	No annotated gene

Table 2-9 Continued

	3	190,318,172	5	GRMZM2G138802	No annotated gene
	3	190,318,172	5	AC195817.3_FG002	No annotated gene
	4	174,920,478	5	GRMZM2G570369	No annotated gene
	4	174,920,478	5	GRMZM2G146330	No annotated gene
No annotation	4	174,954,655	5	GRMZM5G893801	No annotated gene
	4	183,922,262	9	AC204776.3_FG003	No annotated gene
	4	183,922,262	9	GRMZM2G138931	No annotated gene
	4	183,922,262	9	GRMZM2G138918	No annotated gene
	6	105,842,426	7	AC219020.4_FG001	No annotated gene

2.5.2 Summarization of Candidate Genes

2.5.2.1 Challenges of Characterizing Stay-green

Stay-green is a complex, quantitative trait. Further complicating stay-green is the intricacy of accurately phenotyping and analyzing data from multiple populations and models. The AMES diversity panel utilizes a standard association mapping model accounting for population structure using principle components and kinship using background markers and days-to-anthesis as covariates in the model. The NAM populations uses QTL identified from joint-linkage analysis as cofactors in the association mapping model. This regression model also controls population structure. The two methods for analyzing stay-green data increases the complexity of drawing relationships between the populations.

In the NAM analysis, association mapping results can be supported by linkage peaks from joint-linkage QTL mapping. However, we observed significant SNPs that did not contain any linkage support. These association mapping peaks may represent potential false positives and should be carefully examined.

Phenotyping stay-green presents unique challenges. First, obtaining enough stress on the population can be difficult in certain locations where drought does not occur regularly. While stress was present in most of these studies, the types of drought stress can alter the genetic characterization and expression of stay-green. Phenotyping efficiently at peak segregation can also be difficult for stay-green, where disease symptoms and heat-stress related phenotypes can distort stay-green measurements. Finally, testing both inbreds and testcrosses can make comparing association mapping results difficult and is further complicated by using only one tester.

The stay-green traits of maize exhibit low heritability that make genetic and association mapping difficult. However, there appears to be four to ten major QTL controlling the trait across four different phenotypes in maize. It is remarkable that a trait so difficult to phenotype and characterize exhibited collocating SNPs between different maize populations using different analytical models.

Based on the characterization of annotated candidate genes, stay-green appears to be regulated by several stress-related gene families. These gene families are: calcium signaling and relay, stress-related transcription factors, cell-wall related genes, phytohormones, vesicular transportation, sugar transportation, and secondary stress messengers. Disease related gene families were identified in the NAM RILs and NAM testcrosses. The presence of disease related gene families supports visual evidence of disease in 2012 and 2013 in Indiana. Common rust and gray leaf spot were identified in the inbred populations in 2012 and 2013 (Dr. Kiersten Wise, personal communication). No information is available about the field and disease conditions in the NAM testcrosses, however; SNP associations for disease resistance were identified in association mapping results. Heat stress-related gene families and some maturity related genes were also identified and it is reasonable to detect these families based on environmental conditions present at the time of the experiment.

Another factor influencing interpretation of association mapping in maize is the characterization of annotated and non-annotated genes. For our analyses, only genes with annotations were considered as candidates regardless if non-annotated genes were closer to the significant SNP in an LD block. Therefore, while there are many encouraging

annotated candidate genes, non-annotated genes could potentially be involved to various degrees in regulating stay-green on a genetic and physiological level.

2.5.2.2 Gene Families Regulating Stay-green Expression

Stay-green phenotypes appear to be regulated by several gene families. Significant SNPs were identified across all phenotypes and QTL provided linkage support. However, there were SNP associations that did not have linkage support but contained candidate genes related to stay-green and abiotic stress responses. Therefore, SNPs without any linkage support cannot be immediately discarded as false positives. It is reasonable to conclude that stay-green is regulated in part by calcium-related signaling and transduction genes that sense a dynamic change in the plant cell equilibrium initiating a cascade response. Cell wall related genes involved in manipulating the cellular membrane and structure along with vesicular transport genes. Additionally, sugar transporters and other secondary messengers, general stress transcription factors, and phytohormones are actively regulating expression of stay-green.

While there are over 250+ genes identified across four stay-green phenotypes in maize, some candidates are more interesting than others because of their detection in more than one maize population. An ethylene response element binding factor associated with stay-green terminal in the AMES and NAM RIL populations is an interesting candidate since it is a phytohormone involved in regulating senescence. A pectin methyltransferase inhibitor was also associated with terminal stay-green in the AMES and NAM RIL populations. While not as compelling of a candidate gene as an ethylene-related protein, pectin and other cell wall genes are interesting candidates for a phenotype such as stay-green terminal. It is hard to speculate the causative or response nature of

this gene. Stay-green anthesis was the only other phenotype with close enough genomic relationships between two populations to speculate the nature of candidate genes as discussed previously in this section.

2.5.2.3 Implications and Future Characterization of Stay-green in Maize

Identification of stay-green candidate genes ushers in an exciting era for crop improvement for challenging environments. Elite temperate material has a genetic gain ceiling to yield and abiotic stress tolerance. Enhancing elite germplasm with stay-green alleles from tropical and temperate donors promises to increase the genetic diversity of maize while increasing abiotic stress tolerance, thereby indirectly increasing yield. Future work in maize stay-green requires the following steps to successfully enhance germplasm sources.

1. Cloning and functional characterization of major stay-green alleles

We have identified a few hundred SNP associations corresponding to annotated genes for four stay-green phenotypes. Follow up work to identify and functional characterize the major influencers of stay-green, most likely the genes identified in multiple populations and/or from linkage populations, will be critical for future success. Near-isogenic lines will need to be developed to characterize the candidate genes in multiple genetic backgrounds and testcrosses to account for the genetic mode of inheritance and agronomic value. This process will also identify the ideal lines to release into breeding programs. Molecular characterization will be essential to confirming the relationship of the candidate genes to the agronomic and physiological response. Additionally, this project increases the scientific knowledge of plant adaptation to abiotic stresses, specifically utilizing stay-green. Once this process is complete, donor lines from

either the NAM population, AMES panel, or breeding populations can be made available per se or in hybrid combination to the private and public sectors to enhance maize germplasm for abiotic stress tolerance.

2. Leveraging genomic information into other cereals

Maize is a highly invested crop in terms of research support and agronomic value globally. Its relationship to other cereal species provides a powerful platform for leveraging scientific knowledge into other cereal genomes. We examined stay-green relationships in other cereal species, specifically sorghum, and report the results in chapter three of this dissertation.

The potential benefits from leveraging genomic knowledge between species are limitless. Genomic information is quickly becoming overwhelming to analyze, but once harnessed, lesser invested crop species can be dissected and evaluated using comparative genomics. The ability for crop improvement is greatly enhanced through this process, and we provide evidence that this is a reliable and cost-effective method of crop improvement in the areas of climate variability and genomics in Chapter 3.

2.6 Conclusion

Climate variability is challenging crop improvement efforts and will continue to hinder the progress of researchers to develop varieties and hybrids for complex traits. In an effort to further understand maize responses to drought and other abiotic stresses, we characterized three diverse populations of maize for stay-green. Stay-green is the ability of annual crop species to delay senescence throughout the grain fill period and is associated with an increase in yield and decreased lodging under drought stress. We leveraged multiple association mapping approaches to maximize the discovery of SNP

associations to identify potential candidate genes. We report around 250 candidate genes for four stay-green phenotypes and highlight major genomic relationships of regions consistently shown to be significant between two or more populations.

We propose that the stay-green response in maize is orchestrated by specific gene families under drought stress. These families are: calcium signaling and transduction, cell wall structure and function, sugar transportation and other secondary messengers, vesicular transportation, general abiotic stress and transcription factors, and phytohormone-related genes. Additionally, we have identified disease-related and heat response genes that coincide with an abiotic stress like drought in maize.

Further characterization and agronomic evaluation will be needed to better understand the potential impacts of stay-green candidate genes in maize. Once properly understood, advantageous alleles and donors can be deployed for germplasm enhancement and make a substantial contribution to understanding abiotic stress regulation in maize.

CHAPTER 3. COMPARATIVE GENOMIC RELATIONSHIPS OF STAY-GREEN IN MAIZE AND SORGHUM

3.1 Abstract

Substantial investments in comparative genomics and breeding for climate resilient crops have been made over the last 15 years. However, leveraging comparative genomics between crops for abiotic stress traits has been underutilized in modern plant breeding. In this study, we report important genomic relationships between maize and sorghum for the drought-stress phenotype stay-green. Stay-green, or delayed plant senescence under drought-stress, has been well characterized genetically and agronomically in sorghum. There appears to be four to six major QTL modulating the expression of stay-green in sorghum. We characterized the Nested Association Mapping panel (NAM) of maize for stay-green at anthesis and the end of season and uncovered substantial genetic variation for the trait. Upon examining the candidate genes identified from association mapping studies in maize, we leveraged the genomic information into sorghum. We identified substantial genomic relationships between maize and sorghum stay-green QTL based on reported sorghum QTL positions in the available literature and maize genomic information from mapping studies. Furthermore, we detected associations in maize for all four of the major stay-green sorghum QTL, Stg1, Stg2, Stg3, and Stg4, that are commercially selected for yield under drought stress conditions. Additional characterization is required for both of these crops to fine-tune the

genetic, physiological, and agronomic value of breeding for stay-green for challenging environments.

3.2 Introduction

Advances in high throughput sequencing and an increased focus on genetic characterization of alternative crops have led to a higher capacity for comparative genomics in crop species. Comparative genomics has successfully estimated the biological similarity or synteny of two or more species with some level of organization. Successful organization and comparison of these species leads to a better understanding of the evolution, genetic structure, and future applications for crop improvement. Additionally, comparative genomics studies provide insight into crop species of less economic importance. Increased marker density and improving online database resources will contribute to increasing the power of comparative genomics. The field will continue to evolve as new technologies are developed and researchers continue to increase the amount of knowledge in individual crops species that then can be leveraged into comparative studies.

Since the advent of molecular markers and other genotyping systems, comparative chromosomal maps have been constructed for several members of the Poaceae family across multiple agronomic traits. Examples of successful comparative genomics studies in grass species are dwarfing, shattering, flowering, and seed color. Seed shattering has been successfully characterized in rice, sorghum, wheat, and maize (Lin et al., 2012). Comparative studies have shown rice, sorghum, and maize share orthologs of YABBY-like transcription factors for shattering (Lin et al., 2012). Furthermore, sorghum grain color is conditioned by differing alleles of Tannin1 which

has orthologs in arabidopsis (Wu et al., 2012). Understanding this relationship through comparative mapping presents potential nutritional applications of phenolic compounds for human health. Additionally, comparative maps for maize and sorghum flowering times showed 40 QTLs, where 24 of these QTL collocated to previously known positions in sorghum and 16 were novel (Mace et al., 2013). Two-thirds of the QTL in this study were syntenous with maize QTL identified from the NAM population. Finally, RFLP markers showed orthologous relationships for plant height between maize and sorghum (Multani et al., 2003). Four different genomic regions were identified as syntenous for plant height and represented 63.4% of the phenotypic variation for the trait.

Comparative genomics has an exciting future in the understanding of abiotic stress tolerance and contains direct implications for breeding programs. Increased climate variability throughout the world is creating new challenges to breed climate resilient crops in areas where abiotic stress has previously been unknown.

There have been successful contributions to comparative abiotic stress genomics in crop species. Diab et al. (2007) creatively identified several drought related genomic regions between durum wheat, barley, and rice. Combining several crop-specific QTL studies and aligning them to consensus maps, they were able to construct synteny intervals for several drought related traits. They showed a relationship between barley chromosome 5H and durum wheat chromosomes 5A and 5B for chlorophyll content, water soluble carbohydrates, accumulation of water soluble carbohydrates at full turgor, and water index. These relationships were highly conserved. Additionally, they showed unique QTL that were orthologous for one species of durum wheat on chromosome 1A and 1B for chlorophyll content, canopy temperature depression, photosynthetic active

radiation, transpiration, and osmotic potential. They also showed unrelated drought traits that were collocating to the same location in two species. Specifically, they showed this for durum wheat 1B and rice 10 for transpiration and root penetration index/root thickness. Similarly, they showed collocated QTL for durum 2B and barley 2H for quantum yield, carbon isotope discrimination, water soluble carbohydrates, osmotic potential, and accumulation of water soluble content at full turgor (Diab et al., 2007).

Early comparisons between maize and sorghum revealed a high amount of synteny between the two species. These two species diverged around 12 million years ago. Modern maize is a functionally acting diploid consisting of 10 chromosomes that all pair normally. However, substantial evidence shows that maize descended as an ancient polyploid in tetraploidy form. Around the same time as the divergence from sorghum, maize experienced a form of allopolyploidy resulting in a tetraploid, thus creating two subgenomes of maize. Sorghum is closely aligned with both subgenomes of maize. Confirming these relationships between sorghum and maize is relatively simple to test as there should be two genomic positions in maize for each locus in sorghum.

Advances in comparative genomics of maize and sorghum and improving knowledge of abiotic stresses are allowing scientists to increase the knowledge and breeding capacity for crop improvement. In this study, we examine the genomic relationships between maize and sorghum for stay-green. We hypothesize that there will be several genomic relationships for QTL and SNP associations between the two species based on the knowledge we have of existing synteny and comparative biology for stay-green from the NAM and reported sorghum literature.

3.3 Materials and Methods

Marker data for sequence information, synteny/comparative biology, genomic or linkage position, and any other pertinent information were found at the following databases depending on the species being analyzed.

Marker Information

Maize - www.maizegdb.org

Maize - www.panzea.org

All species - www.wheat.pw.usda.gov/GG2/index.shtml

All species - http://www.gramene.org

Sequence Information

Maize - www.maizegdb.org

Sorghum - www.phytozome.net/sorghum

Rice – www.rice.plantbiology.msu.edu/index.shtml

All species - www.ncbi.nlm.nih.gov

All species - http://www.gramene.org

Synteny/Comparative Biology

http://www.gramene.org

BLAST and Sequence Comparisons

www.phytozome.net/sorghum

Candidate genes from maize association mapping studies were BLASTed into the sorghum genome. Only significant hits into protein containing regions of sorghum were considered potential comparative associations of stay-green between the two species. These genomic regions were compared to the stay-green sorghum literature.

3.4 Results

3.4.1 General Sorghum Stay-green Genetic Information

Substantial genetic information is available in the scientific literature cataloging the extent of stay-green characterization in sorghum. For comparison analyses, we compiled a comprehensive review of the literature for sorghum stay-green (Table 3-1, 3-2). Flanking marker information, genetic distance, QTL LOD and R2, and published QTL name (published symbol) were leveraged in predicting the physical positions on the sorghum map. Sorghum information was provided courtesy of Drs. Emma Mace, David Jordan, Andrew Borrell, and Barbara George-Jaeggli (Mace et al., Unpublished).

Table 3-1 Summary of sorghum studies mapping genes for stay-green.

Reference	Population pedigree	Population size	No. loci mapped	No. LGs	Map length	Marker density	Mapping Function[ϯ]	Analysis method[ϕ]
Crasta et al. 1999	B35/Tx430	96	128	14	1602		K	CIM
Haussmann et al. 2002	IS9830/E36-1	226	128	10	1291.2	10.0875	H	CIM
Haussmann et al. 2002	N13/E36-1	226	146	12	1438.1	9.85	H	CIM
Kebede et al. 2001	SC56/Tx7000	125	144	10	1355	9.40972	K	CIM
Srinivas et al. 2009	296B/IS18551	168	152	15	1098.7	7.22829	K	SMA, IM, MQM
Subudhi et al. 2000	B35/Tx7000	98	232	10	-	-	H	SIM, CIM
Tao et al. 2000	QL39/QL41	160	311	10	~2750	8.84244	U	SMA, IM
Xu et al. 2000	B35/Tx7000	98	145	10	837	5.77241	H	SIM

[ϯ] Mapping Function: K (Kosambi), H (Haldene), and U (Unknown)

[ϕ] Analysis Method: CIM (Composite Interval Mapping), IM (Interval Mapping), SMA (Single Marker Analysis), MQM (Multiple QTL Mapping), and SIM (Simple Interval Mapping).

Table 3-2 Reported stay-green QTL in sorghum. Genetic positions, LODS, and R^2 are reported from the literature. Physical positions are predicted from linkage data and markers from literature.

	Genetic Positions		Physical Positions					
LG	CI Start	CI End	CI Start	CI End	LOD	R^2	Publication	Published symbol
SBI-01	18.432	21.568	7,305,943	7,498,895	12	23	Hausmann et al 2002	%GL15 #2
	17.160	22.840	6,957,503	7,789,286	6.2	12.7	Hausmann et al 2002	%GL30 #4
	15.655	24.345	6,601,819	8,599,598	4	8.3	Hausmann et al 2002	%GL45 #3
	34.209	40.791	13,340,116	16,835,360	5.8	25.8	Crasta et al 1999	SGG
	45.565	59.435	20,023,900	46,286,695	2.6	5.2	Hausmann et al 2002	%GL30 #1
	46.282	58.718	20,498,918	45,698,158	2.9	5.8	Hausmann et al 2002	%GL45 #2
	61.122	68.878	47,444,531	51,453,672	4.8	9.3	Hausmann et al 2002	%GL30 #2
	66.112	73.888	50,338,344	52,612,025	3.08	13.1	Tao et al 2000	not named
	93.389	101.611	55,163,162	57,460,960	3.97	11.8	Srinivas et al 2009	QGlaa-sbi01
	91.924	103.076	54,713,042	57,506,577	3.31	8.7	Srinivas et al 2009	QGlam-sbi01-2
	125.944	139.056	61,293,458	66,636,190	2.69	7.4	Srinivas et al 2009	QGlam-sbi01-1
	143.684	155.316	67,073,183	68,342,385	3.1	6.2	Hausmann et al 2002	%GL15 #1
	143.388	155.612	67,038,796	68,386,222	3	5.9	Hausmann et al 2002	%GL30 #1
	143.388	155.612	67,038,796	68,386,222	3	5.9	Hausmann et al 2002	%GL45 #1
SBI-02	70.414	83.586	14,203,578	56,181,567	2.66	9.9	Kebede et al 2001	Stg D
	114.770	125.230	60,089,659	61,594,335	2.86	15.9	Xu et al 2000	Chl3
	121.487	128.513	60,438,145	61,675,900	3.71	14.5	Tao et al 2000	not named
	123.598	133.102	61,412,988	62,121,125	3.49	17.5	Subudhi et al 2000	stg3
	121.643	135.057	60,450,213	62,383,481	2.8	12.4	Subudhi et al 2000	stg3
	123.398	133.602	61,324,258	62,193,365	3.34	16.3	Xu et al 2000	Stg3
	124.078	139.622	61,572,631	63,435,887	1.9	10.7	Subudhi et al 2000	stg3
	130.640	145.360	61,754,092	65,036,819	2.5	4.9	Hausmann et al 2002	%GL15 #3
	131.782	144.218	61,923,733	64,284,484	3	5.8	Hausmann et al 2002	%GL30 #5
	134.204	141.796	62,261,965	63,634,080	4.9	9.5	Hausmann et al 2002	%GL45 #4

Table 3-2 Continued

SBI-03	31.671	38.329	7,570,337	9,835,674	3.88	15.3	Tao et al 2000	not named
	71.108	83.892	55,204,764	56,500,632	2.63	10.2	Kebede et al 2001	Stg A
	79.060	90.940	55,814,195	58,046,499	2.65	14	Subudhi et al 2000	stg2
	82.047	97.953	56,228,544	58,305,138	2.65	6.1	Srinivas et al 2009	QGlaa-sbi03
	83.532	96.468	56,443,470	58,281,040	2.6	5.2	Srinivas et al 2009	QPglam-sbi03
	85.821	94.179	56,775,084	58,252,295	3.66	19.9	Subudhi et al 2000	stg2
	87.152	92.848	56,993,522	58,240,511	5.52	29.2	Subudhi et al 2000	stg2
	86.320	93.680	56,856,140	58,252,295	5.44	22.6	Subudhi et al 2000	stg2
	92.147	98.853	58,234,385	58,305,138	5.6	24.8	Xu et al 2000	Chl2
	92.755	98.245	58,234,385	58,305,138	6.23	30.3	Xu et al 2000	Stg2
	92.882	98.818	58,240,511	58,305,138	6.6	28.6	Crasta et al 1999	SGA
	92.060	104.940	58,234,385	59,052,530	2.8	5.6	Hausmann et al 2002	%GL45 #5
	120.570	134.430	62,207,313	67,212,079	2.69	12	Xu et al 2000	Chl1
	123.257	131.743	62,841,197	66,318,409	4.59	19.6	Xu et al 2000	Stg1
	124.600	135.400	63,241,387	67,694,738	3.18	15.4	Subudhi et al 2000	Stg1
	125.405	134.595	63,482,399	67,351,512	3.61	18.1	Subudhi et al 2000	Stg1
	131.129	133.871	66,129,723	66,758,123	14.9	26.3	Hausmann et al 2002	%GL15 #1
	129.592	135.408	65,303,733	67,694,738	6.5	12.4	Hausmann et al 2002	%GL30 #2
SBI-04	0.000	12.031	83,230	1,751,452	2.52	6.9	Srinivas et al 2009	QGlaa-sbi04
	73.622	80.378	48,579,647	50,150,591	4.66	19.3	Kebede et al 2001	s C
	85.134	94.866	52,570,786	53,840,245	3.63	13.4	Kebede et al 2001	Stg C.1
	84.088	95.912	51,761,082	55,097,491	3.1	6.1	Hausmann et al 2002	%GL15 #2
	83.443	96.557	51,175,809	55,150,649	2.8	5.5	Hausmann et al 2002	%GL30 #3
	82.929	97.071	50,866,536	55,194,144	2.6	5.1	Hausmann et al 2002	%GL45 #4
	85.682	94.318	52,570,786	53,138,114	4.11	15.1	Kebede et al 2001	Stg C.2

Table 3-2 Continued

SBI-05	54.181	68.819	9,942,964	47,138,942	2.3	11.6	Crasta et al 1999	SGJ
	54.508	69.492	10,116,867	48,435,793	2.23	11.1	Xu et al 2000	Stg4
	55.153	72.847	10,407,015	52,892,020	1.81	9.4	Subudhi et al 2000	stg4
	62.566	71.034	13,115,727	52,038,094	4.21	15.4	Kebede et al 2001	Stg J
	77.244	86.756	57,411,681	57,420,675	3.42	10.2	Srinivas et al 2009	QGlaa-sbi05
SBI-06	38.781	50.219	8,015,809	41,422,674	2.86	11.4	Kebede et al 2001	Stg F
	41.913	47.087	18,873,510	39,257,769	6.36	25.2	Kebede et al 2001	Prf F
	76.650	91.350	47,853,564	51,863,938	2.85	6.6	Srinivas et al 2009	QGlam-sbi06
SBI-07	17.885	30.115	1,635,890	2,774,392	2.22	13.6	Subudhi et al 2000	not named
	57.726	63.274	4,559,583	7,617,971	6.8	13	Hausmann et al 2002	%GL15 #4
	57.942	63.058	4,584,864	7,547,514	7.5	14.1	Hausmann et al 2002	%GL30 #6
	57.978	63.022	4,587,055	7,547,514	7.6	14.3	Hausmann et al 2002	%GL45 #7
	62.485	72.515	7,435,638	43,742,113	3.53	13	Kebede et al 2001	Stg E
	62.065	75.935	7,347,284	53,641,687	2.6	5.2	Hausmann et al 2002	%GL15 #3
	121.560	134.440	61,205,894	63,776,848	2.8	5.6	Hausmann et al 2002	%GL15 #5
	122.618	133.382	61,393,105	63,776,848	3.4	6.7	Hausmann et al 2002	%GL30 #7
	121.782	134.218	61,243,343	63,776,848	2.9	5.8	Hausmann et al 2002	%GL45 #8
SBI-08	51.888	64.112	4,755,254	7,734,326	2.6	5.9	Hausmann et al 2002	%GL30 #6
	51.990	64.010	4,770,017	7,700,210	2.6	6	Hausmann et al 2002	%GL45 #6
	97.196	110.804	52,218,412	54,277,680	2.6	5.3	Hausmann et al 2002	%GL30 #7
	98.536	109.464	52,400,642	54,057,570	3.3	6.6	Hausmann et al 2002	%GL45 #7
SBI-09	43.600	56.537	3,032,531	5,260,505	2.9	7.5	Srinivas et al 2009	QPglam-sbi09
	64.611	77.005	7,330,224	46,593,685	2.9	13.7	Crasta et al 1999	SGI.2
	66.820	76.166	7,894,112	45,357,691	2.46	10.9	Tao et al 2000	not named

Table 3-2 Continued

SBI-10	21.475	30.925	1,280,253	2,902,322	3.65	13.8	Kebede et al 2001	Stg B
	41.452	50.548	7,736,603	8,963,984	2.76	11.2	Tao et al 2000	not named
	58.848	69.152	44,984,327	51,757,522	3.5	7	Hausmann et al 2002	%GL15 #4
	57.888	70.112	15,445,079	52,026,416	2.9	5.9	Hausmann et al 2002	%GL30 #4
	84.943	98.057	56,038,744	57,800,351	2.7	5.5	Hausmann et al 2002	%GL30 #8
	84.565	98.435	55,994,289	57,849,024	2.6	5.2	Hausmann et al 2002	%GL45 #9
	92.036	102.964	56,952,356	58,549,190	3.3	6.6	Hausmann et al 2002	%GL15 #5
	91.388	103.612	56,924,176	60,140,101	2.9	5.9	Hausmann et al 2002	%GL30 #5
	91.49	103.51	56,924,176	59,861,785	3	6	Hausmann et al 2002	%GL45 #5
	98.604	110.396	57,880,377	60,382,370	3	14.4	Crasta et al 1999	SGB

Stay-green QTL from each of these studies represented a specific proportion of the sorghum genome. When all QTL are included in the dataset regardless of size, 45.86% of the genome is represented by sorghum stay-green QTL. To improve precision, excessively large linkage QTL (>20mb) were removed from consideration and the remaining stay-green QTL represented 8.8% of the sorghum genome (Table 3-3). Removal of excessively large QTL (>20mb) is justified by the lack of marker coverage in earlier mapping studies as well as small population sizes used in field studies, which increase interval size (Table 3-3).

Table 3-3 Sorghum stay-green QTL expressed as a percentage of the entire genome. To improve precision, QTL that contained predicted genomic distances greater than 20mb were removed in the Major QTL and all QTL were included in the combined row.

	Stay-green Genome Representation (bp)	Genome Coverage
Major QTL (<20mb)	64,569,979	8.89%
All Reported QTL	333,239,660	45.86%
Sb Genome Size (2.1)	726,616,606	

3.4.2 Maize and Sorghum Stay-green Genomic Comparisons

The maize NAM RILs and testcrosses indicated several significant QTL for stay-green. The AMES dataset (reported in Chapter 2) did not contain any significant SNPs from association mapping and was used as a validation set for confirming and supporting associations identified in the NAM populations.

For comparison analyses, we used maize stay-green anthesis (NAM RILs) and terminal (NAM RILs and NAM testcrosses) for evaluation because these phenotypes are commonly assessed in mapping stay-green QTL in sorghum. The maize stay-green phenotypes difference and ratio, which were mapped in the NAM RILs and AMES, were not compared to sorghum as there is no reported phenotype for comparison in sorghum.

In the following tables, we report the genomic relationships for three maize phenotypes and the associated sorghum genomic relationships (Table 3-4: NAM RILs Anthesis. Table 3-5: NAM RILs Terminal. Table 3-6: NAM Testcrosses Terminal).

Table 3-4 Summary of Maize candidate gene associations from the NAM RILs anthesis phenotype compared to reported sorghum stay-green QTL.

Maize LG	SNP Position	RMIP	Maize ID	Description	Sb LG	Sb Genomic Position	Publication	Published symbol
2	185,691,621	47	GRMZM2G110107	AT1G68130.1(AtIDD14, IDD14): indeterminate(ID)-domain 14	2	61368078-61372487	Xu et al 2000	Chl3
2	185,691,621	47	GRMZM2G110107	AT1G68130.1(AtIDD14, IDD14): indeterminate(ID)-domain 14	2	61368078-61372487	Tao et al 2000	not named
2	185,691,621	47	GRMZM2G110107	AT1G68130.1(AtIDD14, IDD14): indeterminate(ID)-domain 14	2	61368078-61372487	Subudhi et al 2000	stg3
2	185,691,621	47	GRMZM2G110107	AT1G68130.1(AtIDD14, IDD14): indeterminate(ID)-domain 14	2	61368078-61372487	Xu et al 2000	Stg3

Table 3-4 Continued

2	185,691,621	47	GRMZM2G110107	AT1G68130.1(AtIDD14,IDD14): indeterminate(ID)-domain 14	7	57388305-57391408	No Relationship	
2	186,183,071	36	GRMZM2G002131	AT4G36990.1(AT-HSFB1,ATHSF4,HSF4,HSFB1): heat shock factor4	2	61754036-61758207	Subudhi et al 2000	stg3
2	186,183,071	36	GRMZM2G002131	AT4G36990.1(AT-HSFB1,ATHSF4,HSF4,HSFB1): heat shock factor4	2	61754036-61758207	Xu et al 2000	Stg3
2	186,183,071	36	GRMZM2G002131	AT4G36990.1(AT-HSFB1,ATHSF4,HSF4,HSFB1): heat shock factor4	2	61754036-61758207	Hausmann et al 2002	%GL15 #3
5	5,005,874	26	AC191251.3_FG005	AT3G20800.1: Cell differentiation, Rcd1-like protein	1	5077035-5081214	No Relationship	
1	58,475,918	21	GRMZM2G075502	AT3G06130.1: Heavy metal transport/detoxification superfamily protein	1	59192242-59193491	No Relationship	
1	183,804,764	18	GRMZM2G113726	AT3G13340.1: Transducin/WD40 repeat-like superfamily protein	7	63521275-63524843	No Relationship	

Table 3-4 Continued

1	183,804,764	18	GRMZM2G113726	AT3G13340.1: Transducin/WD40 repeat-like superfamily protein	4	59688441-59691245	No Relationship	
1	183,804,764	18	GRMZM2G113840	AT4G39170.1: Sec14p-like phosphatidylinositol transfer family protein	7	60976744-60981646	No Relationship	
1	183,804,764	18	GRMZM2G113840	AT4G39170.1: Sec14p-like phosphatidylinositol transfer family protein	2	63166278-63168330	Subudhi et al 2000	stg3
1	183,804,764	18	GRMZM2G113840	AT4G39170.1: Sec14p-like phosphatidylinositol transfer family protein	2	63166278-63168330	Hausmann et al 2002	%GL15 #3
1	183,804,764	18	GRMZM2G113840	AT4G39170.1: Sec14p-like phosphatidylinositol transfer family protein	2	63166278-63168330	Hausmann et al 2002	%GL30 #5
1	183,804,764	18	GRMZM2G113840	AT4G39170.1: Sec14p-like phosphatidylinositol	2	63166278-63168330	Hausmann et al 2002	%GL45 #4
5	181,386,025	18	GRMZM2G029583	AT4G24820.1: 26S proteasome, regulatory subunit Rpn7;Proteasome component (PCI) domain	4	54946225-54949288	Hausmann et al 2002	%GL15 #2
5	181,386,025	18	GRMZM2G029583	AT4G24820.1: 26S proteasome, regulatory subunit Rpn7;Proteasome component (PCI) domain	4	54946225-54949288	Hausmann et al 2002	%GL30 #3
5	181,386,025	18	GRMZM2G029583	AT4G24820.1: 26S proteasome, regulatory subunit Rpn7;Proteasome component (PCI) domain	4	54946225-54949288	Hausmann et al 2002	%GL45 #4

Table 3-4 Continued

5	181,386,025	18	GRMZM2G029583	AT4G24820.1: 26S proteasome, regulatory subunit Rpn7;Proteasome component (PCI) domain	4	54946225-54949288	Kebede et al 2001	Stg C.2
5	181,386,025	18	GRMZM2G029583	AT4G24820.1: 26S proteasome, regulatory subunit Rpn7;Proteasome component (PCI) domain	4	54946225-54949288	Srinivas et al 2009	QGlam-sbi06
5	181,386,025	18	GRMZM2G031496	AT5G50960.1(ATNBP35,NBP35): nucleotide binding protein 35	4	54963829-54967694	Hausmann et al 2002	%GL15 #2
5	181,386,025	18	GRMZM2G031496	AT5G50960.1(ATNBP35,NBP35): nucleotide binding protein 35	4	54963829-54967694	Hausmann et al 2002	%GL30 #3
5	181,386,025	18	GRMZM2G031496	AT5G50960.1(ATNBP35,NBP35): nucleotide binding protein 35	4	54963829-54967694	Hausmann et al 2002	%GL45 #4
4	230,895,626	16	GRMZM2G080056	AT1G14420.1(AT59): Pectate lyase family	4	7791363-7793358	No Relationship	
4	230,895,626	16	GRMZM2G080056	AT1G14420.1(AT59): Pectate lyase family	10	51161633-51162707	Hausmann et al 2002	%GL15 #4
4	230,895,626	16	GRMZM2G080056	AT1G14420.1(AT59): Pectate lyase family protein	10	51161633-51162707	Hausmann et al 2002	%GL30 #4
4	230,895,626	16	GRMZM2G080056	AT1G14420.1(AT59): Pectate lyase family protein	1	22320239-22321787	Hausmann et al 2002	%GL30 #1

Table 3-4 Continued

4	230,895,626	16	GRMZM2G080056	AT1G14420.1(AT59): Pectate lyase family protein	1	22320239-22321787	Hausmann et al 2002	%GL45 #2
4	230,895,626	16	GRMZM2G080056	AT1G14420.1(AT59): Pectate lyase family protein	6	2054207-2055548	No Relationship	
9	18,521,596	16	GRMZM5G800535	PFAM ID: PF05678: VQ motif	10	3446598-3447010	No Relationship	
10	143,670,200	15	GRMZM2G180471	AT1G34750.1: Protein phosphatase 2C family protein	6	58068926-58072700	No Relationship	
10	143,670,200	15	GRMZM2G480282	LOC_Os06g30760.1: transposon protein, putative, CACTA, En/Spm sub-class, expressed	7	37433156-37433213	Kebede et al 2001	Stg E
10	143,670,200	15	GRMZM2G480282	LOC_Os06g30760.1: transposon protein, putative, CACTA, En/Spm sub-class, expressed	7	37433156-37433213	Hausmann et al 2002	%GL15 #3
5	4,944,136	14	GRMZM2G089361	AT4G18390.1(TCP2): TEOSINTE BRANCHED 1, cycloidea and PCF transcription factor 2	1	5025646-5027065	No Relationship	

Table 3-4 Continued

5	4,944,136	14	GRMZM2G089361	AT4G18390.1(TCP2): TEOSINTE BRANCHED 1, cycloidea and PCF transcription factor 2	2	3348415-3348415	No Relationship	
1	287,270,801	13	GRMZM2G342856	AT2G32030.1: Acyl-CoA N-acyltransferases (NAT) superfamily protein	1	4450852-4456632	No Relationship	
4	4,992,844	13	GRMZM5G877647	AT2G06255.1(ELF4-L3): ELF4-like 3	5	58229716-58230888	No Relationship	
4	4,992,844	13	GRMZM2G058340	AT3G49310.1: Major facilitator superfamily protein	4	83908-84500	Srinivas et al 2009	QGlaa-sbi04
4	179,091,367	11	GRMZM2G107414	LOC_Os02g52300.1: CPuORF38 - conserved peptide uORF-containing transcript, expressed	4	63819968-63822410	No Relationship	
5	122,046,355	11	AC186500.3_FG001	AT2G42490.1: Copper amine oxidase family protein	6	49542037-49543118	Srinivas et al 2009	QGlam-sbi06
5	175,865,828	11	GRMZM2G072146	AT4G39910.1(ATUBP3, UBP3): ubiquitin-specific protease 3	4	53375804-53381020	No Relationship	
5	175,865,828	11	GRMZM2G072146	AT4G39910.1(ATUBP3, UBP3): ubiquitin-specific protease 3	6	48123031-48129764	Srinivas et al 2009	QGlam-sbi06
5	175,865,828	11	GRMZM2G072146	AT4G39910.1(ATUBP3, UBP3): ubiquitin-specific protease 3	1	62205339-62208784	Srinivas et al 2009	QGlam-sbi01-1

Table 3-4 Continued

3	11,032,448	10	GRMZM2G074466	AT1G49040.1(SCD1): stomatal cytokinesis defective / SCD1 protein (SCD1)	3	52030777-52038166	No Relationship	
3	11,032,448	10	GRMZM2G074466	AT1G49040.1(SCD1): stomatal cytokinesis defective / SCD1 protein	8	4558998-4559320	No Relationship	
3	11,032,448	10	GRMZM5G849600	AT5G56960.1: basic helix-loop-helix (bHLH) DNA-binding family	3	52013142-52016767	No Relationship	
4	239,498,890	10	GRMZM2G169871	AT3G54170.1(ATFIP37, FIP37): FKBP12 interacting protein 37	4	2677015-2684918	No Relationship	
4	239,498,890	10	GRMZM2G169998	AT5G58130.1(ROS3): RNA-binding (RRM/RBD/RNP motifs) family protein	4	2936328-2939154	No Relationship	
4	239,498,890	10	GRMZM2G169927	AT4G31120.1(ATPRMT5,PRMT5,SKB1): SHK1 binding protein 1	4	2950192-2960459	No Relationship	
3	22,568,001	9	GRMZM2G337815	AT4G34555.1: Ribosomal protein S25 family protein	3	64941263-64941906	Xu et al 2000	Chl1
3	22,568,001	9	GRMZM2G337815	AT4G34555.1: Ribosomal protein S25 family protein	3	64941263-64941906	Xu et al 2000	Stg1
3	22,568,001	9	GRMZM2G337815	AT4G34555.1: Ribosomal protein S25 family protein	3	64941263-64941906	Subudhi et al 2000	Stg1

Table 3-4 Continued

3	22,568,001	9	GRMZM2G337815	AT4G34555.1: Ribosomal protein S25 family protein	3	64941263-64941906	Hausmann et al 2002	%GL15 #1
3	22,568,001	9	GRMZM2G337815	AT4G34555.1: Ribosomal protein S25 family protein	3	64941263-64941906	Hausmann et al 2002	%GL30 #2
3	22,568,001	9	GRMZM2G032107	LOC_Os01g04010.1: expressed protein	3	7460254-7461414	No Relationship	
6	34,893,105	9	GRMZM2G700901	PFAM ID: PF06813: Nodulin-like , PF00579: tRNA synthetases class I (W and Y)	3	62492603-62493321	Xu et al 2000	Chl1
6	34,893,105	9	GRMZM2G305856	AT3G46130.1(ATMYB48,ATMYB48-1,ATMYB48-2,ATMYB48-3,MYB48): myb domain protein 48	9	1546626-1548493	No Relationship	
8	13,790,821	9	GRMZM2G477503	AT5G01220.1(SQD2): sulfoquinovosyldiacylglycerol 2	3	6617797-6621899	No Relationship	
8	13,790,821	9	GRMZM2G477503	AT5G01220.1(SQD2): sulfoquinovosyldiacylglycerol 2	2	138869-141647	No Relationship	
8	13,790,821	9	GRMZM2G176568	AT5G58900.1: Homeodomain-like transcriptional regulator	3	6605257-6606239	No Relationship	

Table 3-4 Continued

8	13,790,821	9	GRMZM2G079458	AT2G38090.1: Duplicated homeodomain-like superfamily protein	3	6589536-6592429	No Relationship	
9	18,334,400	9	GRMZM5G838414	AT1G53290.1: Galactosyltransferase family protein	10	3429104-3434799	No Relationship	
9	18,334,400	9	AC231745.1_FG003	AT5G45910.1: GDSL-like Lipase/Acylhydrolase superfamily protein	10	3436008-3438395	No Relationship	
1	53,630,920	8	GRMZM2G011598	AT3G04070.1(anac047,NAC047): NAC domain containing protein 47	3	9665554-9666868	Tao et al 2000	not named
1	53,630,920	8	GRMZM2G011598	AT3G04070.1(anac047,NAC047): NAC domain containing protein 47	1	60188250-60190515	No Relationship	
1	53,630,920	8	GRMZM2G011598	AT3G04070.1(anac047,NAC047): NAC domain containing protein 47	2	73839404-73840631	No Relationship	
1	53,630,920	8	GRMZM2G020940	AT2G39050.1: hydroxyproline-rich glycoprotein family protein	1	60201668-60203540	No Relationship	
1	53,630,920	8	GRMZM2G020940	AT2G39050.1: hydroxyproline-rich glycoprotein family protein	2	73832201-73840631	No Relationship	

Table 3-4 Continued

1	296,649,227	8	GRMZM2G167428	LOC_Os03g62170.1: cyclase/dehydrase family protein, expressed	1	1713107-1717885	No Relationship	
5	119,472,884	8	GRMZM2G052654	AT2G02880.1: mucin-related	1	57398576-57401785	Srinivas et al 2009	QGlaa-sbi01
5	119,472,884	8	GRMZM2G052654	AT2G02880.1: mucin-related	1	57398576-57401785	Srinivas et al 2009	QGlam-sbi01-2
5	204,317,772	8	GRMZM2G012213	AT4G16835.1: Tetratricopeptide repeat (TPR)-like superfamily protein	4	59508301-59510417	No Relationship	
5	204,317,772	8	GRMZM2G012044	AT1G55850.1(ATCSLE1,CSLE1): cellulose synthase like E1	4	59504139-59507781	No Relationship	
5	204,317,772	8	GRMZM2G011951	AT5G55850.1(NOI): RPM1-interacting protein 4 (RIN4) family protein	4	59502383-59504001	No Relationship	
7	2,360,774	8	GRMZM2G128693	AT3G50950.1(ZAR1): HOPZ-ACTIVATED RESISTANCE 1	2	1126432-1127885	No Relationship	
1	187,592,684	7	GRMZM2G132763	AT1G17750.1(AtPEPR2, PEPR2): PEP1 receptor 2	7	62882190-62885649	Hausmann et al 2002	%GL15 #5
1	187,592,684	7	GRMZM2G132763	AT1G17750.1(AtPEPR2, PEPR2): PEP1 receptor 2	7	62882190-62885649	Hausmann et al 2002	%GL30 #7
1	187,592,684	7	GRMZM2G132763	AT1G17750.1(AtPEPR2, PEPR2): PEP1 receptor 2	7	62882190-62885649	Hausmann et al 2002	%GL45 #8
1	285,904,918	7	GRMZM2G134917	AT5G22060.1(ATJ2,J2): DNAJ homologue 2	1	4880000-4883216	No Relationship	

Table 3-4 Continued

1	289,518,674	7	GRMZM2G101682	LOC_Os03g58850.1: uncharacterized PE-PGRS family protein PE_PGRS3 precursor, putative, expressed	1	3758486-3759280	No Relationship	
2	233,674,088	7	GRMZM2G170934	AT3G22440.1: FRIGIDA-like protein	2	4646463-4653632	No Relationship	
2	233,674,088	7	GRMZM2G469469	AT2G32040.1: Major facilitator superfamily protein	2	4624645-4630564	No Relationship	
2	233,674,088	7	GRMZM2G469469	AT2G32040.1: Major facilitator superfamily protein	1	4417412-4420996	No Relationship	
5	182,133,946	7	GRMZM2G137399	AT1G28580.1: GDSL-like Lipase/Acylhydrolase superfamily protein	4	55110278-55115720	Hausmann et al 2002	%GL30 #3
5	182,133,946	7	GRMZM2G137409	AT5G60600.1(CLB4,CSB3,GCPE,HDS,ISPG): 4-hydroxy-3-methylbut-2-enyl diphosphate synthase	4	55097586-55104013	Hausmann et al 2002	%GL45 #4
7	172,488,742	7	GRMZM2G113863	AT5G27690.1: Heavy metal transport/detoxification superfamily protein	2	68032888-68034345	No Relationship	
1	297,962,777	6	GRMZM2G001661	AT5G16490.1(RIC4): ROP-interactive CRIB motif-containing protein 4	1	1274640-1276680	No Relationship	

Table 3-4 Continued

1	297,962,777	6	AC207546.3_FG004	AT3G08947.1: ARM repeat superfamily protein	1	1274640-1276680	No Relationship	
3	17,433,280	6	GRMZM2G451327	AT2G39550.1(ATGGT-IB,GGB,PGGT-I): Prenyltransferase family	3	6139305-6153146	No Relationship	
3	17,433,280	6	GRMZM2G151087	AT5G10480.3(PAS2,PEP): Protein-tyrosine phosphatase-like, PTPLA	3	6139305-6153146	No Relationship	
3	209,021,937	6	GRMZM2G164674	AT5G19580.1: glyoxal oxidase-related protein	3	59356868-59359229	No Relationship	
3	209,021,937	6	GRMZM2G164674	AT5G19580.1: glyoxal oxidase-related protein	9	57225717-57227462	No Relationship	
5	204,928,300	6	GRMZM5G824439	PFAM ID: PF11573: Mediator complex subunit 23	4	58916633-58925419	No Relationship	
8	161,388,771	6	GRMZM2G423456	AT1G27320.1(AHK3,HK3): histidine kinase 3	3	68028418-68034345	No Relationship	
9	19,163,887	6	GRMZM2G443985	AT4G26270.1(PFK3): phosphofructokinase 3	10	3056731-3077162	No Relationship	
9	20,459,109	6	GRMZM2G173693	AT5G37370.1(ATSRL1): PRP38 family protein	10	2608009-2611580	Kebede et al 2001	Stg B
9	20,459,109	6	GRMZM2G173641	AT5G11380.1(DXPS3): 1-deoxy-D-xylulose 5-phosphate synthase 3	10	2574863-2579870	Kebede et al 2001	Stg B
9	20,459,109	6	GRMZM2G173628	AT5G23310.1(FSD3): Fe superoxide dismutase 3	10	2581328-2583532	Kebede et al 2001	Stg B
9	140,431,872	6	GRMZM2G131539	AT2G29560.1(ENOC): cytosolic enolase	1	60977443-60981646	No Relationship	

Table 3-4 Continued

1	285,941,597	5	GRMZM2G434533	AT3G11780.1: MD-2-related lipid recognition domain-containing protein / ML domain-containing protein	8	52424514-52426469	No Relationship
1	285,941,597	5	GRMZM2G434533	AT3G11780.1: MD-2-related lipid recognition domain-containing protein / ML domain-containing protein	3	4451342-4452714	No Relationship
1	285,941,597	5	GRMZM2G434533	AT3G11780.1: MD-2-related lipid recognition domain-containing protein / ML domain-containing protein	1	4787177-4790160	No Relationship
3	17,030,869	5	AC215260.3_FG004	AT5G16450.1: Ribonuclease E inhibitor RraA/Dimethylmenaquinone methyltransferase	3	6011633-6011723	No Relationship
3	17,030,869	5	AC215260.3_FG003	AT5G48930.1(HCT): hydroxycinnamoyl-CoA shikimate/quinate hydroxycinnamoyl transferase	3	6011633-6011723	No Relationship
4	4,448,482	5	GRMZM2G039408	AT3G18830.1(ATPLT5, ATPMT5,PMT5): polyol/monosaccharide transporter 5	5	58598972-58600771	No Relationship

Table 3-4 Continued

4	4,448,482	5	GRMZM2G039408	AT3G18830.1(ATPLT5, ATPMT5,PMT5): polyol/monosaccharide transporter 5	2	13278297-13280038	No Relationship	
5	59,254,396	5	GRMZM2G084521	AT2G29960.1(ATCYP5, CYP19-4,CYP5): cyclophilin 5	10	59276049-59287698	Hausmann et al 2002	%GL30 #5
5	59,254,396	5	GRMZM2G385945	AT3G02790.1: zinc finger (C2H2 type) family protein	10	59289995-59291725	Hausmann et al 2002	%GL30 #5
5	91,602,155	5	GRMZM2G174785	AT5G25060.1: RNA recognition motif (RRM)-containing protein	4	5271716-5280709	No Relationship	
5	199,972,074	5	AC233960.1_FG005	AT1G06170.1: basic helix-loop-helix (bHLH) DNA-binding superfamily protein	4	60841878-60843904	No Relationship	
5	199,972,074	5	GRMZM5G861093	AT5G27080.1: Transducin family protein / WD-40 repeat family protein	4	60835987-60839090	No Relationship	
5	199,972,074	5	GRMZM5G861093	AT5G27080.1: Transducin family protein / WD-40 repeat family protein	6	56293977-56295543	No Relationship	
5	199,972,074	5	AC233960.1_FG003	AT5G45580.1: Homeodomain-like superfamily protein	4	60829285-60831667	No Relationship	

Table 3-4 Continued

5	204,914,413	5	GRMZM2G089454	AT5G37680.1(ARLA1A, ATARLA1A): ADP-ribosylation factor-like	4	58940294-58943162	No Relationship
8	27,648,546	5	GRMZM2G058491	AT1G64110.2: P-loop containing nucleoside triphosphate hydrolases superfamily protein	3	957049-964951	No Relationship
8	27,648,546	5	GRMZM2G058491	AT1G64110.2: P-loop containing nucleoside triphosphate hydrolases superfamily protein	9	58516984-58522078	No Relationship
9	8,020,744	5	GRMZM2G080696	AT2G03220.1(ATFT1,ATFUT1,FT1,MUR2): fucosyltransferase 1	10	6956300-6958077	No Relationship
9	8,020,744	5	GRMZM2G080696	AT2G03220.1(ATFT1,ATFUT1,FT1,MUR2): fucosyltransferase 1	4	60976514-60981646	No Relationship
9	18,332,206	5	GRMZM5G838414	AT1G53290.1: Galactosyltransferase family protein	10	3429104-3434799	No Relationship
9	18,332,206	5	AC231745.1_FG003	AT5G45910.1: GDSL-Lipase/Acylhydrolase superfamily protein	10	3436008-3438395	No Relationship
10	1,728,072	5	GRMZM2G129954	AT3G57040.1(ARR9,ATRR4): response regulator 9	8	1082610-1084957	No Relationship
10	1,728,072	5	GRMZM2G129954	AT3G57040.1(ARR9,ATRR4): response regulator 9	5	2752276-2754263	No Relationship

Table 3-4 Continued

10	1,728,072	5	GRMZM2G130062	AT1G74040.1(IMS1,IPMS2,MAML-3): 2-isopropylmalate synthase 1	8	1096996-1102868	No Relationship
10	1,728,072	5	GRMZM2G130062	AT1G74040.1(IMS1,IPMS2,MAML-3): 2-isopropylmalate synthase 1	5	2691891-2696552	No Relationship
10	1,728,072	5	GRMZM2G129907	AT5G43210.1: Excinuclease ABC, C subunit, N-terminal	8	982316-984390	No Relationship

Table 3-5 Summary of candidate gene associations for maize stay-green terminal from the NAM RILs compared to reported sorghum stay-green QTL.

Maize LG	RMIP	Maize ID	Description	Sb LG	Sb Genomic Position	Publication	Published symbol
2	39	GRMZM2G021129	AT1G26690.1: emp24/gp25L/p24 family/GOLD family protein	2	55458809-55460251	Kebede et al 2001	Stg D
2	39	GRMZM2G021129	AT1G26690.1: emp24/gp25L/p24 family/GOLD family protein	1	26419739-26422832	Hausmann et al 2002	%GL30 #1
2	39	GRMZM2G021129	AT1G26690.1: emp24/gp25L/p24 family/GOLD family protein	1	26419739-26422832	Hausmann et al 2002	%GL45 #2
9	37	GRMZM5G865819	AT2G20370.1(KAM1,MUR3): Exostosin family protein	1	70389010-70390665	No Relationship	
9	37	GRMZM5G865819	AT2G20370.1(KAM1,MUR3): Exostosin family protein	8	49358197-49359316	No Relationship	
9	37	GRMZM2G178072	AT3G24010.1(ATING1,ING1): RING/FYVE/PHD zinc finger superfamily protein	1	55457063-55460251	Srinivas et al 2009	QGlaa-sbi01
9	37	GRMZM2G178072	AT3G24010.1(ATING1,ING1): RING/FYVE/PHD zinc finger superfamily protein	1	55457063-55460251	Srinivas et al 2009	QGlam-sbi01-2
6	30	GRMZM2G156255	AT3G02850.1(SKOR): STELAR K+ outward rectifier	10	9471103-9477532	No Relationship	
6	30	GRMZM2G156255	AT3G02850.1(SKOR): STELAR K+ outward rectifier	6	47245325-47247967	No Relationship	
6	30	GRMZM2G156310	AT1G47480.1: alpha/beta-Hydrolases superfamily protein	2	62009104-62009408	Subudhi et al 2000	stg3

Table 3-5 Continued

6	30	GRMZM2G156310	AT1G47480.1: alpha/beta-Hydrolases superfamily protein	2	62009104-62009408	Xu et al 2000	Stg3
6	30	GRMZM2G156310	AT1G47480.1: alpha/beta-Hydrolases superfamily protein	2	62009104-62009408	Subudhi et al 2000	stg3
6	30	GRMZM2G156310	AT1G47480.1: alpha/beta-Hydrolases superfamily protein	2	62009104-62009408	Hausmann et al 2002	%GL15 #3
6	30	GRMZM2G156310	AT1G47480.1: alpha/beta-Hydrolases superfamily protein	2	62009104-62009408	Hausmann et al 2002	%GL30 #5
9	28	GRMZM2G107651	AT2G20320.1: DENN (AEX-3) domain-containing protein	1	70297442-70305481	No Relationship	
5	23	GRMZM2G166027	AT2G05940.1: Protein kinase superfamily protein	4	64705811-64709498	No Relationship	
5	23	GRMZM2G463904	AT2G26330.1(ER,QRP1): Leucine-rich receptor-like protein kinase family protein	4	64674255-64681191	No Relationship	
5	23	GRMZM2G463904	AT2G26330.1(ER,QRP1): Leucine-rich receptor-like protein kinase family protein	10	6248199-6254351	No Relationship	
3	21	GRMZM2G122656	AT4G18590.1: Nucleic acid-binding, OB-fold-like protein	3	10474067-10476759	No Relationship	
3	21	GRMZM2G421742	AT5G49350.1: Glycine-rich protein family	3	10490075-10490799	No Relationship	
7	20	GRMZM2G120574	AT5G53890.1(AtPSKR2,PSKR2) : phytosylfokine-alpha receptor 2	2	598353-602274	No Relationship	
10	20	GRMZM2G001195	AT4G33140.1: Haloacid dehalogenase-like hydrolase (HAD) superfamily protein	10	5620661-5621855	No Relationship	
2	18	GRMZM2G160523	AT1G73880.1(UGT89B1): UDP-glucosyl transferase 89B1	6	59270739-59273589	No Relationship	

Table 3-5 Continued

2	18	GRMZM2G160523	AT1G73880.1(UGT89B1): UDP-glucosyl transferase 89B1	10	12730662-12731886	No Relationship	
2	18	GRMZM2G160523	AT1G73880.1(UGT89B1): UDP-glucosyl transferase 89B1	7	60980340-60981646	No Relationship	
4	17	GRMZM2G131329	AT4G21060.2: Galactosyltransferase family protein	7	2842107-2846704	No Relationship	
4	17	GRMZM2G131378	AT2G38110.1(ATGPAT6,GPAT6): glycerol-3-phosphate acyltransferase 6	9	52101160-52101993	No Relationship	
4	17	GRMZM2G131378	AT2G38110.1(ATGPAT6,GPAT6): glycerol-3-phosphate acyltransferase 6	3	56944241-56945073	Subudhi et al 2000	stg2
4	17	GRMZM2G131378	AT2G38110.1(ATGPAT6,GPAT6): glycerol-3-phosphate acyltransferase 6	3	56944241-56945073	Srinivas et al 2009	QGlaa-sbi03
4	17	GRMZM2G131378	AT2G38110.1(ATGPAT6,GPAT6): glycerol-3-phosphate acyltransferase 6	3	56944241-56945073	Srinivas et al 2009	QPglam-sbi03
4	17	GRMZM2G131378	AT2G38110.1(ATGPAT6,GPAT6): glycerol-3-phosphate acyltransferase 6	3	56944241-56945073	Subudhi et al 2000	stg2

Table 3-5 Continued

4	17	GRMZM2G131378	AT2G38110.1(ATGPAT6,GPAT6): glycerol-3-phosphate acyltransferase 6	7	2867975-2869614	No Relationship	
4	17	GRMZM2G089421	AT1G57860.1: Translation protein SH3-like family protein	1	64339789-64342021	Srinivas et al 2009	QGlam-sbi01-1
9	17	GRMZM2G089686	AT3G24310.1(ATMYB71,MYB305): myb domain protein 305	1	70563106-70564580	No Relationship	
9	17	GRMZM2G089686	AT3G24310.1(ATMYB71,MYB305): myb domain protein 305	6	48621508-48622859	Srinivas et al 2009	QGlam-sbi06
9	17	GRMZM2G089699	AT1G65680.1(ATEXPB2,ATHEXPBETA1.4,EXPB2): expansin	1	62208003-62208784	Srinivas et al 2009	QGlam-sbi01-1
3	16	GRMZM5G856738	AT4G23650.1(CDPK6,CPK3): calcium-dependent protein kinase 6	3	56124094-56128697	Kebede et al 2001	Stg A
3	16	GRMZM5G856738	AT4G23650.1(CDPK6,CPK3): calcium-dependent protein kinase 6	3	56124094-56128697	Subudhi et al 2000	stg2
3	16	GRMZM5G856738	AT4G23650.1(CDPK6,CPK3): calcium-dependent protein kinase 6	9	58613859-58616901	No Relationship	
3	16	GRMZM5G856738	AT4G23650.1(CDPK6,CPK3): calcium-dependent protein kinase 6	8	1344788-1346924	No Relationship	
3	16	GRMZM5G856738	AT4G23650.1(CDPK6,CPK3): calcium-dependent protein kinase 6	5	2284302-2286332	No Relationship	
3	16	GRMZM5G856738	AT4G23650.1(CDPK6,CPK3): calcium-dependent protein kinase 6	6	55593503-55595641	No Relationship	

Table 3-5 Continued

10	15	GRMZM2G063394	AT1G76390.1: ARM repeat superfamily protein	8	24301730-24307012	No Relationship	
9	14	GRMZM2G137779	LOC_Os03g05110.1: xyloglucan galactosyltransferase KATAMARI1, putative,	1	70357565-70360177	No Relationship	
9	14	GRMZM2G438840	AT4G28650.1: Leucine-rich repeat transmembrane protein kinase family protein	1	68030886-68034345	Hausmann et al 2002	%GL15 #1
9	14	GRMZM2G438840	AT4G28650.1: Leucine-rich repeat transmembrane protein kinase family protein	1	68030886-68034345	Hausmann et al 2002	%GL30 #1
9	14	GRMZM2G438840	AT4G28650.1: Leucine-rich repeat transmembrane protein kinase family protein	1	68030886-68034345	Hausmann et al 2002	%GL45 #1
9	14	GRMZM2G438840	AT4G28650.1: Leucine-rich repeat transmembrane protein kinase family protein	4	763649-766771	Srinivas et al 2009	QGlaa-sbi04
6	13	GRMZM2G136058	AT1G09580.1: emp24/gp25L/p24 family/GOLD family protein	10	6750688-6753852	No Relationship	
8	13	GRMZM2G169398	alcohol O-acetyltransferase	3	60979810-60981646	No Relationship	
8	13	GRMZM2G169412	AT5G06140.1(ATSNX1,SNX1): sorting nexin 1	3	68239828-68242480	No Relationship	
3	8	GRMZM2G114552	LOC_Os01g03680.1: BBTI8 - Bowman-Birk type bran trypsin inhibitor precursor, expressed	3	68239828-68242480	No Relationship	
7	8	GRMZM2G350205	LOC_Os07g03140.1: ternary complex factor MIP1, putative, expressed	2	1925842-1930101	No Relationship	

Table 3-5 Continued

8	8	GRMZM2G124047	AT5G65760.1: Serine carboxypeptidase S28 family protein	3	63680513-63684777	Xu et al 2000	Chl1
8	8	GRMZM2G124047	AT5G65760.1: Serine carboxypeptidase S28 family protein	3	63680513-63684777	Xu et al 2000	Stg1
8	8	GRMZM2G124047	AT5G65760.1: Serine carboxypeptidase S28 family protein	3	63680513-63684777	Subudhi et al 2000	Stg1
2	7	GRMZM2G122614	AT4G30080.1(ARF16): auxin response factor 16	2	66974211-66975373	No Relationship	
2	7	GRMZM2G122614	AT4G30080.1(ARF16): auxin response factor 16	6	52026582-52027932	No Relationship	
2	7	GRMZM2G473709	LOC_Os07g48244.1: ubiquinol-cytochrome c reductase complex 6.7 kDa protein, putative, expressed	2	62206967-62208784	Subudhi et al 2000	stg3
2	7	GRMZM2G473709	LOC_Os07g48244.1: ubiquinol-cytochrome c reductase complex 6.7 kDa protein, putative, expressed	2	62206967-62208784	Hausmann et al 2002	%GL15 #3

Table 3-5 Continued

2	7	GRMZM2G473709	LOC_Os07g48244.1: ubiquinol-cytochrome c reductase complex 6.7 kDa protein, putative, expressed	2	62206967-62208784	Hausmann et al 2002	%GL30 #5
3	7	AC182482.3_FG003	AT1G16310.1: Cation efflux family protein	3	7540778-7544143	No Relationship	
3	7	GRMZM2G022052	LOC_Os01g48810.1: transcription initiation factor TFIID subunit 11, putative, expressed	3	59582691-59585182	No Relationship	
3	7	GRMZM2G041015	AT2G46225.2(ABIL1): ABI-1-like 1	3	56129320-56132961	Kebede et al 2001	Stg A
3	7	GRMZM5G856738	Ca2+/calmodulin-dependent protein kinase, EF-Hand protein	3	56124094-56128697	Subudhi et al 2000	stg2
4	7	AC233922.1_FG004	AT5G64050.1(ATERS,ERS,OVA3): glutamate tRNA synthetase	4	1438505-1438733	Srinivas et al 2009	QGlaa-sbi04
4	7	AC233922.1_FG005	LOC_Os02g02850.1: bifunctional protein folD, putative, expressed	4	1434239-1437382	No Relationship	
4	7	GRMZM5G846811	AT4G35020.1(ARAC3,ATROP6, RAC3,RHO1PS,ROP6): RAC-like 3	4	1428147-1432056	No Relationship	
4	7	GRMZM5G878607	AT1G78570.1(ATRHM1,RHM1, ROL1): rhamnose biosynthesis 1	1	62767665-62768669	Srinivas et al 2009	QGlam-sbi01-1
4	7	GRMZM5G878607	AT1G78570.1(ATRHM1,RHM1, ROL1): rhamnose biosynthesis 1	9	15520516-15521523	Crasta et al 1999	SGI.2
4	7	GRMZM5G878607	AT1G78570.1(ATRHM1,RHM1, ROL1): rhamnose biosynthesis 1	9	15520516-15521523	Tao et al 2000	not named
6	7	GRMZM2G175676	RNA recognition motif. (a.k.a. RRM, RBD, or RNP domain)	9	50515460-50518998	No Relationship	

Table 3-5 Continued

4	6	GRMZM2G319056	AT4G10150.1: RING/U-box superfamily protein	4	10718953-10719725	No Relationship	
6	6	GRMZM2G412470	AT5G63190.1: MA3 domain-containing protein	7	2230093-2235422	Subudhi et al 2000	not named
6	6	GRMZM2G412470	AT5G63190.1: MA3 domain-containing protein	6	49958897-49960583	Srinivas et al 2009	QGlam-sbi06
7	6	GRMZM2G120652	AT5G01410.1(ATPDX1,ATPDX 1.3,PDX1,PDX1.3,RSR4): Aldolase-type TIM barrel family protein	2	571811-573542	No Relationship	
7	6	GRMZM2G120574	LEUCINE-RICH REPEAT RECEPTOR-LIKE PROTEIN KINASE	2	598353-602274	No Relationship	
7	6	GRMZM2G137676	AT2G26450.1: Plant invertase/pectin methylesterase inhibitor superfamily	2	60346475-60348983	Xu et al 2000	Chl3
7	6	GRMZM2G137676	AT2G26450.1: Plant invertase/pectin methylesterase inhibitor superfamily	7	56379675-56381798	No Relationship	
7	6	GRMZM2G137676	AT2G26450.1: Plant invertase/pectin methylesterase inhibitor superfamily	6	48489499-48490503	Srinivas et al 2009	QGlam-sbi06
9	6	GRMZM2G126682	24-methylenesterol C-methyltransferase	1	62206947-62208784	Srinivas et al 2009	QGlam-sbi01-1
1	5	GRMZM2G110298	AT5G47630.1(mtACP3): mitochondrial acyl carrier protein	1	14753530-14758382	Crasta et al 1999	SGG
2	5	GRMZM2G471931	AT2G28305.1(ATLOG1,LOG1): Putative lysine decarboxylase family protein	6	52003894-52007409	No Relationship	

Table 3-5 Continued

2	5	GRMZM2G122618	Glucose-6-phosphate/phosphate and phosphoenolpyruvate/phosphate antiporter	6	52010744-52016141	No Relationship	
2	5	GRMZM2G122618	Glucose-6-phosphate/phosphate phosphoenolpyruvate/phosphate antiporter	4	56495357-56497337	No Relationship	
3	5	GRMZM2G171677	Tyrosine kinase specific for activated (GTP-bound) p21cdc42Hs	3	9237657-9243340	Tao et al 2000	not named
5	5	GRMZM2G060253	AT4G23800.2: HMG (high mobility group) box protein	4	12111925-12114165	No Relationship	
5	5	GRMZM2G060167	LOC_Os02g15820.1: extra-large G-protein-related, putative, expressed	4	12120082-12125173	No Relationship	
5	5	GRMZM2G060167	LOC_Os02g15820.1: extra-large G-protein-related, putative, expressed	10	43914629-43918413	No Relationship	
6	5	GRMZM2G054946	AT3G14470.1: NB-ARC domain-containing disease resistance protein	10	43914629-43918413	No Relationship	
6	5	GRMZM2G059314	AT2G37790.1: NAD(P)-linked oxidoreductase superfamily protein	9	52026350-52037477	No Relationship	
6	5	GRMZM2G059314	AT2G37790.1: NAD(P)-linked oxidoreductase superfamily protein	3	67425562-67437932	Hausmann et al 2002	%GL30 #2
6	5	GRMZM2G059624	AT5G59850.1: Ribosomal protein S8 family protein	9	52044924-52045541	No Relationship	

Table 3-5 Continued

7	5	GRMZM2G137676	AT2G26450.1: Plant invertase/pectin methylesterase inhibitor superfamily	2	60346475-60348983	Xu et al 2000	Chl3
7	5	GRMZM2G137676	AT2G26450.1: Plant invertase/pectin methylesterase inhibitor superfamily	7	56379675-56381798	No Relationship	
8	5	AC232238.2_FG008	LOC_Os01g64250.1: hemerythrin family protein, expressed	2	64340186-64342021	Hausmann et al 2002	%GL15 #3
8	5	AC232238.2_FG008	LOC_Os01g64250.1: hemerythrin family protein, expressed	5	34662847-34665172	Xu et al 2000	Stg4
8	5	AC232238.2_FG008	LOC_Os01g64250.1: hemerythrin family protein, expressed	5	34662847-34665172	Subudhi et al 2000	stg4
8	5	AC232238.2_FG008	LOC_Os01g64250.1: hemerythrin family protein, expressed	5	34662847-34665172	Kebede et al 2001	Stg J
8	5	AC232238.2_FG008	LOC_Os01g64250.1: hemerythrin family protein, expressed	3	68221744-68223579	No Relationship	
9	5	GRMZM2G169365	AT5G12040.1: Nitrilase/cyanide hydratase and apolipoprotein N-acyltransferase family protein	1	68568757-68573014	No Relationship	
9	5	GRMZM2G169384	LOC_Os09g04670.1: DAG protein, chloroplast precursor, putative, expressed	1	68558366-68568013	No Relationship	
9	5	GRMZM2G107651	AT2G20320.1: DENN (AEX-3) domain-containing protein	1	70297442-70305481	No Relationship	

Table 3-5 Continued

10	5	GRMZM2G080516	AT4G17500.1(ATERF-1,ERF-1): ethylene responsive element binding factor 1	6	53447205-53449740	No Relationship
10	5	GRMZM2G084586	AT3G13530.1(MAP3KE1,MAPKKK7): mitogen-activated protein kinase kinase kinase 7	6	59938234-59942713	No Relationship
10	5	GRMZM2G084576	AT2G43060.1(IBH1): ILI1 binding bHLH 1	6	59908096-59909157	No Relationship

Table 3-6 Summary of maize candidate gene associations for stay-green terminal from the NAM Testcrosses compared to reported sorghum stay-green QTL.

Maize LG	RMIP	Maize ID	Description	Sb LG	Sb Genomic Position	Publication	Published symbol
2	27	GRMZM2G374203	PFAM ID: PF08381: Transcription factor regulating root and shoot growth via Pin3	6	56338195-56345720	No Relationship	
2	27	GRMZM2G074743	AT3G22370.1(AOX1A,ATAOX1A): alternative oxidase 1A	6	56332430-56332700	No Relationship	
5	25	GRMZM2G173674	AT5G17530.3: phosphoglucosamine mutase family protein	2	17048717-17051775	Kebede et al 2001	Stg D
8	23	GRMZM2G055219	AT2G19950.2(GC1): golgin candidate 1	3	62544904-62551856	Xu et al 2000	Chl1
6	20	GRMZM2G170646	AT1G28580.1: GDSL-like Lipase/Acylhydrolase superfamily protein	3	1479900-1490112	No Relationship	
6	20	GRMZM2G170646	AT1G28580.1: GDSL-like Lipase/Acylhydrolase superfamily protein	9	10655297-10658206	Crasta et al 1999	SGI.2
6	20	GRMZM2G162702	AT1G56720.1: Protein kinase superfamily protein	9	10696640-10700524	Tao et al 2000	not named
2	18	GRMZM2G021831	AT3G14180.1: sequence-specific DNA binding transcription factors	6	47401201-47402842	No Relationship	
2	18	GRMZM2G021464	AT3G14080.1: Small nuclear ribonucleoprotein family protein	6	47406107-47411017	No Relationship	
4	16	GRMZM2G108147	AT2G25620.1(AtDBP1,DBP1): DNA-binding protein phosphatase 1	10	4838243-4840662	No Relationship	
4	16	GRMZM2G344376	AT5G11090.1: serine-rich protein-related	4	60981111-60981646	No Relationship	

Table 3-6 Continued

4	16	GRMZM2G344376	AT5G11090.1: serine-rich protein-related	4	65965620-65966719	No Relationship	
5	16	GRMZM2G436710	LOC_Os10g35810.1: thylakoid lumenal protein, putative, expressed	1	18525710-18528791	No Relationship	
5	16	GRMZM2G436707	AT1G07280.1: Tetratricopeptide repeat (TPR)-like superfamily protein	1	18528268-18529939	No Relationship	
10	15	GRMZM2G042782	AT1G43690.1: ubiquitin interaction motif-containing protein	6	45236301-45237998	No Relationship	
10	15	GRMZM2G042811	AT2G19130.1: S-locus lectin protein kinase family protein	6	45214678-45216608	No Relationship	
3	12	GRMZM2G439784	AT2G34930.1: disease resistance family protein / LRR family protein	7	9520372-9523288	Kebede et al 2001	Stg E
3	12	GRMZM2G439784	AT2G34930.1: disease resistance family protein / LRR family protein	7	9520372-9523288	Hausmann et al 2002	%GL15 #3
3	12	GRMZM2G439784	AT2G34930.1: disease resistance family protein / LRR family protein	5	53213094-53217196	No Relationship	
3	12	GRMZM2G439799	AT3G47570.1: Leucine-rich repeat protein kinase family protein	6	6486616-6495047	No Relationship	
8	11	GRMZM2G096358	AT1G68320.1(AtMYB62,BW62B,BW62C,MYB62): myb domain protein 62	3	7677202-7679048	Tao et al 2000	not named
9	11	GRMZM2G078933	AT5G58590.1(RANBP1): RAN binding protein 1	1	61912082-61914993	No Relationship	
9	11	GRMZM2G078933	AT5G58590.1(RANBP1): RAN binding protein 1	9	42101221-42101806	Crasta et al 1999	SGI.2
9	11	GRMZM2G078933	AT5G58590.1(RANBP1): RAN binding protein 1	9	42101221-42101806	Tao et al 2000	not named
9	11	GRMZM2G078933	AT5G58590.1(RANBP1): RAN binding protein 1	3	65699538-65700373	Xu et al 2000	Chl1

Table 3-6 Continued

9	11	GRMZM2G078933	AT5G58590.1(RANBP1): RAN binding protein 1	3	65699538-65700373	Xu et al 2000	Stg1
9	11	GRMZM2G078933	AT5G58590.1(RANBP1): RAN binding protein 1	3	65699538-65700373	Subudhi et al 2000	Stg1
9	11	GRMZM2G078933	AT5G58590.1(RANBP1): RAN binding protein 1	3	65699538-65700373	Hausmann et al 2002	%GL30 #2
9	11	GRMZM2G378852	AT2G30040.1(MAPKKK14): mitogen-activated protein kinasekinasekinase 14	1	61916897-61918785	No Relationship	
8	10	GRMZM2G445338	AT1G18390.2: Protein kinase superfamily protein	3	60075074-60076715	No Relationship	
8	10	GRMZM2G144021	AT5G38220.1: alpha/beta-Hydrolases superfamily protein	3	60053879-60058397	No Relationship	
8	10	GRMZM2G144028	LOC_Os01g49529.2: OsWAK10d - OsWAK receptor-like cytoplasmic kinase OsWAK-RLCK, expressed	3	60057699-60070819	No Relationship	
8	10	GRMZM2G144028	LOC_Os01g49529.2: OsWAK10d - OsWAK receptor-like cytoplasmic kinase OsWAK-RLCK, expressed	9	56669583-56674848	No Relationship	
9	10	GRMZM2G147671	AT4G38630.1(ATMCB1,MBP1,MCB1,RPN10): regulatory particle non-ATPase 10	1	59630506-59635592	No Relationship	
9	10	GRMZM2G156388	AT5G64813.1(LIP1): Ras-related small GTP-binding family protein	1	64671213-64675902	Srinivas et al 2009	QGlam-sbi01-1
1	9	GRMZM2G343157	AT3G43440.1(JAZ11,TIFY3A): jasmonate-zim-domain protein 11	1	68348009-68349336	Hausmann et al 2002	%GL15 #1
1	9	GRMZM5G838098	AT1G19180.1(JAZ1,TIFY10A): jasmonate-zim-domain protein 1	1	68342384-68343847	Hausmann et al 2002	%GL30 #1

Table 3-6 Continued

1	9	GRMZM5G838098	AT1G19180.1(JAZ1,TIFY10A): jasmonate-zim-domain protein 1	1	68334761-68335711	Hausmann et al 2002	%GL45 #1
5	8	GRMZM2G071484	AT3G52450.1(PUB22): plant U-box 22	4	51302099-51303468	Hausmann et al 2002	%GL30 #3
5	8	GRMZM2G071484	AT3G52450.1(PUB22): plant U-box 22	4	51302099-51303468	Hausmann et al 2002	%GL45 #4
5	8	GRMZM2G071484	AT3G52450.1(PUB22): plant U-box 22	6	44859659-44860989	No Relationship	
5	8	GRMZM2G071484	AT3G52450.1(PUB22): plant U-box 22	3	62207724-62208784	No Relationship	
8	8	GRMZM2G139574	AT2G41640.1: Glycosyltransferase family 61 protein	9	48132658-48140986	No Relationship	
8	8	GRMZM2G139574	AT2G41640.1: Glycosyltransferase family 61 protein	2	59634559-59635592	No Relationship	
5	7	GRMZM2G124284	AT5G01230.1: S-adenosyl-L-methionine-dependent methyltransferases superfamily protein	4	65997207-65998773	No Relationship	
5	7	GRMZM2G124290	AT1G21326.1: VQ motif-containing protein	1	4718524-4719317	No Relationship	
9	7	GRMZM2G378852	AT2G30040.1(MAPKKK14): mitogen-activated protein kinasekinasekinase 14	1	61916897-61918785	Srinivas et al 2009	QGlam-sbi01-1
10	7	GRMZM2G031721	AT4G13670.1(PTAC5): plastid transcriptionally active 5	6	51740613-51748799	No Relationship	
10	7	GRMZM2G031628	AT4G21760.1(BGLU47): beta-glucosidase 47	6	51733501-51734083	No Relationship	
10	7	GRMZM2G031660	AT1G61820.1(BGLU46): beta glucosidase 46	6	51733501-51734083	No Relationship	
7	6	GRMZM2G330690	AT4G30890.1(UBP24): ubiquitin-specific protease 24	2	62205791-62208784	Subudhi et al 2000	stg3

Table 3-6 Continued

7	6	GRMZM2G330690	AT4G30890.1(UBP24): ubiquitin-specific protease 24	2	62205791-62208784	Hausmann et al 2002	%GL15 #3
7	6	GRMZM2G330690	AT4G30890.1(UBP24): ubiquitin-specific protease 24	2	62205791-62208784	Hausmann et al 2002	%GL30 #5
7	6	GRMZM2G330690	AT4G30890.1(UBP24): ubiquitin-specific protease 24	2	62205791-62208784	Subudhi et al 2000	stg3
10	6	GRMZM2G446737	PFAM ID: PF05757: Oxygen evolving enhancer protein 3 (PsbQ)	6	52108732-52112831	No Relationship	
10	6	GRMZM2G146809	LOC_Os02g41904.1: DEF7 - Defensin and Defensin-like DEFL family,	6	52085272-52086238	No Relationship	
1	5	GRMZM2G107395	AT1G78300.1(14-3-3OMEGA,GF14 OMEGA,GRF2): general regulatory factor 2	7	61684402-61684907	Hausmann et al 2002	%GL15 #5
1	5	GRMZM2G107395	AT1G78300.1(14-3-3OMEGA,GF14 OMEGA,GRF2): general regulatory factor 2	7	61684402-61684907	Hausmann et al 2002	%GL30 #7
1	5	GRMZM2G107395	AT1G78300.1(14-3-3OMEGA,GF14 OMEGA,GRF2): general regulatory factor 2	7	61684402-61684907	Hausmann et al 2002	%GL45 #8
1	5	GRMZM2G107395	AT1G78300.1(14-3-3OMEGA,GF14 OMEGA,GRF2): general regulatory factor 2	5	51517137-51519016	Subudhi et al 2000	stg4
1	5	GRMZM2G107395	AT1G78300.1(14-3-3OMEGA,GF14 OMEGA,GRF2): general regulatory	5	51517137-51519016	Kebede et al 2001	Stg J
2	5	GRMZM2G530263	AT2G16030.1: S-adenosyl-L-methionine-dependent methyltransferases superfamily protein	7	61684402-61684907	Hausmann et al 2002	%GL15 #5

Table 3-6 Continued

2	5	GRMZM2G530263	AT2G16030.1: S-adenosyl-L-methionine-dependent methyltransferases superfamily protein	7	61684402-61684907	Hausmann et al 2002	%GL30 #7
2	5	GRMZM2G530263	AT2G16030.1: S-adenosyl-L-methionine-dependent methyltransferases superfamily protein	7	61684402-61684907	Hausmann et al 2002	%GL45 #8
3	5	GRMZM2G467086	AT1G25260.1: Ribosomal protein L10	8	434873-437341	No Relationship	
3	5	GRMZM2G467086	AT1G25260.1: Ribosomal protein L10	5	321146-323706	No Relationship	
3	5	GRMZM2G467123	AT5G45275.1: Major facilitator	8	563311-567438	No Relationship	
3	5	GRMZM2G467123	AT5G45275.1: Major facilitator superfamily protein	5	423230-428112	No Relationship	
3	5	GRMZM2G054610	AT3G25100.1(CDC45): cell division cycle 45	8	1813024-1814559	No Relationship	
3	5	GRMZM2G054610	AT3G25100.1(CDC45): cell division cycle 45	5	1865248-1866812	No Relationship	
3	5	GRMZM2G353076	AT3G28917.1(MIF2): mini zinc finger	8	1858071-1860694	No Relationship	
4	5	GRMZM2G107414	LOC_Os02g52300.1: CPuORF38 - conserved peptide uORF-containing transcript, expressed	4	55457809-55460251	No Relationship	
4	5	GRMZM2G041699	AT1G22360.1(AtUGT85A2,UGT85A2): UDP-glucosyl transferase 85A2	4	57333427-57335258	No Relationship	
4	5	GRMZM2G041699	AT1G22360.1(AtUGT85A2,UGT85A2): UDP-glucosyl transferase 85A2	6	48069891-48071375	Srinivas et al 2009	QGlam-sbi06
4	5	GRMZM2G041699	AT1G22360.1(AtUGT85A2,UGT85A2): UDP-glucosyl transferase 85A2	7	54762753-54764102	No Relationship	

Table 3-6 Continued

4	5	GRMZM2G041699	AT1G22360.1(AtUGT85A2,UGT85A2): UDP-glucosyl transferase 85A2	10	11669228-11670615	No Relationship	
4	5	GRMZM2G041699	AT1G22360.1(AtUGT85A2,UGT85A2): UDP-glucosyl transferase 85A2	2	60980278-60981646	Xu et al 2000	Chl3
5	5	GRMZM2G121221	AT2G30620.2: winged-helix DNA-binding transcription factor family protein	1	4084076-4085583	No Relationship	
6	5	GRMZM2G054468	AT5G37720.1(ALY4): ALWAYS EARLY 4	10	9965183-9972666	No Relationship	
6	5	GRMZM2G328859	AT2G18180.1: Sec14p-like phosphatidylinositol transfer family protein	4	1659223-1659662	Srinivas et al 2009	QGlaa-sbi04
9	5	GRMZM2G007514	AT2G38440.1(ATSCAR2,DIS3,ITB1,SCAR2,WAVE4): SCAR homolog 2	1	61667355-61673428	Srinivas et al 2009	QGlam-sbi01-1
9	5	GRMZM2G007590	AT2G30260.1(U2B): U2 small nuclear ribonucleoprotein B	1	61660465-61665574	Srinivas et al 2009	QGlam-sbi01-1
9	5	GRMZM2G487359	AT4G02030.1: Vps51/Vps67 family (components of vesicular transport)	1	7557185-7558119	Hausmann et al 2002	%GL30 #4
9	5	GRMZM2G487359	AT4G02030.1: Vps51/Vps67 family (components of vesicular transport)	1	7557185-7558119	Hausmann et al 2002	%GL45 #3
9	5	GRMZM2G487359	AT4G02030.1: Vps51/Vps67 family (components of vesicular transport)	8	5563825-5565387	No Relationship	
10	5	AC233888.1_FG001	PFAM ID: PF05703: Auxin canalisation , PF08458: Plant pleckstrin homology-like region	6	50745192-50747356	Srinivas et al 2009	QGlam-sbi06
10	5	AC233888.1_FG002	AT5G57660.1(ATCOL5,COL5): CONSTANS-like 5	6	50736218-50737298	Srinivas et al 2009	QGlam-sbi06

3.4.3 General Sorghum Stay-green Genetic Information

We identified several comparative relationships between maize and sorghum for stay-green loci. Maize candidate genes were BLASTed into the sorghum genome to provide an avenue of examining stay-green relationships. Sorghum genomic intervals were determined from predicted base-pair positions and flanking markers from the scientific literature. In Table 3-7, we provide the percent of maize associations for all sorghum QTL and removal of large QTL from sorghum linkage studies to examine the comparative relationship of stay-green in the two species. Maize genic regions BLASTed into the sorghum genome identified multiple locations of genome similarity.

Table 3-7 Summary of maize and sorghum stay-green associations. Number of maize genes evaluated are only annotated candidates from association mapping results for the specific population. Multiple sorghum positions are detected when BLASTing maize genic regions into the sorghum genome. Both the entire sorghum stay-green genome representation and a subset of all large intervals removed were examined for maize stay-green genomic associations.

Maize Population	Number of Maize Genes Evaluated	Sorghum Positions Detected	Stay-green Anthesis Associations (All Sb QTL)	Percent of Stay-green Association
NAM RILs	79	102	25	24.50%
Total	79	102	25	24.50%
Maize Population	Number of Maize Genes Evaluated	Sorghum Positions Detected	Stay-green Anthesis Associations (Large Sb Intervals Removed)	Percent of Stay-green Association
NAM RILs	79	102	22	21.57%
Total	79	102	22	21.57%

Maize Population	Number of Maize Genes Evaluated	Sorghum Positions Detected	Stay-green Terminal Associations (All Sb QTL)	Percent of Stay-green Association
NAM RILs	62	85	29	34.10%
NAM Testcrosses	53	74	25	33.70%
Total	115	159	54	33.90%
Maize Population	Number of Maize Genes Evaluated	Sorghum Positions Detected	Stay-green Terminal Associations (Large Sb Intervals Removed)	Percent of Stay-green Association
NAM RILs	62	85	25	29.41%
NAM Testcrosses	53	74	20	27.03%
Total	115	159	45	28.22%

3.5 Discussion

Comparative genomics is an increasingly powerful resource for plant breeders and geneticists. The ability to leverage genomic data from maize into sorghum has been greatly underutilized in plant breeding for abiotic stress traits. Maize and sorghum are closely related crop species that are adapted to several agronomic and climatic environments. Maize possesses a large genomic and agronomic investment globally, whereas sorghum does not have the same support even though it is a staple crop in developing areas of the world.

Sorghum has been characterized and commercialized in challenging environments. Extensive evaluation of the stay-green phenotype has led to yield increases and improvement for drought environments over the last thirty years. Primarily, stay-green at anthesis and end of season are positively correlated to yield increases and/or stability in drought situations (Borrell et al., 2000a, 2000b, 2001). 83 QTL were identified in eight genetic studies of stay-green under drought situations utilizing varying measurements of stay-green in sorghum (Table 3-1, 3-2). However, these studies employed classical linkage mapping methods, where confidence intervals can extend several million base pairs making molecular characterization difficult.

In comparison to sorghum, maize has not been extensively evaluated for stay-green at genetic and agronomic levels. We examined the comparative relationships of stay-green in maize discussed in Chapter 2 with reported sorghum literature. By identifying these relationships, we propose that candidate genes and functions for stay-green under drought conditions are potentially expressed in both maize and sorghum. Understanding the specific gene function of these candidate genes will aid breeders and

researchers in developing climate resilient crops and leveraging genomic data for crop improvement.

We identified several genomic relationships for stay-green that appear to be similar in maize and sorghum. Sorghum breeders and scientists are actively selecting and characterizing four stay-green QTL identified as Stg1, Stg2, Stg3, and Stg4 (Table 3-1). These QTL provide a baseline for examining the biological relationship of stay-green with maize. Stg1 and Stg2 are located on sorghum chromosome 3 and account for ~20% and ~ 30% of the phenotype variation, while Stg3 and Stg4 encompass ~16% and ~10% of the phenotypic variation. Depending on the population, phenotypic contribution of Stg loci rank as Stg2>Stg1>Stg3>Stg4 (Harris et al., 2007). However, additional minor QTL can modulate the expression of stay-green in different backgrounds and environments. For the three maize populations corresponding to stay-green at anthesis and end-of-season, we report the comparative relationships of stay-green for major sorghum stay-green QTL.

3.5.1 Characterization and Evaluation of *Stg1* in Sorghum

The sorghum Stg1 QTLs were associated with numerous genomic regions and candidate genes for stay-green anthesis and stay-green terminal in maize. Markers for all of the sorghum Stg1 QTL were associated with a region for stay-green anthesis in the maize NAM RILs (Table 3-8). A maize candidate gene was identified for this region on chromosome 3 (Table 3-4). GRMZM2G337815 (Ribosomal protein S25 family protein - AT4G34555.1) (3:22,566,318-22,568,842) and had a RMIP of nine (Table 3-4). Ribosomal protein S25 does not have any known genomic and physiological role in drought tolerance or delayed senescence in plants (Table 3-8).

The sorghum Stg1.1 QTL (Published symbol: Chl1) was also associated with a maize candidate gene for stay-green terminal in the maize NAM RILs (Table 3-8). GRMZM2G700901 (3:34,894,177-34,897,527) encodes a HEAT repeat domain (Table 3-5). HEAT repeat domains are similar to ARM proteins in both molecular structure and function (Andrade et al., 2001). HEAT domains are common to the protein phosphatase 2A gene families that are involved in signal transduction of stress responses under water limited situations (Samuel et al., 2008). However, not enough is known about the function of this gene to speculate a specific role related to abiotic stress tolerance (Table 3-8).

Sorghum Stg1.1, 1.2, 1.3, and 1.4 QTLs were associated with a region for stay-green terminal in the maize NAM RILs on chromosome 8 (Table 3-8). A maize candidate gene was identified in this region (Table 3-5). GRMZM2G124047 (8:173,029,283-173,035,156) encodes a Serine carboxypeptidase S28 family protein (AT5G65760.1) (Table 3-5). Very little is known about this gene or its function in plants.

Sorghum Stg1.1 1.2, 1.3, 1.4, and 1.6 were associated with a region for stay-green terminal in the NAM Testcrosses on chromosome 9 (Table 3-8). A maize candidate gene was identified in this region (Table 3-6). GRMZM2G078933 (9:137,487,958-137,491,564) encoding a (RANBP1): RAN binding protein 1 (AT5G58590.1) (Table 3-6). RAN proteins are known to be involved in HEAT repeats. HEAT repeats contain many diverse functions, one of which is involved in regulating transportation in the cell from the nucleus to the cytoplasm. RANBP1 is known to be involved in mediating the hydrolysis of GTP in the nucleus by interacting with karyopherin B for nuclear import

(Lounsbery and Macara, 1997). The relationship between this process and stay-green remains unclear (Table 3-8).

Sorghum Stg1.1 was associated with a region for stay-green terminal in the NAM testcrosses on chromosome 8 (Table 3-8). A maize candidate gene was identified in this region (Table 3-6). GRMZM2G055219 (8:174,780,979-174,788,170) encodes (GC1): golgin candidate 1 (AT2G19950.2) (Table 3-6). Very preliminary research suggests that golgin candidate 1 is involved in maintenance of the Golgi apparatus or tethering vesicles to the organelle (UniProt) (Table 3-8).

Table 3-8 *Stg1* QTL reported from the literature. Genomic positions are generated through prediction of the linkage positions previously reported.

Stg1 QTL	Pop	Source allele	Additive effect	Flanking markers	Published symbol	Publication
Stg1.1	B35/Tx7000	B35	-6.403	bnl6.16/txs1114	Chl1	Xu et al 2000
Stg1.2	B35/Tx7000	B35	0.071	bnl6.16/txs1114	Stg1	Xu et al 2000
Stg1.3	B35/Tx7000	B35	0.2333	NPI414/bnl15.20	Stg1	Subudhi et al 2000
Stg1.4	B35/Tx7000	B35	0.0205	NPI414/bnl15.20	Stg1	Subudhi et al 2000
Stg1.5	IS9830/E36-1	IS9830	-4.4	umc7/txp114	%GL15 #1	Hausmann et al 2002
Stg1.6	IS9830/E36-1	IS9830	-2.7	umc7/txp114	%GL30 #2	Hausmann et al 2002

Table 3-8 Continued

Stg1 QTL	LG	CI Start	CI End	QTL size	CI Start	CI End	QTL size	LOD	R^2
Stg1.1	SBI-3	120.56	134.43	13.86	62,207,313	67,212,079	5,004,766	2.69	12
Stg1.2	SBI-3	123.25	131.74	8.49	62,841,197	66,318,409	3,477,212	4.59	19.6
Stg1.3	SBI-3	124.59	135.40	10.80	63,241,387	67,694,738	4,453,351	3.18	15.4
Stg1.4	SBI-3	125.41	134.59	9.19	63,482,399	67,351,512	3,869,113	3.61	18.1
Stg1.5	SBI-3	131.13	133.87	2.74	66,129,723	66,758,123	628,400	14.9	26.3
Stg1.6	SBI-3	129.59	135.41	5.82	65,303,733	67,694,738	2,391,005	6.5	12.4

3.5.2 Characterization and Evaluation of *Stg2* in Sorghum

The sorghum Stg2 genomic region overlapped with maize markers on that were associated with stay-green terminal in the NAM RILs (Table 3-9). Sorghum Stg2.2, 2.3, 2.4, 2.5, 2.6 and 2.7 overlapped with maize markers associated with stay-green terminal on chromosome 4 (Table 3-9). A single maize candidate gene was identified in this region (Table 3.5). GRMZM2G131378 (4:36,040,438-36,042,330) encodes a glycerol-3-phosphate acyltransferase 6 (AT2G38110.1 (ATGPAT6, GPAT6)) and the associated SNP was significant at a RMIP = 17 (Table 3-5). GPAT6 is involved in cutin formation in plants, which is associated with cuticle formation (TAIR). The cuticle, a waxy layer on the aerial surface of plants, is associated with water-use efficiency in plants, making it an interesting candidate for stay-green in maize and sorghum (Yoo et al., 2009).

Sorghum Stg2.1 and Stg2.2 also overlapped with maize markers associated with stay-green terminal on chromosome 3 (Table 3-9). Two maize candidate gene were identified in this region (Table 3.5). GRMZM2G041015 (3:217,692,785-217,696,057/RMIP = 7) encodes an ABI-1-like protein (AT2G46225.2 (ABIL1)), and GRMZM5G856738 (3:217,700,066-217,705,147/RMIP = 7) encodes a calcium-dependent protein kinase 6 protein (AT4G23650.1 (CDPK6, CPK3)) (Table 3-5).

The first candidate gene was abscisic acid insensitive 1 (ABI1). ABI1 is involved in regulating and signaling global plant responses for growth and development (Leung et al., 1994, 1997). This protein is involved in regulating stomatal aperture and mitotic activity in the root meristem and differs from other serine-threonine phosphatases 2C proteins by its possession of an amino-terminal extension with an EF hand calcium-binding site (Leung et al., 1994, 1997). This unique motif allows ABI1 to interact

intimately with calcium signaling and ties together ABA and calcium responses (Leung et al., 1994, 1997). The ABI1 mutation is dominant, which made follow up experiments determining regulation characteristics difficult (Leung et al., 1994, 1997). Further characterization of the ABI1 loci showed that this gene is a negative regulator of ABA responses in plants (Gosti et al., 1999). ABI1 and homologous ABI2 wild type plants were tolerant to drought conditions, while mutant plants were susceptible to water-limited conditions (Chak et al., 2000). ABA and its role in regulating plant responses to drought and senescence are well described, and ABI1 is a plausible candidate gene for stay-green in maize and sorghum.

The second candidate gene was a calcium-dependent protein kinase 6/EF-hand calcium domain. These proteins contain a calcium activation domain and additional EF hand domains and have been implicated in multiple plant signaling and downstream transduction cascades of calcium responses. CPK3 is involved in regulating guard cell ion channeling and is active in both the guard and mesophyll cells. ABA is also involved in regulating the expression of CPK3, and double mutants of cpk3cpk6 exhibited impaired stomatal closing (Mori et al., 2003). CPK3 is involved in salt-stress acclimation in arabidopsis through signal relay and transduction (Mehlmer et al., 2010). Furthermore, CPK3 has been implicated in drought stress response in arabidopsis, whereby the inactivation of the gene expression led to a reduction of ion channel activation, impaired ability to sense ABA, and decreased stomata sensitivity to ABA (Kwak et al., 2002).

Table 3-9 *Stg2* QTL reported from the literature. Genomic positions are generated through prediction of the linkage positions

Stg2 QTL	Pop	Source allele	Additive effect	Flanking markers	Published symbol	Publication
Stg2.1	SC56/Tx7000	SC56	0.146	txs584/csu58	Stg A	Kebede et al 2001
Stg2.2	B35/Tx7000	B35	0.0838	rz323/A12RFLP	stg2	Subudhi et al 2000
Stg2.3	296B/IS18551	296B	60.29	txp59/Stgnhsbm21	QGlaa-sbi03	Srinivas et al 2009
Stg2.4	296B/IS18551	296B	3.54	txp59/Stgnhsbm21	QPglam-sbi03	Srinivas et al 2009
Stg2.5	B35/Tx7000	B35	0.2677	wg889/txs584	stg2	Subudhi et al 2000
Stg2.6	B35/Tx7000	B35	0.0703	wg889/txs584	stg2	Subudhi et al 2000
Stg2.7	B35/Tx7000	Tx7000	-5.2845	wg889/txs584	stg2	Subudhi et al 2000
Stg2.8	B35/Tx7000	Tx7000	-7.082	wg889/R	Chl2	Xu et al 2000
Stg2.9	B35/Tx7000	B35	0.089	wg889/R	Stg2	Xu et al 2000
Stg2.10	B35/Tx430	B35	0.27	txs307	SGA	Crasta et al 1999
Stg2.11	N13/E36-1	E36-1	2	11/49-320 / umc63	%GL45 #5	Hausmann et al 2002

Table 3-9 Continued

Stg2 QTL	LG	CI Start	CI End	QTL size	CI Start	CI End	QTL size	LOD	R^2
Stg2.1	SBI-03	71.11	83.89	12.78	55,204,764	56,500,632	1,295,868	2.63	10.2
Stg2.2	SBI-03	79.06	90.94	11.88	55,814,195	58,046,499	2,232,304	2.65	14
Stg2.3	SBI-03	82.05	97.95	15.91	56,228,544	58,305,138	2,076,594	2.65	6.1
Stg2.4	SBI-03	83.53	96.47	12.94	56,443,470	58,281,040	1,837,570	2.6	5.2
Stg2.5	SBI-03	85.82	94.18	8.358	56,775,084	58,252,295	1,477,211	3.66	19.9
Stg2.6	SBI-03	87.15	92.85	5.696	56,993,522	58,240,511	1,246,989	5.52	29.2
Stg2.7	SBI-03	86.32	93.68	7.359	56,856,140	58,252,295	1,396,155	5.44	22.6
Stg2.8	SBI-03	92.15	98.85	6.71	58,234,385	58,305,138	70,753	5.6	24.8
Stg2.9	SBI-03	92.76	98.24	5.49	58,234,385	58,305,138	70,753	6.23	30.3
Stg2.10	SBI-03	92.88	98.82	5.94	58,240,511	58,305,138	64,627	6.6	28.6
Stg2.11	SBI-03	92.06	104.94	12.88	58,234,385	59,052,530	818,145	2.8	5.6

3.5.3 Characterization and Evaluation of *Stg3* in Sorghum

The Stg3 locus of sorghum was detected in numerous genetic mapping studies (Table 3-10). This region also exhibited considerable overlap with QTL detected for stay-green in maize (Table 3-4).

The Sorghum Stg3 QTL overlapped with maize markers associated with the stay-green anthesis trait on chromosomes 1 and 2 (Table 3-4). GRMZM2G110107 (2: 185,690,953-185,695,004) encodes an indeterminate (ID)-domain 14 protein (AT1G68130.1 (AtIDD14,IDD14)) and was in the most significant SNP in the NAM RILs anthesis analysis with an RMIP of 47 (Table 3-4). Indeterminate (ID)-domain 14 protein contains two splicing variants that differentially regulate starch metabolism in cold conditions in arabidopsis (Seo et al., 2011). These proteins functioned to competitively inhibit starch metabolism. Ultimately, Seo et al. proposed that IDD14 generates a self-controlled regulatory loop that modulates starch accumulation in cold stress situations. Furthermore, in conjunction with IDD15 and IDD16, IDD14 works to regulate lateral organ morphogenesis and gravitropism by encouraging auxin biosynthesis and transport in arabidopsis (Cui et al., 2013). Phenotypic presentations of IDD proteins in this study included alter leaf shape, flower development, gravitropic responses, fertility, and plant architecture. Thus these proteins, with the assistance of auxin, are regulating plant growth and development by targeting downstream proteins involved in anatomical plant formation, such as YUCCA5, TAA1, and PIN1 genes. In conclusion, IDD14 and other indeterminate domains, are involved in regulating plant growth and development during the transition from vegetative to reproductive growth. Ultimately, it is plausible that these genes are modulating stay-green expression at anthesis through

phytohormone regulation and expression of other plant growth and development-related gene families. This domain genomically corresponds to sorghum Stg3.1-3.5 (Table 3-10).

GRMZM2G002131 (2: 186,183,204-186,187,268) is the second maize candidate that overlapped with Stg3 of sorghum (Table 3-4). GRMZM2G002131 encodes a heat shock factor 4 protein (AT4G36990.1(AT-HSFB1,ATHSF4,HSF4,HSFB1)) and was the second most significant SNP in this study with an RMIP of 36 (Table 3-4). Heat shock protein 4 is involved in regulating the expression of heat shock proteins in response to heat shock, but it did not have increased or decreased expression of heat shock protein (HSP) when overexpressed in arabidopsis (TAIR). Detection of a heat-related gene such as HSP4 is not surprising due to excessive high temperatures present in the NAM RILs study in 2012. This protein is genomically related to sorghum Stg3.3-3.7 (Table 3-10).

GRMZM2G113840 is the third maize candidate that overlapped with Stg3 of sorghum (Table 3-4). GRMZM2G113840 was identified on chromosome 1 with a RMIP of 18 (Table 3-4). GRMZM2G113840 (1: 183,806,997-183,811,541) encodes a Sec14p-like phosphatidylinositol transfer family protein (AT4G39170.1) (Table 3-4). Sec14p-like phosphatidylinositol transfer family protein was characterized in yeast as regulating lipid transport and phosphoinositide homeostasis (Mousley et al., 2007). Translating this function into plants under abiotic stress suggests that this protein could be involved in manipulating the plant cell under water-deficit conditions to overcome cellular damage, thereby conferring stay-green. The second candidate gene was a calcium-dependent protein kinase 6/EF-hand calcium domain. These proteins contain a calcium activation domain and additional EF hand domains and have been implicated in multiple plant

signaling and downstream transduction cascades of calcium responses. CPK3 is involved in regulating guard cell ion channeling and is active in both the guard and mesophyll cells. ABA is also involved in regulating the expression of CPK3, and double mutants of cpk3cpk6 exhibited impaired stomatal closing (Mori et al., 2003). CPK3 is involved in salt-stress acclimation in arabidopsis through signal relay and transduction (Mehlmer et al., 2010). Furthermore, CPK3 has been implicated in drought stress response in arabidopsis, whereby the inactivation of the gene expression led to a reduction of ion channel activation, impaired ability to sense ABA, and decreased stomata sensitivity to ABA (Kwak et al., 2002) evidence, the exact relationship of this protein to stay-green at anthesis remains unclear. This protein is genomically related to sorghum Stg3.6-3.9 (Table 3-10).

The Sorghum Stg3 QTL also overlapped with maize markers associated with the stay-green terminal trait on chromosomes 2, 6, and 7 (Table 3-5). GRMZM2G156310 (6: 115,546,691-115,548,383) is the maize candidate gene on chromosome 6 that encodes an alpha/beta-hydrolase superfamily protein (AT1G47480.1) and is closely linked to the third most significant SNP for this phenotype with a RMIP of 30 (Table 3-5). Alpha/beta hydrolases are a large family of proteins involved in numerous plant functions. It is unclear at this time what the specific function of this hydrolase would be in relation to stay-green. This protein is genomically related to sorghum Stg3.3-3.8 (Table 3-10). GRMZM2G473709 (2:217,008,458-217,009,689) is the maize candidate gene on chromosome 2 and encodes an ubiquinol-cytochrome c reductase complex 6.7 kDa protein (LOC_Os07g48244.1) (Table 3-5). Ubiquinol-cytochrome c reductase complex 6.7 kDa protein is located in the mitochondria of a plant cell and is involved in the

mitochondrial respiratory chain (TAIR). It is related to sorghum Stg3.5-3.8(Table 3-10). No known function associated with an abiotic stress is reported for this protein. GRMZM2G137676 (7:119,973,818-119,976,271) is the maize candidate on chromosome 7 and encodes a plant invertase/pectin methylesterase inhibitor superfamily (AT2G26450.1) (Table 3-5). Plant invertases/pectin methylesterases are involved in demethylesterification of cell wall polygalacturonans (Micheli et al., 2001). Most of these enzymes are at the beginning of the pectin biosynthetic pathway, where it is synthesized in the Golgi apparatus and secreted into the cell wall. Additionally, in relation to abiotic stress, pectin methylesterases can regulate pectin structure through stem elongation, cellular adhesion, plasticity, pH, and ionic contents of the cell wall (Pelloux et al., 2007). Thus pectin remodeling under an abiotic stress can be critical to survival of a plant. Additionally, it highlights other association mapping results where Golgi apparatus genes were identified as significantly correlated with stay-green phenotypes in maize (Table 3-10). Plant invertase/pectin methylesterase inhibitors have a direct role in regulating kiwi fruit development, carbohydrate metabolism, and cell wall extension (Giovane et al., 1995). In wheat, pectin methyl esterases and their related inhibitors were regulated under stress responses by intron retention of different alleles (Rocchi et al., 2011). French et al. (2014) identified a link between auxin, and cell wall invertases and inhibitors during grain development in rice. The link between stay-green and end of season greenness is plausible based on the known genomic and physiological characterization of this gene (Table 3-10). This specific plant invertase/pectin methylesterase inhibitor was detected in both the NAM RILs terminal and AMES terminal phenotypes genomewide association mapping studies.

The Sorghum Stg3 QTL also overlapped with maize markers associated with the stay-green terminal trait of the NAM testcrosses (Table 3-6). A maize candidate gene was identified near marker on chromosome 7 that corresponds to Stg3.3, 3.4, and 3.6-3.8 (Table 3-10). GRMZM2G330690 (7: 171,482,361-171,486,120) encodes an ubiquitin-specific protease 24 (AT4G30890.1(UBP24), RMIP = 6) (Table 3-6). UBP24 is an uncharacterized, putative protein with no known physiological role in plants (Table 3-10).

Table 3-10 *Stg3* QTL reported from the literature. Genomic positions are generated through prediction of the linkage positions

Stg3 QTL	Pop	Source allele	Additive effect	Flanking markers	Published symbol	Publication
Stg3.1	B35/Tx7000	Tx7000	-5.713	bnl15.40/umc5	Chl3	Xu et al 2000
Stg3.2	QL39/QL41	QL41	-	MB6-84/TS136	not named	Tao et al 2000
Stg3.3	B35/Tx7000	B35	0.0573	txs1307/umc5	stg3	Subudhi et al 2000
Stg3.4	B35/Tx7000	B35	-4.4913	txs1307/umc5	stg3	Subudhi et al 2000
Stg3.5	B35/Tx7000	B35	0.065	txs1307/umc116	Stg3	Xu et al 2000
Stg3.6	B35/Tx7000	B35	0.0728	umc5/umc116	stg3	Subudhi et al 2000
Stg3.7	N13/E36-1	N13	-1.4	txp1 / 14/61-115	%GL15 #3	Hausmann et al 2002
Stg3.8	N13/E36-1	N13	-1.6	14/61-115 / 13/61-259	%GL30 #5	Hausmann et al 2002
Stg3.9	N13/E36-1	N13	-2.5	14/61-115 / 13/61-259	%GL45 #4	Hausmann et al 2002

Table 3-10 Continued

Stg3 QTL	LG	CI Start	CI End	QTL size	CI Start	CI End	QTL size	LOD	R^2
Stg3.1	SBI-02	114.77	125.23	10.46	60,089,659	61,594,335	1,504,676	2.86	15.9
Stg3.2	SBI-02	121.49	128.51	7.03	60,438,145	61,675,900	1,237,755	3.71	14.5
Stg3.3	SBI-02	123.59	133.10	9.50	61,412,988	62,121,125	708,137	3.49	17.5
Stg3.4	SBI-02	121.64	135.069	13.41	60,450,213	62,383,481	1,933,268	2.8	12.4
Stg3.5	SBI-02	123.39	133.60	10.20	61,324,258	62,193,365	869,107	3.34	16.3
Stg3.6	SBI-02	124.08	139.62	15.54	61,572,631	63,435,887	1,863,256	1.9	10.7
Stg3.7	SBI-02	130.64	145.36	14.72	61,754,092	65,036,819	3,282,727	2.5	4.9
Stg3.8	SBI-02	131.78	144.22	12.44	61,923,733	64,284,484	2,360,751	3	5.8
Stg3.9	SBI-02	134.20	141.79	7.592	62,261,965	63,634,080	1,372,115	4.9	9.5

3.5.4 Characterization and Evaluation of *Stg4* in Sorghum

The Stg4 locus of sorghum was detected in several genetic mapping studies (Table 3-11). This region also exhibited considerable overlap with QTL detected for stay-green terminal in the NAM RILs and NAM testcrosses.

The sorghum Stg4 QTL overlapped with maize markers associated with the stay-green terminal trait on chromosomes 1 and 8. The candidate gene on chromosome 8 was detected in the NAM RILs (Table 3-5). AC232238.2_FG008 (8: 166,713,976-166,743,525; RMIP = 5) encodes a hemerythrin family protein (LOC_Os01g64250.1) (Table 3-5). Hemerythrin proteins are involved in regulating oxygen and iron homeostasis in plant cells (TAIR). Although it is well described in human and mammalian physiology, little characterization is known about hemerythrin in plant physiology. This protein is genomically related to sorghum Stg4.2, 4.3, and 4.4 (Table 3-11). The candidate gene on chromosome 1 was detected in the NAM testcrosses (Table 3-6). GRMZM2G107395 (1:22,283,210-22,284,981; RMIP = 5) encodes a general regulatory factor 2 (AT1G78300.1(14-3-3OMEGA,GF14 OMEGA,GRF2)) (Table 3-6). General regulatory factor 2 is a G-box binding factor encoding a 14-3-3 protein, which is expressed in a variety of plant tissues throughout the growth and development of a plant (Denison et al., 2011). 14-3-3 proteins are a relatively small molecule family with 300 individuals represented (Denison et al., 2011). Denison et al., provides a summary of 14-3-3 functions in plant growth and development. Denison et al. (2011) show 14-3-3 protein involvement in abiotic stresses through interaction with KAT1, ABFs, and H-ATPases, biotic stress responses through APX3, MAPKKK, MAPKK, NtrBohD, RPW8.2, primary metabolism through protein interactions with GS, NR, SS, and SPS,

light responses through Hd3A/FT/SP, CO, and PHOT1, regulation of growth and cell division through EDE1, WEE1, CDC25, and PNek1, and finally related hormones ABF1, 2, and 5, BRZ1 and BRZ2, VP1, RSG, and ABF3. Needless to say, these proteins are critical in many plant stress responses and the list of functions will only continue to increase with further characterization of this gene family. This protein is genomically related to Stg4.3 and 4.4 (Table 3-11).

Table 3-11 *Stg4* QTL reported from the literature. Genomic positions are generated through prediction of the linkage positions

Stg4 QTL	Pop	Source allele	Additive effect	Flanking markers	Published symbol	Publication
Stg4.1	B35/Tx430	B35	0.14	txs713	SGJ	Crasta et al 1999
Stg4.2	B35/Tx7000	B35	0.056	txs713/rcb	Stg4	Xu et al 2000
Stg4.3	B35/Tx7000	B35	0.0305	txs387/csu166C	stg4	Subudhi et al 2000
Stg4.4	SC56/Tx7000	SC56	0.171	csu166/txs173	Stg J	Kebede et al 2001

Table 3-11 Continued

Stg4 QTL	LG	CI Start	CI End	QTL size	CI Start	CI End	QTL size	LOD	R^2
Stg4.1	SBI-05	54.18	68.82	14.64	9,942,964	47,138,942	37,195,978	2.3	11.6
Stg4.2	SBI-05	54.51	69.49	14.98	10,116,867	48,435,793	38,318,926	2.23	11.1
Stg4.3	SBI-05	55.15	72.85	17.69	10,407,015	52,892,020	42,485,005	1.81	9.4
Stg4.4	SBI-05	62.57	71.03	8.47	13,115,727	52,038,094	38,922,367	4.21	15.4

Table 3-12 Summary of maize and sorghum stay-green associations for major sorghum stay-green QTL. NAM RILs – A (Anthesis), NAM RILs – T (Terminal), and NAM TC (Testcrosses)

Sb QTL	Sb LG	Sb Stg QTL	Maize Population	Maize Candidate Gene	ZM LG	Arabidopsis/Rice Ortholog	Description	RMIP
Stg1	3	1.1	NAM RILs - A	GRMZM2G700901	6	Os07g38760.1	HEAT repeat family protein, putative, expressed	9
		1.1 – 1.4	NAM RILs - T	GRMZM2G124047	8	AT5G65760.1	Serine carboxypeptidase S28	9
		1.1 - 1.4 1.6	NAM TC	GRMZM2G078933	9	AT5G58590.1	(RANBP1):RAN binding protein 1	11
		1.1	NAM TC	GRMZM2G055219	8	AT2G19950.2	(GC1): golgin candidate 1	23
Stg2	3	2.2 - 2.7	NAM RILs - T	GRMZM2G131378	4	AT2G38110.1	(ATGPAT6,GPAT6): glycerol-3-phosphate acyltransferase 6	17
		2.1, 2.2	NAM RILs - T	GRMZM2G041015	3	AT2G46225.2	(ABIL1): ABI-1-like 1	7
		2.1, 2.2	NAM RILs - T	GRMZM5G856738	3	AT4G23650.1	(CDPK6,CPK3): calcium-dependent protein kinase 6	7
Stg3	2	3.1 - 3.5	NAM RILs - A	GRMZM2G110107	2	AT1G68130.1	(AtIDD14,IDD14): indeterminate (ID)-domain 14 protein	47
		3.3 - 3.7	NAM RILs - A	GRMZM2G002131	2	AT4G36990.1	(AT-HSFB1,ATHSF4,HSF4): heat shock factor 4 protein	36
		3.6 - 3.9	NAM RILs - A	GRMZM2G113840	1	AT4G39170.1	Sec14p-like phosphatidylinositol transfer family protein	18
		3.3 - 3.8	NAM RILs - T	GRMZM2G156310	6	AT1G47480.1	alpha/beta-hydrolase superfamily	30
		3.5 - 3.8	NAM RILs - T	GRMZM2G473709	2	Os07g48244.1	ubiquinol-cytochrome c reductase complex 6.7 kDa protein	7
		3.1	NAM RILs - T	GRMZM2G137676	7	AT2G26450.1	plant invertase/pectin methylesterase inhibitor	6
		3.3 - 3.8	NAM TC	GRMZM2G330690	7	AT4G30890.1	(UBP24): ubiquitin protease 24	6
Stg4	5	4.2 - 4.4	NAM RILs - T	AC232238.2_FG008	8	Os01g64250.1	hemerythrin family protein	5
		4.3, 4.4	NAM TC	GRMZM2G107395	1	AT1G78300.1	(14-3-3OMEGA,GF14 OMEGA,): general regulatory factor 2	5

Figure 3-1 Summary of genomic relationships between NAM stay-green terminal and anthesis phenotypes to reported sorghum linkage positions and Stg QTL. All sorghum stay-green QTL are denoted as yellow bars on the figure. Stg QTL are represented as linkage blocks and consist of several studies combined to encompass the maximum genomic representation. Annotated maize genic regions blasted into sorghum are represented for their respective populations. Non annotated genes are not included. Refer to Table 3-7 for the further information in regards to genomic representation of maize genes.

3.5.5 Further Characterization of Stay-green in Maize and Sorghum

We provide substantial evidence for a genomic and potential physiological relationship between maize and sorghum for stay-green under abiotic stress conditions. A summary of all maize annotated candidate genes associated with sorghum stay-green QTL is provided in Table 3-12 and Figure 3-1. Our initial analysis potentially underestimates the amount of genomic relation between the two species. Only annotated genes from two populations examining two phenotypes were used to compare against sorghum. There are several unannotated genes that upon further characterization and genetic analysis could be regulating and modulating stay-green in maize and sorghum. Additionally, stay-green generally exhibited lower heritabilities than other traits makings it harder to detect comparative relationships between species. However, improvements in phenotyping and modelling will enhance heritability of stay-green in the future.

Maize and sorghum on a cytogenetic level are similar, as maize is a duplicative genome compared to sorghum. In an analysis of sorghum and maize flowering time (Mace et al., 2013), known QTL from maize were generally located in two positions on two chromosomes compared to a single location in sorghum. In the characterization of stay-green, there appears to be similar trends with the duplicative genome of maize to sorghum albeit a weaker association. Additionally, a comprehensive BLASTing protocol was used in these analyses, where maize genes were examined in the sorghum genome and only BLAST hits into genes were considered for potential associations between the two species.

Further genetic analysis is required to confirm and support the stay-green associations in maize and sorghum. While sorghum contains a comprehensive genomic

database for stay-green characterization, these positions are massive in genomic size. Precise genetic mapping using new and more statistically powerful plant populations are needed to precisely narrow the genomic regions of stay-green to a more manageable size. Maize stay-green is less developed agronomically, physiologically, and genetically compared to sorghum. More research is needed to confirm the genetic associations reported in this dissertation. Additionally, better physiological and agronomic characterization is needed to understand the mechanisms of drought and yield that are either improved or non-advantageous in maize. Improvements in phenotyping and agronomic characterization of stay-green in maize is needed to provide better genomic and agronomic support to compare to sorghum.

Validation studies are needed to confirm the candidate genes listed above. Stg1-4 are commercially relevant QTL for sorghum production in drought-stressed conditions. Knowing the genetic architecture of the trait allows plant breeders to select on a specific gene(s) and better characterize the agronomic advantages and disadvantages of stay-green. Substantial progress has been made in this area; however, fine mapping and characterization of major and subsequent minor stay-green QTL in sorghum presents an outstanding opportunity for crop improvement for challenging environments.

3.6 Conclusion

Maize and sorghum represent globally important cereals that are grown in a variety of challenging environments. Both crops are grown in drought-prone environments and substantial research investments are supporting the development of climate resilient hybrids and varieties. Additionally, the genetic relatedness of maize and sorghum

provides another angle for crop improvement, as comparative genomics becomes an increasing powerful tool for plant breeders.

Delayed plant senescence, also known as stay-green, is a commercially relevant trait in sorghum crop improvement and breeding in drought stress environments. Extensive genetic mapping has revealed four to six major genetic loci modulating the expression of the trait. Phenotypic characterization of stay-green in maize revealed substantial genetic variation for multiple traits in the Nested Association Mapping populations and testcrosses.

Stay-green at anthesis and terminal are critical components of stay-green sorghum cultivars and were characterized in maize. Leveraging candidate genes from linkage disequilibrium blocks in maize uncovered substantial genomic relationships for stay-green QTL reported in sorghum. Furthermore, major sorghum Stg1, Stg2, Stg3, and Stg4 displayed maize representation in one or more populations and phenotypes. Further validation and characterization of sorghum and maize stay-green relationships is warranted to understand the genetic and agronomic value of breeding for drought stress tolerance.

CHAPTER 4. GENETIC CONSTITUTION OF MAIZE PREMATURE SENESCENCE THROUGH SINK-INHIBITION

4.1 Abstract

The demand for climate resilient crops for environmental extremes continues to increase globally. Drought and other abiotic stresses during maize reproduction can result in an extended lag period between anthesis and silking resulting in lower yields. B73 is a major contributor to the seed parent heterotic pattern in elite maize breeding programs. However, it is susceptible to abiotic stress conditions. B73 rapidly and prematurely senesces when pollination is disrupted. We examined the phenotyping protocols of ear removal and pollination inhibition to disrupt seed set in maize. The onset of the hyper-senescence phenotype occurred 800 GDDs post anthesis and was initiated from the top of the plant before descending downward. Complete senescence occurs within four to six days of the onset of the phenotype. Our studies showed no significant difference in early onset senescence between ear removal and inhibition treatments in maize, while both forms are significantly different compared to open-pollinated plants. These results suggest that absence of pollination of the ear initiates varying plant responses, resulting in different forms of remobilization and senescence in maize. We characterized the inheritance of this premature hyper-senescence phenotype in the Nested Association Mapping (NAM) population of maize.

Association mapping in the NAM population identified genes involved in regulating genes involved in light perception and signal transduction. FAR1 (far-red light), CRY1 and NPH3/BTBN NYP1 (blue light), and DLF1 and APRR5 (red light interaction with auxin) in tandem with COP1 (second level of light regulation and signal – all three types of light modulate COP1 expression) were associated with expression of the premature senescent phenotype. These results suggested a potential model for premature senescence in maize involving light perception and signaling with auxin. We propose that light signaling interacts with DFL1, a rapidly induced auxin-responsive gene known to interact with COP1, Spotted Leaf Protein 11, and light regulating genes involved in photomorphogenesis and skotomorphogenesis to orchestrate the premature senescence phenotype. In this model, plants sense the lack of remobilization to the sink during shortening days and produce auxin to induce the expression of SPL11 and skotomorphogensis. Further characterization of the premature senescence phenotype is critical in understanding the role of these candidate genes. Selection against allele(s) for premature senescence in B73 presents a substantial opportunity to enhance active breeding germplasm to engineer climate resilient crops

4.2 Introduction

Effects of climate variability constrain global agricultural production and food security. Extreme weather and climate events such as excess heat, drought and flooding negate potential positive plant improvements (Easterling et al., 2007). Food demand is expected to double within the next 30 years, and the effects of climate change will impact the ability of scientists to combat the detrimental outcomes of adverse environmental conditions (Foley et al., 2011). Abiotic stress events already have major socioeconomical

and economic impacts on crop production throughout the world (Bänziger et al., 2006). Scientific efforts to adapt crops to climate variability have been slowed by the complexity of breeding for both yield and abiotic stress adaptation traits in crop plants (Bruce et al., 2002; Duvick, 1997). Nevertheless, production has continued to increase despite these challenges (FAOSTAT). As global demand for food crops continues to increase, efforts to understand the biochemical and genetic elements of abiotic stress tolerance will be critical in mitigating future challenges.

Maize is most susceptible to drought stress during flowering as the plant is reaching peak water-use. Grain yield of maize is nearly double under optimal conditions compared to maize under flowering or grain-fill drought stress (Duvick et al., 2004b). Water stress during the grain fill period leads to increased leaf senescence, loss of photosynthetic activity, reduced dry matter accumulation, and reduced yield resulting from lower kernel weights (Baker et al., 2005; Caker, 2004). Additionally, maize lines under drought stress exhibit extended anthesis-silking intervals (ASI), which have a high negative correlation with yield. This coincides with the increased water use necessary for maize reproductive physiology (Bolanos and Edmeades, 1993; 1996).

Maize senescence is a highly regulated process and during an extended ASI, pollination of the sink is missed. The lack of a sink can initiate premature senescence in maize that is genotype dependent. Some genotypes will prematurely senesce in the absence of a sink, while others will continue to undergo normal senescence rates (Crafts-Brander et al., 1984).

Crafts-Brandner et al. (1984) described a form of rapid, premature senescence associated with maize ear removal. They observed a premature senescence, beginning in

the upper leaves of maize hybrids, when the ear was physically removed. After 25 days post-anthesis, a reddish discoloration occurred in plants with no ear in B73xMo17 hybrids, while alternate hybrids remained green throughout grain fill even after the removal of the sink. Metabolomics data of B73xMo17 hybrids showed an accumulation of carbohydrates in the leaves and a loss of nitrogen from the leaves with the cessation of nitrate uptake. Nitrogen flux was examined in a follow-up study by observing the leaf above the ear over a set period of days after anthesis. They observed the loss of nitrate reductase activity, reduced nitrogen, and lower carboxylating enzyme activity which appeared to be regulated during the premature senescence. They concluded that the rate of nitrogen flux was a regulating factor for the phenotype but could not rule out effects of growth regulators and other metabolites as possible explanations of the premature senescence phenotype (Crafts-Brandener et al., 1984).

Sekhon et al. (2012) conducted a transcriptional and metabolic analysis of the premature senescence phenotype through pollination prevention of B73. They observed an increase in free glucose and starch occurring with the loss of chlorophyll 12 days after anthesis from the highest ear-leaf. Whole plant gene transcription changed with the onset of premature senescence at 24 DAA and internodal gene transcription changed at 30 DAA.

We characterized a subset of the Nested Association Mapping (NAM) population of maize for sink-inhibited senescence phenotypes. Understanding the genetic bases of this phenotype is relevant in hybrid production systems where premature senescence can devastate yields under prolonged ASI. We hypothesize that there are different alleles

controlling the expression of this trait and genetic modifiers regulating the expression of the phenotype in the NAM populations of maize.

4.3 Materials and Methods

4.3.1 Genetic Materials and Experimental Design

4.3.1.1 Genome-wide Mapping Experiment

We evaluated 1295 NAM RILs representing 24 of the 25 NAM families excluding Hp301. RILs from each NAM family were selected based on flowering relative to B73. Lines were selected with equal representation of each RIL family in the experiment. RILs were evaluated at flowering using Ratio Vegetation Index (RVI) on a family average basis and measured again on a family basis at 800 GDDs post-anthesis.

4.3.1.2 Comparison of Sink-Inhibition and Removal

B73 (rapid senescence pattern) and Mo17 (normal senescence pattern) genotypes were used to study the effects of sink-inhibition and ear removal on premature senescence.

4.3.2 Phenotypic Evaluation for Sink-Inhibited Senescence

4.3.2.1 Genome-wide Mapping Experiment

Field trials were conducted in 2012 and 2013 at the Agronomy Center for Research and Education in West Lafayette, Indiana USA. Trials were planted on May 6, 2012 and May 20, 2013. RILs were planted as single-row plots 3.81 m in length with 0.76 m alleys between ranges and 0.76 m spacing between the rows. Trials were laid out in a randomized complete block design with two replications per year. NAM families were nested and randomized within replications and lines were randomized within each

NAM family. Each family contained two checks: B73 as a field check and a purple-maize line as a planting check.

Characterization of sink-inhibited senescence required the shoot-capping (glassine bags) of three random plants per plot to prevent pollination of all ears. Plants were phenotyped for ratio of vegetation index (RVI) using a CCM-200 chlorophyll meter (Opti-Sciences, Inc.) at 800 GDD after anthesis. Three non-shoot-capped (NSC) plants were measured for RVI along with three shoot-capped (SC) plants per plot. Each plant was measured at the leaf above the ear-leaf, midway between the leaf tip and collar and between the midrib and leaf edge. Open-pollinated Senescence (OPS), Shoot-cap Induced Senescence (SIS), Senescence Difference (SD), and Senescence Ratio (SR) were calculated and used as senescence phenotypes as described in Table 4-1. Plot scores was calculated as the mean of each trait measured at 800GDDs post silking. GDDs were calculated using Method 2 from McMaster and Wilhelm (McMaster and Wilhelm, 1997).

Table 4-1 Sink-inhibited senescence phenotypes collected in the NAM RILs

Senescence Phenotype	Measurement Time Points	Calculation
Open-pollinated Senescence (OPS)	RVI of open-pollinated plants at 800 GDDs	RVI at 800GDDs
Shoot-cap Induced Senescence (SIS)	RVI of shoot-capped plants at 800 GDDs	RVI at 800GDDs
Senescence Difference (SD)	Shootcapped RVI at 800 GDDs Non-shootcapped RVI at 800 GDDs	RVI of open-pollinated plants - RVI of shoot-capped plants
Senescence Ratio (SR)	Shootcapped RVI at 800 GDDs Non-shootcapped RVI at 800 GDDs	(RVI of open-pollinated plants - RVI of shoot-capped plants)/ RVI of open-pollinated plants

4.3.2.2 Comparison of Sink Inhibition and Removal

A field trial was conducted to compare senescence phenotypes of plants allowed to open pollinate (open-pollinated), plants with ears removed (sink-removal), and plants with ears shoot-capped to inhibit pollination (sink-inhibition). The trial was planted on May 20, 2013 at the Agronomy Center for Research and Education in West Lafayette, Indiana USA in 2013. B73 and Mo17 were planted as single-row plots 3.81 m in length with 0.76 m alleys between ranges and 0.76 m spacing between the rows with five replications. Nine plants were randomly selected for comparison in each plot. Three plants were tagged and were allowed to open pollinate, three plants were shoot-capped to inhibit pollination, and three plants had their ear(s) removed. Individual plants were phenotyped for ratio of vegetation index (RVI) using a CCM-200 chlorophyll meter (Opti-Sciences, Inc.) at 800 GDD after anthesis as described above.

4.3.3 General Weather Information

During the 2012 growing season, Indiana experienced the 10th warmest year in 118 years of records. Conversely, the 2013 growing season was moderate with Indiana experiencing the 64th warmest year in 119 years of records. Indiana had the 15th driest year on record in 2012 and the 85th driest year on record in 2013. According to the Drought Monitor (http://droughtmonitor.unl.edu), West Lafayette started the growing season in 2012 in a D1 drought situation. By the end of May, the drought progressed into a D2 situation and this condition persisted through the month of June. By the end of July, West Lafayette had deteriorated into a D3 drought. By the end of August, the drought conditions only slightly improved to a D2 situation. In 2013, the effects of the 2012 drought were no longer present, and West Lafayette started the season in a non-drought

condition. This condition endured through the end of July. However, by the end of August, West Lafayette was on the verge of a D1 drought condition (Drought information - United States Drought Monitor; Weather information – NOAA).

4.3.4 Genotypic Information

Joint-linkage mapping was conducted using a genetic map with 1 cM resolution based on GBS v2.3 SNPs available at www.panzea.org. For association mapping, HapMapV2 SNPs (Chia et al., 2012) were projected onto the NAM RILs based on linkage information. HapMap V2 consists of random-sheared, paired-end Illumina GAII reads from 103 maize inbreds, teosinte, and landraces with 4-30x coverage. Overall, 55+ million SNPs and indels were generated for genetic analyses. For each SNP, the values for a RIL were assigned based on the SNP value of the RIL parents and on the genotype of the flanking NAM markers in that RIL.

4.3.5 Statistical Analyses

4.3.5.1 Spatial Analysis for Best Linear Unbiased Estimators (NAM RILs)

A combined mixed model across years was fitted for the NAM experiment. Best Linear Unbiased Estimators (BLUE)s were calculated to account for year and field effects using a weighted multivariate mixed model in ASReml (ASReml 3.0, VSN International). Within the model, the effects of blocks, rows, ranges, replications, and number of observations per plot were fit to identify the best model as appropriate. Additionally, first-order autoregressive for range and row were included as needed in the populations for spatial correction. When appropriate, likelihood ratio tests or Akaike's Bayesian Information Criteria for the random effects or the F-tests for the fixed effects were used to identify which factors were significant for a given phenotype and thus were

retained in the model. When statistical comparisons between different models were not possible, the best model was chosen based on the highest significance for the variety F-test and the lowest pairwise variety mean comparison standard error.

4.3.5.2 Heritability Calculations

Heritabilities were calculated on a plot and mean basis for all populations (Hung et al., 2011). Plot-basis heritabilities were calculated on the entire NAM population, using the following general equation which was modified to correctly account for the number of families, individuals, and environment used in each population:

$$h^2_p = \frac{\sigma^2_{family} + \frac{1}{26}\sum_{p=1}^{26}\sigma^2_{RIL(family)p}}{\sigma^2_{family} + \frac{1}{26}\sum_{p=1}^{26}\sigma^2_{RIL(family)p} + \sigma^2_{env*RIL(family)} + \sigma^2_{\epsilon}}$$

Line-mean heritabilities were calculated for the NAM experiment using an equation described by Cullis et al., (2006) shown below. We modified this equation to correctly account for the number of families, individuals, and environment used in each population:

$$h^2_c = 1 - \frac{V_{PPE}}{2\left(\sigma^2_{family} + \sigma^2_{RIL*family}\right)}$$

In the equation above, V_{PPE} is the average prediction error variance for all possible pairwise comparisons, which includes the checks, obtained directly from the ASReml prediction output.

Line-mean heritabilities were calculated using a modified form of the following equation to correctly account for the number of families, individuals, and environment used in each population:

$$h^2_l = \frac{\sigma^2_{family} + \frac{1}{26}\sum_{p=1}^{26}\sigma^2_{RIL(family)p}}{\sigma^2_{family} + \frac{1}{26}\sum_{p=1}^{26}\sigma^2_{RIL(family)p} + \frac{\sigma^2_{env*RIL(family)}}{n_{env(l)}} + \frac{\sigma^2_{\epsilon}}{n_{plot}}}$$

Harmonic means were used to account for unbalanced data in the experiment. N_{envl} is the harmonic mean of the number of environments in which each RIL was observed and n_{plot} is the harmonic mean of the total number of plots in which each RIL was observed.

For equations h^2_l and $h^2_{p,}$ heritability equations were calculated based on the model selection for an individual trait. Some components for heritability were not calculated in the model selection and therefore were not included in the heritability calculations.

4.3.5.3 Joint-Linkage Stepwise Regression (NAM RILs)

QTL identification utilized a joint stepwise regression model described by Buckler et al., (2009) for mapping flowering time traits in the NAM populations. This method combines all NAM families evaluated to test for QTL associated with a given trait. To account for variation associated with maturity, the residual of the model:

$$y = b_0 + b_1 \times DTA + \varepsilon$$

y is the BLUE of the stay-green trait and days to anthesis (DTA) is the covariate. b_0 is the intercept estimate and b_1 is the slope estimate. ε is the residual.

Backward stepwise selection in Tassel 4 (Bradbury et al., 2007) was used to determine which markers would be selected or removed from the model. Permutation analyses were used to determine the p-value threshold by permuting RVI values for a phenotype 1000 times. The lowest p-values of a single marker scan were collected after each permutation and a threshold p-value was determined at an experimental α of 0.05.

QTL were identified using a genome-wide joint linkage scan where significant markers from the stepwise regression were used as covariates in the model when

analyzing family and marker within family as fixed effects. The joint-linkage protocol removed covariates in the model when a marker was within 10cM of the original covariate markers. QTL intervals were determined using a 0.01 confidence interval.

4.3.5.4 Genome-wide SNP Association

We used the statistical power of the NAM to leverage both the ancestral recombination events from the diversity of the founders and the linkage of individual recombinant inbred populations to conduct genome-wide association for premature senescence. Using HapMapV2, we projected SNPs onto the RIL progeny using linkage marker information and pedigree knowledge which is described in detail in section 4.3.4.

The protocol used for the GWAS followed the one proposed by Tian et al. (2012). For the first step, individual chromosome residuals for each trait were calculated from a model where the population term and all significant markers from the joint-linkage analysis in the other chromosomes were fitted against the mapping trait. Later, those residuals were used as phenotypes and fit into 100 stepwise linear models using a bootstrapping resampling protocol. Bootstrap posterior probability (BBP or RMIP) corresponding to how many times a SNP was deemed significant out of the 100 total runs was calculated as the test statistic. Each of these 100 model runs were analyzed using 80% of the genotypes randomly subsampled from the population.

4.3.5.5 Statistical Analysis of Sink-Inhibition versus Ear Removal

PROC ANOVA (SAS 9.3, SAS Institute) was used to compare senescence phenotypes of B73 and Mo17 with open-pollinated, sink-removal, and sink-inhibition treatments. Least-significant difference values were calculated for each genotype and treatment with an alpha of 0.05.

4.3.5.6 Linkage Disequilibrium Analysis

Linkage disequilibrium (LD) was examined using TASSEL 5.0 and published NAM and AMES GBS SNPs. R-squared and p-values were generated using this software. LD was examined 20 kb in each direction of the SNP association for an individual population. From the NAM population, linkage disequilibrium was examined using the NAM HapMapV2 SNPs available at www.panzea.org.

4.4 Results

4.4.1 Sink Removal versus Sink Inhibition

We examined the RVI phenotypes of B73 and Mo17 with open-pollinated, sink-removal, and sink-inhibition treatments (Figure 4-1). We observed no significant differences between sink-removal and sink-inhibition treatments indicating a similar physiological response for premature senescence in both genotypes (Tables 4-2, 4-3). The RVI values of plants with sink-removal and sink-inhibition treatments were significantly lower than open-pollinated plants with normal ear development. For B73, we observed a high RVI score in the open pollinated plants but RVI values were significantly lower in plants with ear covered or ear removed. A similar pattern was observed in Mo17 where the RVI values of open pollinated plants was significantly higher than plants with ear covered and ear removed. However, the RVI values for both removal types were higher in Mo17 than B73 indicating a slower rate of premature senescence.

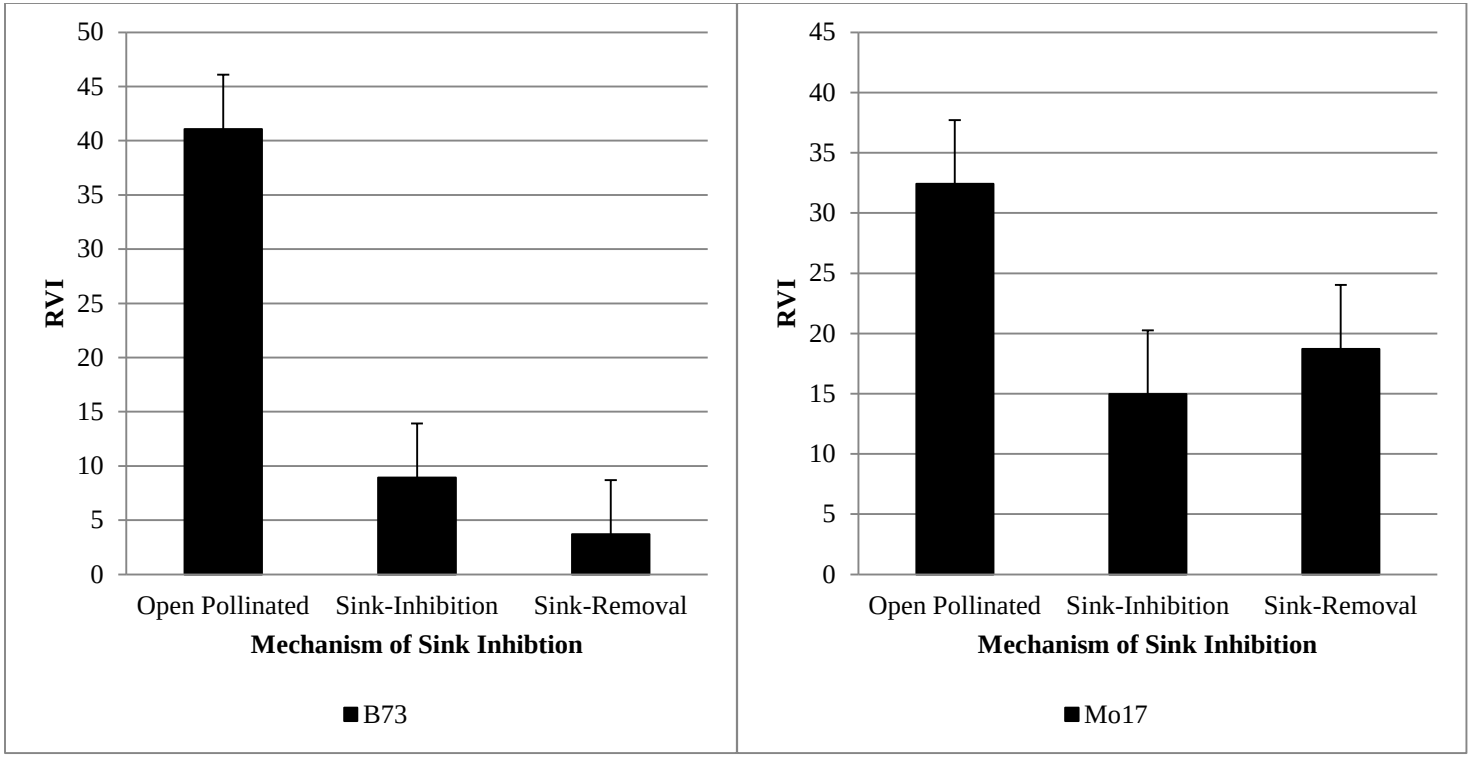

Figure 4-1 Comparison of RVI values of B73 and Mo17 plants with open-pollinated, sink-removal, and sink-inhibition treatments. Error bars indicate least significant difference (LSD) between treatments.

Table 4-2 Analysis of Variance Table for the B73 genotype comparing open pollinated, ear covered, and ear removal treatments.

B73 ANOVA and Pairwise Multiple Comparisons

Source	DF	Sums of Squares	Mean Square	F-Value	Pr > F
Treatment	2	12114.27	6057.14	152.49	<0.0001
Error	38	1509.41	39.721		
Corrected Total	40	13623.67			

R-Square	Coeff Var	Root MSE	B73 Mean
0.889	33.97	6.302	18.55

Treatment Comparison	Difference between Means	95% Confidence Limits		
Open-pollinated vs Sink-inhibition	33.480	28.645	38.315	***
Open-pollinated vs Sink-removal	37.572	32.738	42.407	***
Sink-inhibition vs Sink-removal	4.092	-0.912	9.097	

*** Significant at 0.001

Table 4-3 Analysis of Variance Table for the Mo17 genotype comparing open pollinated, ear covered, and ear removal treatments.

Mo17 ANOVA and Pairwise Multiple Comparisons

Source	DF	Sums of Squares	Mean Square	F-Value	Pr > F
Treatment	2	2504.414	1252.21	29.37	<0.0001
Error	41	1748.217	42.64		
Corrected Total	43	4251.63			

R-Square	Coeff Var	Root MSE	Mo17 Mean
0.589	29.43	6.53	22.19

Treatment Comparison	Difference between Means	95% Confidence Limits		
Open-pollinated vs Sink-inhibition	17.500	12.685	22.315	***
Open-pollinated vs Sink-removal	13.413	8.512	18.313	***
Sink-inhibition vs Sink-removal	4.087	-0.813	8.988	

*** Significant at 0.001

4.4.2 Phenotypic Correlations in the NAM RILs

Days to anthesis and silking were significantly correlated (Table 4-4). These flowering traits were also significantly correlated with the senescence traits described in Table 4-3. OPS, SD, and SR were negatively correlated with flowering time traits while SIS was positively correlated. Each of the senescence traits was significantly correlated with one another. OPS, SD, and SR were positively correlated with each other and negatively correlated with SIS. SD and SR exhibited very high positive correlations and very high negative correlations with SIS (Table 4-4).

Table 4-4 Phenotypic correlations of flowering time and senescence phenotypes in the NAM RILs

	Days to Anthesis	Days to Silking	SR	SIS	SD
Days to Silking	0.93136 <.0001				
SR	-0.34008 <.0001	-0.37431 <.0001			
SIS	0.19417 <.0001	0.21324 <.0001	-0.76183 <.0001		
SD	-0.39445 <.0001	-0.42458 <.0001	0.88983 <.0001	-0.64924 <.0001	
OPS	-0.2101 <.0001	-0.22682 <.0001	0.08824 0.0009	0.46802 <.0001	0.3533 <.0001

4.4.3 Sink-inhibited Senescence Heritabilities

Significant genetic variation was detected for all sink-inhibited senescence phenotypes (Appendix B – ASReml Output; Appendix C – Phenotypic Distribution of Sink-Inhibited Senescence Phenotypes). Heritabilities were calculated for all sink-inhibited senescence phenotypes on a line-means basis and a plot basis depending on the population. SIS NSC, difference, and ratio contained mixed heritabilities. Substantial variation is introduced when combining two different phenotypic responses (shootcapped and non-shootcapped) in the SIS ratio and difference phenotypes. As seen in stay-green in chapter two, confounding factors of maturity can influence the heritability of non-shootcapped ears resulting in lowering heritabilities. Heritabilities were generally high for SIS SC as the phenotype is extremely penetrant in the NAM. Heritabilities for all phenotypes are recorded in Table 4-5.

Table 4-5 Heritabilities of the senescence traits measured in the NAM RILs. Plot and line-means heritabilities were calculated for the respective populations.

NAM RILs	OPS	SIS	SD	SR
Plot-Basis (Hung et al)	0.2531	0.8362	0.2616	0.2378
Line-Means Basis (Cullis et al)	0.365	0.9646	0.5324	0.8301

4.4.4 Genome-wide Association Results

4.4.4.1 Senescence Difference (SD)

Senescence Difference (SD) is a normally distributed phenotype with values ranging from -34.33 to 80. Significant genetic variation was associated with this trait ($P = <0.001$, $F = 5.57$). Joint-linkage analysis identified five QTLs for SD on chromosomes 1, 2, 4, 5, and 9 and explained 36.4% of the phenotypic variation associated with the trait. Permutation analysis was conducted to determine threshold values for each trait using

1000 random iterations. The QTL identified were used as cofactors within the association mapping model. There were 69 SNP associations identified in the model with a RMIP statistic > RMIPx100 = 4. Candidate genes were identified in a genomic interval of 20,000 bp flanking the significant SNP. Linkage disequilibrium was examined for all candidate SNPs using TASSEL 5.0 to identify genomic regions with linkage blocks extending past the 20,000bp window (Figure 4-2).

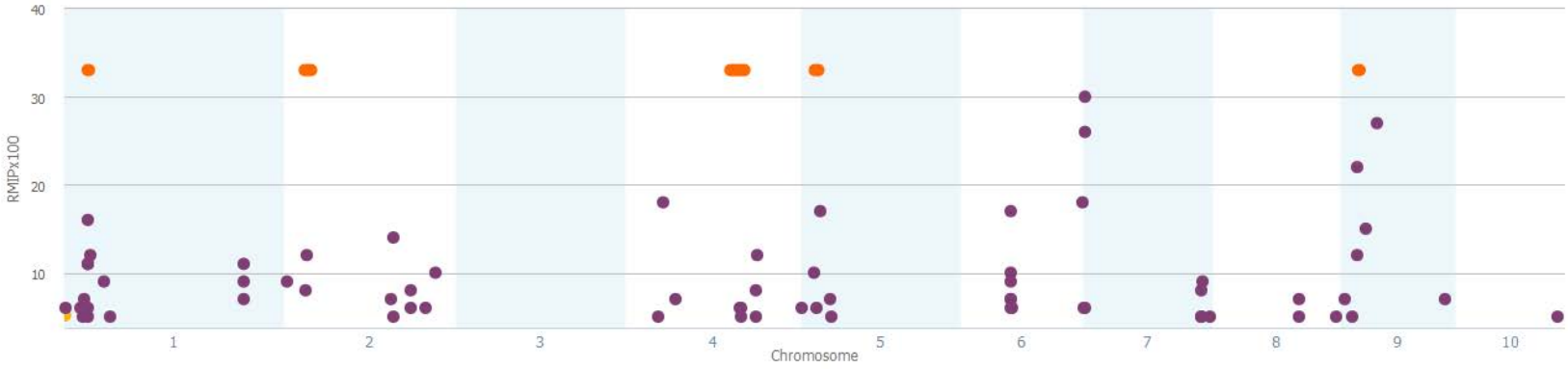

Figure 4-2 Manhattan plot of SNPs associated with senescence difference in the NAM RILs. SNPs with a RMIP > 4 are shown as purple dots. Joint-linkage QTL used as cofactors in the association mapping model are shown as orange bars.

4.4.4.2 Senescence Ratio (SR)

Senescence Ratio (SR) is a normally distributed phenotype and utilizes the OPS value to standardize the data. Standardized values measure the rate of premature senescence rather than difference only which examines the difference in chlorophyll content that could be associated in hyper-senescence or normal senescence. Significant genetic variation was associated with this trait ($P = <0.001$, $F = 5.58$). Joint-linkage analysis identified four QTLs for SR on chromosomes 1, 2, 4, and 5 and explained 31.2% of the phenotypic variation associated with the trait. Permutation analysis was conducted to determine threshold values for the trait using 1000 random iterations. QTL identified were used as cofactors within the association mapping model. Candidate genes were identified in a genomic interval of 20,000 bp flanking the significant SNP which is roughly the LD block for equal SNP coverage across the maize genome. Linkage disequilibrium was examined for all candidate SNPs using TASSEL 5.0 to identify genomic regions with linkage blocks extending past the 20,000bp window (Figure 4-3).

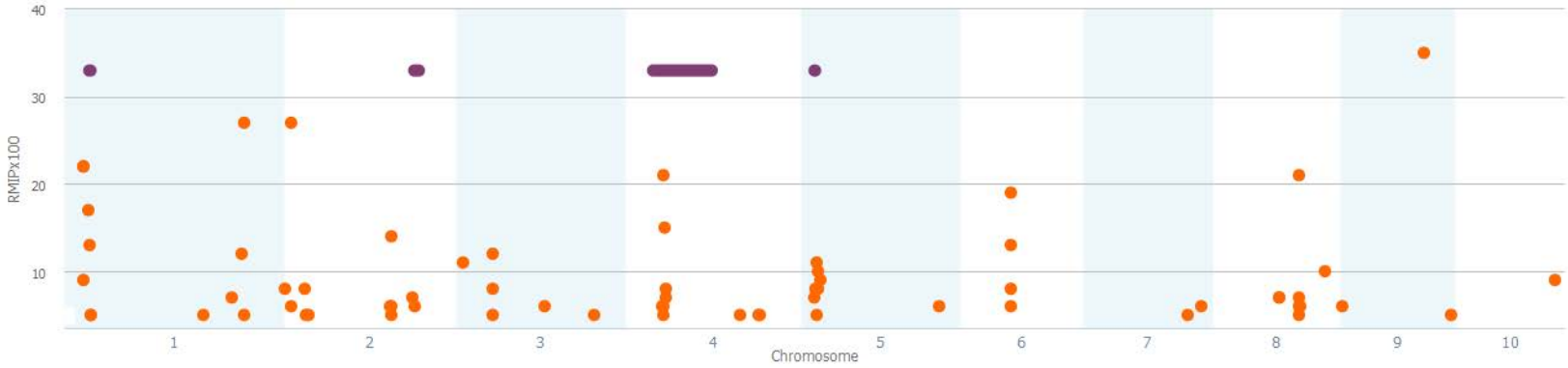

Figure 4-3 Manhattan plot of SNPs associated with senescence ratio in the NAM RILs. SNPs with a RMIP > 4 are shown as orange dots. Joint-linkage QTL used as cofactors in the association mapping model are shown as purple bars.

4.4.4.3 Sink-Induced Senescence (SIS)

Shoot-cap Induced Senescence (SIS) is a normally distributed phenotype. Joint-linkage analysis identified six QTLs for SIS located on chromosomes 1, 2, 3, 4, 8, and 10 and explained 38.3% of the phenotypic variation associated with the trait. Significant genetic variation was associated with this trait ($P = <0.001$, $F = 4.92$). Permutation analysis was conducted to determine threshold values for the trait using 1000 random iterations. The QTL identified were used as cofactors within the association mapping model. Candidate genes were identified in a genomic interval of 20,000 bp flanking the significant SNP which is roughly the LD block for equal SNP coverage across the maize genome. Additionally, linkage disequilibrium was examined for all candidate SNPs using TASSEL 5.0 to identify genomic regions with linkage blocks extending past the 20,000bp window (Figure 4-4).

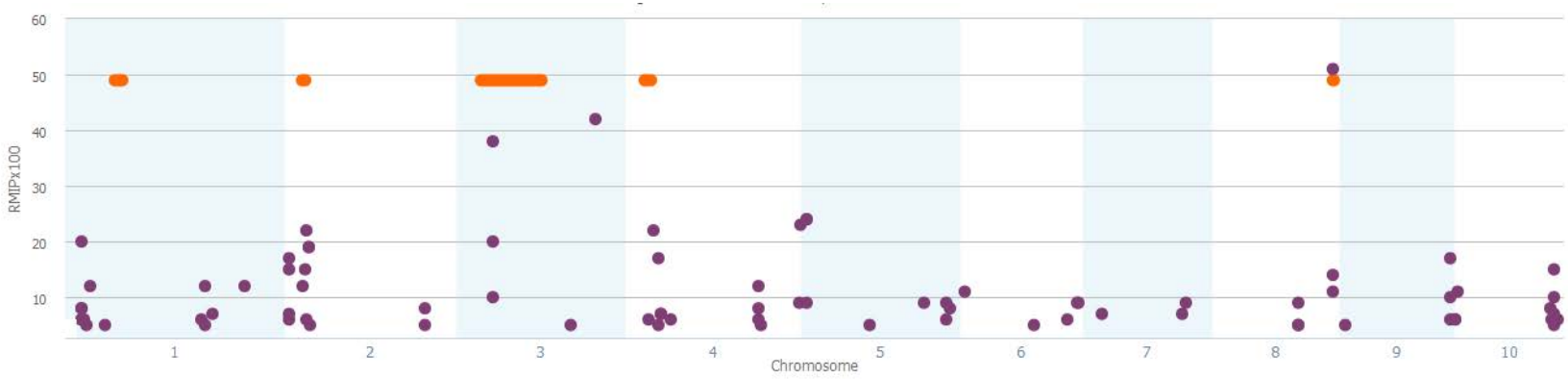

Figure 4-4 Manhattan plot of SNPs associated with shootcap senescence in the NAM RILs. SNPs with a RMIP > 4 are shown as purple dots. Joint-linkage QTL used as cofactors in the association mapping model are shown as orange bars.

4.5 Discussion

Premature senescence under abiotic stress presents an agronomic challenge to plant breeders. Advancements in the development of climate resilient crops continue to positively impact crop improvement as specific plant populations are developed to rapidly dissect complex traits. The NAM panel provides an excellent platform for rapid analysis of diverse germplasm for a variety of climate variability-associated traits (Yu et al., 2008, Buckler et al., 2009). As discussed previously, the backbone of the NAM population, B73, exhibits a form of premature senescence associated with the absence of pollination (Crafts-Brander et al., 1984). Therefore, dissecting the genetic nature of this form of premature senescence is simply obtained by the extreme expressivity of the trait. Additionally, the phenotype is interesting to many plant breeders due to the substantial genetic contribution of B73 to the temperate maize female heterotic pool (Mikel et al., 2006).

Evaluating and phenotyping sink-inhibited senescence in the NAM is a daunting endeavor. The NAM population is large and multiple replications are needed to create enough power for association mapping. Additionally, it takes a group of individuals to manually remove or shootcap all ears over multiple weeks to accurately produce the premature senescent phenotype. It is critical that all sinks are covered on the plant to eliminate confounding factors and obtain the phenotype. Prior to this study, the scientific community was ambiguous concerning sink removal compared to inhibition via shootcapping to initiate the desired plant phenotype (Crafts-Brander et al., 1984, Sekhon et al., 2012). However, in this study we demonstrate that there is no difference between shootcapping and removing the ear on plant senescence.

Flowering time can potentially confound premature senescence in an experiment representing genetically diverse populations. Therefore, we reduced the number of lines used in the experiment to individuals that flowered within a week of B73. We additionally ensured that there was an equal representation of individuals within each NAM family. Finally, we used days to anthesis as a covariate to account for statistical variation associated with flowering.

4.5.1 Sink Removal versus Inhibition

Crafts-Brandner et al. (1984) were the first to report on premature senescence in B73 inbreds and hybrids associated with ear removal. Additionally, they identified hybrids and inbreds that did not exhibit the premature senescence phenotype. However, no discussion was given to potential physiological and genetic responses of manual sink removal such as wounding and altered carbon partitioning.

There may be physiological differences between removing and inhibiting the sink of maize that could elicit differing premature senescent responses. Physical ear removal can elicit a wounding response in the plant, leading to altered plant metabolism and carbon partitioning as well as reallocation of metabolic energy to create a new sink. Inhibiting kernel set by shoot capping can alter plant metabolism and carbon partitioning in a different manner than ear removal. Additionally, inhibition with a shootcap blocks or filters the reception of light in the plant and can create a different physiological response from altering plant metabolism.

We report that there are no significant differences in senescence patterns of plants with ears removed and plants with unpollinated ears in B73 and Mo17 based on RVI at 800 GDDs after flowering (Table 4-2, Table 4-3). There is no immediate need to test for

the phenotype in hybrid combinations since Craft-Brander et al. (1984) demonstrated the premature-senescence phenotype in B73xMo17 hybrids. Therefore, sink removal and sink inhibition produce similar premature senescence phenotypes.

Significant differences in senescence were observed between open-pollinated plants with normal sink development, unpollinated plants with ears covered by shoot caps, and unpollinated plants with ears physically removed (Table 4-2, Table 4-3). Mo17 plants displayed no visibly premature senescent phenotype and maintained a higher level of chlorophyll content in unpollinated plants with ears covered by shoot caps and unpollinated plants with ears physically removed (Table 4-3, Figure 4-1). B73 displayed a similar trend; however, sink-impaired B73 plants had lower chlorophyll content than Mo17 and presented a premature senescent phenotype (Table 4-2, Figure 4-1). It is reasonable to expect that some form of genetic variation is modulating the premature senescent phenotypes in Mo17 and B73. It is agronomically advantageous to maintain chlorophyll content and delay senescence in absence of pollination, especially in stress periods of extended anthesis-silking intervals.

4.5.2 Identification of Candidate Genes in the Nested Association Mapping Panel

The NAM panel provides an excellent platform for dissecting complex traits in maize, especially traits specific to B73. B73 is a major contributor to the United States female heterotic pattern and commonly used in elite temperate hybrids (Mikel et al., 2006). Therefore, identifying traits associated with agronomic characteristics specific to B73 can shed insight on potential breeding objectives for crop improvement such as premature senescence. All candidate genes linked to SNPs associated with the premature

senescence phenotypes are shown in Appendix D-1. In this section, we highlight selected genes that might be associated with senescence observed in the NAM population.

4.5.2.1 Spotted leaf protein 11 – GRMZM2G341166

Spotted leaf protein 11 on chromosome 8 near NAM SNP 166,561,819 was associated with the sink-inhibited shootcapped only phenotype. With a RMIP of 51, it was the most frequently called significant SNP of all four phenotypes evaluated in this study. There were two other genes within the LD block examined. One gene encoded a generic RING/U-Box family protein and the other gene was not annotated.

Spotted leaf protein 11 (spl11) was first characterized by Zeng et al. (2004) as a negative regulator of plant cell death and defense functioning as a U-box/armadillo repeat protein endowed with E3 ubiquitin ligase (Zeng et al., 2004). Several lesion mimic mutants, such as spl11, have been identified across multiple species and encoded several different proteins involved in a plethora of molecular functions. spl11 is involved in controlling spontaneous plant cell death through regulation of ubiquitination and plant defense. Furthermore, spl11 was described as a convergence point of plant defense and flowering signaling in plants. For background purposes, there are three classes of ubiquitin-proteasome systems in plants: E1 – ubiquitin activating enzymes, E2 – ubiquitin conjugating enzymes, and E3 – ubiquitin ligases. E3 systems are abundant in plants and involved in many biological processes; however, these proteins are specific to a biological process. Liu et al. (2012) describe a specific U-box E3 ligase, spl11/PUB13, that is a convergence point for disease defense and initiation of flower development. In rice, lesion mimic mutants of spl11 were accentuated in short day plants compared to long day plants, whereas the PUB13 mutants displayed more lesion formation under long

day conditions. This suggests that both mutations are affected by light and the circadian clock (Liu et al., 2012). Additionally, spl11 appears to be involved in regulating flowering time, as mutants in this gene exhibit delayed flowering time in long day conditions. PUB13 appears to act in the opposite manner to spl11 and interacts with COP1 through LONG HYPOCOTYL IN FAR-RED LIGHT (HFR1). HFR1 is responsible for promoting photomorphogenesis, plant growth, flowering shape, and flowering time (Jang et al., 2008). However, the regulation mechanism of COP1 by HFR1 through PUB13 is unknown.

Shikata et al. (2009) showed that spl11 and two other proteins, spl2 and spl10, are involved in controlling the morphological change in shoot maturation during reproduction in arabidopsis. These data present a break from the reported literature, which showed only a vegetative presentation of spl11 and provided evidence that spl11 is involved during reproductive development in plants (Shikata et al., 2009).

Taken together, these reports and our data suggest that spl11 is active in vegetative and reproductive growth in plants and is regulated by light in conjunction with other proteins that are potentially modulating COP1 expression.

4.5.2.2 (DFL1) indole-3-acetic acid-amido synthetase GH3.1 – GRMZM2G061515

DFL1 is an auxin-responsive GH3 gene homolog. Nakazawa et al. (2008) described DFL1 as a negative regulator of shoot cell elongation and lateral root formation, and as a positive regulator of light response for hypocotyl length. DFL1 is in a genomic region associated with the shootcap-only phenotype. Located on chromosome 3 at SNP 190,031,176, it is the third most frequently called significant SNP of all four phenotypes with a RMIP of 42 and also had support from joint linkage-mapping.

Auxin is a major phytohormone involved in numerous plant responses. GH3 classes of auxin-induced genes are characterized as rapidly expressed in the presence of auxin (Hagen et al., 1998). There already exists a link between auxin and light in the form of gravitropism (Hagen et al., 1998). Furthermore, we hypothesize that loss of sink in conjunction with shorter day-length in the growing season results in the premature senescence response. DFL1 is known to be involved in light responses in plants resulting in shoot cell elongation and root formation in arabidopsis (Nakazawa et al., 2008). Speculatively, the loss of the ability to sense auxin through changing day length could initiate a cascade response of gene expression leading to premature senescence. GH3 gene WES1 has been implicated in reception of red light in conjunction with phytochrome B and regulates hypocotyl growth (Park et al., 2007). GH3 proteins are diverse in plants; however, DFL1 appears to be specific to the light pathway described above. COP1 and DFL1 have an interaction mediated by fin219 in response to light and stem growth. fin219 is a component of the phyA/far-red light sensing pathway. fin219 mutants exhibit a long hypocotyl in soybeans when under continuous far-red light and are rapidly induced by a GH3 auxin gene(s) (Hsieh et al., 2000). Thus, fin219 can indirectly influence the inactivation/activation of COP1 proteins through light perception and changes in auxin. The identification of fin219 provides a link between auxin, specifically GH3 proteins discussed in the previous section, and red light.

4.5.2.3 COP1 associated protein – GRMAM2G015739

COP1 is a protein involved in reception of light and a regulator of photomorphogenesis and skotomorphogenesis. Skotomorphogenesis in plants, most often in seedlings, is characterized by etiolation from no chlorophyll production, limited

leaf growth, radial stem elongation, limited root elongation, limited radial expansion of the stem, and limited production of lateral roots. Photomorphogenesis is characterized by de-etiolation and as coleoptile opening, leaf growth promotion, chlorophyll production, stem elongation suppression, radial expansion of the stem, root elongation and lateral development promotion. While characterized extensively in seedlings, photomorphogenesis and light reception affects the entire plant through reproduction. COP1 is part of a complicated pathway involving far-red light, red-light, and blue light in conjunction with other genes (Figure 4-5, 4-6). This gene was associated with the senescence difference phenotype and is found on chromosome 7 near SNP 2,631,177 with a RMIP of 30. Several other genes described in this section are involved to some extent with COP1 and these relationships will be discussed in relation to the specific gene of interest.

4.5.2.4 Cryptochrome 1 – GRMZM2G171736

Cryptochrome 1 (Cry1) is involved in reception and signal relay of blue light. Additionally, cryptochrome 2 is involved in the same signaling transduction pathway. Specifically, these enzymes repress the expression of COP1 with the reception of blue light through ubiquitin E3 ligase. In mutant phenotypes, plants exhibit hypocotyl elongation. Cry1 is involved in inducing stomatal opening and electron transportation through blue-light interactions. Furthermore, CRY1 and COP1 molecularly interact to regulate photomorphogenesis through the reception of blue light (Yang et al., 2001). Cry1 is a candidate gene associated with the senescence ratio phenotype with a RMIP of 13.

4.5.2.5 Phototropic-responsive NPH3 family protein – GRMZM2G40115

NPH3 is involved in phototropic response of blue light encoding a NPH1 interacting domain in arabidopsis (Motchoulski and Liscum, 1999). This interaction occurs downstream of NPH1 and encodes a light-activated serine/threonine kinase. The gene annotation for NPH3 is slightly different in rice where it is classified as "BTBN13 - Bric-a-Brac, Tramtrack, Broad Complex BTB domain with non-phototropic hypocotyl 3 NPH3 and coiled-coil domains (www.maizegdb.org)." BTBN13 –NPH3 in arabidopsis has a component classified as NPY1 that is critical to plant organogenesis through auxin regulation. Mutants of NYP1 did not develop any flowers in arabidopsis and resembled mutants extremely phenotypically similar that were deficient in auxin transport and signaling. These mutants, classified as NPH3, regulate phototropic responses. Additionally, auxin regulates both organogenesis and phototropic responses using auxin response factors (ARF) and NPH. Mutants that did not have these complexes did not develop proper plant organs (Cheng et al., 2007). Phototropic-responsive NPH3 family protein was a candidate gene associated with senescence ration in the NAM population on chromosome 2 near SNP 2,034,526 with a RMIP of 8.

4.5.2.6 FAR1 DNA Binding domain – GRMZM2G001663

Phytochrome A is the main receptor of far-red light and mediates plant responses to other sources of light through various regulatory pathways and mechanisms (Figures 4-5 and 4-6). FAR1 and FHY3 are proteins critical in responding to far-red light and activating gene expression of proteins involved in light-induced phytochrome A nuclear accumulation (Wang et al., 2002). In short, these genes are transcription factors involved in regulating photomorphogenesis through far-red light. FAR1 does not have any

sequence similarities to any other known proteins (Hudson et al., 1999). FAR1 is a candidate gene associated with senescence difference phenotype and had a RMIP of 12.

4.5.2.7 APRR5 – GRMZM2G179024

APRR5 was a candidate gene for the senescence ratio phenotype with a RMIP of 5. APRR5 is part of a gene family involved in the APPR1/TOC1 quintet gene family. These genes accumulate at dawn in arabidopsis and continue to accumulate in continuous light, controlling early flowering and hypersensitiveness in early photomorphogenesis. This gene family is activated rhythmically and increases transcription accumulation in a specific order: APRR9 → APRR7 → APRR5 → APRR3 → APRR1/TOC1. Specifically, APRR5 mutants (overexpressed) exhibited earlier flowering time compared to wild type and showed hypersensitiveness to red light in early photomorphogenesis (Sato et al., 2002).

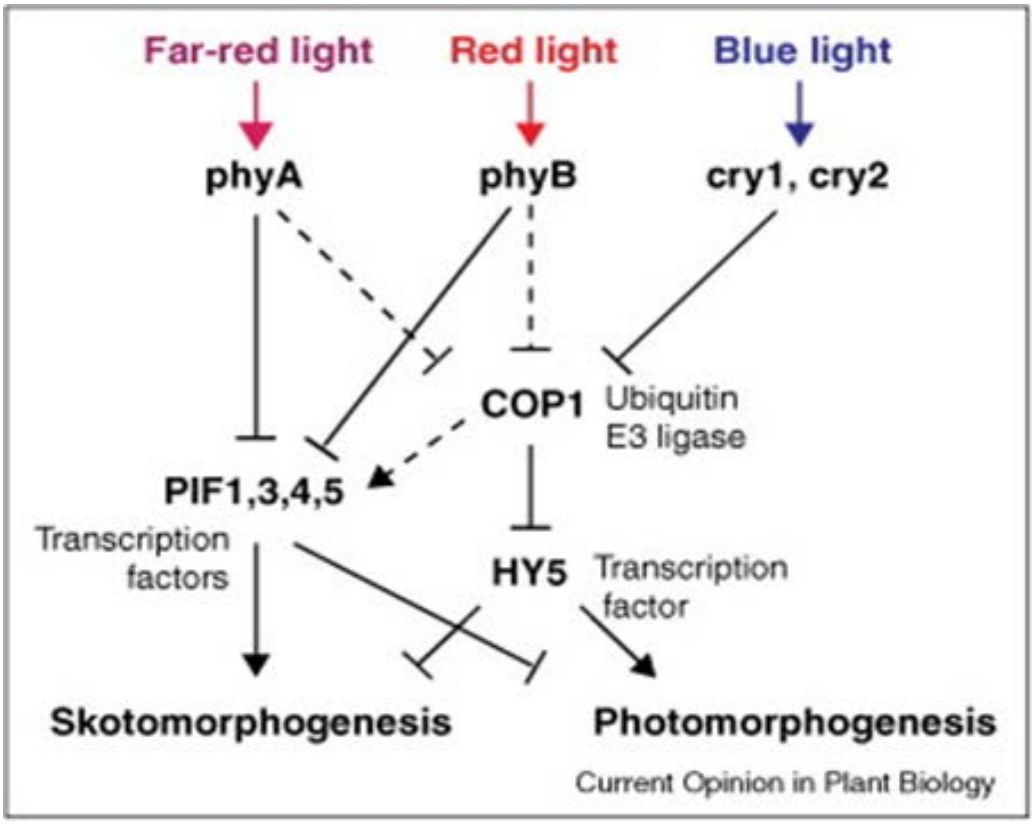

Figure 4-5 Generic outline of light reception and regulation in plants (Current Opinion in Plant Biology)

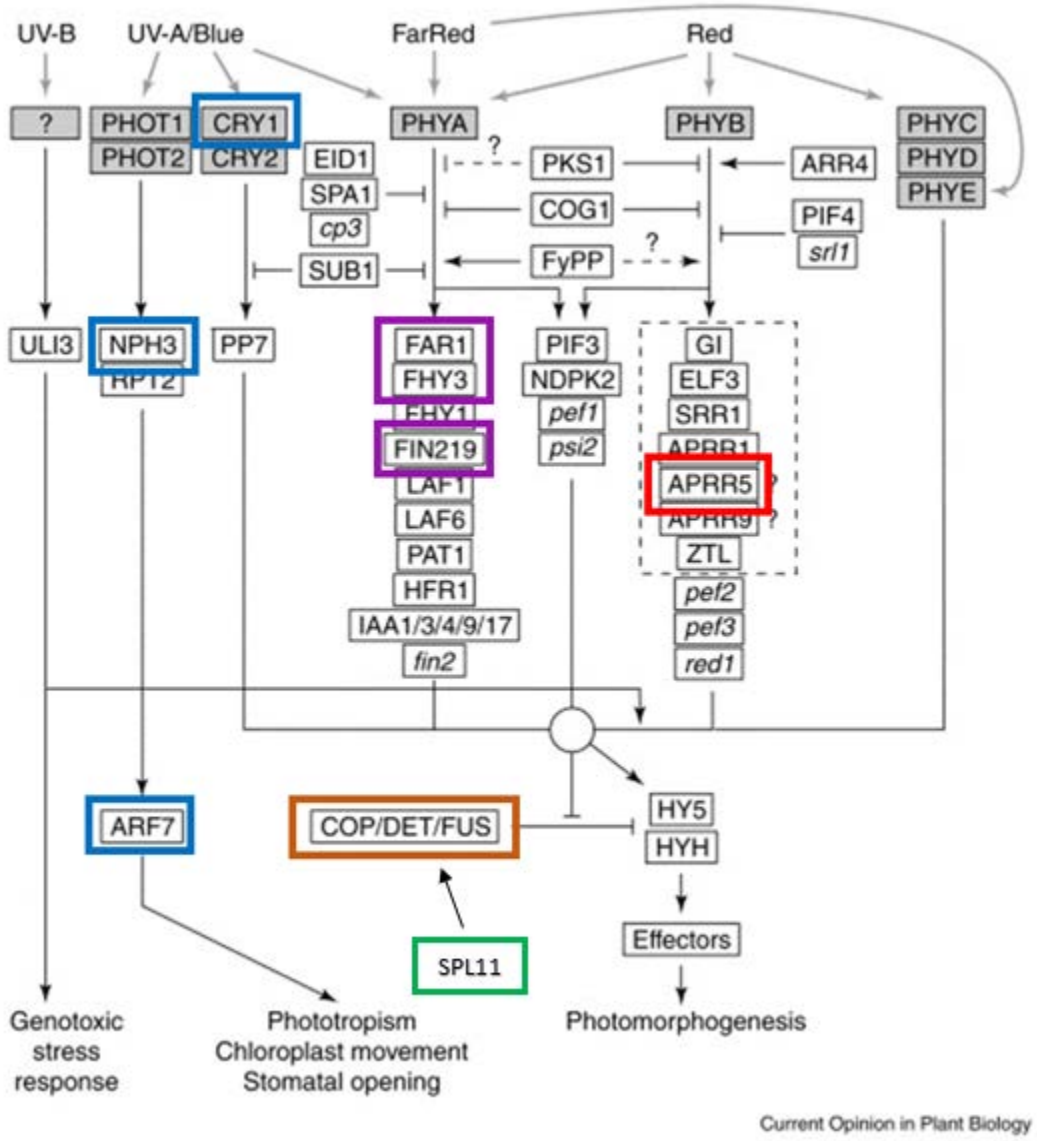

Figure 4-6 Detailed outline of light reception and signaling in plants. Red boxes correspond to NAM RIL candidate genes that interact with red light. Purple boxes correspond to far-red light interactions. Blue boxes correspond to blue light. Brown boxes correspond to second level of light regulation. The green box corresponds to spl11, which is known to interact with COP1. (Current Opinion in Plant Biology)

4.5.3 Proposed Model for Genetic Regulation of the Premature Senescence Phenotype in Maize

The premature senescence phenotype presented in B73 appears to be genotype specific and a consequence of a mutation coinciding with human selection. Although unfortunate for plant breeding efforts, the mutation provides a unique opportunity to examine premature senescence in maize. This mutation does not appear to provide adaptive advantage to maize as there is no fitness advantage to prematurely senescence without reproduction. Conversely, plant fitness is potentially conferred through genetic variation in light perception and circadian rhythm to adapt to broader geographical areas and changes in environments (Michael et al., 2003).

Identification of candidate genes associated with light regulation and signaling, in addition to auxin and spotted leaf protein 11, suggests a model of premature senescence modulated by day-length and light perception coinciding with remobilization to the sink. The detection of all major spectra of light candidates in association mapping suggests that the plant is responding changing light conditions as day length shortens during the latter part of maize development (Figures 4-5, 4-6).

As maize begins grain fill, considerable photosynthates and leaf proteins are remobilized to the ear. Remobilization begins during the latter half of the summer season when day lengths begin to shorten following the summer solstice in June. As the day length begins to shorten, the three wavelengths of light- far-red, red, and blue light - that plants interact with decline.

Therefore, we propose the following model for premature senescence in maize. Maize senses the day length shortening coinciding with grain fill post anthesis through

the interaction of light with Phytochrome A (far-red light), Phytochrome B (red light), and Cryptochrome 1 and 2 (blue light). FAR1 (far-red light), CRY1 and NPH3/BTBN NYP1 (blue light), DLF1 (red light interaction with auxin) and APRR5 (red light), and COP1 mediates the response to the changing light conditions. While there are several genes involved in light signaling in plants, only a subset were detected in association analyses. An explanation of the limited number of genes detected in association analyses lies in the underlying genetic and allelic diversity of the maize population characterized. Therefore, in our analyses, we only detected SNP associations that had substantial genetic variation associated with premature senescence, resulting in a limited number of gene candidates.

Two candidate genes for premature senescence were extremely compelling. DLF1, an auxin GH3 rapid accumulation gene with a RMIP of 42, is capable of detecting the light signal relay. Specifically, auxin interacts with COP1, the second level of light reception following red, blue, and far-red interaction, to regulate plant growth and development (Figure 4-5, 4-6). These genes contribute to regulation of photomorphogenesis or skotomorphogenesis and the identification of these genes by GWAS suggests that premature senescence is conditioned by light regulation and perception.

spl11 is the number one candidate for premature senescence in this population with a RMIP of 51 in association with the shootcap only phenotype. spl11 is involved in light regulation and signaling and is associated with rapid senescence when exposed to short day conditions in the field. Likewise, spl11 regulates flowering time through an

E3- ubiquitin ligase, which is the same protein involved in regulating the inactivation/ activation of COP1.

This model suggests that premature senescence in B73 is initiated through the detection of shorting day lengths through proteins involved in reception and signaling of all spectra of photosynthetically active radiation. Thereby, initiating the expression of spl11 conferring premature senescence.

4.5.4 Future Characterization of Premature Senescence in Maize

Phenotypically speaking, physically removing or inhibiting the pollination of the maize ear result in the premature senescence phenotype. In our association mapping analyses, major candidate genes with high RMIP values were identified in the shootcap only phenotype. Genes that are identified from this phenotype may be directly involved in mediating the phenotype whereas other phenotypes are more indirect measures premature senescence. However, it is critical to obtain the difference and ratio measurements to detect differences in light regulation and signaling present in the non-shootcapped plants compared to the shootcapped plants. Furthermore, the ratio phenotype is valuable as it provides a form of standardization of the data set to quantify the amount of premature senescence in the plant instead of natural loss of chlorophyll from remobilization. Finally, when working with diverse types of germplasm, utilizing population structure and statistical protocols helps alleviate confounding effects of maturity. Candidate genes for premature senescence now require further molecular and physiological characterization to better quantify and identify causative alleles for selection. It is critical that specific alleles are identified to allow plant breeders to select against premature senescence in plant populations. Due to B73's substantial contribution

to temperate maize heterotic pools and susceptibility to drought conditions, selection against this allele will enhance elite germplasm.

4.6 Conclusion

Sink inhibition occurs naturally in periods of stress when the anthesis silking interval in maize extends to the point of no pollination of the ear. In this study, we propose a model for regulation of the premature senescence phenotype in maize associated with sink inhibition. This model leverages candidate genes identified in association mapping studies and describes a plausible cascade of events leading to the premature senescent phenotype. Implication of the major phytohormone auxin gene (DFL1) and a protein involved in spontaneous cell death (spl11) as well as light perception and relay proteins, provides an avenue for whole plant response to sink inhibition. Additionally, we show that scientific recreation of the premature phenotype can be achieved through sink inhibition or removal, which was previously ambiguous in the literature. Continued characterization of sink-inhibition and premature senescence is critical for breeding climate resilient crops. Further characterization of this phenotype will empower plant breeders to select against negative alleles for premature senescence, especially in B73 derived lines. Sustained scientific progress in characterizing premature senescence in maize will contribute to engineering climate resilient crops for a challenging future.

REFERENCES

REFERENCES

Agarwal, Pradeep K., Parinita Agarwal, M. K. Reddy, and Sudhir K. Sopory. "Role of DREB transcription factors in abiotic and biotic stress tolerance in plants." Plant cell reports 25, no. 12 (2006): 1263-1274.

Albacete, Alfonso, Michel Edmond Ghanem, Cristina Martínez-Andújar, Manuel Acosta, José Sánchez-Bravo, Vicente Martínez, Stanley Lutts, Ian C. Dodd, and Francisco Pérez-Alfocea. "Hormonal changes in relation to biomass partitioning and shoot growth impairment in salinized tomato (Solanum lycopersicum L.) plants." Journal of Experimental Botany 59, no. 15 (2008): 4119-4131.

Allen, Randy D. "Dissection of oxidative stress tolerance using transgenic plants." Plant Physiology 107, no. 4 (1995): 1049.

Andrade, Miguel A., Carlo Petosa, Sean I. O'Donoghue, Christoph W. MuÈller, and Peer Bork. "Comparison of ARM and HEAT protein repeats." Journal of molecular biology 309, no. 1 (2001): 1-18.

Apelbaum, Akiva, and Shang Fa Yang. "Biosynthesis of stress ethylene induced by water deficit." Plant Physiology 68, no. 3 (1981): 594-596.

Armstead, Ian, Iain Donnison, Sylvain Aubry, John Harper, Stefan Hörtensteiner, Caron James, Jan Mani et al. "Cross-species identification of Mendel's I locus." *Science* 315, no. 5808 (2007): 73-73.

Asano, Takayuki, Nagao Hayashi, Shoshi Kikuchi, and Ryu Ohsugi. "CDPK-mediated abiotic stress signaling." *Plant Signal Behav* 7, no. 7 (2012): 817-821.

Bai, Ling, Guozeng Zhang, Yun Zhou, Zhaopei Zhang, Wei Wang, Yanyan Du, Zhongyi Wu, and Chun-Peng Song. "Plasma membrane-associated proline-rich extensin-like receptor kinase 4, a novel regulator of Ca2+ signalling, is required for abscisic acid responses in Arabidopsis thaliana."*The Plant Journal* 60, no. 2 (2009): 314-327.

Bañon, Sebastián, J. A. Fernandez, J. A. Franco, A. Torrecillas, J. J. Alarcón, and María Jesús Sánchez-Blanco. "Effects of water stress and night temperature preconditioning on water relations and morphological and anatomical changes of Lotus creticus plants." *Scientia horticulturae*101, no. 3 (2004): 333-342.

Bänziger, Marianne, Peter S. Setimela, David Hodson, and Bindiganavile Vivek. "Breeding for improved abiotic stress tolerance in maize adapted to southern Africa." *Agricultural Water Management* 80, no. 1 (2006): 212-224.

Barker, T., Campos, H., Cooper, M., Dolan, D., Edmeades, G., Habben, J., Schussler, J., Wright, D., and Zinselmeier, C. (2005). Improving drought tolerance in maize. Plant Breed. Rev. 25, 173–253.

Barnabás, Beáta, Katalin Jäger, and Attila Fehér. "The effect of drought and heat stress on reproductive processes in cereals." *Plant, Cell & Environment* 31, no. 1 (2008): 11-38.

Barry, Cornelius S. "The stay-green revolution: Recent progress in deciphering the mechanisms of chlorophyll degradation in higher plants."*Plant Science* 176, no. 3 (2009): 325-333.

Beavis, W. D., O. S. Smith, D. Grant, and R. Fincher. "Identification of quantitative trait loci using a small sample of topcrossed and F4 progeny from maize." *Crop Science* 34, no. 4 (1994): 882-896.

Bekavac, Goran, Božana Purar, and Đorđe Jocković. "Relationships between line per se and testcross performance for agronomic traits in two broad-based populations of maize." *Euphytica* 162, no. 3 (2008): 363-369.

Beuchat, Julien, Emanuele Scacchi, Danuse Tarkowska, Laura Ragni, Miroslav Strnad, and Christian S. Hardtke. "BRX promotes Arabidopsis shoot growth." *New Phytologist* 188, no. 1 (2010): 23-29.

Blilou, Ikram, Jian Xu, Marjolein Wildwater, Viola Willemsen, Ivan Paponov, Jiří Friml, Renze Heidstra, Mitsuhiro Aida, Klaus Palme, and Ben Scheres. "The PIN auxin efflux facilitator network controls growth and patterning in Arabidopsis roots." *Nature* 433, no. 7021 (2005): 39-44.

Blum, Abraham. *Plant breeding for stress environments*. CRC Press, Inc., 1988.

Blum, A. "Drought resistance, water-use efficiency, and yield potential—are they compatible, dissonant, or mutually exclusive?." *Crop and Pasture Science* 56, no. 11 (2005): 1159-1168.

Bogard, Matthieu, Matthieu Jourdan, Vincent Allard, Pierre Martre, Marie Reine Perretant, Catherine Ravel, Emmanuel Heumez et al. "Anthesis date mainly explained correlations between post-anthesis leaf senescence, grain yield, and grain protein concentration in a winter wheat population segregating for flowering time QTLs." *Journal of experimental botany* 62, no. 10 (2011): 3621-3636.

Bohnert, Hans J., and Bo Shen. "Transformation and compatible solutes."*Scientia Horticulturae* 78, no. 1 (1998): 237-260.

Bolaños J, Edmeades GO (1996) The importance of the anthesis-silking interval in breeding for drought tolerance in tropical maize. Field Crops Research 48:65-80

Borrell, Andrew K., and Graeme L. Hammer. "Nitrogen dynamics and the physiological basis of stay-green in sorghum." *Crop science* 40, no. 5 (2000): 1295-1307.

Borrell, Andrew K., Graeme L. Hammer, and Robert G. Henzell. "Does maintaining green leaf area in sorghum improve yield under drought? II. Dry matter production and yield." *Crop Science* 40, no. 4 (2000): 1037-1048.

Bota, Josefina, Hipólito Medrano, and Jaume Flexas. "Is photosynthesis limited by decreased Rubisco activity and RuBP content under progressive water stress?." *New phytologist* 162, no. 3 (2004): 671-681.

Boudsocq, Marie, and Jen Sheen. "Stress signaling II: calcium sensing and signaling." In *Abiotic Stress Adaptation in Plants*, pp. 75-90. Springer Netherlands, 2010.

Bowler, Chris, M. van Montagu, and Dirk Inze. "Superoxide dismutase and stress tolerance." *Annual review of plant biology* 43, no. 1 (1992): 83-116.

Bradbury, Peter J., Zhiwu Zhang, Dallas E. Kroon, Terry M. Casstevens, Yogesh Ramdoss, and Edward S. Buckler. "TASSEL: software for association mapping of complex traits in diverse samples." Bioinformatics 23, no. 19 (2007): 2633-2635.

Brown, M. S., Ye, J., Rawson, R. B. & Goldstein, J. L. Cell 100, 391-38

Bruce, Wesley B., Gregory O. Edmeades, and Thomas C. Barker. "Molecular and physiological approaches to maize improvement for drought tolerance." *Journal of Experimental Botany* 53, no. 366 (2002): 13-25.

Buckler ES, et al. (2009) The genetic architecture of maize flowering time. Science 325:714–718.

Bukhov, Nikolai G., Christian Wiese, Spidola Neimanis, and Ulrich Heber. "Heat sensitivity of chloroplasts and leaves: leakage of protons from thylakoids and reversible activation of cyclic electron transport."*Photosynthesis Research* 59, no. 1 (1999): 81-93.

Chae, Lee, Girdhar K. Pandey, Sheng Luan, Yong Hwa Cheong, and Kyung-Nam Kim. "Protein kinases and phosphatases for stress signal transduction in plants." In *Abiotic Stress Adaptation in Plants*, pp. 123-163. Springer Netherlands, 2010.

Chaitanya, K. V., D. Sundar, and A. Ramachandra Reddy. "Mulberry leaf metabolism under high temperature stress." *Biologia Plantarum* 44, no. 3 (2001): 379-384.

Çakir R (2004) Effect of water stress at different development stages on vegetative and reproductive growth of corn. Field Crops Research 89:1-16.

Campos H, Cooper M, Habben JE, Edmeades GO, Schussler JR (2004) Improving drought tolerance in maize: a view from industry. Field Crops Res 90:19-34.

Ceppi D, Sala M, Gentinetta E, Verderio A, Motto M (1987) Genotype-dependent leaf senescence in maize: inheritance and effects of pollination-prevention. Plant Physiol 85: 720–725.

Chak, Regina KF, Terry L. Thomas, Ralph S. Quatrano, and Christopher D. Rock. "The genes ABI1 and ABI2 are involved in abscisic acid-and drought-inducible expression of the Daucus carota L. Dc3 promoter in guard cells of transgenic Arabidopsis thaliana (L.) Heynh." Planta 210, no. 6 (2000): 875-883.

Chalker-Scott, Linda. "Do anthocyanins function as osmoregulators in leaf tissues?." *Advances in Botanical Research* 37 (2002): 103-127.

Champoux, M. C., G. Wang, S. Sarkarung, D. J. Mackill, J. C. O'Toole, N. Huang, and S. R. McCouch. "Locating genes associated with root morphology and drought avoidance in rice via linkage to molecular markers." *Theoretical and Applied Genetics* 90, no. 7-8 (1995): 969-981.

Chao, Qimin, Madge Rothenberg, Roberto Solano, Gregg Roman, and William Terzaghi. "Activation of the ethylene gas response pathway in Arabidopsis by the nuclear protein ETHYLENE-INSENSITIVE3 and related proteins." *Cell* 89, no. 7 (1997): 1133-1144.

Chen, Wenqiong, Nicholas J. Provart, Jane Glazebrook, Fumiaki Katagiri, Hur-Song Chang, Thomas Eulgem, Felix Mauch et al. "Expression profile matrix of Arabidopsis transcription factor genes suggests their putative functions in response to environmental stresses." *The Plant Cell Online* 14, no. 3 (2002): 559-574.

Cheng, Shu-Hua, Matthew R. Willmann, Huei-Chi Chen, and Jen Sheen. "Calcium signaling through protein kinases. The Arabidopsis calcium-dependent protein kinase gene family." *Plant Physiology* 129, no. 2 (2002): 469-485.

Cheng, Youfa, Genji Qin, Xinhua Dai, and Yunde Zhao. "NPY1, a BTB-NPH3-like protein, plays a critical role in auxin-regulated organogenesis in Arabidopsis." Proceedings of the National Academy of Sciences 104, no. 47 (2007): 18825-18829.

Chia, Jer-Ming, Chi Song, Peter J. Bradbury, Denise Costich, Natalia de Leon, John Doebley, Robert J. Elshire et al. "Maize HapMap2 identifies extant variation from a genome in flux." Nature genetics 44, no. 7 (2012): 803-807.

Christensen, Leslie E., Frederick E. Below, and Richard H. Hageman. "The effects of ear removal on senescence and metabolism of maize." Plant physiology 68, no. 5 (1981): 1180-1185.

Close, Timothy J. "Dehydrins: emergence of a biochemical role of a family of plant dehydration proteins." *Physiologia Plantarum* 97, no. 4 (1996): 795-803.

Cominelli, Eleonora, Massimo Galbiati, Alain Vavasseur, Lucio Conti, Tea Sala, Marnik Vuylsteke, Nathalie Leonhardt, Stephen L. Dellaporta, and Chiara Tonelli. "A guard-cell-specific MYB transcription factor regulates stomatal movements and plant drought tolerance." *Current Biology* 15, no. 13 (2005): 1196-1200.

Cook, Jason P., Michael D. McMullen, James B. Holland, Feng Tian, Peter Bradbury, Jeffrey Ross-Ibarra, Edward S. Buckler, and Sherry A. Flint-Garcia. "Genetic architecture of maize kernel composition in the nested association mapping and inbred association panels." Plant Physiology 158, no. 2 (2012): 824-834.

Cornic, Gabriel. "Drought stress inhibits photosynthesis by decreasing stomatal aperture–not by affecting ATP synthesis." *Trends in plant science*5, no. 5 (2000): 187-188.

Coque, M., A. Martin, J. B. Veyrieras, B. Hirel, and A. Gallais. "Genetic variation for N-remobilization and postsilking N-uptake in a set of maize recombinant inbred lines. 3. QTL detection and coincidences." *Theoretical and Applied Genetics* 117, no. 5 (2008): 729-747.

Crafts-Brandner, Steven J., Frederick E. Below, James E. Harper, and Richard H. Hageman. "Differential senescence of maize hybrids following ear removal I. Whole plant." Plant physiology 74, no. 2 (1984): 360-367.

Crafts-Brandner, Steven J., Frederick E. Below, Vernon A. Wittenbach, James E. Harper, and Richard H. Hageman. "Differential senescence of maize hybrids following ear removal II. Selected leaf." *Plant physiology* 74, no. 2 (1984): 368-373.

Crafts-Brandner, Steven J., and Charles G. Poneleit. "Carbon dioxide exchange rates, ribulose bisphosphate carboxylase/oxygenase and phosphoenolpyruvate carboxylase activities, and kernel growth characteristics of maize." *Plant physiology* 84, no. 2 (1987): 255-260.

Crafts-Brandner, Steven J., and Michael E. Salvucci. "Sensitivity of photosynthesis in a C4 plant, maize, to heat stress." *Plant Physiology* 129, no. 4 (2002): 1773-1780.

Crasta, O. R., W. W. Xu, D. T. Rosenow, J. Mullet, and H. T. Nguyen. "Mapping of post-flowering drought resistance traits in grain sorghum: association between QTLs influencing premature senescence and maturity." *Molecular and General Genetics MGG* 262, no. 3 (1999): 579-588.

Cui, Dayong, Jingbo Zhao, Yanjun Jing, Mingzhu Fan, Jing Liu, Zhicai Wang, Wei Xin, and Yuxin Hu. "The Arabidopsis IDD14, IDD15, and IDD16 cooperatively regulate lateral organ morphogenesis and gravitropism by promoting auxin biosynthesis and transport." PLoS genetics 9, no. 9 (2013): e1003759.

Cullis, Brian R., Alison B. Smith, and Neil E. Coombes. "On the design of early generation variety trials with correlated data." Journal of agricultural, biological, and environmental statistics 11, no. 4 (2006): 381-393.

Darbishire, Arthur Dukinfield. *Breeding and the Mendelian discovery*. Cassell and company, ltd., 1911.

Davletova, Sholpan, Karen Schlauch, Jesse Coutu, and Ron Mittler. "The zinc-finger protein Zat12 plays a central role in reactive oxygen and abiotic stress signaling in Arabidopsis." *Plant Physiology* 139, no. 2 (2005): 847-856.

Demirevska-Kepova, K., R. Holzer, L. Simova-Stoilova, and U. Feller. "Heat stress effects on ribulose-1, 5-bisphosphate carboxylase/oxygenase, Rubisco binding protein and Rubisco activase in wheat leaves." *Biologia Plantarum* 49, no. 4 (2005): 521-525.

Denison, Fiona C., Anna-Lisa Paul, Agata K. Zupanska, and Robert J. Ferl. "14-3-3 proteins in plant physiology." In Seminars in cell & developmental biology, vol. 22, no. 7, pp. 720-727. Academic Press, 2011.

De Ronde, J. A., W. A. Cress, G. H. J. Krüger, R. J. Strasser, and J. Van Staden. "Photosynthetic response of transgenic soybean plants, containing an< i> Arabidopsis P</i> 5< i> CR</i> gene, during heat and drought stress." *Journal of plant physiology* 161, no. 11 (2004): 1211-1224.

del Río, Luis A., Gabriela M. Pastori, José M. Palma, Luisa M. Sandalio, Francisca Sevilla, Francisco J. Corpas, Ana Jiménez, Eduardo López-Huertas, and José A. Hernández. "The activated oxygen role of peroxisomes in senescence." *Plant Physiology* 116, no. 4 (1998): 1195-1200.

DeWald, Daryll B., Javad Torabinejad, Christopher A. Jones, Joseph C. Shope, Amanda R. Cangelosi, James E. Thompson, Glenn D. Prestwich, and Hiroko Hama. "Rapid accumulation of phosphatidylinositol 4, 5-bisphosphate and inositol 1, 4, 5-trisphosphate correlates with calcium mobilization in salt-stressed Arabidopsis." *Plant Physiology* 126, no. 2 (2001): 759-769.

Diab, Ayman A., Béatrice Teulat-Merah, Dominique This, Neslihan Z. Ozturk, David Benscher, and Mark E. Sorrells. "Identification of drought-inducible genes and differentially expressed sequence tags in barley." *Theoretical and Applied Genetics* 109, no. 7 (2004): 1417-1425.

Diab, Ayman A., Ramesh Kantety, Carlos Mauricio La Rota, and Mark E. Sorrells. "Comparative Genetics of Stress-Related Genes and Chromosomal Regions Associated with Drought Tolerance in Wheat, Barley and Rice." *Genes, Genomes and Genomics* 1, no. 1 (2007): 47-55.

Doong, Howard, Alysia Vrailas, and Elise C. Kohn. "What's in the 'BAG'?–a functional domain analysis of the BAG-family proteins." *Cancer letters* 188, no. 1 (2002): 25-32.

Dupuis, Isabelle, and Christian Dumas. "Influence of temperature stress on in vitro fertilization and heat shock protein synthesis in maize (Zea mays L.) reproductive tissues." *Plant Physiology* 94, no. 2 (1990): 665-670.

Duvick, Donald N. "What is yield?." In *Proceedings of a Symposium, El Batan, Mex.(Mexico), 25-29 Mar 1996*. CIMMYT, 1997.

Duvick, D. N., J. S. C. Smith, and M. Cooper. "Long-term selection in a commercial hybrid maize breeding program." *Plant breeding reviews* 24, no. 2 (2004): 109-152.

Easterling W, Aggarwal P, Batima P, Brander K, Erda L, Howden M, Kirilenko A, Morton J, Soussana JF, Schmidhuber J, Tubiello F (2007) Food fibre and forest products. In: Oarry ML, Canziani OF, Palutikof JP, van der Lindin PJ, Hanson CE, eds. Climate Change 2007: Impacts, Adaptation and Vulnerability. Cambridge University Press, Cambridge , UK . pp. 273–313.

Echarte, Laura, Steven Rothstein, and Matthijs Tollenaar. "The response of leaf photosynthesis and dry matter accumulation to nitrogen supply in an older and a newer maize hybrid." *Crop Science* 48, no. 2 (2008): 656-665.

El Maarouf, Hayat, Yasmine Zuily-Fodil, Monique Gareil, Agnès d'Arcy-Lameta, and Anh Thu Pham-Thi. "Enzymatic activity and gene expression under water stress of phospholipase D in two cultivars of Vigna unguiculata L. Walp. differing in drought tolerance." *Plant molecular biology* 39, no. 6 (1999): 1257-1265.

Elstner, ERICH F. "Metabolism of activated oxygen species." *The biochemistry of plants: A comprehensive treatise* 11 (1987).

Eltayeb, Amin Elsadig, Naoyoshi Kawano, Ghazi Hamid Badawi, Hironori Kaminaka, Takeshi Sanekata, Isao Morishima, Toshiyuki Shibahara, Shinobu Inanaga, and Kiyoshi Tanaka. "Enhanced tolerance to ozone and drought stresses in transgenic tobacco overexpressing dehydroascorbate reductase in cytosol." *Physiologia Plantarum* 127, no. 1 (2006): 57-65.

Eltayeb, Amin Elsadig, Naoyoshi Kawano, Ghazi Hamid Badawi, Hironori Kaminaka, Takeshi Sanekata, Toshiyuki Shibahara, Shinobu Inanaga, and Kiyoshi Tanaka. "Overexpression of monodehydroascorbate reductase in transgenic tobacco confers enhanced tolerance to ozone, salt and polyethylene glycol stresses." *Planta* 225, no. 5 (2007): 1255-1264.

Federer, Walter T. "Augmented designs with one-way elimination of heterogeneity." *Biometrics* 17, no. 3 (1961): 447-473.

Federer, Walter T., and D. Raghavarao. "On augmented designs." Biometrics (1975): 29-35.

Foley, Jonathan A., Navin Ramankutty, Kate A. Brauman, Emily S. Cassidy, James S. Gerber, Matt Johnston, Nathaniel D. Mueller et al. "Solutions for a cultivated planet." *Nature* 478, no. 7369 (2011): 337-342.

French, Sarah Russell, Yousef Abu-Zaitoon, Md Myn Uddin, Karina Bennett, and Heather M. Nonhebel. "Auxin and Cell Wall Invertase Related Signaling during Rice Grain Development." *Plants* 3, no. 1 (2014): 95-112.

Fujimoto, Susan Y., Masaru Ohta, Akemi Usui, Hideaki Shinshi, and Masaru Ohme-Takagi. "Arabidopsis ethylene-responsive element binding factors act as transcriptional activators or repressors of GCC box–mediated gene expression." *The Plant Cell Online* 12, no. 3 (2000): 393-404

Fujita, Miki, Yasunari Fujita, Yoshiteru Noutoshi, Fuminori Takahashi, Yoshihiro Narusaka, Kazuko Yamaguchi-Shinozaki, and Kazuo Shinozaki. "Crosstalk between abiotic and biotic stress responses: a current view from the points of convergence in the stress signaling networks." *Current opinion in plant biology* 9, no. 4 (2006): 436-442.

Gechev, Tsanko S., Frank Van Breusegem, Julie M. Stone, Iliya Denev, and Christophe Laloi. "Reactive oxygen species as signals that modulate plant stress responses and programmed cell death." *Bioessays* 28, no. 11 (2006): 1091-1101.

Gentinetta, E., D. Ceppl, C. Lepori, G. Perico, M. Motto, and F. Salamini. "A major gene for delayed senescence in maize. Pattern of photosynthates accumulation and inheritance." *Plant Breeding* 97, no. 3 (1986): 193-203.

Gibson, Susan, Vincent Arondel, Koh Iba, and Chris Somerville. "Cloning of a Temperature-Regulated Gene Encoding a Chloroplast [omega]-3 Desaturase from Arabidopsis thaliana." *Plant Physiology* 106, no. 4 (1994): 1615-1621.

Gill, Sarvajeet Singh, and Narendra Tuteja. "Reactive oxygen species and antioxidant machinery in abiotic stress tolerance in crop plants." *Plant Physiology and Biochemistry* 48, no. 12 (2010): 909-930.

Gilroy, S., NoDa Read, and A. J. Trewavas. "Elevation of cytoplasmic calcium by caged calcium or caged inositol trisphosphate initiates stomatal closure." *Nature* 346, no. 6286 (1990): 769-771.

Giovane, Alfonso, Ciro Balestrieri, Lucio Quagliuolo, Domenico Castaldo, and Luigi Servillo. "A glycoprotein inhibitor of pectin methylesterase in kiwi fruit." *European Journal of Biochemistry* 233, no. 3 (1995): 926-929

Giuliani, Silvia, Maria Corinna Sanguineti, Roberto Tuberosa, Massimo Bellotti, Silvio Salvi, and Pierangelo Landi. "Root-ABA1, a major constitutive QTL, affects maize root architecture and leaf ABA concentration at different water regimes." *Journal of Experimental Botany* 56, no. 422 (2005): 3061-3070.

Gosti, Françoise, Nathalie Beaudoin, Carine Serizet, Alex AR Webb, Nicole Vartanian, and Jérôme Giraudat. "ABI1 protein phosphatase 2C is a negative regulator of abscisic acid signaling." *The Plant Cell Online* 11, no. 10 (1999): 1897-1909.

Grbić, Vojislava, and Anthony B. Bleecker. "Ethylene regulates the timing of leaf senescence in Arabidopsis." *The Plant Journal* 8, no. 4 (1995): 595-602.

Grabov, Alexander, and Michael R. Blatt. "Membrane voltage initiates Ca2+ waves and potentiates Ca2+ increases with abscisic acid in stomatal guard cells." *Proceedings of the National Academy of Sciences* 95, no. 8 (1998): 4778-4783.

Griffiths, Jayne, Kohji Murase, Ivo Rieu, Rodolfo Zentella, Zhong-Lin Zhang, Stephen J. Powers, Fan Gong et al. "Genetic characterization and functional analysis of the GID1 gibberellin receptors in Arabidopsis." *The Plant Cell Online* 18, no. 12 (2006): 3399-3414.

Hagen, Gretchen, and Tom Guilfoyle. "Auxin-responsive gene expression: genes, promoters and regulatory factors." Plant molecular biology 49, no. 3-4 (2002): 373-385.

Halfter, Ursula, Manabu Ishitani, and Jian-Kang Zhu. "The Arabidopsis SOS2 protein kinase physically interacts with and is activated by the calcium-binding protein SOS3." *Proceedings of the National Academy of Sciences* 97, no. 7 (2000): 3735-3740.

Harmon, Alice C., Michael Gribskov, and Jeffrey F. Harper. "CDPKs–a kinase for every Ca< sup> 2+</sup> signal?." *Trends in plant science* 5, no. 4 (2000): 154-159.

Harper, JEFFREY F., Michael R. Sussman, G. Eric Schaller, Cindy Putnam-Evans, Harry Charbonneau, and Alice C. Harmon. "A calcium-dependent protein kinase with a regulatory domain similar to calmodulin." *Science*252, no. 5008 (1991): 951-954.

Harper, Jeffrey F., Ghislain Breton, and Alice Harmon. "Decoding Ca2+ signals through plant protein kinases." *Annu. Rev. Plant Biol.* 55 (2004): 263-288.

Harris, Karen, P. K. Subudhi, Andrew Borrell, David Jordan, Darrell Rosenow, Henry Nguyen, Patricia Klein, Robert Klein, and John Mullet. "Sorghum stay-green QTL individually reduce post-flowering drought-induced leaf senescence." *Journal of experimental botany* 58, no. 2 (2007): 327-338.

Haussmann, B., V. Mahalakshmi, B. Reddy, N. Seetharama, C. Hash, and H. Geiger. "QTL mapping of stay-green in two sorghum recombinant inbred populations." *Theoretical and Applied Genetics* 106, no. 1 (2002): 133-142.

Havaux, Michel. "Carotenoids as membrane stabilizers in chloroplasts."*Trends in Plant Science* 3, no. 4 (1998): 147-151.

He, Ping, Mitsuru Osaki, Masako Takebe, and Takuro Shinano. "Changes of photosynthetic characteristics in relation to leaf senescence in two maize hybrids with different senescent appearance." *Photosynthetica* 40, no. 4 (2002): 547-552.

He, Ping, Mitsuru Osaki, Masako Takebe, Takuro Shinano, and Jun Wasaki. "Endogenous hormones and expression of senescence-related genes in different senescent types of maize." *Journal of experimental botany* 56, no. 414 (2005): 1117-1128.

Heddad, Mounia, and Iwona Adamska. "Light stress-regulated two-helix proteins in Arabidopsis thaliana related to the chlorophyll a/b-binding gene family." *Proceedings of the National Academy of Sciences* 97, no. 7 (2000): 3741-3746.

Hetherington, Alistair M., and Colin Brownlee. "The generation of Ca2+ signals in plants." *Annu. Rev. Plant Biol.* 55 (2004): 401-427.

Hicks, Karen A., Tina M. Albertson, and D. Ry Wagner. "EARLY FLOWERING3 encodes a novel protein that regulates circadian clock function and flowering in Arabidopsis." *The Plant Cell Online* 13, no. 6 (2001): 1281-1292.

Hideg, Éva, Csengele Barta, Tamás Kálai, Imre Vass, Kálmán Hideg, and Kozi Asada. "Detection of singlet oxygen and superoxide with fluorescent sensors in leaves under stress by photoinhibition or UV radiation." *Plant and Cell Physiology* 43, no. 10 (2002): 1154-1164.

Hochholdinger, Frank, Katrin Woll, Michaela Sauer, and Diana Dembinsky. "Genetic dissection of root formation in maize (Zea mays) reveals root-type specific developmental programmes." *Annals of Botany* 93, no. 4 (2004): 359-368.

Horton, Peter, and Alexander Ruban. "Molecular design of the photosystem II light-harvesting antenna: photosynthesis and photoprotection." *Journal of experimental botany* 56, no. 411 (2005): 365-373.

Howarth, C. J. "Genetic improvements of tolerance to high temperature."*Abiotic stresses: plant resistance through breeding and molecular approaches. Howarth Press Inc., New York* (2005).

Hrabak, Estelle M., Catherine WM Chan, Michael Gribskov, Jeffrey F. Harper, Jung H. Choi, Nigel Halford, Jörg Kudla et al. "The Arabidopsis CDPK-SnRK superfamily of protein kinases." *Plant physiology* 132, no. 2 (2003): 666-680.

Hsieh, Hsu-Liang, Haruko Okamoto, Mingli Wang, Lay-Hong Ang, Minami Matsui, Horward Goodman, and Xing Wang Deng. "FIN219, an auxin-regulated gene, defines a link between phytochrome A and the downstream regulator COP1 in light control of Arabidopsis development." Genes & development 14, no. 15 (2000): 1958-1970.

Huang, Xin-Yuan, Dai-Yin Chao, Ji-Ping Gao, Mei-Zhen Zhu, Min Shi, and Hong-Xuan Lin. "A previously unknown zinc finger protein, DST, regulates drought and salt tolerance in rice via stomatal aperture control." *Genes & Development* 23, no. 15 (2009): 1805-1817.

Huang, Guo-Tao, Shi-Liang Ma, Li-Ping Bai, Li Zhang, Hui Ma, Ping Jia, Jun Liu, Ming Zhong, and Zhi-Fu Guo. "Signal transduction during cold, salt, and drought stresses in plants." *Molecular biology reports* 39, no. 2 (2012): 969-987.

Hudson, Matthew, Christoph Ringli, Margaret T. Boylan, and Peter H. Quail. "The FAR1 locus encodes a novel nuclear protein specific to phytochrome A signaling." Genes & development 13, no. 15 (1999): 2017-2027.

Huh, Won-Ki, Seong-Tae Kim, Kap-Seok Yang, Yeong-Jae Seok, Yung Chil Hah, and Sa-Ouk Kang. "Characterisation of D-arabinono-1, 4-lactone oxidase from Candida albicans ATCC 10231." *European Journal of Biochemistry* 225, no. 3 (1994): 1073-1079.

Hung, H. Y., Christopher Browne, Katherine Guill, Nathan Coles, Magen Eller, Arturo Garcia, Nicholas Lepak et al. "The relationship between parental genetic or phenotypic divergence and progeny variation in the maize nested association mapping population." Heredity 108, no. 5 (2011): 490-499.

Iba, Koh. "Acclimative response to temperature stress in higher plants: approaches of gene engineering for temperature tolerance." *Annual Review of Plant Biology* 53, no. 1 (2002): 225-245.

Igarashi, Daisuke, Yoshihiro Izumi, Yuko Dokiya, Kazuhiko Totsuka, Eiichiro Fukusaki, and Chieko Ohsumi. "Reproductive organs regulate leaf nitrogen metabolism mediated by cytokinin signal." *Planta* 229, no. 3 (2009): 633-644.

Ingram, J., and D1 Bartels. "The molecular basis of dehydration tolerance in plants." *Annual review of plant biology* 47, no. 1 (1996): 377-403.

Irigoyen, J. J., D. W. Einerich, and M. Sánchez-Díaz. "Water stress induced changes in concentrations of proline and total soluble sugars in nodulated alfalfa (Medicago sativd) plants." *Physiologia Plantarum* 84, no. 1 (1992): 55-60.

Ishitani, Manabu, Jiping Liu, Ursula Halfter, Cheol-Soo Kim, Weiming Shi, and Jian-Kang Zhu. "SOS3 function in plant salt tolerance requires N-myristoylation and calcium binding." *The Plant Cell Online* 12, no. 9 (2000): 1667-1677.

Iuchi, Satoshi, Hiroyuki Suzuki, Young-Cheon Kim, Atsuko Iuchi, Takashi Kuromori, Miyako Ueguchi-Tanaka, Tadao Asami et al. "Multiple loss-of-function of Arabidopsis gibberellin receptor AtGID1s completely shuts down a gibberellin signal." *The Plant Journal* 50, no. 6 (2007): 958-966.

Jacob, Tobias, Sian Ritchie, Sarah M. Assmann, and Simon Gilroy. "Abscisic acid signal transduction in guard cells is mediated by phospholipase D activity." *Proceedings of the National Academy of Sciences* 96, no. 21 (1999): 12192-12197.

Jang, Seonghoe, Virginie Marchal, Kishore Panigrahi, Stephan Wenkel, Wim Soppe, Xing-Wang Deng, Federico Valverde, and George Coupland. "Arabidopsis COP1 shapes the temporal pattern of CO accumulation conferring a photoperiodic flowering response." The EMBO journal 27, no. 8 (2008): 1277-1288.

Jiang, Huawu, Meiru Li, Naiting Liang, Hongbo Yan, Yubo Wei, Xinlan Xu, Jian Liu, Zhifang Xu, Fan Chen, and Guojiang Wu. "Molecular cloning and function analysis of the stay green gene in rice." *The Plant Journal* 52, no. 2 (2007): 197-209.

Johanson, Urban, Joanne West, Clare Lister, Scott Michaels, Richard Amasino, and Caroline Dean. "Molecular analysis of FRIGIDA, a major determinant of natural variation in Arabidopsis flowering time." *Science* 290, no. 5490 (2000): 344-347.

Kadir, Sorkel, Michael Von Weihe, and Kassim Al-Khatib. "Photochemical efficiency and recovery of photosystem II in grapes after exposure to sudden and gradual heat stress." *Journal of the American Society for Horticultural Science* 132, no. 6 (2007): 764-769.

Karim, M. A., Y. Fracheboud, and P. Stamp. "Heat tolerance of maize with reference of some physiological characteristics." *Ann. Bangladesh Agri* 7 (1997): 27-33.

Karim, M. D., Yvan Fracheboud, and Peter Stamp. "Photosynthetic activity of developing leaves of Zea mays is less affected by heat stress than that of developed leaves." *Physiologia Plantarum* 105, no. 4 (1999): 685-693.

Kebede, H., P. K. Subudhi, D. T. Rosenow, and H. T. Nguyen. "Quantitative trait loci influencing drought tolerance in grain sorghum (Sorghum bicolor L. Moench)." Theoretical and Applied Genetics 103, no. 2-3 (2001): 266-276.

Kirigwi, F. M., M. Van Ginkel, G. Brown-Guedira, B. S. Gill, G. M. Paulsen, and A. K. Fritz. "Markers associated with a QTL for grain yield in wheat under drought." *Molecular Breeding* 20, no. 4 (2007): 401-413.

Kishor, PB Kavi, S. Sangam, R. N. Amrutha, P. Sri Laxmi, K. R. Naidu, K. R. S. S. Rao, Sreenath Rao, K. J. Reddy, P. Theriappan, and N. Sreenivasulu. "Regulation of proline biosynthesis, degradation, uptake and transport in higher plants: its implications in plant growth and abiotic stress tolerance."*Curr Sci* 88, no. 3 (2005): 424-438.

Knight, Heather, Anthony J. Trewavas, and Marc R. Knight. "Calcium signalling in Arabidopsis thaliana responding to drought and salinity." *The Plant Journal* 12, no. 5 (1997): 1067-1078.

Kobilka, Brian K., and Xavier Deupi. "Conformational complexity of G-protein-coupled receptors." *Trends in pharmacological sciences* 28, no. 8 (2007): 397-406.

Koo, Abraham JK, Thomas F. Cooke, and Gregg A. Howe. "Cytochrome P450 CYP94B3 mediates catabolism and inactivation of the plant hormone jasmonoyl-L-isoleucine." *Proceedings of the National Academy of Sciences*108, no. 22 (2011): 9298-9303.

Krishna, Priti, Melanie Sacco, James F. Cherutti, and Sylvia Hill. "Cold-induced accumulation of hsp90 transcripts in Brassica napus." *Plant physiology* 107, no. 3 (1995): 915-923.

Kumari, M., V. P. Singh, R. Tripathi, and A. K. Joshi. "Variation for staygreen trait and its association with canopy temperature depression and yield traits under terminal heat stress in wheat." In *Wheat Production in Stressed Environments,* pp. 357-363. Springer Netherlands, 2007.

Kumari, Uttam, Arun K. Joshi, Maya Kumari, Rajneesh Paliwal, Sundeep Kumar, and Marion S. Röder. "Identification of QTLs for stay green trait in wheat (Triticum aestivum L.) in the 'Chirya 3'×'Sonalika'population."*Euphytica* 174, no. 3 (2010): 437-445.

Kump, Kristen L., Peter J. Bradbury, Randall J. Wisser, Edward S. Buckler, Araby R. Belcher, Marco A. Oropeza-Rosas, John C. Zwonitzer et al. "Genome-wide association study of quantitative resistance to southern leaf blight in the maize nested association mapping population." Nature genetics 43, no. 2 (2011): 163-168.

Kurakawa, Takashi, Nanae Ueda, Masahiko Maekawa, Kaoru Kobayashi, Mikiko Kojima, Yasuo Nagato, Hitoshi Sakakibara, and Junko Kyozuka. "Direct control of shoot meristem activity by a cytokinin-activating enzyme."*Nature* 445, no. 7128 (2007): 652-655.

Kwak, June M., and M. Ć. Pascal. "The clickable guard cell, version II: interactive model of guard cell signal transduction mechanisms and pathways." The Arabidopsis book/American Society of Plant Biologists 6 (2008).

Lee, Youngsook, Young B. Choi, Sujeoung Suh, Joonsang Lee, Sarah M. Assmann, Cheol O. Joe, Joseph F. Kelleher, and Richard C. Crain. "Abscisic acid-induced phosphoinositide turnover in guard cell protoplasts of Vicia faba." *Plant Physiology* 110, no. 3 (1996): 987-996.

Lee, Sang-Hoon, Nagib Ahsan, Ki-Won Lee, Do-Hyun Kim, Dong-Gi Lee, Sang-Soo Kwak, Suk-Yoon Kwon, Tae-Hwan Kim, and Byung-Hyun Lee. "Simultaneous overexpression of both CuZn superoxide dismutase and ascorbate peroxidase in transgenic tall fescue plants confers increased tolerance to a wide range of abiotic stresses." *Journal of plant physiology*164, no. 12 (2007): 1626-1638.

Lemtiri-Chlieh, Fouad, Enid AC MacRobbie, and Charles A. Brearley. "Inositol hexakisphosphate is a physiological signal regulating the K+-inward rectifying conductance in guard cells." *Proceedings of the National Academy of Sciences* 97, no. 15 (2000): 8687-8692.

Lemtiri-Chlieh, Fouad, Enid AC MacRobbie, Alex AR Webb, Nick F. Manison, Colin Brownlee, Jeremy N. Skepper, Jian Chen, Glenn D. Prestwich, and Charles A. Brearley. "Inositol hexakisphosphate mobilizes an endomembrane store of calcium in guard cells." *Proceedings of the National Academy of Sciences* 100, no. 17 (2003): 10091-10095.

Li, Hai, Phoebe Johnson, Anna Stepanova, Jose M. Alonso, and Joseph R. Ecker. "Convergence of Signaling Pathways in the Control of Differential Cell Growth in< i> Arabidopsis</i>." *Developmental cell* 7, no. 2 (2004): 193-204.

Li, Jisheng, Xinhua Dai, and Yunde Zhao. "A role for auxin response factor 19 in auxin and ethylene signaling in Arabidopsis." *Plant Physiology* 140, no. 3 (2006): 899-908.

Lillo, Cathrine, Christian Meyer, Unni S. Lea, Fiona Provan, and Satu Oltedal. "Mechanism and importance of post-translational regulation of nitrate reductase." *Journal of experimental botany* 55, no. 401 (2004): 1275-1282.

Lim, Pyung Ok, Hyo Jung Kim, and Hong Gil Nam. "Leaf senescence."*Annu. Rev. Plant Biol.* 58 (2007): 115-136.

Lin, Zhongwei, Xianran Li, Laura M. Shannon, Cheng-Ting Yeh, Ming L. Wang, Guihua Bai, Zhao Peng et al. "Parallel domestication of the Shattering1 genes in cereals." Nature genetics 44, no. 6 (2012): 720-724.

Lindahl, Marika, Cornelia Spetea, Torill Hundal, Amos B. Oppenheim, Zach Adam, and Bertil Andersson. "The thylakoid FtsH protease plays a role in the light-induced turnover of the photosystem II D1 protein." *The Plant Cell Online* 12, no. 3 (2000): 419-431.

Lindquist, S., and E. A. Craig. "The heat-shock proteins." *Annual review of genetics* 22, no. 1 (1988): 631-677.

Lipka, Alexander E., Feng Tian, Qishan Wang, Jason Peiffer, Meng Li, Peter J. Bradbury, Michael A. Gore, Edward S. Buckler, and Zhiwu Zhang. "GAPIT: genome association and prediction integrated tool." Bioinformatics 28, no. 18 (2012): 2397-2399.

Liu, Jiping, and Jian-Kang Zhu. "A calcium sensor homolog required for plant salt tolerance." *Science* 280, no. 5371 (1998): 1943-1945.

Liu, Jiping, Manabu Ishitani, Ursula Halfter, Cheol-Soo Kim, and Jian-Kang Zhu. "The Arabidopsis thaliana SOS2 gene encodes a protein kinase that is required for salt tolerance." *Proceedings of the National Academy of Sciences* 97, no. 7 (2000): 3730-3734.

Liu, Qiang, Nanming Zhao, K. Yamaguch-Shinozaki, and K. Shinozaki. "Regulatory role of DREB transcription factors in plant drought, salt and cold tolerance." *Chinese Science Bulletin* 45, no. 11 (2000): 970-975.

Liu, Jinling, Wei Li, Yuese Ning, Gautam Shirsekar, Yuhui Cai, Xuli Wang, Liangying Dai, Zhilong Wang, Wende Liu, and Guo-Liang Wang. "The U-box E3 ligase SPL11/PUB13 is a convergence point of defense and flowering signaling in plants." Plant physiology 160, no. 1 (2012): 28-37.

Llusia, Joan, Josep Penuelas, and Sergi Munné-Bosch. "Sustained accumulation of methyl salicylate alters antioxidant protection and reduces tolerance of holm oak to heat stress." *Physiologia Plantarum* 124, no. 3 (2005): 353-361.

Lohse, Gabi, and Rainer Hedrich. "Characterization of the plasma-membrane H+-ATPase from Vicia faba guard cells." *Planta* 188, no. 2 (1992): 206-214.

López-Ráez, Juan A., Wouter Kohlen, Tatsiana Charnikhova, Patrick Mulder, Anna K. Undas, Martin J. Sergeant, Francel Verstappen et al. "Does abscisic acid affect strigolactone biosynthesis?." *New phytologist* 187, no. 2 (2010): 343-354.

Luan, Sheng. "Protein phosphatases in plants." *Annual Review of Plant Biology* 54, no. 1 (2003): 63-92.

Leung, Jeffrey, et al. "Arabidopsis ABA response gene ABI1: features of a calcium-modulated protein phosphatase." Science 264.5164 (1994): 1448-1452.

Leung, Jeffrey, Sylvain Merlot, and Jerome Giraudat. "The Arabidopsis ABSCISIC ACID-INSENSITIVE2 (ABI2) and ABI1 genes encode homologous protein phosphatases 2C involved in abscisic acid signal transduction." The Plant Cell Online 9, no. 5 (1997): 759-771.

K.M. Lounsbury, I.G. Macara. “Ran-binding protein 1 (RanBP1) forms a ternary complex with Ran and Karyopherin β and reduces GTPase-activating protein (RanGAP) inhibition by karyopherin β.” *J. Biol. Chem.*, 272 (1997), pp. 551–555.

Lynch, Daniel V. "Chilling injury in plants: the relevance of membrane lipids." *Environmental injury to plants* (1990): 17-34.

Ma, B. L., and L. M. Dwyer. "Nitrogen uptake and use of two contrasting maize hybrids differing in leaf senescence." *Plant and soil* 199, no. 2 (1998): 283-291.

Mace, E. S., C. H. Hunt, and D. R. Jordan. "Supermodels: sorghum and maize provide mutual insight into the genetics of flowering time." Theoretical and Applied Genetics 126, no. 5 (2013): 1377-1395.

Mahajan, Shilpi, and Narendra Tuteja. "Cold, salinity and drought stresses: an overview." *Archives of biochemistry and biophysics* 444, no. 2 (2005): 139-158.

Mansfield, T. A., A. M. Hetherington, and C. J. Atkinson. "Some current aspects of stomatal physiology." *Annual review of plant biology* 41, no. 1 (1990): 55-75.

Mansfield, Terry A., and Martin R. McAinsh. "Hormones as regulators of water balance." In *Plant hormones*, pp. 598-616. Springer Netherlands, 1995.

Martin, Antoine, Xana Belastegui-Macadam, Isabelle Quilleré, Mathieu Floriot, Marie-Hèlène Valadier, Bernard Pommel, Bruno Andrieu, Iain Donnison, and Bertrand Hirel. "Nitrogen management and senescence in two maize hybrids differing in the persistence of leaf greenness: agronomic, physiological and molecular aspects." *New phytologist* 167, no. 2 (2005): 483-492.

McKersie, Bryan D., and Stephen R. Bowley. "Active oxygen and freezing tolerance in transgenic plants." In *Plant Cold Hardiness*, pp. 203-214. Springer US, 1997.

McMaster GS, Wilhelm WW (1997) Growing degree-days: one equation, two interpretations. Agricultural Forest Meteorology 87:291-300

McMullen MD, et al. (2009) Genetic properties of the maize nested association mapping population. Science 325:737–740.

Mehlmer, Norbert, Bernhard Wurzinger, Simon Stael, Daniela Hofmann-Rodrigues, Edina Csaszar, Barbara Pfister, Roman Bayer, and Markus Teige. "The Ca2+-dependent protein kinase CPK3 is required for MAPK-independent salt-stress acclimation in Arabidopsis." The Plant Journal 63, no. 3 (2010): 484-498.

Mendel, Gregor. "Versuche über Pflanzenhybriden." *Verhandlungen des naturforschenden Vereines in Brunn 4: 3* 44 (1866).

Merlot, Sylvain, Francoise Gosti, Daniele Guerrier, Alain Vavasseur, and Jerome Giraudat. "The ABI1 and ABI2 protein phosphatases 2C act in a negative feedback regulatory loop of the abscisic acid signalling pathway."*The Plant Journal* 25, no. 3 (2001): 295-303.

Messmer, Rainer, Yvan Fracheboud, Marianne Bänziger, Mateo Vargas, Peter Stamp, and Jean-Marcel Ribaut. "Drought stress and tropical maize: QTL-by-environment interactions and stability of QTLs across environments for yield components and secondary traits." *Theoretical and Applied Genetics* 119, no. 5 (2009): 913-930.

Meyer, Knut, Martin P. Leube, and Erwin Grill. "A protein phosphatase 2C involved in ABA signal transduction in Arabidopsis thaliana." *Science* 264, no. 5164 (1994): 1452-1455.

Mi, Guohua, Jian-an Liu, Fanjun Chen, Fusuo Zhang, Zhenling Cui, and Xiangsheng Liu. "Nitrogen uptake and remobilization in maize hybrids differing in leaf senescence." *Journal of plant nutrition* 26, no. 1 (2003): 237-247.

Michael, Todd P., Patrice A. Salome, J. Yu Hannah, Taylor R. Spencer, Emily L. Sharp, Mark A. McPeek, Jose M. Alonso, Joseph R. Ecker, and C. Robertson McClung. "Enhanced fitness conferred by naturally occurring variation in the circadian clock." Science 302, no. 5647 (2003): 1049-1053.

Micheli, Fabienne. "Pectin methylesterases: cell wall enzymes with important roles in plant physiology." *Trends in plant science* 6, no. 9 (2001): 414-419.

Mikel, Mark A., and John W. Dudley. "Evolution of North American dent corn from public to proprietary germplasm." Crop science 46, no. 3 (2006): 1193-1205.

Miroshnichenko, Sergey, Joanna Tripp, Uta zur Nieden, Dieter Neumann, Udo Conrad, and Renate Manteuffel. "Immunomodulation of function of small heat shock proteins prevents their assembly into heat stress granules and results in cell death at sublethal temperatures." *The Plant Journal* 41, no. 2 (2005): 269-281.

Mizoguchi, Tsuyoshi, Nobuaki Hayashida, Kazuko Yamaguchi-Shinozaki, Hiroshi Kamada, and Kazuo Shinozaki. "ATMPKs: a gene family of plant MAP kinases in< i> Arabidopsis thaliana</i>." *FEBS letters* 336, no. 3 (1993): 440-444.

Mizoguchi, Tsuyoshi, Kenji Irie, Takashi Hirayama, Nobuaki Hayashida, Kazuko Yamaguchi-Shinozaki, Kunihiro Matsumoto, and Kazuo Shinozaki. "A gene encoding a mitogen-activated protein kinase kinase kinase is induced simultaneously with genes for a mitogen-activated protein kinase and an S6 ribosomal protein kinase by touch, cold, and water stress in Arabidopsis thaliana." Proceedings of the National Academy of Sciences 93, no. 2 (1996): 765-769.

Moh'd I, Hozain, Michael E. Salvucci, Mohamed Fokar, and A. Scott Holaday. "The differential response of photosynthesis to high temperature for a boreal and temperate Populus species relates to differences in Rubisco activation and Rubisco activase properties." *Tree physiology* 30, no. 1 (2010): 32-44.

Monroy, Antonio F., and Rajinder S. Dhindsa. "Low-temperature signal transduction: induction of cold acclimation-specific genes of alfalfa by calcium at 25 degrees C." *The Plant Cell Online* 7.3 (1995): 321-331.

Mori, Izumi C., Yoshiyuki Murata, Yingzhen Yang, Shintaro Munemasa, Yong-Fei Wang, Shannon Andreoli, Hervé Tiriac et al. "CDPKs CPK6 and CPK3 function in ABA regulation of guard cell S-type anion-and Ca2+-permeable channels and stomatal closure." PLoS biology 4, no. 10 (2006): e327.

Morse, M. J., Richard C. Crain, Gary G. Coté, and Ruth L. Satter. "Light-Stimulated Inositol Phospholipid Turnover in Samanea saman Pulvini Increased Levels of Diacylglycerol." *Plant physiology* 89, no. 3 (1989): 724-727.

Motchoulski, Andrei, and Emmanuel Liscum. "Arabidopsis NPH3: a NPH1 photoreceptor-interacting protein essential for phototropism." Science 286, no. 5441 (1999): 961-964.

Mouchel, Céline F., Georgette C. Briggs, and Christian S. Hardtke. "Natural genetic variation in Arabidopsis identifies BREVIS RADIX, a novel regulator of cell proliferation and elongation in the root." *Genes & development* 18, no. 6 (2004): 700-714.

Mousley, Carl J., Kimberly R. Tyeryar, Patrick Vincent-Pope, and Vytas A. Bankaitis. "The Sec14-superfamily and the regulatory interface between phospholipid metabolism and membrane trafficking." Biochimica et Biophysica Acta (BBA)-Molecular and Cell Biology of Lipids 1771, no. 6 (2007): 727-736.

Multani, Dilbag S., Steven P. Briggs, Mark A. Chamberlin, Joshua J. Blakeslee, Angus S. Murphy, and Gurmukh S. Johal. "Loss of an MDR transporter in compact stalks of maize br2 and sorghum dw3 mutants." Science 302, no. 5642 (2003): 81-84.

Munné-Bosch, Sergi, and Leonor Alegre. "The function of tocopherols and tocotrienols in plants." *Critical Reviews in Plant Sciences* 21, no. 1 (2002): 31-57.

Munnik, Teun, Harold JG Meijer, Bas Ter Riet, Heribert Hirt, Wolfgang Frank, Dorothea Bartels, and Alan Musgrave. "Hyperosmotic stress stimulates phospholipase D activity and elevates the levels of phosphatidic acid and diacylglycerol pyrophosphate." The Plant Journal 22, no. 2 (2000): 147-154.

Mukhopadhyay, Arnab, Shubha Vij, and Akhilesh K. Tyagi. "Overexpression of a zinc-finger protein gene from rice confers tolerance to cold, dehydration, and salt stress in transgenic tobacco." *Proceedings of the National Academy of Sciences of the United States of America* 101, no. 16 (2004): 6309-6314.

Nakajima, Masatoshi, Asako Shimada, Yoshiyuki Takashi, Young-Cheon Kim, Seung-Hyun Park, Miyako Ueguchi-Tanaka, Hiroyuki Suzuki et al. "Identification and characterization of Arabidopsis gibberellin receptors."*The Plant Journal* 46, no. 5 (2006): 880-889.

Neta-Sharir, Inbal, Tal Isaacson, Susan Lurie, and David Weiss. "Dual role for tomato heat shock protein 21: protecting photosystem II from oxidative stress and promoting color changes during fruit maturation." *The Plant Cell Online* 17, no. 6 (2005): 1829-1838.

Neumann, D., M. Emmermann, J-M. Thierfelder, U. Zur Nieden, M. Clericus, H-P. Braun, L. Nover, and U. K. Schmitz. "HSP68—a DnaK-like heat-stress protein of plant mitochondria." *Planta* 190, no. 1 (1993): 32-43.

Oldham, William M., Ned Van Eps, Anita M. Preininger, Wayne L. Hubbell, and Heidi E. Hamm. "Mechanism of the receptor-catalyzed activation of heterotrimeric G proteins." *Nature structural & molecular biology* 13, no. 9 (2006): 772-777.

Olien, C. R., and Myrtle N. Smith. "Ice adhesions in relation to freeze stress."*Plant Physiology* 60, no. 4 (1977): 499-503.

Ort, Donald R., and Neil R. Baker. "A photoprotective role for O< sub> 2</sub> as an alternative electron sink in photosynthesis?." *Current opinion in plant biology* 5, no. 3 (2002): 193-198.

Osakabe, Yuriko, Kyonoshin Maruyama, Motoaki Seki, Masakazu Satou, Kazuo Shinozaki, and Kazuko Yamaguchi-Shinozaki. "Leucine-rich repeat receptor-like kinase1 is a key membrane-bound regulator of abscisic acid early signaling in Arabidopsis." *The Plant Cell Online* 17, no. 4 (2005): 1105-1119.

Osakabe, Yuriko, Kazuko Yamaguchi-Shinozaki, Kazuo Shinozaki, and Lam-Son Phan Tran. "Sensing the environment: key roles of membrane-localized kinases in plant perception and response to abiotic stress."*Journal of experimental botany* 64, no. 2 (2013): 445-458.

Park, Jung-Eun, Ju-Young Park, Youn-Sung Kim, Paul E. Staswick, Jin Jeon, Ju Yun, Sun-Young Kim, Jungmook Kim, Yong-Hwan Lee, and Chung-Mo Park. "GH3-mediated auxin homeostasis links growth regulation with stress adaptation response in Arabidopsis." Journal of Biological Chemistry 282, no. 13 (2007): 10036-10046.

Parkinson, John S., and Eric C. Kofoid. "Communication modules in bacterial signaling proteins." *Annual review of genetics* 26, no. 1 (1992): 71-112.

Peleg, Zvi, and Eduardo Blumwald. "Hormone balance and abiotic stress tolerance in crop plants." *Current opinion in plant biology* 14, no. 3 (2011): 290-295.

Peleg, Zvi, Maria Reguera, Ellen Tumimbang, Harkamal Walia, and Eduardo Blumwald. "Cytokinin-mediated source/sink modifications improve drought tolerance and increase grain yield in rice under water-stress." *Plant Biotechnology Journal* 9, no. 7 (2011): 747-758.

Pelloux, Jérôme, Christine Rusterucci, and Ewa J. Mellerowicz. "New insights into pectin methylesterase structure and function." *Trends in plant science* 12, no. 6 (2007): 267-277.

Perera, Imara Y., Ingo Heilmann, and Wendy F. Boss. "Transient and sustained increases in inositol 1, 4, 5-trisphosphate precede the differential growth response in gravistimulated maize pulvini." *Proceedings of the National Academy of Sciences* 96, no. 10 (1999): 5838-5843.

Poland, Jesse A., Peter J. Bradbury, Edward S. Buckler, and Rebecca J. Nelson. "Genome-wide nested association mapping of quantitative resistance to northern leaf blight in maize." Proceedings of the National Academy of Sciences 108, no. 17 (2011): 6893-6898.

Pospisilova, Jana, Daniel Haisel, and Radomira Vankova. "Responses of transgenic tobacco plants with increased proline content to drought and/or heat stress." *American Journal of Plant Sciences* 2 (2011): 318.

Qiu, Quan-Sheng, Yan Guo, Margaret A. Dietrich, Karen S. Schumaker, and Jian-Kang Zhu. "Regulation of SOS1, a plasma membrane Na+/H+ exchanger in Arabidopsis thaliana, by SOS2 and SOS3." *Proceedings of the National Academy of Sciences* 99, no. 12 (2002): 8436-8441.

R Core Team (2014). R: A language and environment for statistical computing. R Foundation for Statistical Computing, Vienna, Austria. URL http://www.R-project.org/.

Reape, Theresa J., and Paul F. McCabe. "Apoptotic-like programmed cell death in plants." *New Phytologist* 180, no. 1 (2008): 13-26.

Renaud, A. L., and M. R. Tuinstra, 2013: Role of Engineering Plants for Abiotic Stresses. Climate Vulnerability: Understanding and Addressing Threats to Essential Resources. Elsevier Inc., Academic Press, 51–55 pp

Ribeiro, Dimas M., Radhika Desikan, J. O. Bright, A. N. A. Confraria, Judith Harrison, John T. Hancock, Raimundo S. Barros, Steven J. Neill, and Ian D. Wilson. "Differential requirement for NO during ABA-induced stomatal closure in turgid and wilted leaves." *Plant, cell & environment* 32, no. 1 (2009): 46-57.

Ristic, Zoran, and David D. Cass. "Chloroplast structure after water and high-temperature stress in two lines of maize that differ in endogenous levels of abscisic acid." *International journal of plant sciences* (1992): 186-196.

Rivero, Rosa M., Jacinta Gimeno, Allen Van Deynze, Harkamal Walia, and Eduardo Blumwald. "Enhanced cytokinin synthesis in tobacco plants expressing PSARK:: IPT prevents the degradation of photosynthetic protein complexes during drought." *Plant and cell physiology* 51, no. 11 (2010): 1929-1941.

Rhodes, David, Paul E. Verslues, and Robert E. Sharp. "Role of amino acids in abiotic stress resistance." *Plant amino acids: biochemistry and biotechnology* (1999): 319-356.

Rhodes, David, A. Nadolska-Orczyk, and P. J. Rich. "Salinity, osmolytes and compatible solutes." In *Salinity: Environment-plants-molecules*, pp. 181-204. Springer Netherlands, 2002.

Robson PR, Donnison IS, Wang K, Frame B, Pegg SE, Thomas A, Thomas H (2004) Leaf senescence is delayed in maize expressing the Agrobacterium IPT gene under the control of a novel maize senescence-enhanced promoter. Plant Biotechnology Journal 2:101-112

Rocchi, V., M. Janni, D. Bellincampi, T. Giardina, and R. D'Ovidio. "Intron retention regulates the expression of pectin methyl esterase inhibitor (Pmei) genes during wheat growth and development." *Plant Biology* 14, no. 2 (2012): 365-373.

Rodriguez, Pedro L., Martin P. Leube, and Erwin Grill. "Molecular cloning in Arabidopsis thaliana of a new protein phosphatase 2C (PP2C) with homology to ABI1 and ABI2." *Plant molecular biology* 38, no. 5 (1998): 879-883.

Roig-Villanova, Irma, Jordi Bou-Torrent, Anahit Galstyan, Lorenzo Carretero-Paulet, Sergi Portolés, Manuel Rodríguez-Concepción, and Jaime F. Martínez-García. "Interaction of shade avoidance and auxin responses: a role for two novel atypical bHLH proteins." *The EMBO journal* 26, no. 22 (2007): 4756-4767.

Rosenow, D. T. "Breeding for resistance to root and stalk rots in Texas."*Sorghum Root and Stalk Rots a Critical Review. Bellagio, Italy. ICRISAT, Patancheru, AP India* (1984): 209-236.

Růžička, Kamil, Karin Ljung, Steffen Vanneste, Radka Podhorská, Tom Beeckman, Jiří Friml, and Eva Benková. "Ethylene regulates root growth through effects on auxin biosynthesis and transport-dependent auxin distribution." *The Plant Cell Online* 19, no. 7 (2007): 2197-2212.

Sakamoto, A., and N. Murata. "The role of glycine betaine in the protection of plants from stress: clues from transgenic plants." *Plant, cell & environment*25, no. 2 (2002): 163-171.

Sakamoto, Hideki, Kyonoshin Maruyama, Yoh Sakuma, Tetsuo Meshi, Masaki Iwabuchi, Kazuo Shinozaki, and Kazuko Yamaguchi-Shinozaki. "Arabidopsis Cys2/His2-type zinc-finger proteins function as transcription repressors under drought, cold, and high-salinity stress conditions." *Plant Physiology* 136, no. 1 (2004): 2734-2746.

Samuel, Marcus A., Yashwanti Mudgil, Jennifer N. Salt, Frédéric Delmas, Shaliny Ramachandran, Andrea Chilelli, and Daphne R. Goring. "Interactions between the S-domain receptor kinases and AtPUB-ARM E3 ubiquitin ligases suggest a conserved signaling pathway in Arabidopsis." Plant Physiology 147, no. 4 (2008): 2084-2095.

Sanders, Dale, Jérôme Pelloux, Colin Brownlee, and Jeffrey F. Harper. "Calcium at the crossroads of signaling." *The Plant Cell Online* 14, no. suppl 1 (2002): S401-S417.

Sato, Eriko, Norihito Nakamichi, Takafumi Yamashino, and Takeshi Mizuno. "Aberrant expression of the Arabidopsis circadian-regulated APRR5 gene belonging to the APRR1/TOC1 quintet results in early flowering and hypersensitiveness to light in early photomorphogenesis." Plant and cell physiology 43, no. 11 (2002): 1374-1385.

Sato, Yutaka, Ryouhei Morita, Susumu Katsuma, Minoru Nishimura, Ayumi Tanaka, and Makoto Kusaba. "Two short-chain dehydrogenase/reductases, NON-YELLOW COLORING 1 and NYC1-LIKE, are required for chlorophyll b and light-harvesting complex II degradation during senescence in rice." *The Plant Journal* 57, no. 1 (2009): 120-131.

Savchenko, G. E., E. A. Klyuchareva, L. M. Abramchik, and E. V. Serdyuchenko. "Effect of periodic heat shock on the inner membrane system of etioplasts." *Russian journal of plant physiology* 49, no. 3 (2002): 349-359.

Schöffl, Fritz, R. Prandl, and Andreas Reindl. "Molecular responses to heat stress." *Molecular responses to cold, drought, heat and salt stress in higher plants. RG Landes Co., Austin, Texas* (1999): 81-98.

Schulze, E. D. "Whole-plant responses to drought." *Functional Plant Biology*13, no. 1 (1986): 127-141.

Schumaker, Karen S., and Heven Sze. "Inositol 1, 4, 5-trisphosphate releases Ca2+ from vacuolar membrane vesicles of oat roots." *Journal of Biological Chemistry* 262, no. 9 (1987): 3944-3946.

Sekhon, Rajandeep S., Kevin L. Childs, Nicholas Santoro, Cliff E. Foster, C. Robin Buell, Natalia de Leon, and Shawn M. Kaeppler. "Transcriptional and metabolic analysis of senescence induced by preventing pollination in maize." *Plant physiology* 159, no. 4 (2012): 1730-1744.

Seo, Mitsunori, Hiroyuki Aoki, Hanae Koiwai, Yuji Kamiya, Eiji Nambara, and Tomokazu Koshiba. "Comparative studies on the Arabidopsis aldehyde oxidase (AAO) gene family revealed a major role of AAO3 in ABA biosynthesis in seeds." *Plant and Cell Physiology* 45, no. 11 (2004): 1694-1703.

Seo, Pil Joon, Jaeyong Ryu, Seok Ki Kang, and Chung-Mo Park. "Modulation of sugar metabolism by an INDETERMINATE DOMAIN transcription factor contributes to photoperiodic flowering in Arabidopsis." The Plant Journal 65, no. 3 (2011): 418-429.

Sheen, Jen. "Mutational analysis of protein phosphatase 2C involved in abscisic acid signal transduction in higher plants." *Proceedings of the National Academy of Sciences* 95, no. 3 (1998): 975-980.

Shi, Huazhong, Manabu Ishitani, Cheolsoo Kim, and Jian-Kang Zhu. "The Arabidopsis thaliana salt tolerance gene SOS1 encodes a putative Na+/H+ antiporter." *Proceedings of the national academy of sciences* 97, no. 12 (2000): 6896-6901.

Shi, Qinghua, Zhiyi Bao, Zhujun Zhu, Quansheng Ying, and Qiongqiu Qian. "Effects of different treatments of salicylic acid on heat tolerance, chlorophyll fluorescence, and antioxidant enzyme activity in seedlings of Cucumis sativa L." *Plant growth regulation* 48, no. 2 (2006): 127-135.

Shikata, Masahito, Tomotsugu Koyama, Nobutaka Mitsuda, and Masaru Ohme-Takagi. "Arabidopsis SBP-box genes SPL10, SPL11 and SPL2 control morphological change in association with shoot maturation in the reproductive phase." Plant and cell physiology 50, no. 12 (2009): 2133-2145.

Snaith, P. J., and T. A. Mansfield. "Stomatal sensitivity to abscisic acid: can it be defined?." *Plant, Cell & Environment* 5, no. 4 (1982): 309-311.

Solano, Roberto, Anna Stepanova, Qimin Chao, and Joseph R. Ecker. "Nuclear events in ethylene signaling: a transcriptional cascade mediated by ETHYLENE-INSENSITIVE3 and ETHYLENE-RESPONSE-FACTOR1."*Genes & development* 12, no. 23 (1998): 3703-3714.

Solomon, Susan, ed. *Climate change 2007-the physical science basis: Working group I contribution to the fourth assessment report of the IPCC*. Vol. 4. Cambridge University Press, 2007.

Somerville, Chris. "Plant lipids: metabolism, mutants, and membranes."*Science* 252, no. 5002 (1991): 80-87.

Sondermann, Holger, Clemens Scheufler, Christine Schneider, Jörg Höhfeld, F-Ulrich Hartl, and Ismail Moarefi. "Structure of a Bag/Hsc70 complex: convergent functional evolution of Hsp70 nucleotide exchange factors." *Science* 291, no. 5508 (2001): 1553-1557.

Srinivas, G., K. Satish, R. Madhusudhana, R. Nagaraja Reddy, S. Murali Mohan, and N. Seetharama. "Identification of quantitative trait loci for agronomically important traits and their association with genic-microsatellite markers in sorghum." Theoretical and applied genetics 118, no. 8 (2009): 1439-1454.

Stepanova, Anna N., Joyce M. Hoyt, Alexandra A. Hamilton, and Jose M. Alonso. "A link between ethylene and auxin uncovered by the characterization of two root-specific ethylene-insensitive mutants in Arabidopsis." *The Plant Cell Online* 17, no. 8 (2005): 2230-2242.

Stepanova, Anna N., Joyce Robertson-Hoyt, Jeonga Yun, Larissa M. Benavente, De-Yu Xie, Karel Doležal, Alexandra Schlereth, Gerd Jürgens, and Jose M. Alonso. "< i> TAA1</i>-Mediated Auxin Biosynthesis Is Essential for Hormone Crosstalk and Plant Development." *Cell* 133, no. 1 (2008): 177-191.

Strasser, Andrea, Hans-Joachim Wittmann, Armin Buschauer, Erich H. Schneider, and Roland Seifert. "Species-dependent activities of G-protein-coupled receptor ligands: lessons from histamine receptor orthologs."*Trends in pharmacological sciences* 34, no. 1 (2013): 13-32.

Stock, J. B., A. J. Ninfa, and A. M. Stock. "Protein phosphorylation and regulation of adaptive responses in bacteria." *Microbiological reviews* 53, no. 4 (1989): 450.

Subudhi, P. K., D. T. Rosenow, and H. T. Nguyen. "Quantitative trait loci for the stay green trait in sorghum (Sorghum bicolor L. Moench): consistency across genetic backgrounds and environments." *Theoretical and Applied Genetics* 101, no. 5-6 (2000): 733-741.

Subedi, K. D., and B. L. Ma. "Nitrogen uptake and partitioning in stay-green and leafy maize hybrids." *Crop Science* 45, no. 2 (2005): 740-747.

Swank, Joan C., Frederick E. Below, Robert J. Lambert, and Richard H. Hageman. "Interaction of carbon and nitrogen metabolism in the productivity of maize." *Plant Physiology* 70, no. 4 (1982): 1185-1190.

Tanaka, Mina, Kentaro Takei, Mikiko Kojima, Hitoshi Sakakibara, and Hitoshi Mori. "Auxin controls local cytokinin biosynthesis in the nodal stem in apical dominance." *The Plant Journal* 45, no. 6 (2006): 1028-1036.

Tao, Y. Z., R. G. Henzell, D. R. Jordan, D. G. Butler, A. M. Kelly, and C. L. McIntyre. "Identification of genomic regions associated with stay green in sorghum by testing RILs in multiple environments." *Theoretical and Applied Genetics* 100, no. 8 (2000): 1225-1232.

Thomas, Howard, and Catherine M. Smart. "Crops that stay green1."*Annals of applied Biology* 123, no. 1 (1993): 193-219.

Thomas, Howard, and Catherine J. Howarth. "Five ways to stay green."*Journal of experimental botany* 51, no. suppl 1 (2000): 329-337.

Tian, Chunjie, Beth Kasiborski, Raman Koul, Peter J. Lammers, Heike Bücking, and Yair Shachar-Hill. "Regulation of the nitrogen transfer pathway in the arbuscular mycorrhizal symbiosis: gene characterization and the coordination of expression with nitrogen flux." *Plant Physiology* 153, no. 3 (2010): 1175-1187.

Tian, Feng, Peter J. Bradbury, Patrick J. Brown, Hsiaoyi Hung, Qi Sun, Sherry Flint-Garcia, Torbert R. Rocheford, Michael D. McMullen, James B. Holland, and Edward S. Buckler. "Genome-wide association study of leaf architecture in the maize nested association mapping population." Nature genetics 43, no. 2 (2011): 159-162.

Tondelli, A., G. Laidò, D. Barabaschi, A. Visioni, A. M. Stanca, E. Francia, and N. Pecchioni. "Mapping candidate genes for drought tolerance in barley."*Options Méditerranéennes. Série A: Séminaires Méditerranéens (CIHEAM)*(2008).

Tripathy, J. N., Jingxian Zhang, S. Robin, Thuy T. Nguyen, and H. T. Nguyen. "QTLs for cell-membrane stability mapped in rice (Oryza sativa L.) under drought stress." *Theoretical and Applied Genetics* 100, no. 8 (2000): 1197-1202.

Tsuchisaka, Atsunari, and Athanasios Theologis. "Unique and overlapping expression patterns among the Arabidopsis 1-amino-cyclopropane-1-carboxylate synthase gene family members." *Plant Physiology* 136, no. 2 (2004): 2982-3000.

Tuinstra, Mitchell R., Edwin M. Grote, Peter B. Goldsbrough, and Gebisa Ejeta. "Genetic analysis of post-flowering drought tolerance and components of grain development in Sorghum bicolor (L.) Moench."*Molecular Breeding* 3, no. 6 (1997): 439-448.

Van Oosterom, E. J., R. Jayachandran, and F. R. Bidinger. "Diallel analysis of the stay-green trait and its components in sorghum." *Crop science* 36, no. 3 (1996): 549-555.

Van Oosterom, E. J., S. C. Chapman, A. K. Borrell, I. J. Broad, and G. L. Hammer. "Functional dynamics of the nitrogen balance of sorghum. II. Grain filling period." *Field Crops Research* 115, no. 1 (2010): 29-38.

VanRaden, P. M. "Efficient methods to compute genomic predictions." Journal of dairy science 91, no. 11 (2008): 4414-4423.

Vauquelin, Georges, and Bengt Von Mentzer. *G Protein-Coupled Receptors: Molecular Pharmacology*. John Wiley & Sons, 2008.

Vranová, Eva, Sopapan Atichartpongkul, Raimundo Villarroel, Marc Van Montagu, Dirk Inzé, and Wim Van Camp. "Comprehensive analysis of gene expression in Nicotiana tabacum leaves acclimated to oxidative stress."*Proceedings of the National Academy of Sciences* 99, no. 16 (2002): 10870-10875.

Uemura, Matsuo, Raymond A. Joseph, and Peter L. Steponkus. "Cold acclimation of Arabidopsis thaliana (effect on plasma membrane lipid composition and freeze-induced lesions)." *Plant physiology* 109, no. 1 (1995): 15-30.

Uno, Yuichi, Takashi Furihata, Hiroshi Abe, Riichiro Yoshida, Kazuo Shinozaki, and Kazuko Yamaguchi-Shinozaki. "Arabidopsis basic leucine zipper transcription factors involved in an abscisic acid-dependent signal transduction pathway under drought and high-salinity conditions."*Proceedings of the National Academy of Sciences* 97, no. 21 (2000): 11632-11637.

Van Breusegem, Frank, Luit Slooten, Jean-Marie Stassart, Johan Botterman, Tanya Moens, Marc Van Montagu, and Dirk Inzé. "Effects of overproduction of tobacco MnSOD in maize chloroplasts on foliar tolerance to cold and oxidative stress." *Journal of Experimental Botany* 50, no. 330 (1999): 71-78.

VanRaden, P. M. "Efficient methods to compute genomic predictions." Journal of dairy science 91, no. 11 (2008): 4414-4423.

Vanoosthuyse, Vincent, Gabrielle Tichtinsky, Christian Dumas, Thierry Gaude, and J. Mark Cock. "Interaction of calmodulin, a sorting nexin and kinase-associated protein phosphatase with the Brassica oleracea S locus receptor kinase." *Plant Physiology* 133, no. 2 (2003): 919-929.

Vu, Joseph CV, Russ W. Gesch, and Arja H. Pennanen. "Soybean photosynthesis, Rubisco, and carbohydrate enzymes function at supraoptimal temperatures in elevated CO< sub> 2</sub>." *Journal of plant physiology* 158, no. 3 (2001): 295-307.

Wahid, Abdul, and Alia Ghazanfar. "Possible involvement of some secondary metabolites in salt tolerance of sugarcane." *Journal of plant physiology* 163, no. 7 (2006): 723-730.

Wahid, A., S. Gelani, M. Ashraf, and M. R. Foolad. "Heat tolerance in plants: an overview." *Environmental and Experimental Botany* 61, no. 3 (2007): 199-223.

Wahid, A., and T. J. Close. "Expression of dehydrins under heat stress and their relationship with water relations of sugarcane leaves." *Biologia Plantarum* 51, no. 1 (2007): 104-109.

Walden, Richard, Alexandra Cordeiro, and Antonio F. Tiburcio. "Polyamines: small molecules triggering pathways in plant growth and development."*Plant physiology* 113, no. 4 (1997): 1009.

Wallace, Jason G., Peter J. Bradbury, Nengyi Zhang, Yves Gibon, Mark Stitt, and Edward S. Buckler. "Association Mapping across Numerous Traits Reveals Patterns of Functional Variation in Maize." PLoS genetics 10, no. 12 (2014): e1004845.

Walulu, Richard S., Darrell T. Rosenow, David B. Wester, and Henry T. Nguyen. "Inheritance of the stay green trait in sorghum." *Crop science* 34, no. 4 (1994): 970-972.

Wang, Hong, Qungang Qi, Peter Schorr, Adrian J. Cutler, William L. Crosby, and Larry C. Fowke. "ICK1, a cyclin-dependent protein kinase inhibitor fromArabidopsis thalianainteracts with both Cdc2a and CycD3, and its expression is induced by abscisic acid." *The Plant Journal* 15, no. 4 (1998): 501-510.

Wang, Jing, Hong Zhang, and Randy D. Allen. "Overexpression of an Arabidopsis peroxisomal ascorbate peroxidase gene in tobacco increases protection against oxidative stress." *Plant and Cell Physiology* 40, no. 7 (1999): 725-732.

Wang, Haiyang, and Xing Wang Deng. "Arabidopsis FHY3 defines a key phytochrome A signaling component directly interacting with its homologous partner FAR1." The EMBO journal 21, no. 6 (2002): 1339-1349.

Wang, Yueju, Michael Wisniewski, Richard Meilan, Minggang Cui, Robert Webb, and Leslie Fuchigami. "Overexpression of cytosolic ascorbate peroxidase in tomato confers tolerance to chilling and salt stress." *Journal of the American Society for Horticultural Science* 130, no. 2 (2005): 167-173.

Waters, Elizabeth R., Garrett J. Lee, and Elizabeth Vierling. "Evolution, structure and function of the small heat shock proteins in plants." *Journal of Experimental Botany* 47, no. 3 (1996): 325-338.

Wen, Jiang-Qi, Kiyoharu Oono, and Ryozo Imai. "Two novel mitogen-activated protein signaling components, OsMEK1 and OsMAP1, are involved in a moderate low-temperature signaling pathway in rice." *Plant physiology* 129, no. 4 (2002): 1880-1891.

West, Ann H., and Ann M. Stock. "Histidine kinases and response regulator proteins in two-component signaling systems." *Trends in biochemical sciences* 26, no. 6 (2001): 369-376.

White, Philip J., and Martin R. Broadley. "Calcium in plants." *Annals of botany* 92, no. 4 (2003): 487-511.

Wi, Soo Jin, Woo Taek Kim, and Ky Young Park. "Overexpression of carnation S-adenosylmethionine decarboxylase gene generates a broad-spectrum tolerance to abiotic stresses in transgenic tobacco plants." *Plant cell reports* 25, no. 10 (2006): 1111-1121.

Wilkinson, S., and William J. Davies. "ABA-based chemical signalling: the co-ordination of responses to stress in plants." *Plant, cell & environment*25, no. 2 (2002): 195-210.

Wise, R. R., A. J. Olson, S. M. Schrader, and T. D. Sharkey. "Electron transport is the functional limitation of photosynthesis in field-grown pima cotton plants at high temperature." *Plant, Cell & Environment* 27, no. 6 (2004): 717-724.

Wise, Michael J., and Alan Tunnacliffe. "POPP the question: what< i> do</i> LEA proteins do?." *Trends in plant science* 9, no. 1 (2004): 13-17.

Wong, Vanessa NL, R. S. B. Greene, R. C. Dalal, and B. W. Murphy. "Soil carbon dynamics in saline and sodic soils: a review." *Soil use and management* 26, no. 1 (2010): 2-11.

Wu, Yan, Jennifer Kuzma, Eric Maréchal, Richard Graeff, Hon Cheung Lee, Randy Foster, and Nam-Hai Chua. "Abscisic acid signaling through cyclic ADP-ribose in plants." *Science* 278, no. 5346 (1997): 2126-2130.

Wu, Yuye, Xianran Li, Wenwen Xiang, Chengsong Zhu, Zhongwei Lin, Yun Wu, Jiarui Li et al. "Presence of tannins in sorghum grains is conditioned by different natural alleles of Tannin1." Proceedings of the National Academy of Sciences 109, no. 26 (2012): 10281-10286.

Xiao, Jun, Hongtao Cheng, Xianghua Li, Jinghua Xiao, Caiguo Xu, and Shiping Wang. "Rice WRKY13 regulates cross talk between abiotic and biotic stress signaling pathways by selective binding to different cis-elements." *Plant physiology* 163, no. 4 (2013): 1868-1882.

Xin, Zhanguo. "eskimo1 mutants of Arabidopsis are constitutively freezing-tolerant." *Proceedings of the National Academy of Sciences* 95, no. 13 (1998): 7799-7804.

Xiong, Liming, and Jian-Kang Zhu. "Abiotic stress signal transduction in plants: molecular and genetic perspectives." *Physiologia Plantarum* 112, no. 2 (2001): 152-166.

Xiong, Liming, Karen S. Schumaker, and Jian-Kang Zhu. "Cell signaling during cold, drought, and salt stress." *The Plant Cell Online* 14, no. suppl 1 (2002): S165-S183.

Xu, Deping, Xiaolan Duan, Baiyang Wang, Bimei Hong, Tuan-Hua David Ho, and Ray Wu. "Expression of a late embryogenesis abundant protein gene, HVA1, from barley confers tolerance to water deficit and salt stress in transgenic rice." *Plant physiology* 110, no. 1 (1996): 249-257.

Xu, Wenwei, Prasanta K. Subudhi, Oswald R. Crasta, Darrell T. Rosenow, John E. Mullet, and Henry T. Nguyen. "Molecular mapping of QTLs conferring stay-green in grain sorghum (Sorghum bicolor L. Moench)."*Genome* 43, no. 3 (2000): 461-469.

Xu, Kenong, Xia Xu, Takeshi Fukao, Patrick Canlas, Reycel Maghirang-Rodriguez, Sigrid Heuer, Abdelbagi M. Ismail, Julia Bailey-Serres, Pamela C. Ronald, and David J. Mackill. "Sub1A is an ethylene-response-factor-like gene that confers submergence tolerance to rice." *Nature* 442, no. 7103 (2006): 705-708.

Yamaguchi, Yube, Alisa Huffaker, Anthony C. Bryan, Frans E. Tax, and Clarence A. Ryan. "PEPR2 is a second receptor for the Pep1 and Pep2 peptides and contributes to defense responses in Arabidopsis." *The Plant Cell Online* 22, no. 2 (2010): 508-522.

Yamane, Yoshihiro, Yasuhiro Kashino, Hiroyuki Koike, and Kazuhiko Satoh. "Effects of high temperatures on the photosynthetic systems in spinach: oxygen-evolving activities, fluorescence characteristics and the denaturation process." *Photosynthesis Research* 57, no. 1 (1998): 51-59.

Yang, Hong-Quan, Ru-Hang Tang, and Anthony R. Cashmore. "The signaling mechanism of Arabidopsis CRY1 involves direct interaction with COP1." The Plant Cell Online 13, no. 12 (2001): 2573-2587.

Yang, Liang, Wei Ji, Yanming Zhu, Peng Gao, Yong Li, Hua Cai, Xi Bai, and Dianjing Guo. "GsCBRLK, a calcium/calmodulin-binding receptor-like kinase, is a positive regulator of plant tolerance to salt and ABA stress."*Journal of experimental botany* 61, no. 9 (2010): 2519-2533.

Ye, Bin, Herbert H. Muller, Jian Zhang, and Jonathan Gressel. "Constitutively elevated levels of putrescine and putrescine-generating enzymes correlated with oxidant stress resistance in Conyza bonariensis and wheat." *Plant physiology* 115, no. 4 (1997): 1443-1451.

Yoo, Chan Yul, Heather E. Pence, Paul M. Hasegawa, and Michael V. Mickelbart. "Regulation of transpiration to improve crop water use." Critical Reviews in Plant Science 28, no. 6 (2009): 410-431.

Young, Todd E., Jun Ling, C. Jane Geisler-Lee, Robert L. Tanguay, Christian Caldwell, and Daniel R. Gallie. "Developmental and thermal regulation of the maize heat shock protein, HSP101." *Plant Physiology* 127, no. 3 (2001): 777-791.

Young, Todd E., Robert B. Meeley, and Daniel R. Gallie. "ACC synthase expression regulates leaf performance and drought tolerance in maize."*The Plant Journal* 40, no. 5 (2004): 813-825.

Yu J, Holland JB, McMullen MD, Buckler ES (2008) Genetic design and statistical power of nested association mapping in maize. Genetics 178:539–551.

Zhang, J., H. G. Zheng, A. Aarti, G. Pantuwan, T. T. Nguyen, J. N. Tripathy, A. K. Sarial et al. "Locating genomic regions associated with components of drought resistance in rice: comparative mapping within and across species." *Theoretical and Applied Genetics* 103, no. 1 (2001): 19-29.

Zhang, Jun-Huan, Wei-Dong HUANG, Yue-Ping LIU, and Qiu-Hong PAN. "Effects of Temperature Acclimation Pretreatment on the Ultrastructure of Mesophyll Cells in Young Grape Plants (Vitis vinifera L. cv. Jingxiu) Under Cross-Temperature Stresses." *Journal of Integrative Plant Biology* 47, no. 8 (2005): 959-970.

Zhang, Jianhua, Wensuo Jia, Jianchang Yang, and Abdelbagi M. Ismail. "Role of ABA in integrating plant responses to drought and salt stresses."*Field Crops Research* 97, no. 1 (2006): 111-119.

Zhang, T., Y. Liu, T. Yang, L. Zhang, S. Xu, L. Xue, and L. An. "Diverse signals converge at MAPK cascades in plant." *Plant physiology and Biochemistry* 44, no. 5 (2006): 274-283.

Zhang, Jianhua, Wensuo Jia, Jianchang Yang, and Abdelbagi M. Ismail. "Role of ABA in integrating plant responses to drought and salt stresses."*Field Crops Research* 97, no. 1 (2006): 111-119.

Zhang, Qian, Jingjing Li, Wenjiao Zhang, Shuning Yan, Rui Wang, Junfeng Zhao, Yujing Li, Zhiguang Qi, Zongxiu Sun, and Zhengge Zhu. "The putative auxin efflux carrier OsPIN3t is involved in the drought stress response and drought tolerance." *The Plant Journal* 72, no. 5 (2012): 805-816.

Zhang, Sheng-Wei, Chen-Hui Li, Jia Cao, Yong-Cun Zhang, Su-Qiao Zhang, Yu-Feng Xia, Da-Ye Sun, and Ying Sun. "Altered architecture and enhanced drought tolerance in rice via the down-regulation of indole-3-acetic acid by TLD1/OsGH3. 13 activation." *Plant physiology* 151, no. 4 (2009): 1889-1901.

Zeng, Li-Rong, Shaohong Qu, Alicia Bordeos, Chengwei Yang, Marietta Baraoidan, Hongyan Yan, Qi Xie, Baek Hie Nahm, Hei Leung, and Guo-Liang Wang. "Spotted leaf11, a negative regulator of plant cell death and defense, encodes a U-box/armadillo repeat protein endowed with E3 ubiquitin ligase activity." The Plant Cell Online 16, no. 10 (2004): 2795-2808.

Zhao, F., and H. Zhang. "Expression of Suaeda salsa glutathione S-transferase in transgenic rice resulted in a different level of abiotic stress resistance." *The Journal of Agricultural Science* 144, no. 06 (2006): 547-554.

Zheng, H. J., A. Z. Wu, C. C. Zheng, Y. F. Wang, R. Cai, X. F. Shen, R. R. Xu, P. Liu, L. J. Kong, and S. T. Dong. "QTL mapping of maize (Zea mays) stay-green traits and their relationship to yield." *Plant breeding* 128, no. 1 (2009): 54-62.

Zhu, Jian-Kang, Jiping Liu, and Liming Xiong. "Genetic analysis of salt tolerance in Arabidopsis: evidence for a critical role of potassium nutrition."*The Plant Cell Online* 10, no. 7 (1998): 1181-1191.

Zhu, Jian-Kang. "Cell signaling under salt, water and cold stresses."*Current opinion in plant biology* 4, no. 5 (2001): 401-406.

Zhu, Jian-Kang. "Plant salt tolerance." *Trends in plant science* 6, no. 2 (2001): 66-71.

Zhu, Jian-Kang. "Salt and drought stress signal transduction in plants."*Annual review of plant biology* 53, no. 1 (2002): 247-273.

Zhuo, Degen, Mamoru Okamoto, J. John Vidmar, and Anthony DM Glass. "Regulation of a putative high-affinity nitrate transporter (Nrt2; 1At) in roots ofArabidopsis thaliana." *The Plant Journal* 17, no. 5 (1999): 563-568.

Zhou, Huapeng, Jinfeng Zhao, Yongqing Yang, Changxi Chen, Yanfen Liu, Xuehua Jin, Limei Chen et al. "Ubiquitin-specific protease16 modulates salt tolerance in Arabidopsis by regulating Na+/H+ antiport activity and serine hydroxymethyltransferase stability." *The Plant Cell Online* 24, no. 12 (2012): 5106-5122.

APPENDICES

Appendix A Phenotypic Distributions of Stay-green and Sink Inhibited Senescence Traits

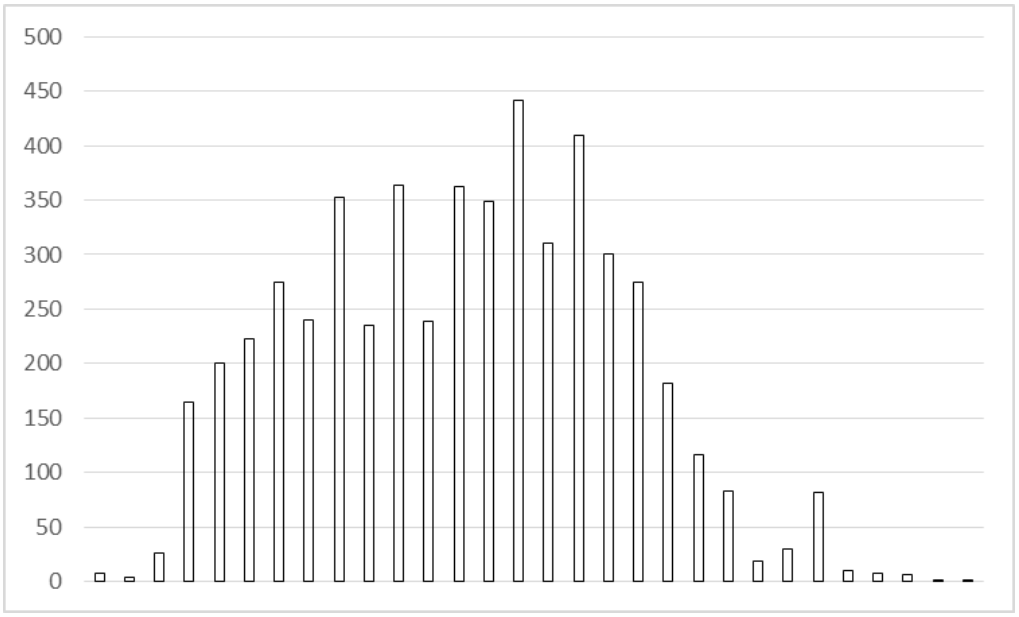

Figure A-1 Phenotypic distribution of days to anthesis of the NAM RILs from a combined year analysis

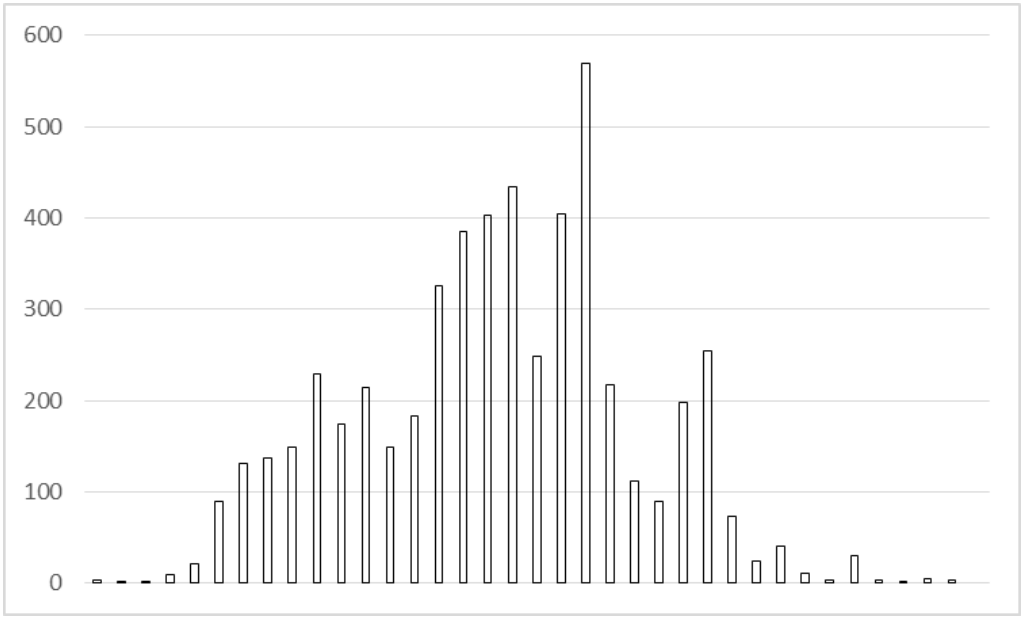

Figure A-2 Phenotypic distribution of days to silking of the NAM RILs from a combined year analysis

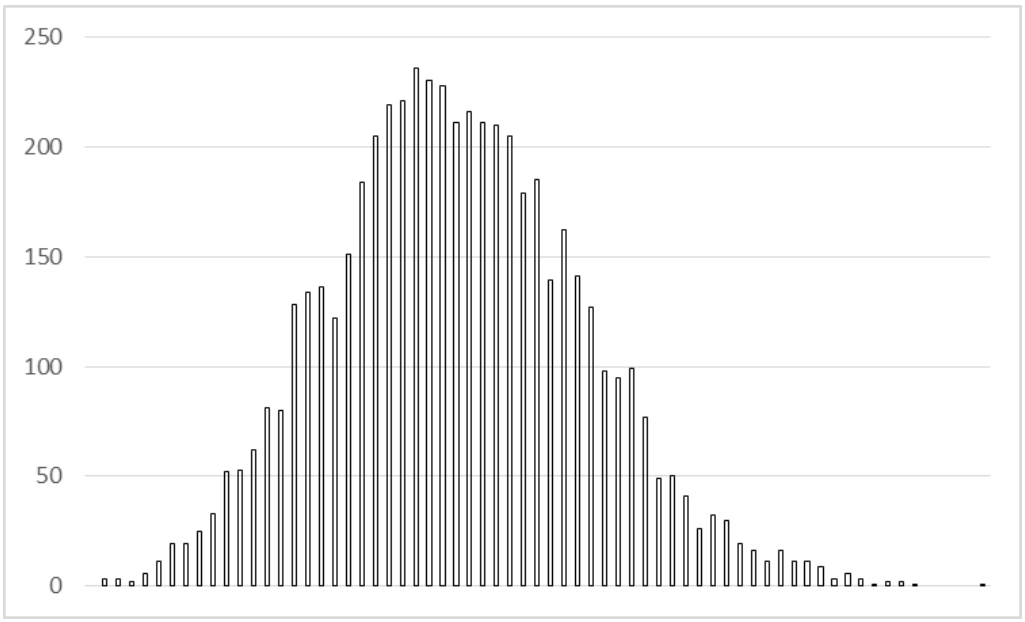

Figure A-3 Phenotypic distribution of stay-green anthesis of the NAM RILs from a combined year analysis

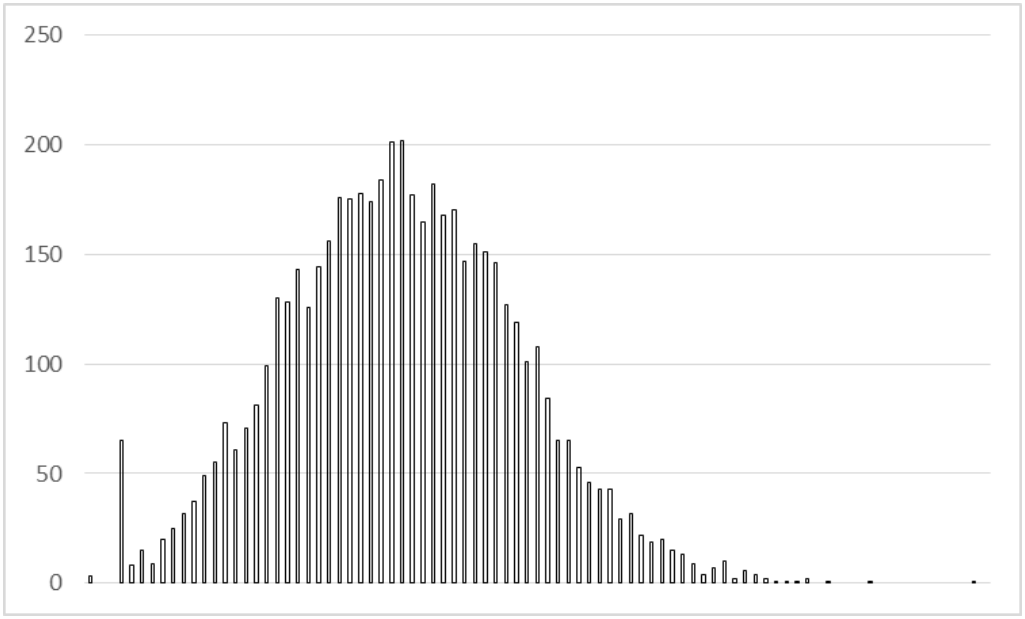

Figure A-4 Phenotypic distribution of stay-green terminal of the NAM RILs from a combined year analysis

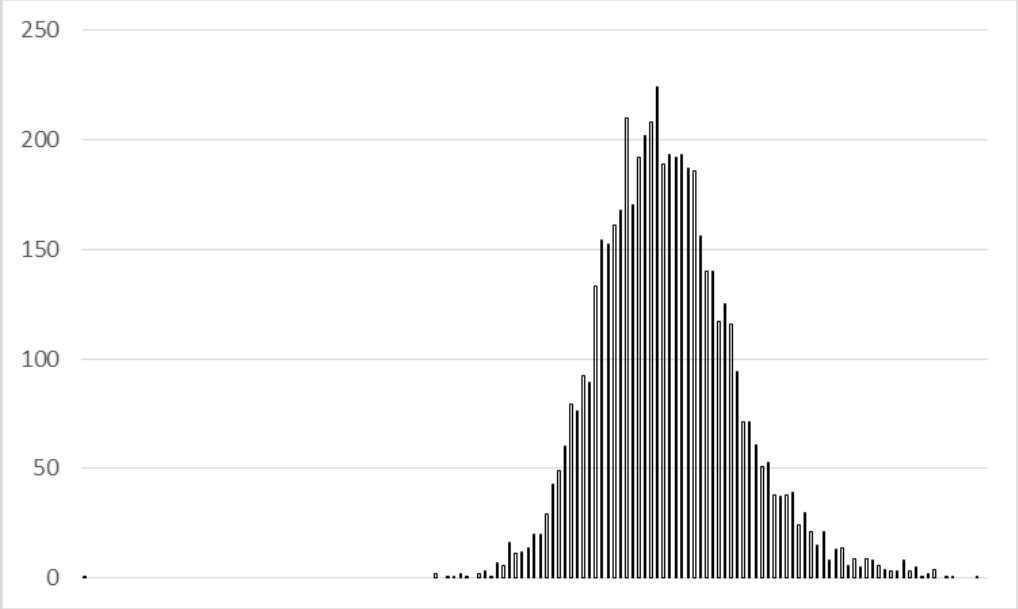

Figure A-5 Phenotypic distribution of stay-green difference of the NAM RILs from a combined year analysis

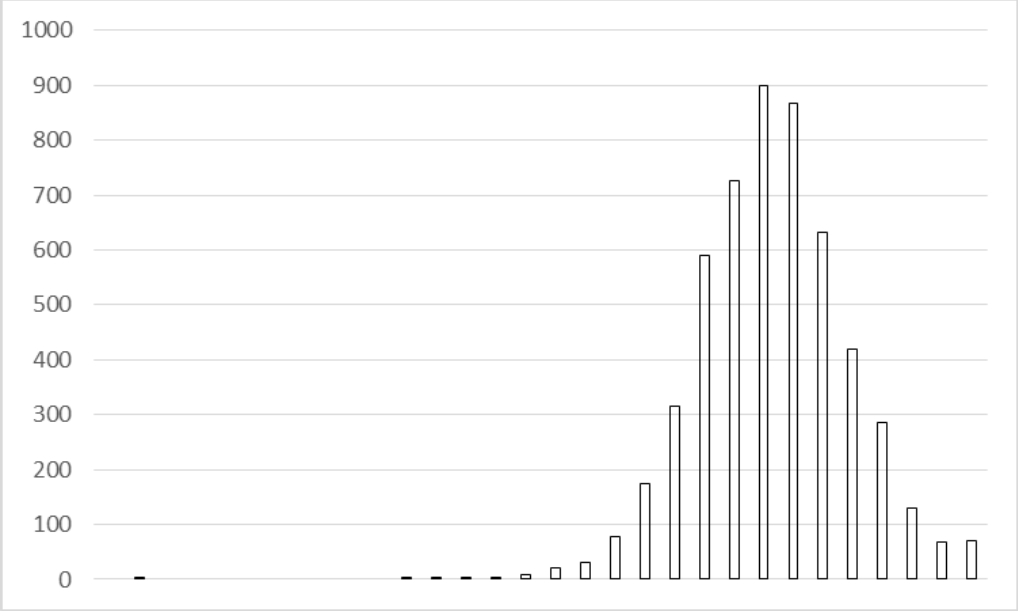

Figure A-6 Phenotypic distribution of stay-green ratio of the NAM RILs from a combined year analysis

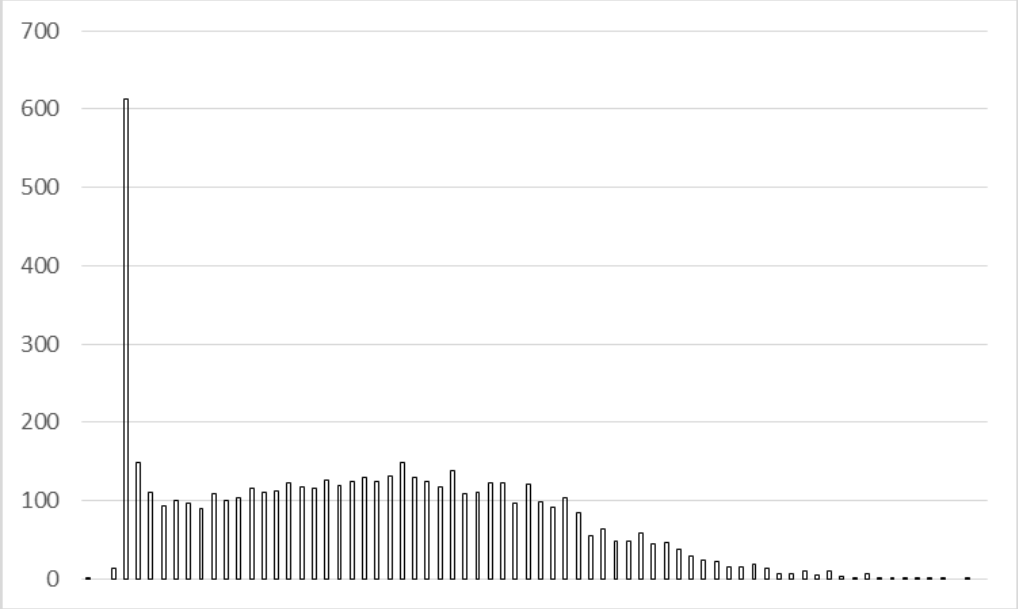

Figure A-7 Phenotypic distribution of sink-inhibited shootcapped only of the NAM RILs from a combined year analysis

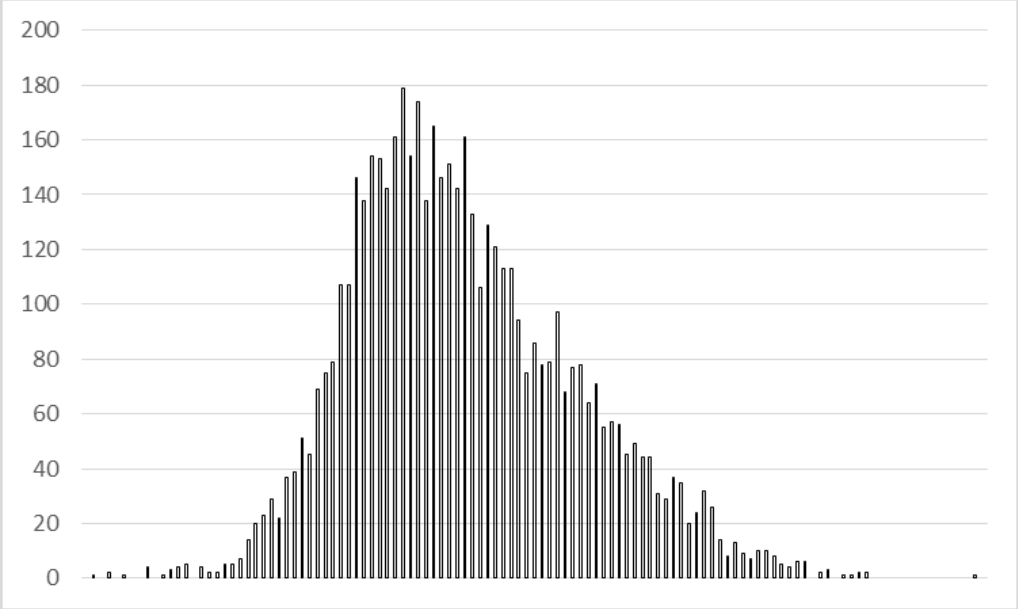

Figure A-8 Phenotypic distribution of sink-inhibited difference of the NAM RILs from a combined year analysis

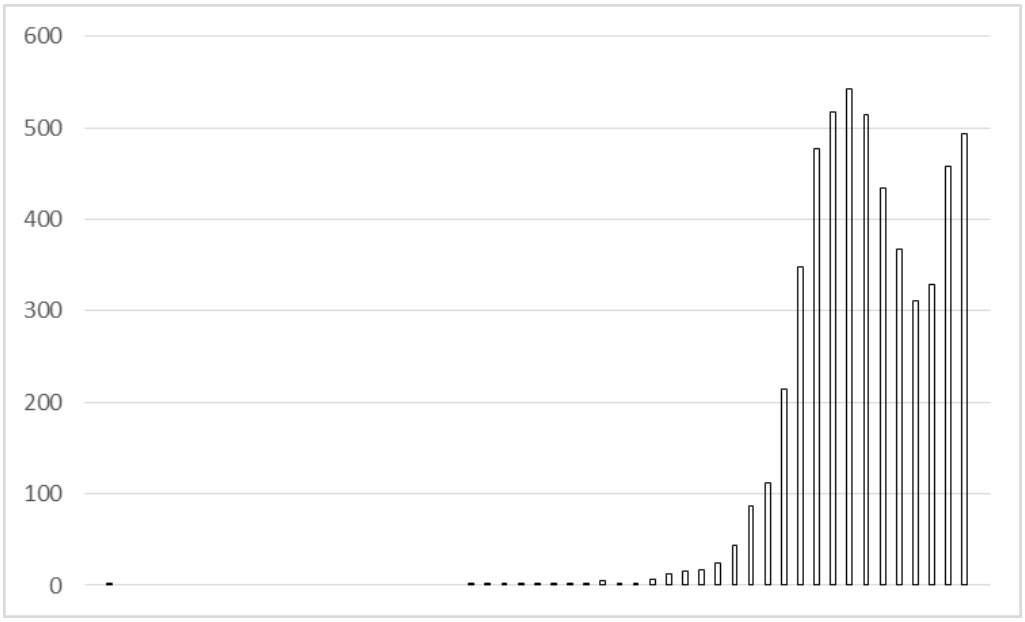

Figure A-9 Phenotypic distribution of sink-inhibited ratio of the NAM RILs from a combined year analysis

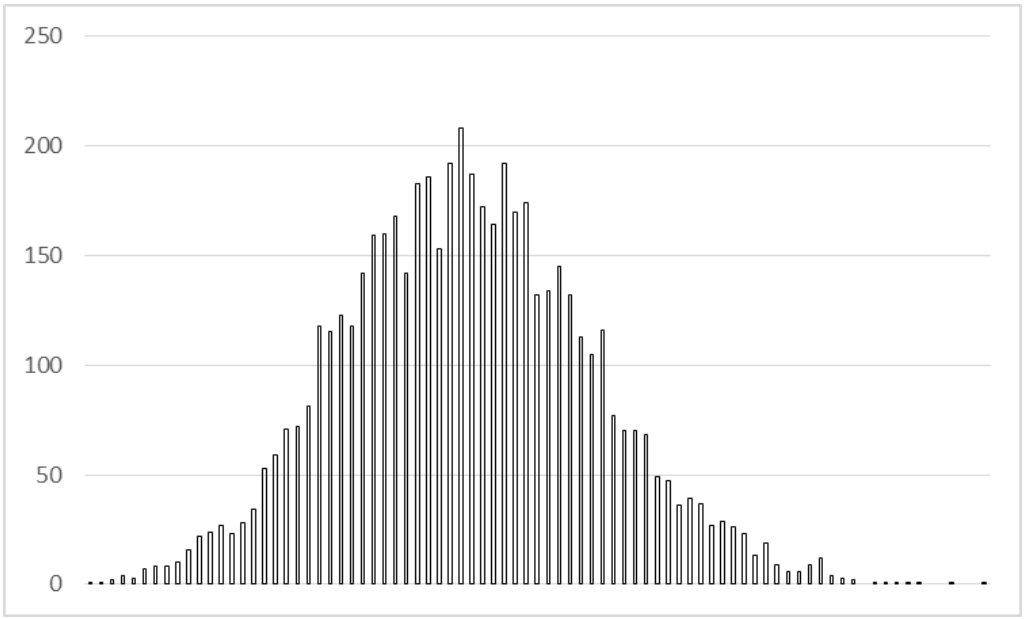

Figure A-10 Phenotypic distribution of sink-inhibited non-shootcapped only of the NAM RILs from a combined year analysis

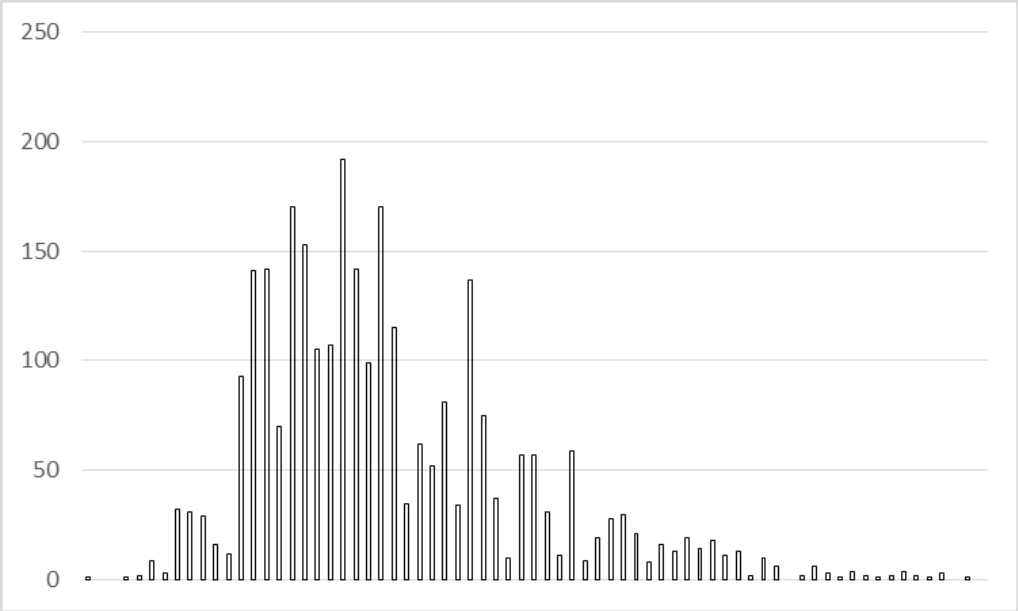

Figure A-11 Phenotypic distribution of days to anthesis of the AMES Diversity Panel from a combined year analysis

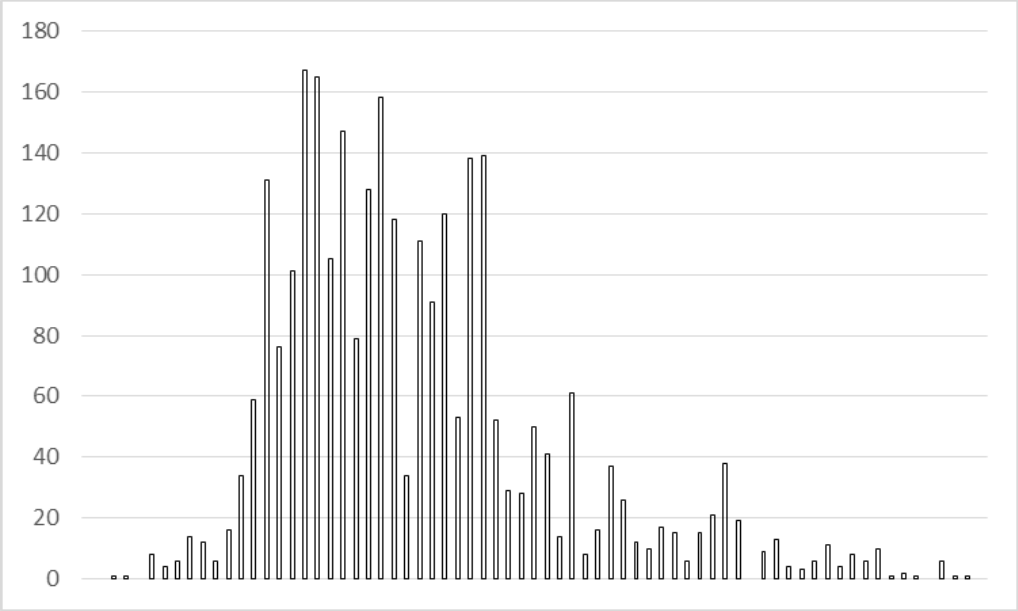

Figure A-12 Phenotypic distribution of days to silking of the AMES Diversity Panel from a combined year analysis

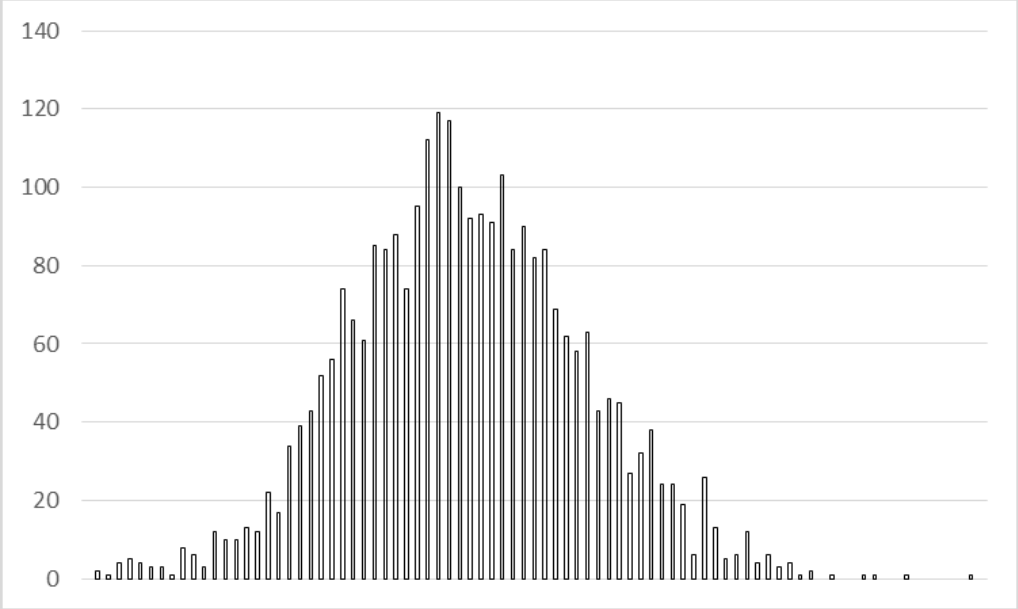

Figure A-13 Phenotypic distribution of stay-green anthesis of the AMES Diversity Panel from a combined year analysis

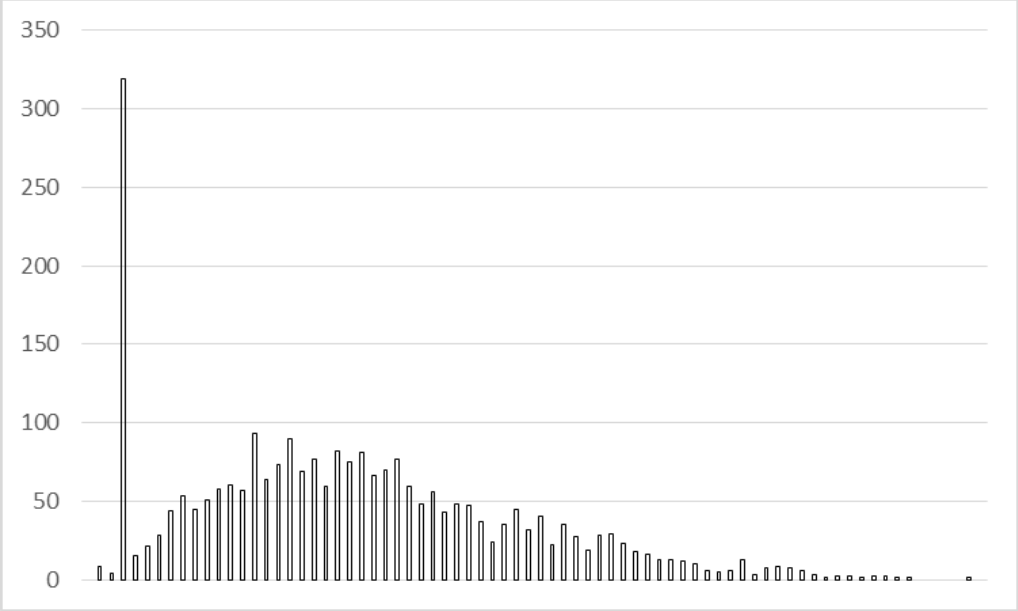

Figure A-14 Phenotypic distribution of stay-green terminal of the AMES Diversity Panel from a combined year analysis

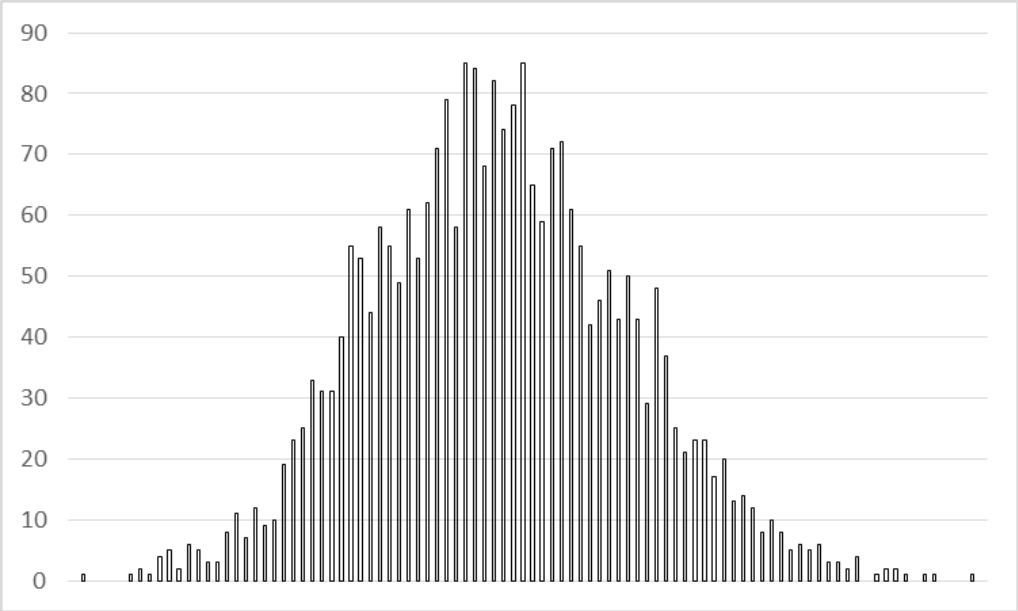

Figure A-15 Phenotypic distribution of stay-green difference of the AMES Diversity Panel from a combined year analysis

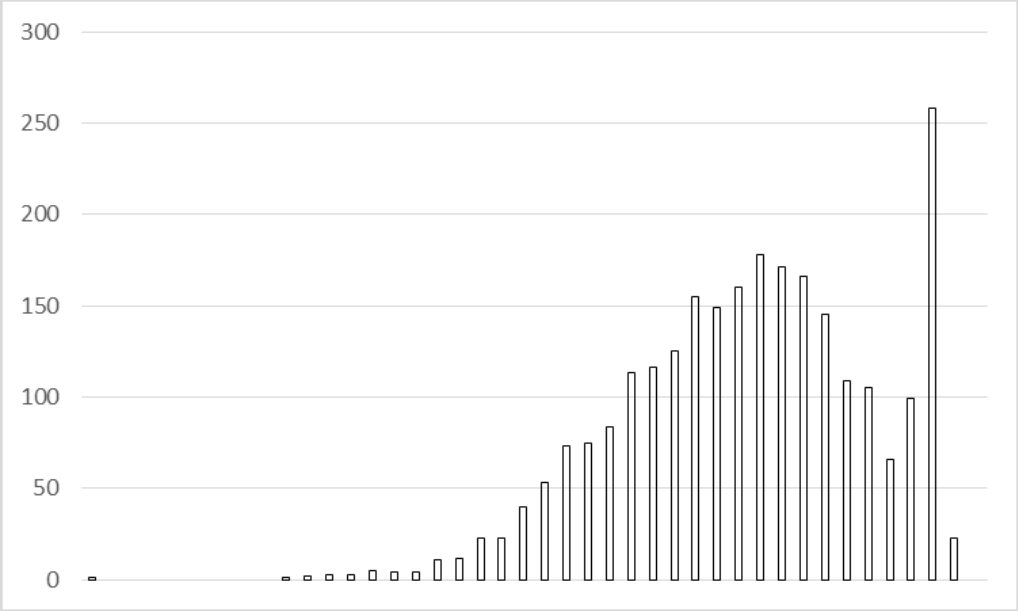

Figure A-16 Phenotypic distribution of stay-green ratio of the AMES Diversity Panel from a combined year analysis

Appendix B SAS Code for Chapter 4

Code Used (Supplementary Materials)

Sink Removal vs. Sink Inhibition

```
Data Sink Removal vs. Sink Inhibition;
Input Rep Treatment$ B73 Mo17;
Datalines;
1	Open	19.5	27.4
1	Open	41	38.6
1	Open	33.6	21.8
2	Open	48.3	25.5
2	Open	50	33.2
2	Open	45.1	25.1
3	Open	38.9	29.5
3	Open	40.6	25.4
3	Open	49.9	42.6
4	Open	41.7	31.5
4	Open	35.7	31.4
4	Open	53.1	31.3
5	Open	40.3	38.3
5	Open	43.6	31.5
5	Open	34.9	53.2
1	Removed	2.3	15
1	Removed	3.1	.
1	Removed	.	14.6
2	Removed	2.4	11.7
2	Removed	3.6	15.7
2	Removed	2.5	9.8
3	Removed	3	19.8
3	Removed	3.2	21.2
3	Removed	2.5	10.3
4	Removed	4.2	23.3
4	Removed	8.7	34.9
4	Removed	.	27.3
5	Removed	3.5	19.9
5	Removed	3.8	19.6
5	Removed	2.8	23
1	Shootcap	2.6	14.2
1	Shootcap	15.5	25.1
1	Shootcap	2.7	11.8
2	Shootcap	18.7	16.9
2	Shootcap	16.2	13.1
```

```
2       Shootcap    .       15.3
3       Shootcap    5.4     16
3       Shootcap    3.6     9.5
3       Shootcap    2.5     14
4       Shootcap    16.6    13.6
4       Shootcap    6.2     21.6
4       Shootcap    .       13.2
5       Shootcap    3.1     11.5
5       Shootcap    2.1     14.2
5       Shootcap    3.6     13.8
;
Run;

PROC ANOVA DATA= Sink Removal vs. Sink Inhibition;
        CLASS Treatment;
        MODEL B73 = Treatment;
        MEANS Treatment/LSD;
RUN;

PROC ANOVA DATA= Sink Removal vs. Sink Inhibition;
        CLASS Treatment;
        MODEL Mo17 = Treatment;
        MEANS Treatment/LSD;
RUN;
```

Appendix C ASReml, R, and SAS Code for Chapter 2

```
AMES Model Selection for Stay-green Traits in ASReml
!WORKSPACE 16000 !NODISPLAY
!CYCLE 1!JOIN

AMES_ALL_DATA_ASREML

#env,loc,year,row,range,maturity,genocode,dta,wt_dta,dts,wt_dts,sg_ant,wt_sg_ant,sg_p
ost,wt_sg_post,sg_diff,wt_sg_diff,sg_ratio,wt_sg_ratio,ef

 env *
 #loc  !A
 year  !I !SKIP 1
 row  *
 range  *
 maturity *
 genocode  !A 2500  !LL 39  !PRUNE
 dta
 wt_dta
 dts
 wt_dts
 sg_ant
 wt_sg_ant
 sg_post
 wt_sg_post
 sg_diff
 wt_sg_diff
 sg_ratio
 wt_sg_ratio
 ef *

"C:\Users\arenaud\Desktop\ASReml\5-12-
2014\AMES\BLUPs\BLUPs\ames_All_data_asreml_NoOut4.csv",
!skip 1 !DOPATH $I !FCON !DENSE !CONTINUE !MAXITER 100

#####################################################################
!PATH 1 # env: comb field: all Model dropped 2 Geno as fixed Reduced poly
dta !WT wt_dta ~ mu,
at(ef,1).pol(range,-3),
at(ef,1).pol(row,-4),
!r,
genocode,
at(ef,2).range,
```

```
at(ef,2).maturity
#ef,
#ef.genocode
predict  genocode !IGNORE at(ef,1).pol(range,-3) at(ef,1).pol(row,-4)

!PATH 1 # env: comb field: all  Model Dropped 2 Geno as fixed
dts !WT wt_dts ~ mu,
at(ef,1).pol(range,-2),
!r,
genocode,
at(ef,2).range,
at(ef,2).maturity
#ef
#ef.genocode
predict  genocode !IGNORE at(ef,1).pol(range,-2)

!PATH 1 # env: comb field: all  Model Dropped 2 Geno as fixed
sg_ant !WT wt_sg_ant ~ mu,
at(ef,1).pol(range,-2),
at(ef,1).pol(row,-2),
!r,
genocode,
#at(ef,2).range,
at(ef,2).maturity,
#ef
ef.genocode
predict  genocode !IGNORE at(ef,1).pol(range,-2) at(ef,1).pol(row,-2)

!PATH 1 # env: comb field: all  Model Dropped 2 Geno as fixed
sg_diff !WT wt_sg_diff ~ mu,
at(ef,1).pol(row,-2),
!r,
genocode,
at(ef,2).maturity,
#ef
ef.genocode
predict  genocode !IGNORE at(ef,1).pol(row,-2)

!PATH 1 # env: comb field: all  Model Dropped 2 Geno as fixed
sg_post !WT wt_sg_post ~ mu,
!r,
genocode,
#at(ef,2).range,
at(ef,2).maturity,
ef,
```

```
ef.genocode
predict  genocode

!PATH 1 # env: comb field: all  Model Dropped 2 Geno as fixed
sg_ratio !WT wt_sg_ratio ~ mu,
at(ef,1).pol(row,-3),
!r,
genocode,
#at(ef,2).range,
at(ef,2).maturity,
#ef,
ef.genocode
predict  genocode !IGNORE at(ef,1).pol(row,-3)
```

NAM RILs Model Selection for Stay-green and Shootcap Induced Senescence Traits in ASReml

```
!WORKSPACE 16000 !NODISPLAY
!CYCLE 1 2 3 4 5 6 7 8 9 10 !JOIN

PHENOTYPES_STAYGREEN_NAM_ALL_ASREMLREVISED

#env,field,pblock,pop,entrynum,entity_id,sample_id,range,row,dta,wt_dta,dts,wt_dts,sg_
ant,wt_ant,sg_post,
#wt_post,sg_diff,wt_sg_diff,sg_ratio,wt_sg_ratio,sis_nsc,wt_sis_nsc,sis_sc,wt_sis_sc,sis
_diff,wt_sis_diff,sis_ratio,wt_sis_ratio,ff,ef

env *
field *
pblock *
pop *
entrynum !A 2500  !LL 39  !PRUNE
entity_id !A 2500  !LL 39  !PRUNE
sample_id !A 2500  !LL 39  !PRUNE
range *
row *
dta
wt_dta
dts
wt_dts
sg_ant
wt_ant
sg_post
wt_post
sg_diff
```

```
wt_sg_diff
sg_ratio
wt_sg_ratio
sis_nsc
wt_sis_nsc
sis_sc
wt_sis_sc
sis_diff
wt_sis_diff
sis_ratio
wt_sis_ratio
ff *
ef *

"C:\Users\arenaud\Desktop\ASReml\5-12-
2014\NAM\phenotypes_staygreen_nam_all_asremlRevised.csv",
!skip 1 !DOPATH $I !FCON !CONTINUE !MAXITER 100 !DDF 1

!PATH 1 # env: combined field: All  Full model: Best model for each field
dta !WT wt_dta ~ mu,
at(ef,1).at(ff,1).pol(row,-1),
#at(ef,1).at(ff,1).pol(range,-1), #NS
at(ef,2).at(ff,3).pol(row,-2),
pop,
at(pop,1,2,3,4,5,6,7,8,9,11,12,13,14,15,16,17,18,19,20,21,22,23,24,25,26,27).entrynum,
!r,
at(ef,1).at(ff,2).pblock,
#at(ef,1).ff,
at(ef,2).ff,
#ef,
ef.pop
#ef.pop.entrynum
predict  pop entrynum !IGNORE at(ef,1).at(ff,1).pol(row,-1) at(ef,1).at(ff,1).pol(range,-1)
at(ef,2).at(ff,3).pol(row,-2)


!PATH 1 # env: combined field: All  Full model: Best model for each field
dts !WT wt_dts ~ mu,
#at(ff,1).pol(range,-1),
at(ff,2).pol(range,-4),
#at(ff,4).pol(row,-2),
pop,
at(pop,1,2,3,4,5,6,7,8,9,11,12,13,14,15,16,17,18,19,20,21,22,23,24,25,26,27).entrynum,
!r,
at(ef,1).ff,
```

```
#at(ef,2).ff,
#ef,
ef.pop,
#ef.pop.entrynum
predict  pop entrynum !IGNORE at(ff,1).pol(range,-1) #at(ff,2).pol(range,-4)
at(ff,4).pol(row,-2)


!PATH 1 # env: combined field: All  Full model: Best model for each field
sg_ant !WT wt_ant ~ mu,
at(ff,1).pol(range,-1),
at(ff,1).pol(row,-3),
at(ff,2).pol(range,-2),
at(ff,4).pol(range,-4),
#at(ff,4).pol(row,-3),
pop,
at(pop,1,2,3,4,5,6,7,8,9,11,12,13,14,15,16,17,18,19,20,21,22,23,24,25,26,27).entrynum,
!r,
at(ef,1).ff,
at(ef,2).ff,
#ef,
ef.pop,
#ef.pop.entrynum
predict  pop entrynum !IGNORE at(ff,1).pol(range,-1) at(ff,1).pol(row,-3)
at(ff,2).pol(range,-2) at(ff,4).pol(range,-4)

!PATH 1 # env: combined field: All  Full model: Best model for each field
sg_post !WT wt_post ~ mu,
at(ff,1).pol(range,-1),
pop,
at(pop,1,2,3,4,5,6,7,8,9,11,12,13,14,15,16,17,18,19,20,21,22,23,24,25,26,27).entrynum,
!r,
at(ff,2).pblock,
at(ff,4).pblock,
#at(ef,1).ff,
#at(ef,2).ff,
#ef,
ef.pop,
ef.pop.entrynum
predict  pop entrynum !IGNORE at(ff,1).pol(range,-1)


!PATH 1 # env: combined field: All  Full model: Best model for each field
sg_diff !WT wt_sg_diff ~ mu,
at(ff,3).pol(range,-4),
```

```
pop,
at(pop,1,2,3,4,5,6,7,8,9,11,12,13,14,15,16,17,18,19,20,21,22,23,24,25,26,27).entrynum,
!r,
at(ff,2).pblock,
at(ff,4).pblock,
#at(ef,1).ff,
#at(ef,2).ff,
#ef,
ef.pop,
ef.pop.entrynum
predict  pop entrynum !IGNORE at(ff,3).pol(range,-4)


!PATH 1 # env: combined field: All  Full model: Best model for each field
sg_ratio !WT wt_sg_ratio ~ mu,
at(ff,2).pol(range,-4),
pop,
at(pop,1,2,3,4,5,6,7,8,9,11,12,13,14,15,16,17,18,19,20,21,22,23,24,25,26,27).entrynum,
!r,
at(ff,3).pblock,
at(ff,4).pblock,
at(ef,1).ff,
#at(ef,2).ff,
#ef,
ef.pop,
ef.pop.entrynum
predict  pop entrynum !IGNORE at(ff,2).pol(range,-4)


!PATH 1 # env: combined field: All  Full model: Best model for each field
sis_diff !WT wt_sis_diff ~ mu,
#at(ff,1).pol(range,-1),
#at(ff,2).pol(row,-1),
at(ff,3).pol(range,-4),
#at(ff,3).pol(row,-4),
pop,
at(pop,1,2,3,4,5,6,7,8,9,11,12,13,14,15,16,17,18,19,20,21,22,23,24,25,26,27).entrynum,
!r,
#at(ef,1).ff,
#at(ef,2).ff,
ef,
ef.pop,
ef.pop.entrynum
predict  pop entrynum !IGNORE at(ff,3).pol(range,-4)
```

```
!PATH 1 # env: combined field: All  Full model: Best model for each field
sis_ratio !WT wt_sis_ratio ~ mu,
at(ff,2).pol(row,-1),
at(ff,3).pol(range,-4),
pop,
at(pop,1,2,3,4,5,6,7,8,9,11,12,13,14,15,16,17,18,19,20,21,22,23,24,25,26,27).entrynum,
!r,
at(ff,4).pblock,
#at(ef,1).ff,
#at(ef,2).ff,
ef,
ef.pop,
ef.pop.entrynum
predict  pop entrynum !IGNORE at(ff,2).pol(row,-1) at(ff,3).pol(range,-4)



!PATH 1 # env: combined field: All  Full model: Best model for each field
sis_sc !WT wt_sis_sc ~ mu,
at(ff,1).pol(row,-4),
at(ff,3).pol(range,-4),
at(ff,4).pol(range,-3),
pop,
at(pop,1,2,3,4,5,6,7,8,9,11,12,13,14,15,16,17,18,19,20,21,22,23,24,25,26,27).entrynum,
!r,
#at(ef,1).ff,
#at(ef,2).ff,
#ef,
ef.pop,
ef.pop.entrynum
predict  pop entrynum !IGNORE at(ff,1).pol(row,-4) at(ff,3).pol(range,-4)
at(ff,4).pol(range,-3)

!PATH 1 # env: combined field: All  Full model: Best model for each field
sis_nsc !WT wt_sis-nsc ~ mu,
at(ff,1).pol(range,-1),
at(ff,2).pol(row,-1),
at(ff,3).pol(range,-4),
at(ff,3).pol(row,-4),
pop,
at(pop,1,2,3,4,5,6,7,8,9,11,12,13,14,15,16,17,18,19,20,21,22,23,24,25,26,27).entrynum,
!r,
at(ef,1).ff,
at(ef,2).ff,
```

#ef,
ef.pop,
ef.pop.entrynum
predict pop entrynum !IGNORE at(ff,1).pol(range,-1) at(ff,2).pol(row,-1)
at(ff,3).pol(range,-4) at(ff,3).pol(row,-4)

AMES Heritabilities in ASReml

DTA
!PIN   !DEFINE   #use this pin definition to get heritability estimate
#F VarG 3 #cross is 3rd variance component in ouput = genotypic variance, but it is not necessary to define this, so flag it out
F Var_plots 3 + 4 #comp 5 Variance for plot heritability = GxE + MeanError
H H_plot 3 5 #herit plot basis
H_plot   = genocode   3/Var_plot   5=   0.4445   0.0310
Cullis heritability for entry mean basis
#h2 = 1 - ((SED)^2)/2 * geno variance)
#h2 = 1 - ((2.860)^2)/(2*8.07288) = 0.51

DTS
!PIN   !DEFINE   #use this pin definition to get heritability estimate
#F VarG 3 #cross is 3rd variance component in ouput = genotypic variance, but it is not necessary to define this, so flag it out
F Var_plots 3 + 4 #comp 5 Variance for plot heritability = GxE + MeanError
H H_plot 3 5 #herit plot basis
H_plot   = genocode   3/Var_plot   5=   0.5187   0.0277
Cullis heritability for entry mean basis
#h2 = 1 - ((SED)^2)/2 * cross variance)
#h2 = 1 - ((3.292)^)/(2*12.3510) = 0.622071087

SG_ANT
!PIN   !DEFINE   #use this pin definition to get heritability estimate
#F VarG 3 #cross is 3rd variance component in ouput = genotypic variance, but it is not necessary to define this, so flag it out
F Var_plots 2+ 3 + 4 #comp 5 Variance for plot heritability = GxE + MeanError
H H_plot 2 5 #herit plot basis
H_plot   = genocode   2/Var_plot   5=   0.3071   0.0212
Cullis heritability for entry mean basis
#h2 = 1 - ((SED)^2)/2 * cross variance)
#h2 = 1 - ((6.733)^)/(2*59.7953) = 0.379070671

SG_POST
!PIN   !DEFINE   #use this pin definition to get heritability estimate
#F VarG 3 #cross is 3rd variance component in ouput = genotypic variance, but it is not necessary to define this, so flag it out

F Var_plots 3 + 4+ 5 #comp 6 Variance for plot heritability = GxE + MeanError
H H_plot 3 6 #herit plot basis
H_plot = genocode 3/Var_plot 6= 0.2485 0.0221
Cullis heritability for entry mean basis
#h2 = 1 - ((SED)^2)/2 * cross variance)
#h2 = 1 - ((8.768)^2)/(2*65.7975) = 0.58420019

SG_DIFF
!PIN !DEFINE #use this pin definition to get heritability estimate
#F VarG 3 #cross is 3rd variance component in ouput = genotypic variance, but it is not necessary to define this, so flag it out
F Var_plots 2 + 3+ 4 #comp 5 Variance for plot heritability = GxE + MeanError
H H_plot 2 5 #herit plot basis
H_plot = genocode 2/Var_plot 5= 0.1245 0.0202
Cullis heritability for entry mean basis
#h2 = 1 - ((SED)^2)/2 * cross variance)
#h2 = 1 - ((8.955)^2)/(2*40.8671) = 1 - 0.981131827 = #

SG_RATIO
!PIN !DEFINE #use this pin definition to get heritability estimate
#F VarG 3 #cross is 3rd variance component in ouput = genotypic variance, but it is not necessary to define this, so flag it out
F Var_plots 2 + 3+ 4 #comp 5 Variance for plot heritability = GxE + MeanError
H H_plot 2 5 #herit plot basis
H_plot = genocode 2/Var_plot 5= 0.1566 0.0201
Cullis heritability for entry mean basis
#h2 = 1 - ((SED)^2)/2 * cross variance)
#h2 = 1 - ((0.1901)^2)/(2*0.230604E-01) = 0.783551239

1 - ((0.1901)^2)/(2*0.230604E-01)

NAM RILs Heritabilities in ASReml

DTA
    - - - Results from analysis of dta - - -

1	at(ef	0.370112
2	at(ef	0.195165
3	pop	14.8174
4	ef.pop	0.363495
5	at(pop	0.762422
6	at(pop	7.08162
7	at(pop	10.8202
8	at(pop	10.6007
9	at(pop	14.9865

10 at(pop	10.9540	
11 at(pop	4.24763	
12 at(pop	7.70201	
13 at(pop	6.97875	
14 at(pop	3.28914	
15 at(pop	15.4152	
16 at(pop	10.9985	
17 at(pop	5.86736	
18 at(pop	4.93572	
19 at(pop	4.75566	
20 at(pop	3.44366	
21 at(pop	7.84263	
22 at(pop	2.11486	
23 at(pop	3.37266	
24 at(pop	4.50942	
25 at(pop	1.50172	
26 at(pop	8.06016	
27 at(pop	3.00378	
28 at(pop	4.36391	
29 at(pop	7.46146	
30 at(pop	4.41333	
31 Variance	3.49208	
32 VarG 3	21.427	4.3491
33 Var_plots 4	25.283	4.3492

H_plot = VarG 3 32/Var_plot 33= 0.8475 0.0267

Notice: The parameter estimates are followed by
their approximate standard errors.

H2 means basis: 21.427(VARG) / ((VARG) + 4/(2 - Harmonic Mean) + ef.pop.entrynum / 2 + (Variance) / 3.41)

21.427 / (21.427 + (0.363495/2) + (3.49/3.41)) = 0.9467 = H2 Means-Basis

DTS

- - - Results from analysis of dts - - -

1 at(ef	0.387305E-01
2 pop	17.7505
3 ef.pop	0.372610
4 at(pop	3.12348
5 at(pop	7.13447
6 at(pop	13.4221
7 at(pop	13.5777
8 at(pop	19.7904

```
 9 at(pop                13.8885
10 at(pop                5.01558
11 at(pop                11.4705
12 at(pop                7.30621
13 at(pop                7.99410
14 at(pop                17.8549
15 at(pop                11.9496
16 at(pop                6.06385
17 at(pop                6.54009
18 at(pop                6.64475
19 at(pop                10.5250
20 at(pop                13.0027
21 at(pop                5.21989
22 at(pop                5.36417
23 at(pop                6.37971
24 at(pop                4.60017
25 at(pop                5.73091
26 at(pop                7.87015
27 at(pop                9.08951
28 at(pop                10.2497
29 at(pop                13.3129
30 Variance              5.77751
31 VarG  2               27.232       5.3431
32 Var_plots  3          33.382       5.3438
   H_plot      = VarG  2   31/Var_plot  32=         0.8158    0.0299
Notice: The parameter estimates are followed by
        their approximate standard errors.
```

H2 means basis: 21.427(VARG) / ((VARG) + ef.pop/(2 : Harmonic Mean) + ef.pop.entrynum / 2 + (Variance) / 3.41)

27.232 / (27.232 + (0.372610/2) + (5.77751/3.417852679)) = 0.9355 = H2 Means-Basis

SG_ANT

- - - Results from analysis of sg_ant - - -

```
 1 at(ef                 0.330879
 2 at(ef                 0.101993E-04
 3 pop                   7.71009
 4 ef.pop                1.28646
 5 at(pop                29.4371
 6 at(pop                32.7713
 7 at(pop                39.4140
 8 at(pop                56.1651
```

9 at(pop	48.8294		
10 at(pop	51.1942		
11 at(pop	19.2640		
12 at(pop	58.7892		
13 at(pop	32.6721		
14 at(pop	52.6952		
15 at(pop	50.4898		
16 at(pop	45.0764		
17 at(pop	46.1588		
18 at(pop	18.0182		
19 at(pop	40.7022		
20 at(pop	47.9548		
21 at(pop	36.8566		
22 at(pop	32.2941		
23 at(pop	42.9649		
24 at(pop	68.9274		
25 at(pop	25.2676		
26 at(pop	55.4592		
27 at(pop	60.1942		
28 at(pop	47.0168		
29 at(pop	36.9645		
30 at(pop	26.5625		
31 Variance	141.021		
32 VarG 3	50.694	3.8489	
33 Var_plots 4	193.00	4.8595	
H_plot = VarG 3 32/Var_plot 33=		0.2627	0.0156

Notice: The parameter estimates are followed by
their approximate standard errors.

H2 means basis: (VARG) / ((VARG) + ef.pop/(2 : Harmonic Mean) + ef.pop.entrynum / 2 + (Variance) / 3.41)

50.694 / (50.694 + (1.28646/2) + (141.021/3.41922529)) = 0.5475 = H2 Means-Basis

SG_POST

- - - Results from analysis of sg_post - - -

1 at(ff	6.43431
2 at(ff	4.45785
3 pop	19.6069
4 ef.pop	4.86542
5 at(pop	40.7440
6 at(pop	57.4560
7 at(pop	28.9908

```
 8 at(pop              26.1664
 9 at(pop              25.8691
10 at(pop               51.9473
11 at(pop               16.7110
12 at(pop               54.1896
13 at(pop               22.7563
14 at(pop               17.4759
15 at(pop               39.9220
16 at(pop               60.6391
17 at(pop               24.7379
18 at(pop               15.3094
19 at(pop               12.6775
20 at(pop               80.5262
21 at(pop               51.6316
22 at(pop               47.2818
23 at(pop               42.6184
24 at(pop               55.2886
25 at(pop               33.9329
26 at(pop               64.4007
27 at(pop               15.5874
28 at(pop               22.0223
29 at(pop               31.7189
30 at(pop               131.216
31 ef.pop.entrynum        10.9654
32 Variance             196.674
33 VarG  3              61.408       11.217
34 Var_plots  4           273.91       12.156
   H_plot      = VarG  3   33/Var_plot  34=         0.2242    0.0322
Notice: The parameter estimates are followed by
        their approximate standard errors.
```

H2 means basis: (VARG) / ((VARG) + ef.pop/(2 : Harmonic Mean) + ef.pop.entrynum / 2 + (Variance) / 3.41)

61.408 / (61.408 + (4.86542/2) + (10.9654/2) +(196.674/3.402825389)) = 0.4831 = H2 Means-Basis

SG_DIFF

```
        - - - Results from analysis of sg_diff - - -

 1 at(ff               6.86053
 2 at(ff               9.75483
 3 pop                 9.71651
 4 ef.pop              7.13821
```

```
 5 at(pop              9.40730
 6 at(pop              48.5024
 7 at(pop              18.2939
 8 at(pop              5.64451
 9 at(pop              9.79591
10 at(pop               37.8839
11 at(pop              0.259957E-04
12 at(pop               33.2103
13 at(pop               5.33218
14 at(pop               38.4654
15 at(pop               44.6256
16 at(pop               13.1137
17 at(pop               23.1803
18 at(pop               5.29553
19 at(pop               10.8519
20 at(pop               30.5204
21 at(pop               39.5626
22 at(pop               22.8803
23 at(pop               8.25027
24 at(pop               35.7629
25 at(pop               2.96354
26 at(pop               36.0687
27 at(pop               59.4130
28 at(pop               32.9306
29 at(pop               22.3467
30 at(pop               24.5984
31 ef.pop.entrynum         12.1026
32 Variance              272.065
33 VarG  3               33.854       5.3617
34 Var_plots  4            325.16       8.4421
   H_plot      = VarG  3   33/Var_plot  34=         0.1041    0.0152
Notice: The parameter estimates are followed by
        their approximate standard errors.
```

H2 means basis: (VARG) / ((VARG) + ef.pop/(2 : Harmonic Mean) + ef.pop.entrynum / 2 + (Variance) / 3.41)

33.854 / (33.854 + (7.13821/2) + (12.1026 /2) +(272.065/3.402825389)) = 0.2742 = H2 Means-Basis

SG_RATIO

```
        - - - Results from analysis of sg_ratio - - -

 1 at(ef                0.702546E-03
```

```
 2 at(ff              0.210510E-02
 3 at(ff              0.330717E-02
 4 pop                0.744746E-02
 5 ef.pop             0.282314E-02
 6 at(pop             0.647817E-02
 7 at(pop             0.256199E-01
 8 at(pop             0.599753E-02
 9 at(pop             0.593903E-08
10 at(pop             0.588270E-02
11 at(pop             0.941110E-02
12 at(pop             0.167714E-02
13 at(pop             0.143326E-01
14 at(pop             0.461231E-02
15 at(pop             0.246816E-01
16 at(pop             0.109706E-01
17 at(pop             0.170138E-01
18 at(pop             0.129024E-01
19 at(pop             0.599984E-02
20 at(pop             0.835072E-03
21 at(pop             0.151361E-01
22 at(pop             0.191980E-01
23 at(pop             0.139162E-01
24 at(pop             0.113105E-01
25 at(pop             0.139953E-01
26 at(pop             0.587236E-02
27 at(pop             0.136696E-01
28 at(pop             0.153806E-01
29 at(pop             0.101830E-01
30 at(pop             0.170939E-01
31 at(pop             0.192100E-01
32 ef.pop.entrynum       0.632070E-02
33 Variance            0.137476
34 VarG  4             0.19201E-01   0.34163E-02
35 Var_plots  5          0.16582      0.47362E-02
   H_plot      = VarG  4   34/Var_plot  35=         0.1158    0.0186
Notice: The parameter estimates are followed by
        their approximate standard errors.
```

H2 means basis: (VARG) / ((VARG) + ef.pop/(2 : Harmonic Mean) + ef.pop.entrynum / 2 + (Variance) / 3.41)

0.19201E-01 / (0.19201E-01 + (0.282314E-02/2) + (0.282314E-02/2) +(0.137476/3.402825389)) = 0.3075 = H2 Means-Basis

SIS_DIFF

- - - Results from analysis of sis_diff - - -

1	ef	19.7931
2	pop	17.0832
3	ef.pop	4.68322
4	at(pop	129.244
5	at(pop	78.4153
6	at(pop	58.2800
7	at(pop	34.4417
8	at(pop	44.0940
9	at(pop	118.607
10	at(pop	12.0836
11	at(pop	81.9419
12	at(pop	27.8234
13	at(pop	66.9090
14	at(pop	73.4376
15	at(pop	25.7480
16	at(pop	12.1366
17	at(pop	14.3261
18	at(pop	53.4119
19	at(pop	103.915
20	at(pop	52.3812
21	at(pop	31.9988
22	at(pop	46.4334
23	at(pop	68.0813
24	at(pop	49.2598
25	at(pop	67.5594
26	at(pop	4.51920
27	at(pop	32.2429
28	at(pop	14.6002
29	at(pop	851.871
30	ef.pop.entrynum	20.9363
31	Variance	259.701
32	VarG 2	101.08 49.211
33	Var_plots 3	386.40 49.544

H_plot = VarG 2 32/Var_plot 33= 0.2616 0.0942

Notice: The parameter estimates are followed by
their approximate standard errors.

H2 means basis: (VARG) / ((VARG) + ef.pop/(2 : Harmonic Mean) + ef.pop.entrynum / 2 + (Variance) / 3.41)

101.08 / (101.08 + (4.68322/2) + (20.9363/2) +(259.701/3.419912009)) = 0.5324 = H2
Means-Basis

SIS_RATIO

- - - Results from analysis of sis_ratio - - -

1	ef	0.914878E-02	
2	at(ff	0.335947E-02	
3	pop	0.104587E-01	
4	ef.pop	0.355337E-02	
5	at(pop	0.679071E-01	
6	at(pop	0.576289E-01	
7	at(pop	0.382190E-01	
8	at(pop	0.380796E-01	
9	at(pop	0.561052E-01	
10	at(pop	0.668841E-01	
11	at(pop	0.154536E-01	
12	at(pop	0.831541E-01	
13	at(pop	0.393739E-01	
14	at(pop	0.552513E-01	
15	at(pop	0.523152E-01	
16	at(pop	0.284231E-01	
17	at(pop	0.306621E-01	
18	at(pop	0.274955E-01	
19	at(pop	0.365142E-01	
20	at(pop	0.796945E-01	
21	at(pop	0.486771E-01	
22	at(pop	0.242568E-01	
23	at(pop	0.622251E-01	
24	at(pop	0.405297E-01	
25	at(pop	0.208359E-01	
26	at(pop	0.419855E-01	
27	at(pop	0.181950E-01	
28	at(pop	0.433207E-01	
29	at(pop	0.208820E-01	
30	at(pop	0.293567	
31	ef.pop.entrynum	0.144299E-01	
32	Variance	0.189035	
33	VarG 3	0.64577E-01	0.17968E-01
34	Var_plots 4	0.27159	0.18456E-01

H_plot = VarG 3 33/Var_plot 34= 0.2378 0.0508

Notice: The parameter estimates are followed by
their approximate standard errors.

H2 means basis: (VARG) / ((VARG) + ef.pop/(2 : Harmonic Mean) + ef.pop.entrynum / 2 + (Variance) / 3.41)

0.064577 / (0.064577 + (0.00355337/2) + (0.0144299/2) +(0.0144299/3.419912009)) = 0.8301 = H2 Means-Basis

SIS_NSC

- - - Results from analysis of sis_nsc - - -

1	at(ef	3.17301
2	at(ef	3.66977
3	pop	17.5284
4	ef.pop	2.31406
5	at(pop	47.1836
6	at(pop	31.7313
7	at(pop	32.9171
8	at(pop	26.9076
9	at(pop	48.7658
10	at(pop	39.4849
11	at(pop	36.5306
12	at(pop	59.1980
13	at(pop	20.7507
14	at(pop	41.0421
15	at(pop	54.0673
16	at(pop	65.4136
17	at(pop	29.3688
18	at(pop	25.4188
19	at(pop	25.1172
20	at(pop	91.2928
21	at(pop	36.0359
22	at(pop	43.4048
23	at(pop	49.9738
24	at(pop	61.0791
25	at(pop	37.4711
26	at(pop	74.9392
27	at(pop	32.9953
28	at(pop	34.9424
29	at(pop	43.8098
30	at(pop	116.108
31	ef.pop.entrynum	6.51229
32	Variance	181.713

```
 33 VarG  3                64.560       9.7667
 34 Var_plots  4           255.10       10.636
   H_plot      = VarG  3   33/Var_plot  34=        0.2531    0.0291
Notice: The parameter estimates are followed by
       their approximate standard errors.

!PIN   !DEFINE
F VarG 3 + 5 * 0.039 + 6 * 0.039 + 7 * 0.039 + 8 * 0.039 + 9 * 0.039 + 10 * 0.039 + 11 *
0.039 + 12 * 0.039 + 13 * 0.039 + 14 * 0.039 + 15 * 0.039 + 16 * 0.039 + 17 * 0.039 +
18 * 0.039 + 19 * 0.039 + 20 * 0.039 + 21 * 0.039 + 22 * 0.039 + 23 * 0.039 + 24 *
0.039 + 25 * 0.039 + 26 * 0.039 + 27 * 0.039 + 28 * 0.039 + 29 * 0.039 + 30 * 0.039
#(Comp 33)
F Var_plots 4 + 32 + 31 + 33#comp33
H H_plot 33 34


# Cullis heritability for entry mean basis
1 - ((9.051^2)/(2*64.560)) = 0.365 = H_Mean
# Cullis heritability for entry mean basis
# Overall Standard Error of Difference    2.860
#h2 = 1 - ((SED)^2)/2 * G variance)

SIS_SC

       - - - Results from analysis of sis_sc - - -

  1 pop              16.7785
  2 ef.pop            7.84091
  3 at(pop          171.567
  4 at(pop          115.080
  5 at(pop          100.905
  6 at(pop           72.3130
  7 at(pop           61.1218
  8 at(pop          138.083
  9 at(pop           45.9184
 10 at(pop           95.4822
 11 at(pop           68.5242
 12 at(pop           90.2964
 13 at(pop           68.6927
 14 at(pop           77.7211
 15 at(pop           41.6504
 16 at(pop           38.6781
 17 at(pop           44.6447
 18 at(pop          101.561
 19 at(pop           80.7264
```

```
 20 at(pop                62.0109
 21 at(pop                77.9457
 22 at(pop                118.482
 23 at(pop                43.3140
 24 at(pop                100.470
 25 at(pop                28.5223
 26 at(pop                69.2066
 27 at(pop                77.5438
 28 at(pop                284.335
 29 ef.pop.entrynum         15.9161
 30 Variance               162.190
 31 VarG  1                105.50        18.949
 32 Var_plots 29           291.44        19.269
   H_plot       = VarG  1   31/Var_plot  32=          0.3620    0.0422
Notice: The parameter estimates are followed by
        their approximate standard errors.
```

H2 means basis: (VARG) / ((VARG) + ef.pop/(2 : Harmonic Mean) + ef.pop.entrynum / 2 + (Variance) / 3.41)

105.50 / (105.50 + (7.84091/2) + (15.9161/2) +(15.9161/3.43786403)) = 0.8646 = H2 Means-Basis

Joint-Linkage Mapping Code – SAS – Buckler et al., 2009

```
DATA GENO;
INFILE 'SCIS SAS.csv' DSD FIRSTOBS=2 LINESIZE=10000;
LENGTH SAMPLE $3.;
*/ (Zeno#) (phenotype) pop m1-m1106;
INPUT genocode nsc sc diff ratio dta dts pop  m1-m1106;
RUN;
PROC PRINT DATA=GENO;
RUN;

/*********************************************/
/*      Use GLMSELECT to build a model.      */
/*      First create a macro to hold the     */
/*      pop and marker*pop terms.            */
/*********************************************/
%let factor = pop;

%macro makefactor;
        %do i = 1 %to 1106;
                %let factor = &factor pop*m&i;
        %end;
```

```
%mend;
%makefactor;
%put &factor;                          /*  checks that factor is correct   */

/*****************************************************************/
/*  Run glmselect.                                               */
/*  The correct significance level to use depends on the markers   */
/*  and should be determined using a permutation analysis.        */
/*  The stop parameter may be set to a higher or lower value       */
/*  to limit the amount of time taken by the analysis.            */
/*****************************************************************/
proc glmselect data=GENO;
class pop;
model ratio = &factor /select=sl sle=1e-4 sls=2e-4 stop=50 showpvalues;
run;

/*****************************************************************
*/
/*  The next section uses the model as background markers (cofactors)   */
/*  to perform a scan of all the markers in the data set excluding      */
/*  background markers in a window around the marker being tested.      */
/*  It uses likelihood ratios to calculate a LOD score for each marker. */
/*                                                                */
/*  Replace the numbers in the cards statement with the marker numbers  */
/*  from the actual model.                                        */
/*****************************************************************
*/

DATA MAP;
INFILE 'markers061208.txt' DLM='09'x;
LENGTH marker $15 name $5;
INPUT marker chr pos mnum;
name = 'm'||left(mnum);
RUN;
*input markers from previously run model;
data modelterms;
length name $5;
input mnum;
name = 'm'||left(mnum);
chr = 0;
pos = 0;
cards;
33
242
472
```

```
;
run;

proc sql;
update modelterms set chr=(select chr from map where modelterms.name=map.name);
update modelterms set pos=(select pos from map where modelterms.name=map.name);
quit;

%let trait = ratio;
%global model;
%global rmodel;
%macro getreducedmodel(marker, window);
	%let mname = m&marker;
	proc sql;
	select chr,pos into :chr,:pos from map where map.name="&mname";
	quit;

	data _null_;
	set modelterms end=stop;
	length model $1000;
	retain model "&trait = pop";
	if chr^=&chr then model = trim(model)||" pop*"||left(name);
	else if abs(pos - &pos) > &window then model = trim(model)||"
pop*"||left(name);
	if stop then call symput('model',trim(model));
	run;
%mend;

%macro testAMarker(marker, window);
	%getreducedmodel(&marker, &window);

	%if "&rmodel"^="&model" %then %do;
		%put calculating the reduced model for m&marker;

		proc mixed data=geno method=ml;
		class pop;
		model &model;
		ods output "Fit Statistics"=reduced;
		run;
		%let rmodel = &model;
	%end;

	%let model = &model pop*m&marker;
	%put calculating the full model for m&marker;
	proc mixed data=geno method=ml;
```

```
	class pop;
	model &model;
	ods output "Fit Statistics"=full;
	run;

%mend;

%macro scanmarkers(start, finish, window);
	proc sql;
	create table scanresults(name char(5), LRreduced num, LRfull num, diff num, lod
num);
	quit;
	%let rmodel = blank;
	%do i = &start %to &finish;
		%testAMarker(&i, &window);
		proc sql;
		insert into scanresults(name, LRreduced, LRfull, diff, lod)
			select "m&i",a.value, b.value, a.value-b.value, (a.value-
b.value)/4.61
			from reduced a, full b
			where a.descr=b.descr and b.descr="-2 Log Likelihood";
		quit;
	%end;
%mend;

options nonotes;
ods listing close;
ods results off;
%scanmarkers(1,1106,20);
ods listing;
ods results on;
options notes;
```

Appendix D Sink-Inhibited Senescence Candidate Genes

Table D-1 Candidate Genes for Sink-Inhibited Senescence Phenotypes

Phenotype	Chr	SNP Position	RMIP	Gene ID	Arabidopsis/Rice/PFAM Ortholog
Difference	7	2,631,177	30	GRMZM2G100176	PFAM ID: PF00249: Myb-like DNA-binding domain
	7	2,631,177	30	GRMZM2G542190	No annotated gene
	7	2,631,177	30	GRMZM2G015739	PFAM ID: PF08507: COPI associated protein
	7	2,631,177	30	GRMZM2G015654	PFAM ID: PF03254: Xyloglucan fucosyltransferase
	7	2,631,177	30	GRMZM2G490613	No annotated gene
	7	2,631,177	30	GRMZM2G490599	No annotated gene
	9	50,589,579	27	GRMZM2G573326	No annotated gene
	9	50,589,579	27	AC204296.3_FG001	No annotated gene
	7	2,585,778	26	GRMZM2G101545	AT5G03970.2: F-box associated ubiquitination effector
	7	2,585,778	26	GRMZM5G879345	No annotated gene
	7	2,585,778	26	GRMZM2G403424	No annotated gene
	7	2,585,778	26	GRMZM2G403426	No annotated gene
	7	2,585,778	26	GRMZM5G827455	PFAM ID: PF00931: NB-ARC domain
	7	2,585,778	26	GRMZM2G341621	AT3G06430.1(EMB2750): Tetratricopeptide repeat (TPR)-like superfamily protein
	7	2,585,778	26	GRMZM2G043383	PFAM ID: PF00118: TCP-1/cpn60 chaperonin family
	7	2,585,778	26	GRMZM2G043722	No annotated gene
	7	2,585,778	26	GRMZM2G043368	No annotated gene
	7	2,585,778	26	GRMZM2G043301	AT5G66920.1(sks17): SKU5 similar 17
	7	2,585,778	26	GRMZM5G808940	No annotated gene
	9	23,335,558	22	GRMZM2G110158	PF10192: Rhodopsin-like GPCR transmembrane domain
	9	23,335,558	22	GRMZM2G110117	No annotated gene
	9	23,335,558	22	GRMZM2G548056	No annotated gene

Table D-1 Continued

Difference	9	23,335,558	22	GRMZM2G548053	No annotated gene
	9	23,335,558	22	GRMZM2G548052	No annotated gene
	9	23,335,558	22	GRMZM2G024993	Granule-bound starch synthase - waxy 1
	9	23,335,558	22	GRMZM2G171395	(ANAC043,EMB2301,NST1): NAC (No Apical Meristem) domain transcriptional regulator superfamily protein
	9	23,335,558	22	GRMZM2G171376	AT4G14040.1(EDA38,SBP2): selenium-binding protein 2
	4	52,101,633	18	GRMZM2G069922	AT3G10300.1: Calcium-binding EF-hand family protein
	6	167,702,389	18	GRMZM2G310880	No annotated gene
	6	167,702,389	18	GRMZM2G010953	AT1G56720.1: Protein kinase superfamily protein
	6	167,702,389	18	GRMZM2G011091	No annotated gene
	6	167,702,389	18	GRMZM2G021644	No annotated gene
	6	167,702,389	18	GRMZM2G021661	AT3G26360.1: Ribosomal protein S21 family protein
	6	167,702,389	18	GRMZM2G167786	PFAM ID: PF08263: Leucine rich repeat N-terminal domain
	6	167,702,389	18	GRMZM2G167860	No annotated gene
	5	26,052,001	17	AC210058.3_FG002	No annotated gene
	5	26,052,001	17	GRMZM2G377735	No annotated gene
	5	26,052,001	17	AC210058.3_FG003	No annotated gene
	6	69,934,096	17	GRMZM2G126057	No annotated gene
	6	69,934,096	17	GRMZM2G126053	No annotated gene
	6	69,934,096	17	AC216268.3_FG001	No annotated gene
	1	33,116,200	16	GRMZM2G108138	AT4G24230.6(ACBP3): acyl-CoA-binding domain 3
	1	33,116,200	16	GRMZM2G108032	AT4G38650.1: Glycosyl hydrolase family 10 protein
	1	33,116,200	16	GRMZM2G546229	No annotated gene
	1	33,116,200	16	GRMZM2G546268	No annotated gene
	9	34,020,915	15	GRMZM2G703960	No annotated gene
	9	34,020,915	15	GRMZM2G106113	No annotated gene

Table D-1 Continued

	2	150,254,066	14	GRMZM5G874578	No annotated gene
	2	150,254,066	14	GRMZM2G075384	No annotated gene
	1	35,744,241	12	GRMZM2G001696	PFAM ID: PF01293: Phosphoenolpyruvate carboxykinase
	1	35,744,241	12	GRMZM2G001663	PFAM ID: PF03101: FAR1 DNA-binding domain
	1	35,744,241	12	GRMZM2G001814	AT5G57190.1(PSD2): phosphatidylserine decarboxylase 2
	1	35,744,241	12	GRMZM2G484108	No annotated gene
	2	31,831,353	12	GRMZM2G158083	AT5G48930.1(HCT): hydroxycinnamoyl-CoA shikimate/quinate hydroxycinnamoyl transferase
	2	31,831,353	12	GRMZM2G321210	AT4G02290.1(AtGH9B13,GH9B13): glycosyl hydrolase 9B13
	2	31,831,353	12	GRMZM2G020947	No annotated gene
	2	31,831,353	12	AC200505.4_FG005	No annotated gene
	2	31,831,353	12	GRMZM2G321262	No annotated gene
Difference	4	180,242,001	12	AC197274.4_FG004	No annotated gene
	4	180,242,001	13	GRMZM2G149422	PFAM ID: PF04674: Phosphate-induced protein 1 conserved region
	4	180,242,001	14	GRMZM2G448876	No annotated gene
	4	180,242,001	15	GRMZM2G448881	No annotated gene
	4	180,242,001	16	GRMZM2G448883	PFAM ID: PF04674: Phosphate-induced protein 1 conserved region
	4	180,242,001	17	GRMZM2G338457	No annotated gene
	4	180,242,001	12	GRMZM2G501303	No annotated gene
	9	22,390,491	12	No annotated genes	No annotated gene
	1	33,215,584	11	GRMZM2G346861	AT4G38660.1: Pathogenesis-related thaumatin superfamily protein
	1	33,215,584	11	GRMZM2G346861	AT4G38660.1: Pathogenesis-related thaumatin superfamily protein

Table D-1 Continued

	1	246,542,036	11	GRMZM2G012119	(PIFI): post-illumination chlorophyll fluorescence increase
	1	246,542,036	11	GRMZM2G013600	AT5G51940.1(NRPB6A,NRPD6A,NRPE6A): RNA polymerase Rpb6
	1	246,542,036	11	GRMZM2G012071	AT4G31490.1: Coatomer, beta subunit
	2	207,836,886	10	GRMZM2G130773	AT5G55580.1: Mitochondrial transcription termination
	2	207,836,886	10	GRMZM2G431309	AT1G50600.1(SCL5): scarecrow-like 5
	2	207,836,886	10	GRMZM2G431309	LOC_Os07g39470.1: gibberellin response modulator
	2	207,836,886	10	GRMZM2G130854	AT4G26640.2(AtWRKY20,WRKY20): WRKY family transcription factor family protein
	2	207,836,886	10	GRMZM2G130819	No annotated gene
	5	17,687,519	10	No annotated genes	No annotated gene
	6	69,597,861	10	GRMZM5G819899	No annotated gene
	6	69,597,861	10	GRMZM5G894974	No annotated gene
Difference	1	55,526,001	9	No annotated genes	No annotated gene
	1	246,493,829	9	GRMZM2G011912	AT2G35610.1(XEG113): xyloglucanase 113
	2	4,160,502	9	GRMZM5G826577	No annotated gene
	2	4,160,502	9	GRMZM2G398057	No annotated gene
	2	4,160,502	9	GRMZM5G846720	No annotated gene
	2	4,160,502	9	GRMZM2G096905	No annotated gene
	6	69,982,294	9	GRMZM2G482736	No annotated gene
	6	69,982,294	9	GRMZM2G482733	No annotated gene
	6	69,982,294	9	GRMZM2G482730	No annotated gene
	7	163,274,001	9	No annotated genes	No annotated gene
	2	30,290,372	8	GRMZM2G051952	LOC_Os04g42800.1: photosystem-II repair protein, putative, expressed
	2	30,290,372	8	GRMZM2G052009	No annotated gene
	2	30,290,372	8	GRMZM2G051948	No annotated gene

Table D-1 Continued

Difference	2	174,290,434	8	AC196395.3_FG001	No annotated gene
	4	179,358,319	8	GRMZM2G154389	No annotated gene
	7	161,798,001	8	GRMZM2G179777	AT5G50890.1: alpha/beta-Hydrolases superfamily protein
	7	161,798,001	8	GRMZM2G179779	No annotated gene
	7	161,798,001	8	GRMZM5G888034	No annotated gene
	7	161,798,001	8	GRMZM5G848687	No annotated gene
	7	161,798,001	8	GRMZM2G589996	No annotated gene
	7	161,798,001	8	GRMZM2G396653	No annotated gene
	1	27,254,251	7	No annotated genes	No annotated gene
	1	246,409,076	7	GRMZM2G011078	AT1G61250.1(SC3): secretory carrier 3
	1	246,409,076	7	GRMZM2G307908	No annotated gene
	1	246,409,076	7	GRMZM2G010831	No annotated gene
	1	246,409,076	7	GRMZM2G487196	No annotated gene
	2	148,184,812	7	GRMZM2G545106	No annotated gene
	4	68,643,578	7	AC214531.3_FG004	AT2G32560.1: F-box family protein
	4	68,643,578	7	GRMZM2G029184	LOC_Os08g16130.1: fiber protein Fb34, putative, expressed
	4	68,643,578	7	GRMZM2G029173	No annotated gene
	4	68,643,578	7	GRMZM2G029165	No annotated gene
	5	39,440,001	7	No annotated genes	No annotated gene
	6	69,882,668	7	No annotated genes	No annotated gene
	6	69,954,140	7	No annotated genes	No annotated gene
	8	118,974,331	7	GRMZM2G034421	AT4G11070.1(AtWRKY41,WRKY41): WRKY family transcription factor
	9	5,512,154	7	GRMZM2G152415	PFAM ID: PF00319: SRF-type transcription factor (DNA-binding and dimerisation domain)

Table D-1 Continued

	9	5,512,154	7	GRMZM2G152411	AT5G46860.1(ATSYP22,ATVAM3,SGR3,SYP22,VAM3): Syntaxin/t-SNARE family protein
	9	143,360,715	7	GRMZM2G175642	No annotated gene
	9	143,360,715	7	GRMZM2G175685	No annotated gene
	9	143,360,715	7	GRMZM2G175738	No annotated gene
	9	143,360,715	7	GRMZM2G175743	No annotated gene
	9	143,360,715	7	GRMZM2G477658	No annotated gene
	9	143,360,715	7	GRMZM2G175758	No annotated gene
	9	143,360,715	7	GRMZM2G477666	No annotated gene
	1	2,541,747	6	GRMZM2G052546	AT3G52180.2(ATPTPKIS1,ATSEX4,DSP4,SEX4): dual specificity protein phosphatase (DsPTP1) family protein
	1	23,235,688	6	GRMZM2G005435	PFAM ID: PF05903: PPPDE putative peptidase domain
	1	23,235,688	6	GRMZM2G005624	AT2G18550.1(ATHB21,HB-2,HB21): homeobox protein21
Difference	1	33,042,978	6	No annotated genes	No annotated gene
	2	174,342,922	6	AC203957.3_FG001	AT1G68825.1(DVL5,RTFL15): ROTUNDIFOLIA like 15
	2	174,342,922	6	GRMZM2G149022	No annotated gene
	2	174,342,922	6	AC203957.3_FG002	No annotated gene
	2	174,342,922	6	GRMZM5G857422	No annotated gene
	2	174,342,922	6	GRMZM5G825892	No annotated gene
	2	195,013,286	6	No annotated genes	No annotated gene
	4	157,614,954	6	GRMZM2G004748	PFAM ID: PF00664: ABC transporter transmembrane region , PF00005: ABC transporter
	4	157,614,954	6	GRMZM5G896519	No annotated gene
	4	158,305,199	6	GRMZM2G350157	AT2G31290.1: Ubiquitin carboxyl-terminal hydrolase family protein
	4	158,305,199	6	GRMZM2G050405	AT5G28050.2: Cytidine/deoxycytidylate deaminase family
	4	158,305,199	6	AC184172.3_FG004	No annotated gene

Table D-1 Continued

	4	158,305,199	6	GRMZM2G350106	No annotated gene
	5	362,001	6	No annotated genes	No annotated gene
	5	20,199,518	6	GRMZM2G070523	AT2G32460.1(ATM1,ATMYB101,MYB101): myb domain protein 101
	5	20,199,518	6	GRMZM5G889027	No annotated gene
	5	20,199,518	6	GRMZM2G369119	No annotated gene
	5	20,199,518	6	GRMZM5G854240	No annotated gene
	6	69,758,139	6	No annotated genes	No annotated gene
	6	71,514,973	6	GRMZM2G700957	No annotated gene
	6	71,514,973	6	GRMZM5G815863	No annotated gene
	7	722,100	6	GRMZM2G177104	AT4G21200.1(ATGA2OX8,GA2OX8): gibberellin 2-oxidase 8
	7	722,100	6	GRMZM2G177091	No annotated gene
Difference	7	722,100	6	GRMZM2G588737	No annotated gene
	7	2,586,382	6	GRMZM2G101545	AT5G03970.2: F-box associated ubiquitination effector family protein
	7	2,586,382	6	GRMZM5G879345	No annotated gene
	7	2,586,382	6	GRMZM2G403424	No annotated gene
	7	2,586,382	6	GRMZM2G403426	No annotated gene
	7	2,586,382	6	GRMZM5G827455	PFAM ID: PF00931: NB-ARC domain
	7	2,586,382	6	GRMZM2G341621	AT3G06430.1(EMB2750): Tetratricopeptide repeat (TPR)-like superfamily protein
	7	2,586,382	6	GRMZM2G043383	PFAM ID: PF00118: TCP-1/cpn60 chaperonin family
	7	2,586,382	6	GRMZM2G043722	No annotated gene
	7	2,586,382	6	GRMZM2G043368	No annotated gene
	7	2,586,382	6	GRMZM2G043301	AT5G66920.1(sks17): SKU5 similar 17
	7	2,586,382	6	GRMZM5G808940	No annotated gene

Table D-1 Continued

	1	26,573,277	5	GRMZM2G088309	AT1G69180.1(CRC): Plant-specific transcription factor YABBY family protein
	1	26,573,277	5	GRMZM2G534604	No annotated gene
	1	33,116,201	5	GRMZM2G108138	AT4G24230.6(ACBP3): acyl-CoA-binding domain 3
	1	33,116,201	5	GRMZM2G108032	AT4G38650.1: Glycosyl hydrolase family 10 protein
	1	33,116,201	5	GRMZM2G546229	No annotated gene
	1	33,116,201	5	GRMZM2G546268	No annotated gene
	1	64,146,869	5	GRMZM2G084407	AT2G46950.1(CYP709B2): cytochrome P450, family 709, subfamily B, polypeptide 2
	1	64,146,869	5	GRMZM2G534260	No annotated gene
	2	150,525,724	5	No annotated genes	No annotated gene
	4	45,668,829	5	GRMZM2G355806	No annotated gene
	4	45,668,829	5	GRMZM2G052995	No annotated gene
Difference	4	45,668,829	5	GRMZM5G847573	No annotated gene
	4	158,181,853	5	GRMZM2G576495	No annotated gene
	4	158,181,853	5	GRMZM2G156444	No annotated gene
	4	179,802,574	5	GRMZM2G308193	AT5G65290.1: LMBR1-like membrane protein
	4	179,802,574	5	GRMZM2G008691	AT1G72210.1: basic helix-loop-helix (bHLH) DNA-binding superfamily protein
	4	179,802,574	5	GRMZM2G008819	AT2G32300.1(UCC1): uclacyanin 1
	4	179,802,574	5	GRMZM2G487332	No annotated gene
	5	41,126,001	5	No annotated genes	No annotated gene
	7	160,762,001	5	GRMZM2G104204	AT2G18550.1(ATHB21,HB-2,HB21): homeobox protein 21
	7	161,627,332	5	GRMZM2G066197	No annotated gene
	7	172,818,001	5	GRMZM5G884316	No annotated gene
	7	172,818,001	5	GRMZM2G042347	AT5G05340.1: Peroxidase superfamily protein

Table D-1 Continued

Difference	7	172,818,001	5	GRMZM2G507784	AT5G05340.1: Peroxidase superfamily protein
	7	172,818,001	5	GRMZM5G899449	AT5G05340.1: Peroxidase superfamily protein
	7	172,818,001	5	AC211735.5_FG008	AT5G05340.1: Peroxidase superfamily protein
	8	118,006,292	5	GRMZM2G179728	PFAM ID: PF00657: GDSL-like Lipase/Acylhydrolase
	8	118,006,292	5	GRMZM2G173874	AT3G47300.1(SELT): SELT-like protein precursor
	8	169,476,475	5	AC233788.2_FG009	No annotated gene
	9	16,488,862	5	GRMZM2G017349	AT4G36930.1(SPT): basic helix-loop-helix (bHLH) DNA-binding superfamily protein
	9	16,488,862	5	GRMZM2G338056	AT3G53600.1: C2H2-type zinc finger family protein
	9	16,488,862	5	GRMZM2G016930	AT4G11240.1(TOPP7): Calcineurin-like metallo-phosphoesterase superfamily protein
	9	16,488,862	5	GRMZM2G494762	No annotated gene
	9	16,488,862	5	GRMZM2G494759	No annotated gene
	10	141,004,347	5	GRMZM2G129071	AT1G31410.1: putrescine-binding periplasmic protein-related
	10	141,004,347	5	GRMZM2G109753	AT2G04940.1: scramblase-related
Ratio	9	113,515,721	35	GRMZM2G138429	AT1G32400.1(TOM2A): tobamovirus multiplication 2A
	9	113,515,721	35	GRMZM2G562388	No annotated gene
	9	113,515,721	35	GRMZM2G144841	AT1G32370.2(TOM2B,TTM1): tobamovirus multiplication 2B
	1	246,542,036	27	GRMZM2G012119	(PIFI): post-illumination chlorophyll fluorescence increase
	1	246,542,036	27	GRMZM2G013600	AT5G51940.1(NRPB6A,NRPD6A,NRPE6A): RNA polymerase Rpb6
	1	246,542,036	27	GRMZM2G012071	AT4G31490.1: Coatomer, beta subunit
	2	9,277,549	27	GRMZM2G124560	AT5G21040.1(FBX2): F-box protein 2
	2	9,277,549	27	GRMZM2G107711	No annotated gene
	2	9,277,549	27	GRMZM2G124603	No annotated gene

Table D-1 Continued

	2	9,277,549	27	GRMZM2G124600	No annotated gene
	2	9,277,549	27	AC185413.3_FG002	No annotated gene
	2	9,277,549	27	AC185413.3_FG001	No annotated gene
	2	9,277,549	27	GRMZM2G584478	No annotated gene
	2	9,277,549	27	GRMZM2G469521	No annotated gene
	1	25,787,771	22	AC211140.2_FG010	No annotated gene
	1	25,787,771	22	AC211140.2_FG010	No annotated gene
	4	52,101,633	21	GRMZM2G069922	AT3G10300.1: Calcium-binding EF-hand family protein
	8	119,035,095	21	GRMZM2G432583	AT5G01900.1(ATWRKY62,WRKY62): WRKY DNA-binding protein 62
	8	119,035,095	21	GRMZM2G132759	AT3G08690.1(ATUBC11,UBC11): ubiquitin-conjugating enzyme 11
	8	119,035,095	21	GRMZM2G132740	No annotated gene
Ratio	6	69,934,096	19	GRMZM2G126057	No annotated gene
	6	69,934,096	19	GRMZM2G126053	No annotated gene
	6	69,934,096	19	AC216268.3_FG001	No annotated gene
	1	33,116,200	17	GRMZM2G108138	AT4G24230.6(ACBP3): acyl-CoA-binding domain 3
	1	33,116,200	17	GRMZM2G108032	AT4G38650.1: Glycosyl hydrolase family 10 protein
	1	33,116,200	17	GRMZM2G546229	No annotated gene
	1	33,116,200	17	GRMZM2G546268	No annotated gene
	4	53,858,511	15	GRMZM2G473869	PFAM ID: PF04570: Protein of unknown function (DUF581)
	4	53,858,511	15	GRMZM2G486609	No annotated gene
	2	148,184,812	14	GRMZM2G545106	No annotated gene
	1	34,603,099	13	GRMZM2G089812	AT5G63470.1(NF-YC4): nuclear factor Y, subunit C4
	1	34,603,099	13	GRMZM2G171736	AT4G08920.1(ATCRY1,BLU1,CRY1,HY4,OOP2): cryptochrome 1

Table D-1 Continued

Ratio	1	34,603,099	13	GRMZM5G825312	No annotated gene
	1	34,603,099	13	GRMZM2G089832	No annotated gene
	1	34,603,099	13	GRMZM2G068507	No annotated gene
	6	69,982,294	13	GRMZM2G482736	No annotated gene
	6	69,982,294	13	GRMZM2G482733	No annotated gene
	6	69,982,294	13	GRMZM2G482730	No annotated gene
	1	243,882,001	12	No annotated genes	No annotated gene
	3	50,206,375	12	GRMZM2G463340	No annotated gene
	3	50,206,375	12	GRMZM2G463336	No annotated gene
	3	50,206,375	12	GRMZM2G580724	No annotated gene
	3	50,206,375	12	AC190652.3_FG004	No annotated gene
	3	8,220,888	11	GRMZM2G176489	AT5G15130.1(ATWRKY72,WRKY72): WRKY DNA-binding protein 72
	3	8,220,888	11	GRMZM2G475984	AT5G64810.1(ATWRKY51,WRKY51): WRKY DNA-binding protein 51
	5	19,777,916	11	GRMZM5G853066	PFAM ID: PF00319: SRF-type transcription factor (DNA-binding and dimerisation domain)
	5	19,777,916	11	AC192246.2_FG002	No annotated gene
	5	19,777,916	11	GRMZM2G502484	No annotated gene
	5	22,570,177	10	GRMZM2G082160	No annotated gene
	8	153,620,941	10	GRMZM2G138999	AT5G53370.1(ATPMEPCRF,PMEPCRF): pectin methylesterase PCR fragment F
	1	26,148,892	9	GRMZM2G009638	AT2G33040.1(ATP3): gamma subunit of Mt ATP synthase
	5	26,052,001	9	AC210058.3_FG002	No annotated gene
	5	26,052,001	9	GRMZM2G377735	No annotated gene
	5	26,052,001	9	AC210058.3_FG003	No annotated gene
	10	137,505,644	9	GRMZM5G884137	AT2G02070.1(AtIDD5,IDD5): indeterminate(ID)-domain 5

Table D-1 Continued

	10	137,505,644	9	GRMZM2G702582	No annotated gene
	10	137,505,644	9	AC209206.3_FG009	No annotated gene
	10	137,505,644	9	AC209206.3_FG010	No annotated gene
	2	2,034,526	8	GRMZM2G040115	AT3G19850.1: Phototropic-responsive NPH3 family protein
	2	2,034,526	8	GRMZM2G040247	AT1G08190.1(ATVAM2,ATVPS41,VAM2,VPS41,ZIP2): vacuolar protein sorting 41
	2	2,034,526	8	GRMZM5G827567	No annotated gene
	2	28,664,390	8	GRMZM2G052644	AT2G33385.2(arpc2b): actin-related protein C2B
	2	28,664,390	8	GRMZM5G889644	No annotated gene
	2	28,664,390	8	GRMZM5G806726	No annotated gene
	2	28,664,390	8	GRMZM2G052688	AT1G04020.1(ATBARD1,BARD1,ROW1): breast cancer associated RING 1
Ratio	2	28,664,390	8	AC187787.2_FG007	No annotated gene
	3	50,210,647	8	GRMZM2G463340	No annotated gene
	3	50,210,647	8	GRMZM2G463336	No annotated gene
	3	50,210,647	8	GRMZM2G580724	No annotated gene
	3	50,210,647	8	AC190652.3_FG004	No annotated gene
	4	54,363,620	8	GRMZM2G477032	No annotated gene
	5	19,776,980	8	GRMZM5G853066	PFAM ID: PF00319: SRF-type transcription factor (DNA-binding and dimerisation domain)
	5	19,776,980	8	AC192246.2_FG002	No annotated gene
	5	19,776,980	8	GRMZM2G502484	No annotated gene
	5	22,556,150	8	GRMZM5G869246	AT4G39050.1: Kinesin motor family protein
	6	69,625,973	8	GRMZM2G168299	AT1G02100.1: Leucine carboxyl methyltransferase
	1	229,362,503	7	GRMZM2G108949	PFAM ID: PF05553: Cotton fibre expressed protein
	1	229,362,503	7	GRMZM2G409205	No annotated gene

Table D-1 Continued

Ratio	1	229,362,503	7	GRMZM2G409193	No annotated gene
	1	229,362,503	7	GRMZM2G547826	No annotated gene
	2	176,356,560	7	GRMZM2G113633	AT5G63870.1(ATPP7,PP7): serine/threonine phosphatase 7
	2	176,356,560	7	GRMZM2G055960	No annotated gene
	2	176,356,560	7	AC229978.2_FG002	No annotated gene
	2	176,356,560	7	GRMZM2G113607	No annotated gene
	2	176,356,560	7	GRMZM2G412081	No annotated gene
	2	176,356,560	7	GRMZM2G549433	No annotated gene
	2	176,356,560	7	GRMZM2G412079	No annotated gene
	4	55,502,889	7	No annotated genes	No annotated gene
	5	17,687,519	7	No annotated genes	No annotated gene
	8	91,176,928	7	GRMZM2G347248	No annotated gene
	8	91,176,928	7	GRMZM5G893547	No annotated gene
	8	91,176,928	7	GRMZM2G532340	No annotated gene
	8	91,176,928	7	AC195139.3_FG003	No annotated gene
	8	118,058,509	7	No annotated genes	No annotated gene
	2	10,658,773	6	GRMZM2G098214	AT5G14600.1: S-adenosyl-L-methionine-dependent methyltransferases superfamily protein
	2	10,658,773	6	GRMZM2G098187	AT4G24480.1: Protein kinase superfamily protein
	2	10,658,773	6	GRMZM2G121063	AT5G09400.1(KUP7): K+ uptake permease 7
	2	10,658,773	6	GRMZM5G870342	AT1G03475.1(ATCPO-I,HEMF1,LIN2): Coproporphyrinogen III oxidase
	2	10,658,773	6	GRMZM2G554927	No annotated gene
	2	146,547,891	6	GRMZM2G314166	No annotated gene
	2	147,946,642	6	No annotated genes	No annotated gene
	2	179,437,964	6	GRMZM2G114681	rabidopsis best hit: AT1G74950.1(JAZ2,TIFY10B): TIFY domain/Divergent CCT motif family protein

Table D-1 Continued

	2	179,437,964	7	GRMZM2G548783	No annotated gene
	2	179,437,964	8	GRMZM2G498951	No annotated gene
	3	121,043,869	6	No annotated genes	No annotated gene
	4	50,729,244	6	GRMZM2G106165	AT2G27920.1(SCPL51): serine carboxypeptidase-like 51
	4	50,729,244	6	GRMZM2G106143	AT5G53300.1(UBC10): ubiquitin-conjugating enzyme 10
	4	50,729,244	6	GRMZM2G546782	No annotated gene
	4	51,402,374	6	No annotated genes	No annotated gene
	5	188,477,501	6	GRMZM2G178517	AT5G22300.1(AtNIT4,NIT4): nitrilase 4
	5	188,477,501	6	GRMZM2G178509	AT5G23350.1: GRAM domain-containing protein / ABA-responsive protein-related
	5	188,477,501	6	AC198169.4_FG007	No annotated gene
	5	188,477,501	6	GRMZM2G480911	No annotated gene
	5	188,477,501	6	GRMZM2G590870	No annotated gene
Ratio	5	188,477,501	6	GRMZM2G590871	No annotated gene
	5	188,477,501	6	GRMZM2G178506	No annotated gene
	5	188,477,501	6	GRMZM5G855035	No annotated gene
	5	188,477,501	6	GRMZM2G178592	No annotated gene
	6	69,882,668	6	No annotated genes	No annotated gene
	7	160,996,488	6	No annotated genes	No annotated gene
	8	118,058,503	6	No annotated genes	No annotated gene
	8	119,644,458	6	GRMZM2G300589	AT1G55530.1: RING/U-box superfamily protein
	8	119,644,458	6	GRMZM2G489343	No annotated gene
	8	119,644,458	6	GRMZM2G300586	No annotated gene
	8	119,644,458	6	GRMZM2G012098	No annotated gene
	9	2,810,904	6	No annotated genes	No annotated gene
	1	35,744,241	5	GRMZM2G001696	PFAM ID: PF01293: Phosphoenolpyruvate carboxykinase
	1	35,744,241	5	GRMZM2G001663	PFAM ID: PF03101: FAR1 DNA-binding domain

Table D-1 Continued

	1	35,744,241	5	GRMZM2G001814	AT5G57190.1(PSD2): phosphatidylserine decarboxylase 2
	1	35,744,241	5	GRMZM2G484108	No annotated gene
	1	35,744,246	5	GRMZM2G001696	PFAM ID: PF01293: Phosphoenolpyruvate carboxykinase
	1	35,744,246	5	GRMZM2G001663	PFAM ID: PF03101: FAR1 DNA-binding domain
	1	35,744,246	5	GRMZM2G001814	AT5G57190.1(PSD2): phosphatidylserine decarboxylase 2
	1	35,744,246	5	GRMZM2G484108	No annotated gene
	1	191,204,001	5	GRMZM2G076257	AT4G18750.1(DOT4): Pentatricopeptide repeat (PPR) superfamily protein
	1	246,409,076	5	GRMZM2G011078	AT1G61250.1(SC3): secretory carrier 3
	1	246,409,076	5	GRMZM2G307908	No annotated gene
	1	246,409,076	5	GRMZM2G010831	No annotated gene
	1	246,409,076	5	GRMZM2G487196	No annotated gene
	2	29,674,584	5	GRMZM2G049608	AT1G21230.1(WAK5): wall associated kinase 5
Ratio	2	29,674,584	5	GRMZM2G347361	No annotated gene
	2	29,674,584	5	GRMZM2G171620	AT2G20300.1(ALE2): Protein kinase superfamily protein
	2	29,674,584	5	GRMZM2G085975	No annotated gene
	2	29,674,584	5	GRMZM2G510907	No annotated gene
	2	33,402,437	5	GRMZM2G321354	AT5G11420.1: Protein of unknown function, DUF642
	2	148,228,600	5	AC211891.4_FG001	AT1G02030.1: C2H2-like zinc finger protein
	2	148,228,600	5	GRMZM2G528252	No annotated gene
	3	50,323,040	5	No annotated genes	No annotated gene
	3	188,956,961	5	No annotated genes	No annotated gene
	4	51,867,230	5	GRMZM2G372457	No annotated gene
	4	51,867,230	5	GRMZM2G525705	No annotated gene
	4	157,482,739	5	GRMZM2G091003	AT3G24140.1(FMA): basic helix-loop-helix (bHLH) DNA-binding superfamily protein
	4	157,482,739	5	AC186146.3_FG002	No annotated gene

Table D-1 Continued

Ratio	4	157,482,739	5	GRMZM2G390050	No annotated gene
	4	183,712,001	5	GRMZM2G088847	AT5G01650.1: Tautomerase/MIF superfamily protein
	4	183,712,001	5	GRMZM2G089819	AT3G56100.1(IMK3,MRLK): meristematic receptor-like kinase
	4	183,712,001	5	GRMZM2G089783	AT2G38360.1(PRA1.B4): prenylated RAB acceptor 1.B4
	4	183,712,001	5	GRMZM2G388512	No annotated gene
	4	183,712,001	5	GRMZM5G807550	No annotated gene
	4	183,712,001	5	GRMZM5G878943	No annotated gene
	4	183,712,001	5	GRMZM2G089813	No annotated gene
	5	20,493,495	5	GRMZM2G080231	AT1G05170.1: Galactosyltransferase family protein
	7	143,113,852	5	GRMZM2G179024	AT5G24470.1(APRR5,PRR5): pseudo-response regulator 5
	7	143,113,852	5	GRMZM2G179021	AT5G66350.1(SHI): Lateral root primordium (LRP) protein-related
	7	143,113,852	5	GRMZM2G590541	No annotated gene
	8	118,167,591	5	AC197705.4_FG001	AT4G33070.1: Thiamine pyrophosphate dependent pyruvate decarboxylase family protein
	9	150,820,164	5	GRMZM2G169365	AT5G12040.1: Nitrilase/cyanide hydratase and apolipoprotein N-acyltransferase family protein
	9	150,820,164	5	GRMZM2G169363	AT1G72820.1: Mitochondrial substrate carrier family protein
	9	150,820,164	5	GRMZM2G169384	AT3G15000.1: cobalt ion binding
	9	150,820,164	5	GRMZM2G700128	No annotated gene
Shootcap-only	8	166,561,819	51	GRMZM2G341166	AT4G16490.1: ARM repeat superfamily protein/Spotted leaf protein 11
	8	166,561,819	51	GRMZM2G341159	AT1G49210.1: RING/U-box superfamily protein
	8	166,561,819	51	GRMZM2G700775	No annotated gene
	3	190,031,176	42	GRMZM2G116632	Early nodulin 20

Table D-1 Continued

	3	190,031,176	42	GRMZM2G061515	indole-3-acetic acid-amido synthetase GH3.1
	3	50,210,647	38	AC190652.3_FG004	No annotated gene
	3	50,210,647	38	GRMZM2G580724	No annotated gene
	3	50,210,647	38	GRMZM2G463336	No annotated gene
	3	50,210,647	38	GRMZM2G463340	No annotated gene
	5	6,305,173	24	GRMZM2G035103	AT1G27730.1(STZ,ZAT10): salt tolerance zinc finger
	5	6,305,173	24	GRMZM2G034877	AT5G66850.1(MAPKKK5): mitogen-activated protein kinase kinase kinase 5
	5	6,305,173	24	GRMZM2G034968	No annotated gene
	5	6,305,173	24	GRMZM2G332637	No annotated gene
	5	6,305,173	24	GRMZM2G332641	No annotated gene
	5	6,305,173	24	GRMZM2G077034	GASR3 - Gibberellin-regulated GASA/GAST/Snakin family protein precursor
Shootcap-only	4	239,407,015	23	GRMZM2G073571	AT2G21520.1: Sec14p-like phosphatidylinositol transfer
	4	239,407,015	23	GRMZM2G073731	No annotated gene
	4	239,407,015	23	GRMZM2G374068	No annotated gene
	4	239,407,015	23	GRMZM2G073542	No annotated gene
	4	239,407,015	23	GRMZM2G073532	No annotated gene
	2	29,910,364	22	GRMZM2G173289	AT5G18520.1: Lung seven transmembrane receptor family
	2	29,910,364	22	GRMZM2G473765	No annotated gene
	2	29,910,364	22	GRMZM2G586913	No annotated gene
	2	29,910,364	22	AC208663.3_FG005	No annotated gene
	2	29,910,364	22	GRMZM2G173299	No annotated gene
	4	38,545,804	22	GRMZM2G123246	AT2G02450.2(anac034,ANAC035,LOV1,NAC035): NAC domain containing protein 35
	1	23,225,249	20	GRMZM2G005844	AT1G19340.1: Methyltransferase MT-A70 family protein
	1	23,225,249	20	GRMZM2G304841	No annotated gene

Table D-1 Continued

	3	50,309,401	20	GRMZM2G149747	No annotated gene
	3	50,309,401	20	GRMZM2G572820	No annotated gene
	3	50,309,401	20	GRMZM2G572822	No annotated gene
	2	33,402,437	19	GRMZM2G321354	PFAM ID: PF04862: Protein of unknown function (DUF642)
	2	6,597,595	17	GRMZM2G339117	No annotated gene
	4	44,770,267	17	GRMZM5G896883	AT4G38800.1(ATMTAN1,ATMTN1,MTAN1,MTN1): methylthioadenosine nucleosidase 1
	9	150,815,418	17	GRMZM2G169365	AT5G12040.1: Nitrilase/cyanide hydratase and apolipoprotein N-acyltransferase family protein
	9	150,815,418	17	GRMZM2G169384	LOC_Os09g04670.1: DAG protein, chloroplast precursor, putative, expressed
	9	150,815,418	17	GRMZM2G584442	No annotated gene
Shootcap-only	9	150,815,418	17	GRMZM2G700128	No annotated gene
	2	5,837,290	15	GRMZM5G882708	AT4G32140.1: EamA-like transporter family
	2	5,837,290	15	GRMZM2G023239	AT5G10790.1(UBP22): ubiquitin-specific protease 22
	2	5,837,290	15	GRMZM5G892758	AT1G15290.1: Tetratricopeptide repeat (TPR)-like superfamily protein
	2	5,837,290	15	GRMZM2G023921	AT1G80450.1: VQ motif-containing protein
	2	5,837,290	15	GRMZM2G372145	No annotated gene
	2	28,161,965	15	GRMZM2G445655	No annotated gene
	10	136,705,302	15	GRMZM2G077036	AT4G00750.1: S-adenosyl-L-methionine-dependent methyltransferases superfamily protein
	10	136,705,302	15	GRMZM2G077069	AT3G61060.1(AtPP2-A13,PP2-A13): phloem protein 2-A13
	10	136,705,302	15	GRMZM2G077082	AT5G19160.1(TBL11): TRICHOME BIREFRINGENCE-LIKE 11
	10	136,705,302	15	GRMZM2G529263	No annotated gene

Table D-1 Continued

	8	165,586,261	14	GRMZM2G128248	AT3G08910.1: DNAJ heat shock family protein
	8	165,586,261	14	GRMZM2G128215	AT5G07610.1: F-box family protein
	8	165,586,261	14	GRMZM2G005483	No annotated gene
	1	34,597,029	12	GRMZM2G089812	AT5G63470.1(NF-YC4): nuclear factor Y, subunit C4
	1	34,597,029	12	GRMZM5G825312	No annotated gene
	1	34,597,029	12	GRMZM2G089832	No annotated gene
	1	34,597,029	12	GRMZM2G068507	No annotated gene
	1	193,320,518	12	GRMZM2G424241	AT3G07220.1: SMAD/FHA domain-containing protein
	1	247,399,275	12	GRMZM2G074853	No annotated gene
	1	247,399,275	12	GRMZM2G074809	No annotated gene
	2	25,011,125	12	GRMZM2G081957	AT3G19300.1: Protein kinase superfamily protein
	2	25,011,125	12	GRMZM2G383883	AT5G62950.1: RNA polymerase II, Rpb4, core protein
Shootcap-only	4	182,870,585	12	GRMZM2G451325	AT3G55990.1(ESK1,TBL29): Plant protein of unknown function (DUF828)
	6	6,269,078	11	GRMZM2G134134	AT5G40650.1(SDH2-2): succinate dehydrogenase 2-2
	6	6,269,078	11	GRMZM2G562746	No annotated gene
	6	6,269,078	11	GRMZM2G134130	LOC_Os08g02630.1: photosystem II core complex proteins psbY, chloroplast precursor, putative, expressed
	6	6,269,078	11	GRMZM2G434069	No annotated gene
	8	166,624,558	11	GRMZM2G085035	AT2G36026.1: Ovate family protein
	8	166,624,558	11	GRMZM2G084979	AT2G35980.1(ATNHL10,NHL10,YLS9): Late embryogenesis abundant (LEA) hydroxyproline-rich glycoprotein family
	8	166,624,558	11	GRMZM2G143586	No annotated gene
	8	166,624,558	11	GRMZM2G534657	No annotated gene
	8	166,624,558	11	AC209737.3_FG016	No annotated gene
	10	4,763,003	11	GRMZM2G031150	No annotated gene

Table D-1 Continued

	10	4,763,003	11	GRMZM2G031164	No annotated gene
	3	50,315,894	10	No annotated genes	No annotated gene
	9	150,815,407	10	GRMZM2G169365	AT5G12040.1: Nitrilase/cyanide hydratase and apolipoprotein N-acyltransferase family protein
	9	150,815,407	10	GRMZM2G169384	LOC_Os09g04670.1: DAG protein, chloroplast precursor, putative, expressed
	9	150,815,407	10	GRMZM2G584442	No annotated gene
	9	150,815,407	10	GRMZM2G700128	No annotated gene
	10	137,387,236	10	GRMZM2G054078	No annotated gene
	4	238,228,758	9	GRMZM2G042664	No annotated gene
	4	238,228,758	9	GRMZM5G866636	No annotated gene
	4	238,228,758	9	GRMZM2G043011	No annotated gene
	4	238,228,758	9	GRMZM2G042602	No annotated gene
Shootcap-only	5	6,305,152	9	GRMZM2G035103	AT1G27730.1(STZ,ZAT10): salt tolerance zinc finger
	5	6,305,152	9	GRMZM2G034877	AT5G66850.1(MAPKKK5): mitogen-activated protein kinase kinase kinase 5
	5	6,305,152	9	GRMZM2G034968	No annotated gene
	5	6,305,152	9	GRMZM2G332637	No annotated gene
	5	6,305,152	9	GRMZM2G332641	No annotated gene
	5	167,845,943	9	No annotated genes	No annotated gene
	5	198,788,532	9	GRMZM2G004480	AT3G03550.1: RING/U-box superfamily protein
	5	198,788,532	9	GRMZM2G111146	AT1G22490.1: basic helix-loop-helix (bHLH) DNA-binding superfamily protein
	6	161,288,001	9	GRMZM2G034225	No annotated gene
	6	161,288,001	9	GRMZM2G034128	No annotated gene
	6	161,288,001	9	GRMZM2G501302	No annotated gene
	6	161,288,001	9	GRMZM2G501312	No annotated gene

Table D-1 Continued

	6	161,797,999	9	GRMZM5G847982	LOC_Os05g46340.1: expressed protein
	6	161,797,999	9	GRMZM2G088995	AT1G09830.1: Glycinamide ribonucleotide (GAR) synthetase
	6	161,797,999	9	GRMZM5G899656	AT1G09830.1: Glycinamide ribonucleotide (GAR) synthetase
	6	161,797,999	9	GRMZM2G388502	No annotated gene
	6	161,797,999	9	GRMZM2G507562	No annotated gene
	7	141,643,096	9	GRMZM2G073228	AT3G63530.1(BB,BB2): RING/U-box superfamily protein
	7	141,643,096	9	GRMZM2G073377	AT5G52160.1: Bifunctional inhibitor/lipid-transfer protein/seed storage 2S albumin superfamily protein
	7	141,643,096	9	GRMZM2G073504	AT4G11740.1(SAY1): Ubiquitin-like superfamily protein
	8	117,967,787	9	GRMZM2G173874	AT3G47300.1(SELT): SELT-like protein precursor
Shootcap-only	1	23,235,666	8	GRMZM2G005624	AT2G18550.1(ATHB21,HB-2,HB21): homeobox protein 21
	1	23,235,666	8	GRMZM2G005435	AT1G47740.1: PPPDE putative thiol peptidase family protein
	2	193,280,739	8	No annotated genes	No annotated gene
	4	182,084,001	8	No annotated genes	No annotated gene
	5	204,427,506	8	GRMZM2G145594	AT1G26300.1: BSD domain-containing protein
	10	131,902,889	8	GRMZM5G854655	AT3G53150.1(UGT73D1): UDP-glucosyl transferase 73D1
	1	202,399,165	7	GRMZM2G328309	LOC_Os08g23430.1: starch binding domain containing protein, putative, expressed
	2	6,597,292	7	GRMZM2G339117	No annotated gene
	4	47,552,515	7	GRMZM5G893272	No annotated gene
	4	47,814,585	7	GRMZM2G532086	No annotated gene
	7	25,133,700	7	No annotated genes	No annotated gene
	7	136,421,257	7	No annotated genes	No annotated gene

Table D-1 Continued

	10	137,538,072	7	GRMZM5G800518	AT1G36160.1(ACC1,AT-ACC1,EMB22,GK,PAS3): acetyl-CoA carboxylase 1
	1	23,234,659	6	GRMZM2G005624	AT2G18550.1(ATHB21,HB-2,HB21): homeobox protein 21
	1	23,234,659	6	GRMZM2G005435	AT1G47740.1: PPPDE putative thiol peptidase family protein
	1	26,915,303	6	GRMZM2G178894	AT2G41940.1(ZFP8): zinc finger protein 8
	1	26,915,303	6	GRMZM2G589568	No annotated gene
	1	26,915,303	6	GRMZM2G589559	No annotated gene
	1	187,843,059	6	GRMZM2G580853	No annotated gene
	1	187,843,059	6	GRMZM2G163771	No annotated gene
	1	187,843,059	6	GRMZM2G163783	No annotated gene
	2	6,990,668	6	GRMZM2G106393	AT4G10265.1: Wound-responsive family protein
Shootcap-only	2	6,990,668	6	GRMZM2G106384	AT1G03560.1: Pentatricopeptide repeat (PPR-like) superfamily protein
	2	6,990,668	6	GRMZM2G106245	AT5G13780.1: Acyl-CoA N-acyltransferases (NAT) superfamily protein
	2	6,990,668	6	GRMZM2G106105	AT2G03870.1: Small nuclear ribonucleoprotein family
	2	6,990,668	6	GRMZM2G106056	AT5G54260.1(ATMRE11,MRE11): DNA repair and meiosis protein (Mre11)
	2	6,990,668	6	GRMZM2G406977	AT5G42090.1: Lung seven transmembrane receptor family protein
	2	29,674,082	6	GRMZM2G049608	AT1G21230.1(WAK5): wall associated kinase 5
	2	29,674,082	6	GRMZM2G171620	AT2G20300.1(ALE2): Protein kinase superfamily protein
	2	29,674,082	6	GRMZM2G347361	No annotated gene
	2	29,674,082	6	GRMZM2G510907	No annotated gene
	4	31,513,039	6	GRMZM2G052670	AT1G77140.1(ATVPS45,VPS45): vacuolar protein sorting
	4	31,513,039	6	GRMZM2G106485	No annotated gene

Table D-1 Continued

Shootcap-only	4	62,243,825	6	GRMZM5G806975	LOC_Os08g34700.1: GDU1, putative, expressed
	4	62,243,825	6	GRMZM2G153176	No annotated gene
	4	182,120,435	6	GRMZM2G702728	No annotated gene
	5	198,788,071	6	GRMZM2G111146	AT1G22490.1: basic helix-loop-helix (bHLH) DNA-binding superfamily protein
	5	198,788,071	6	GRMZM2G004480	AT3G03550.1: RING/U-box superfamily protein
	6	147,544,749	6	GRMZM2G147867	AT2G02450.2(anac034,ANAC035,LOV1,NAC035): NAC domain containing protein 35
	9	151,072,090	6	GRMZM2G065237	AT5G52650.1: RNA binding Plectin/S10 domain-
	9	151,072,090	6	GRMZM2G065259	AT5G47550.1: Cystatin/monellin superfamily protein
	9	151,072,090	6	GRMZM5G839889	No annotated gene
	10	1,724,445	6	GRMZM2G430780	LOC_Os03g47470.1: STE_PAK_Ste20_STLK.4 - STE kinases include homologs to sterile 7, sterile 11 and sterile 20 from yeast, expressed
	10	1,724,445	6	GRMZM2G129907	AT5G43210.1: Excinuclease ABC, C subunit, N-terminal
	10	1,724,445	6	GRMZM2G129954	AT3G57040.1(ARR9,ATRR4): response regulator 9
	10	1,724,445	6	GRMZM2G130062	AT1G74040.1(IMS1,IPMS2,MAML-3): 2-isopropylmalate synthase 1
	10	1,724,445	6	GRMZM2G560695	No annotated gene
	10	1,724,445	6	AC195137.2_FG009	No annotated gene
	10	2,254,468	6	GRMZM2G138659	AT5G65180.1: ENTH/VHS family protein
	10	2,254,468	6	GRMZM2G437314	AT3G46710.1: NB-ARC domain-containing disease resistance protein
	10	2,254,468	6	GRMZM2G564717	No annotated gene
	10	134,709,685	6	GRMZM2G018027	AT5G56550.1(ATOXS3,OXS3): oxidative stress 3
	10	134,709,685	6	GRMZM5G887529	No annotated gene
	10	134,709,685	6	GRMZM2G702463	No annotated gene

Table D-1 Continued

	10	137,457,786	6	AC209206.3_FG014	LOC_Os04g53300.1: polyphenol oxidase, putative, expressed
	10	137,457,786	6	AC209206.3_FG001	No annotated gene
	10	142,513,527	6	GRMZM2G354209	AT1G56150.1: SAUR-like auxin-responsive protein family
	10	142,513,527	6	GRMZM2G054537	AT3G06790.2: plastid developmental protein DAG, putative
	10	142,513,527	6	GRMZM2G354187	No annotated gene
	1	29,198,985	5	GRMZM2G476914	AT3G49810.1: ARM repeat superfamily protein
	1	29,198,985	5	GRMZM2G588698	No annotated gene
	1	29,198,985	5	AC191623.3_FG006	No annotated gene
	1	29,198,985	5	GRMZM2G588701	No annotated gene
	1	54,722,001	5	GRMZM2G106283	AT2G37975.1: Yos1-like protein
Shootcap-only	1	54,722,001	5	GRMZM2G106408	AT5G24910.1(CYP714A1): cytochrome P450, family 714, subfamily A, polypeptide 1
	1	193,028,001	5	GRMZM2G012123	AT5G48680.1: Sterile alpha motif (SAM) domain-containing protein
	2	34,841,474	5	No annotated genes	No annotated gene
	2	193,444,001	5	No annotated genes	No annotated gene
	3	157,017,224	5	GRMZM5G863364	AT5G07370.1(ATIPK2A,IPK2a): inositol polyphosphate kinase 2 alpha
	3	157,017,224	5	GRMZM5G898668	AT1G27440.1(ATGUT1,GUT2,IRX10): Exostosin family protein
	3	157,017,224	5	GRMZM2G542752	No annotated gene
	4	44,716,001	5	No annotated genes	No annotated gene
	4	185,758,722	5	GRMZM2G174938	AT5G65180.1: ENTH/VHS family protein
	4	185,758,722	5	GRMZM2G588682	No annotated gene
	5	93,000,001	5	AC184705.4_FG001	No annotated gene

Table D-1 Continued

Shootcap-only	6	102,056,646	5	No annotated genes	No annotated gene
	8	118,074,951	5	AC197705.4_FG011	LOC_Os05g39230.2: low photochemical bleaching 1 protein, putative, expressed
	8	118,074,951	5	AC197705.4_FG009	No annotated gene
	8	118,074,951	5	AC197705.4_FG010	No annotated gene
	8	119,035,095	5	GRMZM2G132759	AT3G08690.1(ATUBC11,UBC11): ubiquitin-conjugating enzyme 11
	8	119,035,095	5	GRMZM2G432583	AT5G01900.1(ATWRKY62,WRKY62): WRKY DNA-binding protein 62
	9	8,116,223	5	AC215605.2_FG003	No annotated gene
	10	136,705,817	5	GRMZM2G077036	AT4G00750.1: S-adenosyl-L-methionine-dependent methyltransferases superfamily protein
	10	136,705,817	5	GRMZM2G077069	AT3G61060.1(AtPP2-A13,PP2-A13): phloem protein 2-A13
	10	136,705,817	5	GRMZM2G077082	AT5G19160.1(TBL11): TRICHOME BIREFRINGENCE-LIKE 11
	10	136,705,817	5	GRMZM2G529263	No annotated gene

VITA

VITA

Alexandar L. Renaud
Department of Agronomy – Purdue University
915 W. State Street, West Lafayette, IN 47907
Work – 765-494-4773 | arenaud@purdue.edu

Education

2011 – May 2015 Ph.D. Plant Breeding and Genetics – *Purdue University*
Dissertation: "Genetic Regulation of Maize Senescence under Abiotic Stress"
Advisor: Dr. Mitchell Tuinstra

2007 – 2011 B.S. Plant Biology (Biotechnology Option), Minor: Biology with Honors – *University of Nebraska - Lincoln*
Thesis: "Molecular Analysis of Maize Mutator Transposon Generated Opaque Endosperm Mutants"
Undergraduate Research Advisor: Dr. David Holding

Professional Experience

February 2015 Monsanto Company (Chesterfield, MO) – Trait Integration Breeder

Summer 2011 Monsanto Company (Huxley, IA) – Corn and Soybean Breeding and Trait Integration Intern

Summer 2010 University of Nebraska (Lincoln, NE) – Field Laboratory Assistant

Summer 2009 DuPont Pioneer (Woodland, CA) – Maize Product Development Intern

May 2009 – May 2011 University of Nebraska (Lincoln, NE) – Maize Biochemistry Laboratory Assistant

Summer 2006 – 2008 Syngenta AG (Slater, IA) – Crew Leader – Corn Line Maintenance and Purification Team

Summer 2005	Garst Seed Company (Slater, IA) – Field Personnel – Corn Line Maintenance and Purification Team

International Experience

May-June 2013	CIMMYT-Asia, ICRISAT Campus, Hyderabad, India – USAID Heat Tolerant Maize for Asia (HTMA) Project

Teaching Experience

Summer/Fall 2014	Lecture Teaching Assistant - Introduction to Plant Breeding (AGRY 520) – *Purdue University* (Dr. Tuinstra)
Spring 2014	Lecture Teaching Assistant - Introduction to Genetics (AGRY 320) – *Purdue University* (Dr. Ma)
Fall 2013	Lecture Teaching Assistant - Introduction to Genetics (AGRY 320) – *Purdue University* (Drs. Bidwell and Anderson)
Fall 2012	Lecture Teaching Assistant - Introduction to Genetics (AGRY 320) – *Purdue University* (Drs. Dilkes and Weil)
Spring 2011	Laboratory Teaching Assistant - Introduction to Genetics (AGRO 315) –*University of Nebraska* (Dr. Lee)

Publications

2013	**Renaud, A. L**., and M. R. Tuinstra, 2013: Role of Engineering Plants for Abiotic Stresses. Climate Vulnerability: Understanding and Addressing Threats to Essential Resources. Elsevier Inc., Academic Press, 51–55 pp.

Invited Presentations

November 2013	ASA-CSSA-SSSA Annual Meeting – Tampa, FL - Adaptation of Agronomic Crops to Climate Change Symposium "Late-season drought tolerance in maize and sorghum"

Invited Presentations Continued

May 2013	Precision Phenotyping for Heat Stress Tolerance in Maize Workshop - CIMMYT-Asia, ICRISAT Campus, Hyderabad, India "Chlorophyll fluorescence and thermal stability in maize"
May 2013	Punjab Agricultural University – Ludhiana, Andhra Pradesh, India "Late-season drought tolerance in maize and sorghum"
May 2013	Lovely Professional University – Phagwara, India "Overview of the Ph.D. program at Purdue University"
January 2013	Hendricks County Purdue Extension - Pesticide Applicator Recertification Program (PARP) "Long and short term drought forecast: state and local level"

Conference and Workshop Activity

April 2014	AFRI Partnership Advisory Council meeting – West Lafayette, IN Poster Title: "Late-season drought tolerance in maize and sorghum"
March 2014	Illinois Corn Breeders School – Champaign-Urbana, IL
December 2013	American Seed Trade Association Corn and Sorghum Seed Conference – Chicago, IL Poster Title: "Late-season drought tolerance in maize and sorghum"
September 2013	AFRI Partnership Advisory Council meeting – West Lafayette, IN Poster Title: "Late-season drought tolerance in maize and sorghum"
May 2013	Accessible, Affordable, Asian (AAA) Drought Tolerant Maize Annual Project Meeting – CIMMYT-Asia, Hyderabad, India
May 2013	Precision Phenotyping for Heat Stress Tolerance in Maize Workshop– CIMMYT-Asia, Hyderabad, India

March 2013	Maize Genetics Conference – St. Charles, IL
March 2013	Illinois Corn Breeders School – Champaign-Urbana, IL
September 2012	Genotype-by-Sequencing Workshop – Cornell University, Ithaca, NY
June 2012	Marker-Assisted Plant Breeding Workshop – St. Paul, MN
March 2012	Maize Genetics Conference – Portland, OR Poster Title: "Functional stay-green in maize"
February 2012	AFRI Partnership Advisory Council meeting – West Lafayette, IN Poster Title: "Functional stay-green in maize"
December 2011	American Seed Trade Association Corn and Sorghum Seed Conference – Chicago, IL Poster Title: "Functional stay-green in maize"

Awards and Certificates

May 2014	John D. Axtell Graduate Student Award in Plant Breeding and Genetics – Department of Agronomy – Purdue University
December 2013	3rd Place Poster Contest – American Seed Trade Association Corn and Sorghum Seed Research Conference – Chicago, IL Poster Title: "Late-season drought tolerance in maize and sorghum"
November 2013	Scarseth Scholarship to attend Annual Meetings of ASA-CSSA-SSSA – Tampa, FL
May 2013	Precision Phenotyping for Heat Stress Tolerance in Maize Certificate – USAID HTMA Project Meeting – ICRISAT, India
December 2011	1st Place Poster Contest – American Seed Trade Association Corn and Sorghum Seed Research Conference – Chicago, IL Poster Title: "Functional stay-green in maize"

Awards and Certificates

2010-2011 Undergraduate Creative Activities & Research Experiences (UCARE) Grant Recipient

Active Collaborations

University of Nebraska-Lincoln – Stay-green in near-isogenic hybrids multi-stress environments

Cornell University – Genetic architecture of stay-green in the NAM and AMES populations of maize

Software Skills

Statistical Analysis Software (SAS)
R Programming
ASReml

Society Memberships

Member since 2013 - National Association of Plant Breeders (NAPB)
Member since 2014 - American Society of Agronomy - Soil Science Society of America - Crop Science Society of America

Strength Finder

Intellection – Learner – Competitive – Deliberative – Individualization

PUBLICATION

PUBLICATION

Renaud, A. L., and M. R. Tuinstra, 2013: Role of Engineering Plants for Abiotic Stresses. Climate Vulnerability: Understanding and Addressing Threats to Essential Resources. Elsevier Inc., Academic Press, 51–55 pp.